SYNTHESIS OF ALCOHOLIC BIOFUELS FROM MULTIPLE INVASIVE WEEDS: PROCESS DESIGN, OPTIMIZATION AND INTENSIFICATION

A Thesis
Submitted in Partial Fulfillment of the Requirements for the Award of the Degree of

DOCTOR OF PHILOSOPHY

Arup Jyoti Borah

CENTER FOR ENERGY
Indian Institute of Technology Guwahati
Guwahati – 781 039, Assam, India
November 2018

Dedicated

To my Jethai

Late Hiranmoyee Borah,

My Parents

&

Mentors

INDIAN INSTITUTE OF TECHNOLOGY GUWAHATI

CENTRE FOR ENERGY

STATEMENT

I do hereby declare that the content embodied in this thesis entitled **"Synthesis of Alcoholic Biofuels from Multiple Invasive Weeds: Process design, Optimization and Intensification"** is the result of investigation carried out by me at Center for Energy, Indian Institute of Technology Guwahati, Guwahati, India under the guidance of Prof. Vijayanand S. Moholkar and Prof. Arun Goyal.

In keeping with the general practice of reporting scientific observations, due acknowledgements have been made wherever the work described is based on the findings of others investigators.

November 2018

Arup Jyoti Borah
(Roll No. 126151008)
Center for Energy
Indian Institute of Technology Guwahati
Guwahati, Assam, India

INDIAN INSTITUTE OF TECHNOLOGY GUWAHATI

CENTRE FOR ENERGY

CERTIFICATE

This is to certify that the work described in this thesis entitled **"Synthesis of Alcoholic Biofuels from Multiple Invasive Weeds: Process design, Optimization and Intensification" by Mr. Arup Jyoti Borah (Roll No. 126151008)** for the award of **Doctoral of Philosophy** is an authentic record of the results obtained from the research work carried out under our supervision in the Center for Energy, Indian Institute of Technology Guwahati, India and this work has not been submitted elsewhere for a degree.

Dr. Vijayanand S. Moholkar
Professor (MTech, PhD)
CEng, FIChemE, FRSC, MAIChE (Sr).
Department of Chemical Engineering
Indian Institute of Technology Guwahati
Guwahati -781 039, Assam, India

Dr. Arun Goyal
Professor (MTech, PhD)
(FAMI, FABAP, FBRS, FNABS,FNAAS,FIFIB)
Department of Bioscience and Bioengineering
Indian Institute of Technology Guwahati
Guwahati – 781 039, Assam, India

Acknowledgements

The tenure in IIT Guwahati as a PhD student has been an amazing and challenging experience for me which I will cherish in my journey to Life. It is full of my patience, support and encouragement from numerous individuals. I take my utmost pleasure to express my deepest gratitude to each and every one who supported me in several ways to complete my PhD Dissertation.

The first and foremost gratitude to my supervisors ***Prof. Vijayanand S. Moholkar*** *and* ***Prof. Arun Goyal*** *for their patience, valuable suggestions, and constant support throughout my research work. I earnestly thank them for their humbleness, spending their valuable time and effort for imbibing scientific temperament and appreciable work ethics in me.*

I would like to express my sincere gratitude to all my doctoral committee members ***Prof. T Punniyamurthy****,* ***Dr. SenthilKumar S.*** *and* ***Dr. Vaibhav V. Goud*** *for their encouragement and insightful advice during my seminars and progress reviews that has led to the successful completion of my thesis.*

I would also like to highly express my heartfelt gratitude to ***Prof. Latha Rangan****, and her lab groups for allowing me to conduct various flow cytometry experiments and guiding me with all their lab expertise. I would specially like to thank my friends* ***Mrs. Reshmi Das****,* ***Ms. Anuma Singh*** *for their constant help and guidance in conducting my experiments.*

I would also like to express my gratitude to ***Prof. Pranab Goswami*** *sir former head of the Centre and his PhD student* ***Mrs. Babina Chakma*** *for helping me to access various instrument for my PhD work.*

I would also like to thank ***Dr. Prasenjit Khanikar*** *&* ***Prof. Anupam Saikia*** *for their motivation and believe in me in various endeavors.*

I wish to acknowledge the support received from earlier and present staffs of Center for Energy, Chemical Engineering, Department of Bioscience and Bioengineering and Central instrument Facility (CIF) ***Dr. Lepakshi Borbora****,* ***Dr. Pankaj Kalita****,* ***Mr. Dhiren Huzuri****,* ***Mr. Debarshi Baruah****,* ***Mr. Parag Jyoti Sharma****,* ***Mr. Lukumoni Bora****,* ***Mr. Harsaraj Biswanath****,* ***Mr. Pranjal Bhuyan****,* ***Mr. Nayan Jyoti Das****,* ***Mrs. Bornali Malakar****,* ***Mr. Nurul islam****,* ***Niranjan Barah*** *and* ***Mrs. Gitanjali Hazarika*** *for their all possible support and facilities to carry out my research work.*

I will be always grateful to my friends at IIT Guwahati ***Garima****,* ***Somnath****,* ***Sourav****,* ***Deep****,* ***Neelkamal****,* ***Sashankar****,* ***Sanjay Da*** *for making my stay comfortable and*

cheerful in campus and ***Jayeeta****,* ***Prachi****,* ***Shivangi****,* ***Shravanika*** *and* ***Bidyutparna*** *for all the love and support. I am immensely thankful to my seniors* ***Dr. Hanif Ahmed Choudhury****,* ***Dr. Swati Khanna****,* ***Dr. Amrita Singh****,* ***Dr. Sankar Chakma*** *and* ***Dr. Jay Bhasarkar*** *and research group members,* ***Pritam****,* ***Shyamali, Ritesh****,* ***Neha****,* ***Niharika****,* ***Kuldeep****,* ***Bhaskar****,* ***Phillip****,* ***Udangshree****,* ***Kajal****,* ***STP****,* ***Mayank****,* ***Mriganka****,* ***Vicky*** *and* ***Sumitha****.*

At last but not the least, I am highly indebted to my parents, ***Mr. Krishna Prasad Bora*** *(Baba),* ***Mrs. Nilima Bora (Ma)****,* ***Late. Hiranmoyee Bora (Jethi)*** *for all the sacrifices they have made for my better future, to have faith in me and giving me freedom to take my own decision. my Ph.D endeavor could not be completed without them. This is for you "****Jethi****", "****Ma****" and "****Baba****."*

Date

Arup Jyoti Borah

Table of Contents

List of Tables

Chapter 1

Chapter 2

List of Figures

Chapter 1

Chapter 2

Chapter 3

Chapter 4

Chapter 5

Chapter 6

Abbreviations

ABE	Acetone, Butanol ethanol
AD	*Arundo donax*
AD	Anaerobic digestion
ATCC	American Type Culture Collection
CAGR	Compound annual growth rate
CBP	Consolidated bioprocessing
CD	Circular dichroism
CMC	Carboxymethyl cellulose
CO	*Chromolena odorata*
CrI	Crystallinity Index
EC	*Eichhornia crassipes*
EH	Enzyme hydrolysis
FID	Flame ionization detector
FSC	Forward Scatter
FTIR	Fourier transform infrared spectroscopy
GA	Genetic Algorithm
GDP	Gross domestic products
g/mol	Gram per mole
HMF	Hydroxymethyl furfural

HPLC	High performance liquid chromatography
IAS`	Invasive alien species
IC	*Ipomea carnea*
K	Kelvin
KDa	Kilo Dalton
KHz	Kilo Hertz
Kpa	Kilo pascal
LC	*Lantana camara*
Lb	Pound
LCA	Life cycle assessment
MA	Mechanical agitation
MJ/L	Mega joule per litre
MM	*Mikania micrantha*
MTCC	Microbial type culture collection
NCIM	National Collection of Industrial Micro-organisms
NRRL	Northern Regional Research Laboratory
ODE	Oridinary differential equation
PH	*Parthenium hysterophorus*
RCM	Reinforced clostridium medium
RI	Refractive index
SS	*Saccharum spontaneum*
SEM	Scanning electron microscope

SHF	Separate hydrolysis and fermentation
SSF	Simultaneous saccharification and fermentation
SSCF	Simultaneous saccharification and co-fermentation
TAPPI	Technical association of pulp industry
TPH	Ton per hectare
TFS	Total fermentable sugar
TRS	Total reducing sugar
US	Ultrasound
XRD	X-ray diffraction

CHAPTER 1: GENERAL INTRODUCTION AND LITERATURE REVIEW

Chapter Highlights

- Biofuel scenario from lignocellulosic biomass and its pretreatments
- Brief discussion and policies for invasive species
- Ultrasound assisted intensification
- Fermentation of lignocellulosic biomass to ethanol
- Butanol as an advanced fuel

CHAPTER 1

INTRODUCTION AND LITERATURE REVIEW

1.1 Introduction

The key to fostering the development and economic upliftment of a country depends heavily on its energy budgets. A nation rich in indigenous energy resources always has an edge over those who depend on import. According to the International Energy Outlook (U.S. IEO 2013), world energy consumption is expected to rise by 56% from 2010-2040, touching 524 quadrillion British thermal units (Btu) to 820 quadrillion Btu per year. This over exploitation of crude oil is severely straining various economies over the world, particularly those of the developing countries. India has only 0.4 % of world proven oil reserves, and is also projected to run out of coal reserves in next forty years **(Patni et al., 2011)**. This necessitates search for alternative energy sources along with the need for conservation of present resources. World over rapid depletion of oil reserves, ever galloping crude prices and impending danger of greenhouse effect have expedited the search for alternative, renewable, sustainable and economically viable fuels. Biofuels, which are derived from biomass either through thermo-chemical or biochemical conversion have recently attained importance. These fuels are either in liquid or gaseous forms. The liquid biofuel are mainly alcoholic fuels such as methanol, ethanol and butanol which can either be used directly or can be blended with petrol or diesel. Biofuels simultaneously provide energy and environment security. Encouraged by this, the European Union has made it mandatory to replace at least 10% transportation fuel with the biofuels by 2020.

1.2 Biofuel scenario in India

In India, the scenario is of grave concern. The domestic crude oil is able to meet only about 23% of the demand, while the rest is met through import. Crude is selling at more than $55 per barrel during 2017-18 and petrol is already selling at around Rs. 76 a liter (an exchange rate of rupees 65 a dollar). India being one of the fastest economies of the world will have to urgently look for alternative and renewable energy sources to reduce dependence on crude and coal based energy. Among the various sources of renewable energy, biofuel attain importance as it has an enormous feedstock generating regularly. Added to this, it ensures environmental security by utilizing the bio-waste.

1.2.1 India's approach to biofuel policy

The Oil minister of India in EU-India Conference on Advance biofuel on 7th March 2018 announced a biofuel policy with proposed investment of rupees one trillion in 2018 under Waste to wealth Project **(Abdi, 2018).** He also mentioned that 95% of transportation depended on fossil fuel, of which 80% was met through import. The target set was to reduce the import by 10% by 2022. A proposal was made for blending 20% bioethanol with petrol by 2030 under Ethanol blending program. The Indian biofuel programme differs from the current international approach in following aspects:

- It is based solely on non-food feedstocks to be raised on degraded or wastelands that are not suited for agriculture and utilizing perpetually regenerated farm domestic and industrial wastes, thus not interfering with food security.
- The National Policy on Biofuel has ensured to meet an aspirational target of 20 percent blending of biofuels by 2017.
- It facilitates and brings about optimal development and utilization of indigenous biomass feedstocks for production of biofuel.

- The policy also envisages development of the next generation of more efficient biofuel conversion technologies based on new feedstocks.
- The policy sets out the vision, medium term goals, strategy and approach to biofuel development and proposes a framework of technological, financial and institutional interventions aimed at developing suitable protocols.
- The policy aims at mainstreaming of biofuel and therefore ideate a central role for it in the energy and transportation sectors of the country in coming decades.
- The policy will bring about accelerated development and promotion of the cultivation, production and use of biofuel to increasingly substitute petrol and diesel for transport.
- It will also contribute to energy security, climate change mitigation, apart from creating new employment opportunities and leading to sustainable development.

1.3. Invasive weedy lignocellulosic biomass

Invasive alien species (IAS) are alien to an ecosystem and when introduced affect native biodiversity. Invasive weeds cause a negative impact on global economy, securing the second largest threat to global biodiversity next to habitat destruction **(Schei, 1996)**. The hardy and unparalleled stress compatibility of these alien plants eliminate the native vegetation through competition, predation, transmission of pathogens and most significantly, disruption of local ecosystems. Since the 17th century, invasive alien species have contributed to nearly 40% of all animal extinctions **(Convention for Biological Diversity CBD, 2006)**. The problem continues to grow at great socio-economic, health and ecological cost around the world. Invasive alien species exacerbate poverty and threaten development through their impact on agriculture, forestry, fisheries and natural systems, which are an important basis of livelihood of people in developing countries. This damage is aggravated by climate change, pollution, habitat loss and human-induced disturbances. A list of weedy species with biological classification screened for biofuel feedstock is shown in **Table 1.1** below.

Table 1.1: List of invasive weedy biomass screened as a feedstock for bioalcohol production.

Biomass	Classification	Salient features
 *Arundo donax*	Division: Magnoliophyta Class: Liliopsida Order: Cyperales Family: Poaceae Genus: *Arundo. L* Species: *A. donax*	Invasive in parts of South Africa, Australia, and the USA, Tolerate wide variety of conditions, high salinity, flourish in many soil types Low input crop and high yield above ground (20-30 ton/h) **Threat:** Infest Kaziranga Nameri and Dibru Saikhowa National Park
 *Chromolena odorata,*	Division: Magnoliophyta Class: Liliopsida Order: Asterales Family: Asteraceae Genus: *Chromolena* Species: *C. odorata*	Serious weed in central and western Africa, India, Australia, Pacific Islands, Southeast Asia (**McFadyen et al., 2003**). Wind-dispersed seeds (up to 800,000/ plant), persist more than a year in soil (QISC, Hawaii dept. of agriculture). **Threat:** Problem in agronomic land such as rubber, palm oil, tea, coffee, cashew, teak and other plantation crops in Asia, Africa savanna etc.
 *Eichhornia crassipes*	Division: Magnoliophyta Class: Liliopsida Order: Liliales Family: Pontederia Genus: *Eichhornia* Species: *E. crassipes*	World's worst aquatic weed. Reproduce both sexually and asexually Viable upto 20 years. Takes 5 days to double its mass. Block irrigation channel, making fish inhabitable and inaccessible. **Threat:** Loktak lake (40 sq km) in Manipur Largest fresh water lake in India, Deepor Beel (10 sq km) in Guwahati is infested by water hyacinth
 *Ipomea carnea*	Division: Magnoliophyta Class: Liliopsida Order: Solanales Family: Convolvulaceae Genus: *Ipomea* Species: *I. carnea*	Covering seven habitats (railway sides, waste lands, road sides, drain and canal banks, road dividers and field edges). **Threat**: Infested Pobitora Wild sanctuary (Assam) (**Lahkar et al., 2011)**

 *Lantana camara*	Division: Magnoliophyta Class: Magnoliopsida Order: lamiales Family: Verbenaceae Genus: *Lantana* Species: *L. camara*	Both vegetative (asexual) and seed reproduction occur. Up to 12,000 fruits by each plants Grow in wide range of soil dry to wet, salt and high draught resistant. **Threat**: Bandipur Tiger reserve, Southern India
 *Mikania micrantha*	Division: Magnoliophyta Class: Liliopsida Order: Asterales Family: Asteraceae Genus: *Mikania* Species: *M. micrantha*	Known as mile a minute vines. A single stalk can produce 20,000 to 40,000 seeds a season. Grow 80 to 90 millimetres (3.1 to 3.5 in) in 24 hours. **Threat:** Chitwan national park, and Kaziranga national park
 *Parthenium hysterophorus*	Division: Magnoliophyta Class: Magnoliopsida Order: Asterales Family: Asteraceae Genus: *Parthenium* Species: *P. hysterophorus*	25,000 seeds/plant, pollen grains, 624 million/plant. Cause asthma, bronchitis (man livestock) Infests 170000 km^2 grazing country in Queensland, losses $16.8 mm/yr to the pasture industry, 40% farmland in Australia In India, decline of up to 40% in agricultural crops, Khosla and Sobti (**Kaur et al., 2014**).
 *Saccharum spontaneum*	Division: Magnoliophyta Class: Liliopsida Order: Cyperales Family: Poaceae Genus: *Saccharum* Species: *S. Spontaneum*	High genetic and morphological diverse polymorphic species. vary from short bunchgrasses to those that produce 4 to 6-meter-tall stems Weed in 33 countries (**Holm et al., 1997**). 3- 4 mm ha of land in India, (**Holm et al., 1997; Raju, 1998**). **Threat**: Infest in almost all grassland of Assam. Shown in Table 1.4

1.3.1 Global and national scenario

At global level, the losses due to IAS invasion have been estimated to be US$ 1.4 trillion per year **(Table 1.2)**, close to 5% of global GDP (gross domestic product) **(Avery 2013). Clavero** and **Garcia-Berthou (2005)** have reported invasive alien species as the main cause of avifaunal extinctions worldwide and indicates their secondary role in

extinctions of freshwater fish and mammals. **Pimentel (2009)** estimated the loss associated with invasive species in the United States at US$ 120 billion per year. Moreover, these species pose primary threat to about 42% of the indigenous threatened and endangered species.

Table 1.2: Estimated economic losses due to invasive weeds across the globe.

Country	Estimated losses (Euro, €, billion/year)
Globally	1000
US	90
EU	12
China	11
New Zealand	2
UK	2

Data Source: adopted from European Parliamentary Service Commission **(Avery, 2013)**

Indian subcontinent also has suffered great economic losses due to IAS, many of which were characterized by a highly invasive nature. **Khuroo et al. (2012)** reported alien flora of India amounts to 1599 species, belonging to 842 genera of 161 families and constituting 8.5% of the total vascular flora found in the country. The negative impact has been felt through loss to grazing, arable land, endangering animal and human health. **Muniappan** and **Bamba (1999)** had described the introduction of few species as ornamental plant in 1845 in Calcutta. Unfortunately, it turned out to be highly invasive, spreading widely across north-eastern India during World War I, followed by West Bengal and Orissa during 1924-25 and Kerala and other southern states in 1942 **(Singh, 1998)**. The northeastern region of India (especially state of Assam) is glutted with the weed flora of diverse species due to the favorable climate. The biomass production of weeds roughly ranges from 5 to 20 t/ha depending upon plant species, growing conditions and the prevailing season (*Lantana camara* 10–12 t/ha, *Eichhornia crassipes* 6–8 t/ha, *Mikania micrantha* 8–10 t/ha) (**Rajkhowa et al., 2005**). State of Conservation Report of

Wildlife Sanctuary, India (2015) has given detailed account of the serious intrusion of invasive weeds and their adverse effects on conservation of indigenous creation of national importance such as one-horn rhino habitat and grasslands that provide wildlife fodder. UNESCO has strongly recommended development and implementation of invasive species management policy for prevention of their intrusion of grassland habitats. Invasive weeds are unwanted plants that are available almost free of cost. Utilization of these invasive weeds for bioalcohol production therefore, could be of great ecological and economic importance. Assam is mainly a grass dominated biome. Till date, 23 grasslands have been listed that include all national parks and wild life sanctuaries ranging from 480 sq. km Kaziranga National park to Nameri national park which is extended to 10 sq. km. A detailed report of weed invasion in the main grassland and national park of Assam is depicted in **Table 1.3** and **Table 1.4** below.

Table 1.3: Background study of weed infestation in different ecosystem of Assam **(Deka and Barua, 2015)**

Ecosystem	Area of Spread	Invasive weeds	Economic loss %	Distinguish information
Agro (Jute) ecosystem		*A. houstonianum, A. sessilis, A. spinosus, A. compressus, C. diffusa, C. dactylon, etc.*	75-80%	NA
Agro-ecosystem (Sugarcane)		*M. micrantha, A. houstonianum* and *B. articularis*	12-75%	NA
Agro-ecosystem (Tea)	3.18 lakh ha	*M. micrantha, P. aspalum* spp., *B. articularis, G. bicolor, C. odorata, L. camara*	50-70%	Assam is the world's largest exporter of tea
Horticulture-ecosystem (Banana)		*Ageratum-Borreria-Commelina, M. micrantha, M. diplotricha*		Daranggiri, in Goalpara, Assam. 2nd highest retail hub of banana in Asia
Horticulture-ecosystem (Pine-apple)		*M. micrantha, M. diplotricha, C. odorata, S. spontaneum, I. cylindrica*		productivity higher than the national average (15.3 t/ha)
Fisheries Ecosystem	3.44 lakh h static water, 1.58 lakh h paddy field	*Nymphoides spp., Trapabisinosa, E. crassipes, Salvinia spp., Azolla, pinnata, C. antiquorum* and *M. quadrifolia*	86 -92% irrigation tanks are infested	Brahamputra river, navigation is hindered by water hyacinth.
Wet land Ecosystem	101232 ha	*Eichhornia crassipes, Salvinia molesta, Chara spp., Nitella spp.* and *algal scum.*		3513 wetlands, 1,29 % of state total area. Deepor Beel (40.2 sq. km.) (Ramsar site)
Forest Ecosystem	26,781.91 sq. km.	*L. camara, M. micrantha, Mimosa spp., Ipomea spp.* and *C. odorata*		34.14% of the total area

NA - Not available

Table 1.4 Some alien species that have detrimental impact on grassland ecosystems **(Lahkar et al., 2011)**

Sites	District	Size (sq. km)	Invasive species	Current impact	Rate of spread	Management by Forest Department
Kaziranga	Golaghat, Nagoan, Sonitpur	480	1,3,5,9	Severe	Increase rapidly	Manual removal, Fire
Manas	Barpeta and Bongaigoan	250	6,	Severe	Increase rapidly	Fire
			4	High	Increase rapidly	None
Dibru Saikhowa	Dibrugarh, Tinsukia	70	1,2,3,4, 5,6,7,8,9	Not reported	Not reported	-
Orang	Darrang Sonitpur	50	3,6	Severe	Increase rapidly	Fire
			4	High	Increase rapidly	None
			5,9	Moderate	Increasing slowly	None
Pabitora	Morigaon	20	3,7,9	High	Increasing rapidly	None
			4	Moderate	Increasing slowly	None
Nameri	Sonitpur	10	1,2,3,4, 5,6,7,8,9	Not studied	Not reported	-

Source: State Biodiversity Strategy and Action Plan, Assam, 2009. Species of weeds: *1 = Arundo donax; 2 = Phragmites karka; 3 = Mimosa; 4 = Mikania 5 = Saccharrum spp.; 6 = Chromolaena, 7 = Ipomea, 8 = Erianthus ravennae (Saccharum spp.), 9 = water hyacinth*

1.4 Pretreatment and hydrolysis of biomasses

Pretreatment of bio-waste is observed as one of the most expensive steps in converting the cellulosic biomass to fermentable sugars **(Lynd et al., 1996).** It represents one-third of the cost of the overall process. Lignin (polymer) another important constituent of bio-waste. It is of high commercial value but is often neglected during hydrolysis. The goal of the pretreatment process is to break down the lignin structure and disrupt the crystalline structure of cellulose, thereby increasing the porosity of the

lignocellulosic material. This provides acids and enzymes access to hydrolyze cellulose by increasing the porosity of the lignocellulosic material so that easy access and hydrolyze the cellulose. These raw lignocellulosic materials are sufficiently abundant and have the potential to cut greenhouse gas emissions by 86%. Approximately 90% of the dry weight of most plant materials is stored in the form of cellulose, hemicellulose, lignin, and pectin **(Kumar et al., 2009).** The carbohydrate polymers are tightly bound to lignin mainly by hydrogen bonds and some covalent bonds. Presence of lignin in lignocelluloses barricades the plant cell against the break down action by fungi and bacteria. Pretreatment is therefore done: (i) to facilitate to formation of sugars by hydrolysis, (ii) avoid the degradation or loss of carbohydrates, (iii) prevent the formation of byproducts that are inhibitory to the subsequent hydrolysis and fermentation processes, and (iv) make it cost-effective. Three major hydrolysis processes are conventionally employed to produce a variety of sugars suitable for ethanol production using dilute acid, concentrated acid and enzymatic hydrolysis. While hemicellulose can be readily hydrolyzed by dilute acids under ambient conditions, comparatively more extreme conditions are needed for cellulose hydrolysis. Numerous pretreatment protocols are employed for treating biomass to overcome the problem faced during pretreatment.

1.4.1 Physical pretreatment

1.4.1.1 *Mechanical comminution*

This process is used to reduce the size of the materials usually 10-30 mm after chipping to 0.2-2 mm by milling or grinding. The energy input for comminution can be kept below 30 kWh per ton of biomass. In pretreatment process, it undergoes irradiation of cellulose by γ-rays, which leads to cleavage of 1,4-glycosidic bonds and gives a larger surface area and a lower crystallinity, which helps in high yield of sugar for fermentation. It is considered as an expensive process due to high energy utilization.

1.4.2 Physicochemical pretreatment

1.4.2.1 *Steam explosion*

It is the most commonly used method. Biomass is treated with saturated steam at high-pressure, and then the pressure is suddenly reduced. This makes the materials undergo an explosive decompression. Temperature initiated here is in the range 160-260°C (corresponding pressure, 0.69-4.83 MPa) for several seconds to a few minutes before the material is exposed to atmospheric pressure. This process causes hemicellulose degradation and lignin transformation due to high temperature, thus increasing the potential of cellulose hydrolysis. Addition of H_2SO_4 (or SO_2) or CO_2 [typically 0.3-3% (w/w)] in steam explosion can decrease the time and temperature, effectively improve hydrolysis, decrease the production of inhibitory compounds, and lead to complete removal of hemicellulose.

1.4.2.2 *Ammonia fiber explosion (AFEX)*

In this process, biomass is exposed to liquid ammonia at high temperature and pressure for a period of time, and then the pressure is suddenly reduced. (similar to steam explosion). The dosage of liquid ammonia required is 1-2 kg of ammonia/kg of dry biomass, the temperature is 90 °C, and the residence time is 30 min. The hemicellulose is degraded to oligomeric sugars and deacetylated, but hemicellulose is not soluble. Over 90% hydrolysis of cellulose and hemicellulose can be done but is not very effective for biomass with higher lignin content.

1.4.2.3 *Carbon dioxide explosion*

The process of supercritical CO_2 explosion has lower temperature than steam explosion and possibly a reduced expense compared to ammonia explosion. It is a fluid

which is in a gaseous form but is compressed at temperatures above its critical point to a liquid like density. CO_2 forms carbonic acid when dissolve in water, which results in increase of hydrolysis rate. The molecular size of CO_2 is similar to water and ammonia which helps in hydrolyzing hemicellulose as well as cellulose. Monosaccharides do not undergo any degradation in the presence of acid due to low temperature treatment.

1.4.3 Chemical pretreatment

1.4.3.1 *Ozonolysis*

Ozone helps in reducing the lignin content of the feedstock by *in vitro* degradation of the treated material without producing any toxic residues unlike other chemical treatment. All reactions are conducted at room temperature and normal pressure. Ozone can be easily decomposed later either by increasing the temperature or by using a catalytic bed. Large amount of ozone is required which makes it an expensive process.

1.4.3.2 *Acid pretreatment*

Acid pretreatment is one of the common pretreatment techniques. This is accomplished by using concentrated or dilute acid. Concentrated acid treatment results in improvement of enzymatic hydrolysis. But it is not an economically feasible process due to corrosion of reactor and no chemical recovery. Dilute acid treatment has been successfully employed as it involves use of acid of strength < 4% w/w. Two types of dilute acid pretreatments are used. High-temperature (T > 160^{o}C), continuous flow process for low solid loadings (5-10%) and a low temperature batch process (T < 160^{o}C) for high solid loadings (10-40%). This is the most widely used and tested process for the generation of xylose from hemicellulose and furfural from xylose.

1.4.3.3 *Alkaline pretreatme*nt

This process utilizes lower temperature and pressure than other pretreatments. It is a time consuming process and yields comparatively less sugar than acid process. Although sodium hydroxide treatment is expensive than calcium hydroxide, it is more effective. This treatment removes amorphous substances increasing the crystallinity index and reducing the lignin content to about 10% in the treated biomass. This significantly increases the susceptibility of cellulose to enzymatic hydrolysis.

1.4.3.4 *Oxidative delignification*

This is a wet oxidation process, which is catalyzed by the peroxidase enzyme in the presence of H_2O_2 resulting in biodegradation of lignin and making the cellulose more susceptible to enzymatic hydrolysis.

1.4.3.5 *Organosolv process*

In this process, an organic or aqueous organic solvent mixture with inorganic acid catalysts (HCl or H_2SO_4) process is used to break the internal lignin and hemicellulose bond. This process causes prehydrolysis and delignification simultaneously. It is comparatively an expensive process.

1.4.3 Biological pretreatment

It is safe and ecofriendly process. It uses microorganisms such as soft, brown rot fungi. Brown rot fungi attack cellulose, whereas white and soft rot fungi attack both lignin and cellulose. Only drawback is the slow kinetics of the process.

1.5 Dilute acid hydrolysis

In the dilute acid process, the reaction is carried out at high temperature and pressure but it yields less glucose from cellulose leading to low ethanol yield. The use of concentrated acid in the hydrolysis process yields more ethanol as almost the entire cellulose is converted to glucose. Unlike the dilute-acid hydrolysis, this process is accomplished at ambient conditions. The acid concentration in the dilute-acid hydrolysis process is in the range of 2-5% as compared to 10-30% for concentrated acid.

After acid pretreatment, hemicellulose fraction of the feedstock gets hydrolyzed into pentose sugars and acetyl group gets converted to acetic acid. However, various byproducts formed during acid hydrolysis depend on efficiency and nature of the biomass. The lignin content in the biomass acts as a barrier for the formation of pentose sugars and reduces the access of enzyme molecules to cellulose which limits the generation of hexose sugars synthesis **(Alvira et al., 2010).**

For high hexose sugar yield during enzymatic hydrolysis, the cellulose moieties in the biomass need to be exposed to enzymatic action. This requires both detoxification and delignification (lignin removal) of pretreated biomass. In the biological process also detoxification and delignification are prerequisites for liberating cellulose and hemicellulose from their complex with lignin, depolymerization of the carbohydrate polymers to produce free sugars and fermentation of mixed hexose and pentose sugars to produce biofuel. Growth of microbes during fermentation is also hindered by the formation of hydroxymethyl furfural, furfural and phenolic compounds. In addition, the lignocellulosic biomasses also resist physical and biological degradation. Thus, selection of best and cost-effective pretreatment process and its parameters is crucial.

1.6 Detoxification of lignocellulose hydrolysate after acid hydrolysis

Lignocellulosic hydrolysate obtained after acid hydrolysis contains phenolic compounds, furan aldehydes and aliphatic acids which inhibit the growth of the micro-organisms during fermentation process. The process which is used to remove such inhibitors prior to fermentation is known as detoxification. **Jonsson et al. (2013)** listed various substances inhibits microorganisms including phenolic compounds and other aromatics, aliphatic acids, furan aldehydes, inorganic ions, and bio alcohols or other fermentation products.

1.6.1 Phenolic compounds

Phenolic compounds (syringaldehyde, vanillin, syringic acid, vanillic acid, *p*-coumaric acid, ferulic acid) and other aromatics are formed during pretreatment regardless of the presence of an acid catalyst **(Martin et al., 2002).** These phenolics interfere with the cell membrane function by changing the protein-to-lipid ratio **(Keweloh et al., 1990).**

1.6.2 Aliphatic acids

Lignocellulose hydrolysates contain aliphatic acids like acetic acid, formic acid, and levulinic acid. Acetic acid is formed primarily by hydrolysis of acetyl groups of hemicellulose, while formic acid and levulinic acid arise as acid-catalyzed thermochemical degradation products from polysaccharides. Formic acid is a degradation product of furfural and HMF (5-hydroxymethylfurfural), while levulinic acid is formed by degradation of HMF **(Ulbricht et al., 1984)**. The aliphatic acids content of slurries and hydrolysates vary widely depending on the feedstock and severity of the pretreatment. Feedstocks with high content of acetylated xylan such as agricultural residues and

hardwood give higher concentration of aliphatic acids than softwood. The total content of aliphatic acids in softwood hydrolysates is often below 100 mM which is beneficial for ethanol yield. Undissociated acid enters the cell through diffusion through the cell membrane and dissociates due to the neutral cytosolic pH. This leads to a decrease in the intracellular pH, which may lead to cell death. This mechanism differs from that proposed for aliphatic acids like acetic acid, as it inhibits the regeneration of ATP in mitochondria reducing the supply of ATP at the plasma membrane. Some aromatic carboxylic acids may act as uncouplers, as shown in experiments with plant cells and salicylic acid **(Norman et al., 2004)**. Salicylic acid is also found in lignocellulose hydrolysates **(Jonsson et al., 1998)**. Conversely another aromatic carboxylic acid, p-hydroxybenzoic acid which is common in lignocellulose hydrolysates, does not exhibit the uncoupling effect **(Norman et al., 2004)**.

1.6.3 Furan aldehydes

The furan aldehydes like furfural and HMF, commonly found in lignocellulose hydrolysates, are formed by dehydration of pentose and hexose sugars, respectively. Under anaerobic conditions, *S. cerevisiae* converts furfural to furfural alcohol and HMF to 2,5-bis-hydroxymethylfuran **(Taherzadeh et al., 2000).** This will result in decreased formation of the undesirable by-product, xylitol, and an increased formation of ethanol. This is sometimes referred to as insitu detoxification.

1.6.4 Inorganic compounds

Inorganic ions mainly originate from the added chemicals present in lignocellulose hydrolysates during pretreatment, conditioning and hydrolysis, and possibly from process equipment. Addition of salts increases the osmotic pressure. This

inhibits the process because of the increased demand of ATP generated by the increased transport over the plasma membrane. The extra ATP required is acquired by increased ethanol production at the expense of biomass formation. **Maiorella et al. (1984)** investigated the effect of different salts on *S. cerevisiae* and found that the inhibition decreased in the following order: $CaCl_2$>$(NH_4)_2SO_4$>NaCl>NH_4Cl>KH_2PO_4> $MgCl_2$> $MgSO_4$>KCl.

1.7 Delignification of acid hydrolyzed biomasses

Lignin is a large group of aromatic polymers resulting from the oxidative combinatorial coupling of 4-hydroxyphenylpropanoids through enzymatic hydrolysis **(Vanholme et al., 2010).** It mainly comprises three monomeric units, coniferyl, sinapyl and *p*-coumeryl alcohols linked randomly mostly via ether linkage at α and β positions to construct the macromolecule. Lignin is predominantly found in the walls of secondarily thickened cells, making them rigid and impervious. Lignin makes the plant biomass resistant to microbial degradation making pulp and biofuel synthesis difficult. Therefore, efforts are now aimed at designing plants with low lignin content that are more amenable to chemical degradation **(Vanholme et al., 2010).**

Lignin is interlinked with carbohydrate moiety by ester, ether and glycosidic linkages which are not easily dissociated. In alkaline medium ester linkage is comparatively readily hydrolyzed than the ether linkage. Delignification process is used to selectively remove the residual lignin left after pretreatment and enhance digestibility of treated biomass. It is generally carried out under acidic, alkaline or oxidative conditions **(Bussemaker and Zhang, 2013)**.

Acidic Environment: Here the degradation of α and β ether lignin units takes place when there is protonation of benzyl oxygen. The protonation is followed by α- ether elimination of phenol or alcohol giving benzylic carbonium ion intermediate.

Alkaline Environment: In alkaline and alkaline-oxidative environments, the *α* and *β*-aryl ether linkage between lignin get cleaved to give in various fragmentation units.

Oxidative Environment: In this case, cleavage of carbon-carbon linkages takes place followed by phenolic degradation by formation of acidic group such as carboxylic acids. The side chain of the lignin may get displaced through electrophilic substitution.

For delignification under alkaline conditions, NaOH is the widely used reagent **(Sun et al., 2012)**. Degradation of lignin is achieved through the cleavage of *α*– and *β*–aryl ether linkages under alkaline and alkaline–oxidative environment. The mechanism for lignin extraction may include depolymerization, separation, degradation and condensation.

1.7.1 Ultrasound induced delignification of acid hydrolyzed biomass

Ultrasound treatment recently is being attempted for intensification by accelerating delignification under alkaline treatment. However, the exact physical mechanism of the ultrasound assisted delignification have not been fully understood. Ultrasound and its secondary effect of cavitation have both physical and chemical implications on the reaction system. The physical effect generated by ultrasound creates a strong micro–turbulence in the system through micro–convection generated by transient bubble motion and micro–streaming (i.e. small amplitude oscillatory motion of liquid elements induced by passage of ultrasound wave). The chemical effect results in transient collapse of the bubbles which results in the production of highly reactive radical species such as •OH, •O and HO_2• generated through thermal dissociation of vapor molecules

entrapped in the bubble. These radicals lead to degradation of lignin through different mechanisms. For effective delignification, the underlying physical and chemical effects of ultrasound have to be clearly understood. Coupling experiments with simulations of cavitation bubble dynamics at the prevalent experimental conditions have been attempted in a few studies. Concurrent analysis of experimental and simulations results reveal interesting mechanistic facets of the delignification process, as outlined in the subsequent sections.

A summary of some representative studies on optimization of pretreatment and fermentation of the invasive weeds is given in **Table 1.5**. Most of these studies employed: acid hydrolysis, followed by delignification, enzymatic hydrolysis and fermentation of the acid/enzyme hydrolyzates to bioethanol. These studies revealed that the optimum pretreatment conditions varied with the type of biomass. Since the same type of bio-waste may not be available throughout the year, biofuel industry may have to use a mixture of biomass as feedstock. It is therefore necessary to identity optimum pretreatment conditions and processing equipment suitable for the pretreatment of individual biomass or mixed biomass feed.

1.8 Saccharification of delignified biomass

Cellulose is the widely prevalent polymer constituting major structural component of plant cell wall (35-70% of dry weight). Cellulose consists of a polymerized linear chain of glucose units joined by β-1,4-glycosidic linkages. One cellulose molecule comprises approximately, 10,000-15,000 glucose units and 30 such cellulose molecules are assembled into elementary fibrils. These elementary fibrils are further linked together by extensive intra- or inter chain hydrogen bonding interactions to form microfibrils. About 250 of such microfibrils join to form a cellulose fiber **(Krassig, 1992)**. Cellulose

rich pretreated lignocellulose is used as substrate for producing fermentable sugar by enzymatic hydrolysis. Lignocellose is a condensed structure insoluble in water, affording very little surface area for cellulase enzymes to carry out enzymatic hydrolysis. Most of the studies are directed to reduce the recalcitrance of cellulose and make it susceptible to enzymatic hydrolysis and facilitate formation of a fermentable form of sugar by decreasing crystallinity and increasing the accessibility to the glucan chain. Removal of lignin helps in better utilization of cellulose substrate for hydrolysis. Enzymatic hydrolysis is the crucial step in determining the economy of biofuel production due to high cost of enzymes and slow kinetics. Economizing the process also involves making it more energy efficient by reducing energy input required for physical pretreatment of feed stock and process operation. Ultrasound irradiation (or sonication) is an efficient method for pretreatment as it induces cavitation, a process of nucleation, growth and implosive collapse of gas/vapor bubbles driven by pressure variation induced by ultrasound. Both sonication and cavitation create intense energy concentration on temporal and spatial scale, which improves the kinetics of the process. Earlier studies on pretreatment to increase the yield of enzyme hydrolysis are summarized in **Table. 1.6**.

1.9 Fermentation of enzymatic hydrolysate to ethanol

In bioethanol production process, the lignocellulosic hydrolysate obtained by acid and enzymatic hydrolysis has been used for fermentation. Four different modes of fermentation process have been employed: i) Separate hydrolysis and fermentation (SHF), ii) simultaneous saccharification and fermentation (SSF), iii) simultaneous saccharification and co-fermentation, and iv) consolidated bioprocessing (CBP). The choice of the process however depends on characteristics of biomass, enzyme and micro-organisms involved. Pentose fermenting organism is employed for fermentation of acid

hydrolysate and hexose fermenting organism for the hydrolysate obtain for enzymatic hydrolysis.

In SHF, the enzymatic hydrolysis and fermentation processes are carried out separately. The main attraction of this process is that both hydrolysis and fermentation can be carried out at their optimum conditions for better results. **Kuhad et al. (2010a)** and **Bharadwaja et al. (2015)** carried out ethanol production by SHF mode, which resulted in total ethanol yield of 0.26 g/g of raw biomass.

SSF has certain advantage over SHF since both processes of saccharification and fermentation take place in one reactor, and thus have high energy efficiency **(Sanchez and Cardona, 2008).** It also prevents glucose inhibition of cellulases since the sugar gets simultaneously utilized by micro-organism thereby reducing sugar levels in the fermentation broth. This also results in reduced microbial contamination. The major limitation regarding SSF is the compromise with the optimum conditions of both enzymatic hydrolysis and fermentation. Optimal activity of cellulase enzyme is best at temperatures 40^{o}-50^{o}C and pH 4.0-5.0 whereas the optimal growth conditions for the fermenting microorganisms is 30^{o}-37^{o}C and pH of 4.0-5.0. Pentose fermenting organism performs best at 30^{o}-70^{o}C and pH of 5.0 -7.0 **(Olsson and Hahn-Hagerdal, 1996).**

When pentose fermentation is included in the same reactor in SSF, the process is termed as simultaneous saccharification and co-fermentation (SSCF). The main advantage of this process is the prevalent best optimal condition for the microbes. **Olsson and Hahn-Hagerdal (1996)** used coculture of *Pichia stiptis* and *Brettanomyces calusennii* at 38^{o}C in SSCF. **Oloffson et al. (2010)** used both acid and enzyme hydrolysis of wheat straw using a recombinant *Saccharomyces cerevisiae* TMB3400 strain. **Koppram et al., (2013)** used recombinant strain of *Saccharomyces cerevisiae* for ethanol production by SSCF process using substrate comprising corn cob slurry and molasses.

Consolidated bioprocessing(CBP), also known as direct microbial conversion (DMC), involves a single community to carry out four successive bioconversions namely cellulases and hemicellulases production, hydrolysis of delignified biomass to sugar and sugar fermentation to ethanol in one reactor. Here, either a microbial consortium or a genetically modified organism is used **(Wyman, 1994; McMillan, 1997; Lynd et al., 2002).** Since, a single wild strain is not capable of performing all these process, *S. cerevisiae* **(Yamada et al., 2013)** and *Trichoderma* sps. (**Huang et al. 2014)** have been studied in recent times. A briefing of literature on ethanol production by various modes of fermentation using various feedstock is given in **Table 1.7**.

Table 1.5: Review on available information on pretreatment of invasive weeds and fermentation of the hydrolysate

Type and summary of pretreatment	Biomass	Major observations and conclusions	Reference
Microwave assisted alkali pretreatment. Two stages pretreatment microwave/dilute NaOH followed by microwave/ dil H_2SO_4.	*Arundo donax*	120°C/5 min/5% w/v NaOH. Total sugar release: 0.89/100g biomass. 120°C/5 min/5% w/v NaOH and 180oC/30 min/0.5% w/v H_2SO_4 31.99/100g biomass. Glucose is the main monomeric sugars	**Komolwanich et al. (2014)**
Optimization of enzymatic hydrolysis (EH) and simultaneous saccharification and fermentation (SSF). Optimization of EH and SSF using response surface methodology (RSM) with 2 input parameters: severity factor (SF) and oxalic acid concentration (OA) Temp range: 150°C – 190°C Treatment time range: 10 – 40 min Dil. oxalic acid concentration range = (2–8% w/v)	*Arundo donax*	Xylan content after dil. oxalic acid pretreatment reduced with increasing SF and OA. Glucan and lignin showed opposite trend with respect to xylan content after dil. OA treatment. Final results: Glucan conversion in EH = 95%, and Ethanol production = 18 g/L (75% of maximum theoretical yield) for pretreatment conditions of SF = 4.05 and OA = 5% w/w	**Scordia et al. (2013)**
Cost effective pretreatment of biomass with protic acid resin Amberlyst 35DRY and ionic liquid 1-butyl-3-methylimidazolium chloride. Two stage treatment: 1. 160°C with ionic liquid for 1.5 h, 2. slurry of ionic liquid and Amberlyst 35DRY resin at 90°C for 1 h.	*Arundo donax*	Reduction in cellulose crystallinity and increased porosity and partial depolymerization of longer cellulose chains of dissolved biomass by Amberlyst catalyst High glucose yield of 92.8% than 42.8% yield for single ionic liquid treatment for enzyme loading of 20 FPU/g of substrate. Reusability of the ionic liquid solid catalyst system.	**You et al. (2014)**

Table 1.5 (continued…….)

Type and summary of pretreatment	Biomass	Major observations and conclusions	Reference
1.75% w/v H_2SO_4 (8.5 ml), 121°C/h 1.2 ml of 10% w/v $Ca(OH)_2$GC 220 Cellulase 5FPU/g biomass, 12U Novozyme 188 Cellubiase	*Arundo donax*	Xylan associated monosaccharide yield: 201 mg/g Ethanol produced from A. donax: 109 mg/g.	**Anderson et al. (2008)**
Dilute acid pretreatment for following conditions: Effect of temperature (170°C-190°C) Acid loading (2-10% w/v); Reaction time (15-40 min) Simultaneous saccharification and fermentation using commercial enzymes and two yeast strains: *S. stipitis* CBS 6054 and *S. carlsbergensis* FPL-450	*Arundo donax*	*S carlsbergenesis* results: Max ethanol concentration of 15.9 g/L after 48 h at pH 5. *S. stipitis* results: Ethanol concentration of 15.9 g/L in 96 h. Increasing pH to 6 reduced lag phase and attained 18 g/L after 72 h	**Scordia et al. (2013)**
Laccase treatment followed by simultaneous saccharification and fermentation (SSF); Crude laccase 400 IU/ml, pH 6.5; 10 g dry substrate liq:solid (2 ml/g) kept 8 h at 37°C. SSF using cellulase from *T. reesei*. Optimization of SSF through CCD based response surface methodology	*Lantana camara*	Maximum bioethanol production: 5.14 % v/v Optimum substrate concentration: 17% w/v Optimum inoculum volume: 9% v/v Inoculum age 60 h and 144 h of incubation time Enhanced bioethanol concentration of 6.01% v/v using mutant strain of *S. cerevisiae*	**Kuila and Banerjee. (2014)**

Table 1.5 (continued…..)

Biomass pretreatment with acid, alkali and chlorite to improve enzymatic saccharification of cellulose 1. For 100 g substrate: Acid concentration 1-5%w/v, Time 15-16 min, Temperature 121^{o}C 2. For 100 g substrate: Alkali concentration 1-5% w/v for 2 h. Thermal pretreatment at 121^{o}C; Time 15, 30, 45 & 60 min. 3. Chlorite pretreatment: Sodium chlorite 1-5% w/v for 121^{o}C for 15, 30, 45, 60 min followed by washing and drying at 60^{o}C.	*Lantana camara*	Chlorite treatment removes maximum lignin with 90% w/w residual holocellulose. Results of enzymatic hydrolysis: 1. Chlorite treatment: 90% w/w initial holocellulose, saccharification of 86-92% fraction 2. Alkali treatment: 66-76% w/w initial holocellulose, saccharification of 55% fraction 3. Acid treatment: 39.5-48% w/w initial holocellulose, saccharification of 38-48% fraction	**Gupta et al. (2011)**
Biomass loading 5% (w/v); Alkaline (NaOH) pretreatment at different concentrations (0.5, 1, 1.5, 2% w/v); Period of treatment: 30, 60, 90,120 min at 121^{o}C. Enzymatic hydrolysis of biomass with crude mixture of cellulase enzymes (20 Units/ g biomass); CMCase, FPAse, xylanase activities of 1.41, 1.12 and 6.23 Units respectively.	*Saccharum spontaneum*	Optimization results: 1. 70.75% lignin removal for 0.5% w/v NaOH treatment at 120^{o}C with total reducing sugar yield in enzymatic saccharification: 350 mg/g 2. Holocellulose increase in biomass from 64.7% to 79.61% 3. 79.3%lignin removal for 2% w/v NaOH in 90 min treatment. Holocellulose content increases to 76.7% with 70 mg/g reducing sugar yield in enzymatic sachharification.	**Kataria and Ghosh, (2014)**

Table 1.5 (continued…..)

Different alkaline pretreatment methods (NaOH, NaOH + 10% urea and aqueous ammonia) were optimized for maximum delignification. Solubilization of solid residue using H_2SO_4 60% (v/v), 10% biomass loading at 30°C for 4 h. Real hydrolysis of cellulose and hemi-cellulose with diluted slurry with acid concentration of 10% at 100 C for 1 h.	*Saccharum spontaneum*	Maximum delignification with alkaline treatment: 1. 47.8% from 7% NaOH, 48 h, and 10% biomass loading); 2. 51% from NaOH + urea (7% NaOH + 10% urea, 48 h and 10% biomass loading); 3. 48% from 30% ammonia (40 days and 10% biomass loading). Best result for reducing sugar yield with ammonia treated biomass: 0.58 g reducing sugar /g of initial biomass after acid hydrolysis. This accounts for nearly 85% of the total sugars present in the biomass.	**Chaudhury et al. (2012)**
Three different pretreatment approaches viz. dil. sulfuric acid (1.5% v/v at160°C), dil. sodium hydroxide (0.4% w/v or 0.1 N at 120°C), and aq. ammonia (15%) treatment at 50°C and 24 h followed by enzymatic hydrolysis (5-35 FPU/g of dry substrate)	*Saccharum spontaneum*	A max. sugar yield of 631.5 ± 3.25 mg/g with 89.38% hydrolytic efficiency (HE) after enzymatic hydrolysis of aq. ammonia pretreated biomass Fermentation results: Yields of 0.36 g/g from acid hydrolyzate, 0.384 g/g from enzymatic hydrolyzate of acid pretreated substrate, 0.391 g/g from enzymatic hydrolyzate of alkali pretreated substrate and 0.4 g/g from enzymatic hydrolyzate of aq. ammonia pretreated substrate.	**Chandel et al. (2011)**
NaOH/H_2O_2-pretreated water hyacinth 1.5% v/v H_2O_2 and 3% (w/v) NaOH at 25°C	*Eichhornia crassipes*	Reducing sugar yield of 223.53 mg/g dry biomass with reduced cellulose crystallinity	**Yan et al. (2015)**
Temperature range 160°−220°C, Hydrothermal pretreatment using ball-mill reactor followed by enzymatic hydrolysis Effects of CH3COOH and K2CO3 on the liquid composition were investigated experimentally.	*Eichhornia crassipes*	Glucose yield at 220°C in absence of CH_3COOH and K_2CO_3 = 0.267 Glucose yield at 200°C with 0.75 wt% CH_3COOH and 10% biomass = 0.855 Glucose yield at 220°C with 0.5 wt% K_2CO_3 = 0.195 Addition of K_2CO_3 did not suppress hydrolysis	**Phothisantikal et al. (2013)**

Table 1.5 (continued…..)

Type and summary of pretreatment	Biomass	Major observations and conclusions	Reference
Preliminary pretreatment with different acids (HCl/H_2SO_4, 2% v/v) and organic acids (acetic/ formic acid, 30% v/v) and autoclaving (121^{o}C, 15 lb) for 60 min and 10 g biomass Further optimization with H_2SO_4 concentration: 1-7% w/v; biomass loading 5-30% w/w, temperature 80^o, 100^o and 121^{o}C; incubation time 15-90 min. Enzymatic saccharification of biomass with commercial cellulase Zytex (30 FPU/g biomass) and surfactant	*Eichhornia crassipes*	Most optimum conditions for pretreatment: 4% w/v H_2SO_4 pretreatment at 10% w/w biomass loading at temperature of 121^{o}C for 75 min to produce 0.356 g/g reducing sugars. Optimum condition for hydrolysis of pretreated biomass: 12.5% w/w biomass loading, incubation period 24 h, surfactant concentration 0.1%, commercial cellulase concentration 70 FPU%	**Satyanaga-lakshmi et al. (2011)**

Table 1.6 Summary of literature on ultrasound assisted enzymatic hydrolysis with cellulase/cellobiase system

Type and summary of pretreatment	Enzyme	Major observation	Reference
Ultrasound assisted enzymatic hydrolysis of corn stover **Alkali hydrolysis parameters** Biomass = 10g, 5% (w/v) Sodium hydrate to water solution ratio = 1:12 Ultrasound frequency= 4 kHz, Power = 80W at 25^{o}C **Enzymatic hydrolysis** Biomass powder = 10 g in 500 ml reactor, pH = 5.5, Cellulase addition = 0.1 g Water bath temp = 55^{o}C, 20 kHz and 80 W, pulse rate = 1:2	Commercial cellulase	Ultrasound application is more suitable for biofuel production. Lignin removal enhance by 23.3% and saccharification rate reaches to 47.6% compared to conventional hydrolysis Cellulose rate loss= 7% Raw biomass decomposition rate= 24.1%	**Zhang et al. (2008)**
Parametric optimization of ultrasonic treatment of free and immobilized cellulase Cellulase 300 mg/ml in citric acid buffer (pH 4.8) **Free cellulase** Time variation: 5 - 30 min, Power variation: 5-40 W, Frequency variation: 18-29 kHz **Immobilized cellulase** Temperature variation: 30 - 80 ^{o}C, pH variation: 2-7, Frequency variation: 18-29 kHz, Power variation: 10-80 W	Commercial cellulase	Free cellulase activity increased by 18.17% over control with low intensity ultrasound at 15W, 24 kHz for 10 min. For immobilized cellulase activity increased by 24.67% over control at 60W, 24 kHz for 10 min. Fluorescence and circular dichroism reveal number of tryptophans increase on surface slightly, deformation of certain α-helix and random coil increase in cellulase.	**Wang et al. (2012)**
Effect of pre-sonication before hydrolysis and intermittent sonication throughout hydrolysis assessed. Organosolv-treated biomass of southern red oak and switch grass used for hydrolysis Sonication using 20 kHz, 1500 W in six pulses of 20 s each in 72 h treatment	Commercial cellulase	Intermittent sonication strategy showed a remarkable improvement(> 20%) in enzymatic hydrolysis for some specimens	**Shi et al. (2013)**
Ultrasound treated enzyme solution was added into the 0.5 M CMC in citrate buffer solution at pH 4.8 under temperature range 20-50^{o}C for 30 min. Ultrasound parameter:probetype sonicator 20 kHz &17.33 W/cm^{2}	Commercial cellulase	Enzyme activity increased by 25%. Significant reduction in thermodynamics parameters observed after ultrasonic irradiation. E_a, ΔH, ΔS and ΔG reduced by 64.7%, 68%, 37.3% and 1.3%, respectively.	**Subhedar and Gogate (2014)**

Table 1.6 (*continued……*)

Type and summary of pretreatment	Enzyme	Major observation	Reference
Conventional enzyme hydrolysis parameters Biomass loading = 5% (w/v), Enzyme loading = 0.14%(w/v), Temperature = 323 K, Treatment time = 72 h Ultrasound assisted enzyme hydrolysis Biomass loading = 3% (w/v), Enzyme loading = 0.8% w/v Sonication power = 60 W, Duty cycle = 70%, hydrolysis time = 6.5 h	Commercial cellulase	Reducing sugar yield in conventional and ultrasound assisted enzyme hydrolysis are 11.569 g/L and 27.6 g/L Approx. 2.4 fold enhancement in sugar yield as compared to conventional method	**Subhedar and Gogate (2014)**
Cellulase preparation range: concentration = 0.84 to 3.37 mg/mL, diluted 100 time to 1.68 mg/ml, reaction volume = 50 ml Temperature range=(10^{o}-30^{o}C) Ultrasound intensity = 6 W/mL. Treatment time = 0-160 s Frequency = 20kHz, maximum ultrasonic power 750W	Commercial cellulase	Decrease in enzyme activity for ultrasound intensity > 6 W/mL with spatial configuration of the cellulase molecule. Sonication time from 0 to 80 s increased the cellulase activity, with subsequent reduction for treatment up to 120 s and 160 s. No difference on protein content	**Le and TTT Nguyen (2013)**
Bioethanol synthesis using *Parthenium hysterophorus*. Enzymatic hydrolysis of pretreated and delignified biomass. Ultrasound bath 35 W, 35 kHz, 10% duty cycle Total reducing sugar release profile fitted to HCH-1 model of enzymatic hydrolysis.	Cellulase + β-glucosidase	K_m decreased by approx. 43%, V_{max} increased by approx.21.7%; sugar yield increased by approx.20%	**Singh *et. al* (2015)**
Evaluation of effects of ultrasound on enzymatic hydrolysis of sugarcane bagasse to obtain fermentable sugars. Evaluation of influences of temperature, enzyme concentration and moisture content 132 W, 40 kHz, 240 min treatment. The ultrasonic transducer surface area = 282.2 cm^2. Ultrasonic intensity of 0.46 W cm^2	Commercial cellulase complex	Highest amount of fermentable sugars with ultrasound: 0.26 g/g dry sugarcane bagasse at 50 °C, 10% mass of enzyme and a moisture content of 75% (dry basis), 240 min treatment 2-fold enhancement in sugar yield with ultrasound	**Lunelli *et al*. (2014)**

Table 1.7 Summary of Literature on ethanol production by enzymatic hydrolysis and fermentation using various lignocellulosic biomass

Lignocellulosic Biomass	Microorganism	Enzyme	Mode of fermentation	Ethanol Yield			Reference
				g/L	g/g	g/L/h	
Cynara Cardunculus	*S. cerevisiae*	cellulase complex from Celluclast	SHF	11.5	0.10	0.48	**Fernandes et al., 2018**
			SSF	12.2	0.10	0.51	
Cistus ladanifer	*S. cerevisiae*	cellulase complex from Celluclast	SHF	4.7	0.04	0.20	**Fernandes et al., 2018**
			SSF	5.2	0.07	0.22	
Pretreated rice straw	*S. cerevisiae* NCIM 3215	Cocktail of cellulase with CMCase, FPase & β glucosidase	SSF	25.2	0.38	1.05	**Akhtar et al., 2017**
Non-detoxified lignocellulosic hydrolysates	*Scheffersomyces shehatae* strain TTC79	NA	NA	29.4	ND	ND	**Senatham et al., 2016**
Pretreated rice straw	*Clavispora* NRRL Y-50464	commercial Cellic Ctec2 cellulase	SHF	36.7	ND	ND	**Kumar et al., 2016**
Whole slurry of pretreated rice straw	*S. cerevisiae*	commercial cellulase	SSF	12.4	ND	ND	**Jung et al., 2015**
Mild alkali- and dilute acid-pretreated rice straw	*Clavispora* sp. (NRRL Y-50464)	N.A	SSF	25.7	0.26	0.71	**Chapla et al., 2015**
Microwave-assisted $FeCl_3$ pretreated rice straw	*S. cerevisiae* and *Pichia stipites*	commercial cellulase	SSF	5.5	0.38	0.11	**Lu and Zhou., 2015**
Pretreated *Parthenium hysterophorus*	*S. cerevisiae* MTCC 170	(CMCase) *B. amyloliquefaciens* SS35 Commercial β-glucosidase	SSF	5.5	0.85	0.21	**Singh et al., 2015**
Timothy grass (*Phleum pretense*)	*Saccharomyces cerevisiae ATCC 96581*	Cellulase, β-glucosidase and xylanase	SHF	ND	0.39	ND	**Nanda et al., 2014**
Sugarcane Bagasse	*Recombinant Trichoderma reesei*	N.A.	CBP	ND	0.10	ND	**Huang et al., 2014**
Pinewood (*Pinus banksiana*)	*Saccharomyces cerevisiae ATCC 96581*	Cellulase, β-glucosidase and xylanase	SHF	ND	0.35	ND	**Nanda et al., 2014**
Phosphoric acid swollen cellulose	*Recombinant S. cerevisiae*	N.A.	CBP	ND	0.19	ND	**Yamada et al., 2013**
Corn cob slurry and molasses	*Recombinant strains S. cerevisiae*	N.A	SSCF	ND	0.46	ND	**Koppram et al., 2013**

Abbreviation: CBP= Consolidated bioprocessing, SHF= Separate hydrolysis and fermentation, SSF= Simultaneous saccharification and fermentation, SSCF= Simultaneous saccharification and co-fermentation, ND- Not determined

1.10 Butanol as a potential biofuel

Biofuel is a carbon neutral fuel derived from biomass and is generally considered as fuel additive rather than a substitute **(Davis and Morton, 2008)**. 1-Butanol (butyl alcohol or n-butanol) is a four carbon straight chain alcohol with a molecular formula C_4H_9OH (MW = 74.12 g/mol) and boiling point of 118ºC. Butanol is the fermentation product of bacteria belonging to the group *Clostridia*. It has the potential to be a direct gasoline substitute due to its similar properties in energy density and octane number as shown in the **Table 1.8 (Jang et al., 2012).** The comparison of fuel properties of n-butanol with other fuels is shown in **Table 1.9**. As a new-generation biofuel, butanol has gained an edge over ethanol in having higher octane value (1.5 times than ethanol). In addition, it is also less corrosive, has low water-solubility (9 ml/100 ml) and volatility. It is therefore does not require advanced distillation and drying for water removal (**Durre, 2007, Lee et al., 2008a; Nigam and Singh, 2011)**. Butanol can be easily blended with gasoline and diesel for use in automobile engines and with the current transportation pipeline without modification **(Durre, 2007; Lee et al., 2008b). Swana et al. (2011)** made a life cycle assessment (LCA) of these biofuels and found that the net energy returns from biobutanol (6.53 MJ/L) were higher than ethanol (0.4 MJ/L). All these features favor biobutanol as the second generation biofuel of choice.

Table 1.8: Comparative fuel properties of n-butanol with other fuels. Adopted **(Jang et al., 2012)**

Fuel properties	n-Butanol	Ethanol	Methanol	Gasoline
Energy density	29.2	19.6	16	32
Heat of vapourization (MJ/kg)	0.43	0.92	1.2	0.36
Research octane number	96	0.92	1.2	91-99
Motor Octane number	78	89	92	81-89
Air to fuel ratio	11.2	9.0	16	32
Specific energy (MJ/kg air)	3.2	3.0	3.1	2.9

1.10.1 Butanol production from lignocellulosic biomass

Lignocellulosic feedstock is the most widely available source of biomass which remains largely unutilized as feedstock for biofuel production. Nearly 90% of globally produced plant biomass constitutes lignocelluloses. This amounts to about 200×10^9 tons per year, of which about $8–20\times10^9$ tons can be effectively utilized for biofuel production. The supply of feedstock however, is plagued with season based sporadic availability, scattered processing stations, and high logistic cost **(Polman, 1994).** Efforts are being made to economize process efficiency, cut on logistic cost by drying and pulverizing the biomass at the spot with insitu production and searching lignocellulolytic and fermenting microbes.

Production cost of butanol mainly depends on substrate selection which in turns regulates the overall economy of ABE fermentation industry (approx. 30~32% on feedstock, **Qureshi and Blaschek, 2000).** The current market price of butanol ($ 1.09 per kg), which can be brought down by at least 40-50% through the use of alternative cheap substrates. In this prospect, a secure supply of multiple feedstocks by scaling both second and third generation biomass can be highly convenient as well as beneficial, since those feedstock does not have direct outlet with respect to the first generation feedstock which competes for food vs fuel economy for biofuel industry. Decentralized production of biofuels utilizing local resources will cut down the logistic cost. In lignocellulosic biomass, the cellulose fibers are surrounded by a hemicellulose bounded by a strong lignin barrier. While the lignin component of lignocellulosic biomass cannot be utilized by the solventogenic *Clostridia*, yet cellulose and hemicellulose can be transformed into fermentable sugars, which can be further metabolized to produce butanol. Thus, a pretreatment process is essential to produce fermentable sugars such as glucose, xylose, and galactose, by enhancing the enzyme accessibility through depolymerization of lignin

barrier. In addition to fermentable sugars, the pretreatment process could also produce fermentation inhibitors such as 5-hydroxymethylfurfural (HMF), furfural, and acetic, ferulic, glucuronic, and phenolic compounds. These microbial inhibitors reduce butanol production requiring detoxification thereof. The fermentable sugars produced from pretreatment and successive enzymatic hydrolysis process are metabolized by *Clostridium spp* during acetone−butanol−ethanol (ABE) fermentation. Clostridium spp can metabolize both hexose (C6) and pentose (C5) sugars efficiently in ABE fermentation. Current n-butanol yield from fermentable sugars is between 15 and 25 wt%. Contamination and failure to switch from acidogenic to solventogenic phase are severe problems in ABE fermentation as these lead to overall halt and complete loss of a fermentation batch. The maximum ABE concentration of 26.27 g/L with a yield of 0.44 g/g and a productivity of 0.31g/L/h has been achieved in batch fermentation of sulfuric acid pretreated corn stover using *C. beijerinckii* P260 **(Baral and Shah., 2016).**

1.10.2 ABE Fermentation: past and current perspectives

Currently commercial butanol is being produced exclusively from petrochemical routes, although its production via microbial fermentation is known for more than a century. The butanol production through microbial intervention was first reported by Louis Pasteur in 1861. Later, in the 20thcentury, the concept was industrialized using *Clostridium acetobutylicum* isolated by Chaim Weizmann. It contributed 66% of butanol consumed worldwide **(Durre, 2008)**. However, during the advent of second World War the petroleum industry got a boost leading to progressive reduction in biobutanol production This was further escalated by the availability of cheap butanol from petrochemical industry coupled with increasing cost of carbohydrate feed substrates and low sugar content of molasses (main substrate at that time), have resulted in the complete

eradication of this industrial activity. However, the oil prices started climbing up since the beginning of 1970s because of ever depleting oil reserves and galloping demand. This along with the emerging environmental awareness led to the revival of interest in biofuel industry **(Durre, 2008)**. Research workers started exploiting *clostridia* to improve solvent yields, enhance volumetric productivity and final product concentration. These are focused on development and of microbes, cataloguing their growth requirement and standardizing fermentation conditions **(Desai, 1999; Nolling, 2001; Scotcher and Bennett, 2005; Papoutsakis, 2008).** Upgrading of this technology that includes upstream processing, media optimization and development of integrated low energy separation–extraction–purification techniques (downstream processing) has also been extensively studied **(Ezeji et al., 2004b; Ezeji et al., 2007a; Lee, 2008a).**

1.10.3 ABE fermentation process

Acetone Butanol Ethanol (ABE) fermentation has several limitations in terms of economic competitiveness over pure chemical processes. The major disadvantage is the complex metabolic pathway that regulates butanol production by these bacteria (Figure 1). In typical ABE fermentation, butyric, propionic and acetic acids are initially produced by *C. acetobutylicum*, which then undergoes a metabolic shift. Solvents (butanol, acetone, and ethanol) are formed in the ratio of 6:3:1 from sugars and starch when the stationary phase is reached (Solventogenesis) **(Fond, 1985; Mitchell,1998)**. This shift induction is controlled either by the decrease in pH (< 5) at the end of the exponential phase and increase of butyric acid concentration (> 2 g/L) **(Gottwald and Gottschalk, 1985; Monot, 1984)**. In conventional ABE fermentation, the butanol yield from glucose is low, typically at ~15% (w/w) and rarely exceeds 25% (0.77–1.3 gallons per bushel corn, as example). The production of butanol is also limited by severe product inhibition.

Typically, butanol at a concentration of 10 g/L can significantly inhibit cell growth and fermentation (although the inhibition concentration may vary from culture to culture). Consequently, butanol titers in conventional ABE fermentations are usually lower than 13 g/L. This process still forms the commonly adopted protocols for biological butanol production process. The low butanol yield and butanol concentration with low cell densities made butanol production from glucose by ABE fermentation uneconomical **(Maddox, 1989)**. Thus, to make them industrially viable we have to improve each and every step of butanol production. A summary of ABE fermentation using different lignocellulosic feedstock is mentioned in **Table 1.9.**

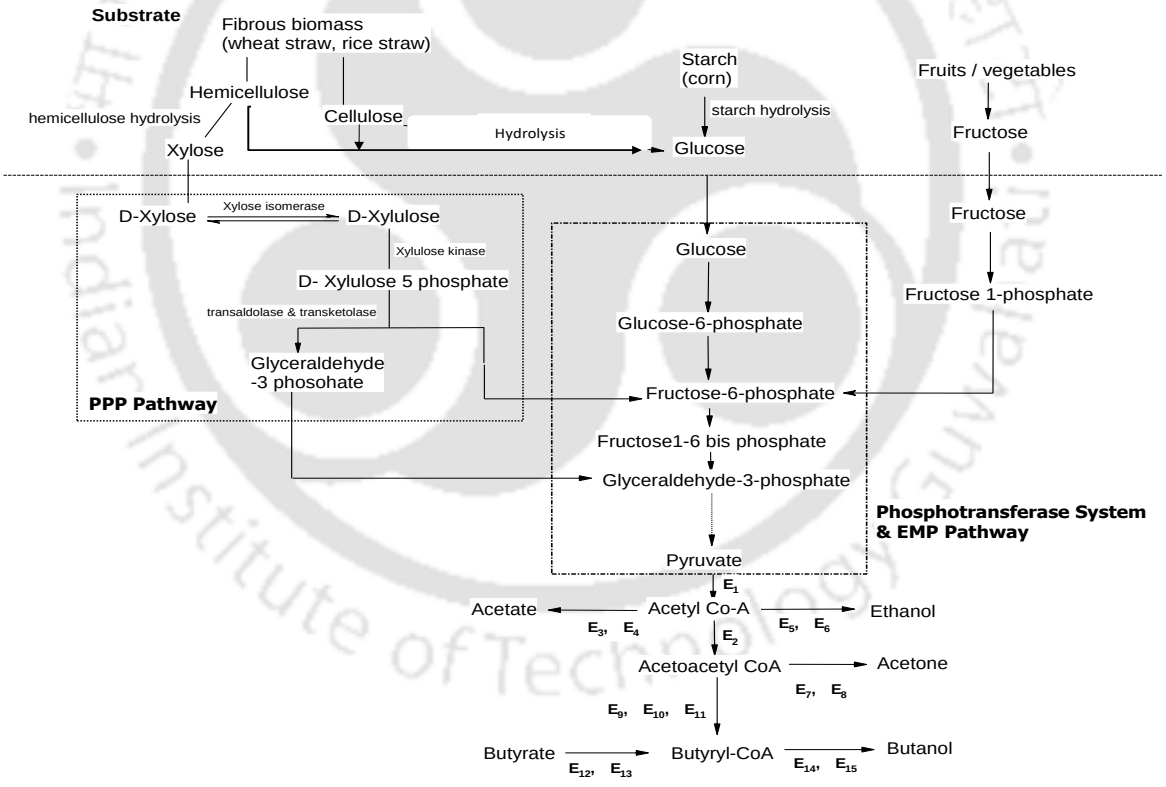

Figure 1: ABE fermentation pathway by *Clostridia* (adopted from Ranjan *et al*., 2013)
Abbreviations: E_1– pyruvate ferrodoxin oxidoreductase; E_2– thiolase; E_3– phosphate acetyltransferase; E_4– acetate kinase; E_5– acetaldehyde dehydrogenase; E_6– ethanol dehydrogenase; E_7– CoA transferase; E_8– acetoacetate decarboxylase; E_9– 3-hydroxybutyryl-CoA dehydrogenase; E_{10}– crotonase; E_{11}– butyryl CoA dehydrogenase; E_{12}– phosphate butyryl transferase; E_{13}– butyrate kinase; E_{14}– butyraldehyde dehydrogenase; E_{15}– butanol dehydrogenase

Table 1.9 Summary of ABE production protocols using different lignocellulosic feedstocks

Feedstock	Pretreatment and hydrolysis	Strain	ABE yield	Reference
Composite feedstock	Dilute acid + enzyme	*C. acetobutylicum (Mechanical shaking)*	ABE titer 9.61 (g/L) (MS) ABE yield 0.17 (g/g) (MS) ABE Productivity 0.08 (MS) g L^{-1} h^{-1}	Present study
Composite feedstock	Dilute acid + enzyme	*C. acetobutylicum (Ultrasound)*	ABE titer 16.5 (g/L) (US) ABE yield0.28 (g/g) (US) ABE Productivity 0.18 (MS) g L^{-1} h^{-1}	Present study
Volatile fatty acid	Two-stage fermentation	*C. beijerinckii* NCIMB 8052	Butanol 13.8 g/L Hydrogen 5897 mL/L	Li *et. al* 2018
Sugarcane bagasse	hydrothermal pretreatment (121°C for 15 min)	*Clostridium sporogenes*	Butanol 0.173 g/g	Sivanarutselvi *et.al* 2017
Brewery liquid waste (BLW) and brewery spent grain (BSG).	Two-phase partitioning detoxification	*C. acetobutylicum* NRRL B-582 *C. beijerinckii* NRRL B-466	Butanol yield 8.0 g/L and 7.2 g/L	Maiti *et.al* 2017
Corn stover / Glucose	Enzymatic hydrolysis with VSVP process	*C. beijerinckii CC101*	ABE titer 306.6-356.1 g/L Butanol 212.0–232.0 g/L	Xue *et. al* 2016
Rice Straw	Dilute Sulphuric acid treatment with stress.	C. *acetobutylicum* NCIM 2337	ABE yield 0.58 g/g Butanol yield 0.34 g/g	Ranjan *et.al* 2013
Wheat bran	Dilute acid	*C. beijerinckii* ATCC 55025	ABE titer 11.8 (g/L) ABE yield 0.32 (g/g) ABE Productivity 0.16 gL^{-1} h^{-1}	Liu *et. al.*, 2010
Barley Straw	Dilute acid	*C.beijerinckii* P260	ABE titer 26.6 (g/L) ABE yield 0.43 (g/g) ABE Productivity 0.39 gL^{-1} h^{-1}	Qureshi *et.al* 2014
Corn Stover	Dilute acid	*C. beijerinckii* P260	ABE titer 26.3 (g/L) ABE yield 0.44 (g/g) ABE Productivity 0.31 gL^{-1} h^{-1}	Qureshi *et.al* 2014
Switch grass	Dilute acid	*C. beijerinckii* P260	ABE titer 14.6 (g/L) ABE yield 0.39 (g/g) ABE Productivity 0.17 gL^{-1} h^{-1}	Qureshi *et.al* 2014
Corn fibre	Dilute acid + enzyme	*C. beijerinckii* BA101	ABE titer 9.3 (g/L) ABE yield 0.39 (g/g) ABE Productivity 0.10 gL^{-1} h^{-1}	Qureshi *et. al* 2008a
Wheat straw	Alkaline peroxide + enzymes	*C. beijerinckii* P260	ABE titer 22.2 (g/L) ABE yield 0.41 (g/g) ABE Productivity 0.55 gL^{-1} h^{-1}	Qureshi *et al.*, 2008b
Liquid corn Starch	*None*	*C. beijerinckii* BA101	ABE titer 18.4 (g/L) ABE yield 0.41 (g/g) ABE Productivity 0.15 gL^{-1} h^{-1}	Ezeji *et al.*, 2007c

1.10.4 Microbes role in ABE fermentation

Micro-organisms are implicated in the production of variety of bakery, brewery and dairy products etc. They are also being recognized as savior's of environment degradation, energy crises and to bring sustainability in agricultural production. The economy of biofuel industry largely depends upon microbial culture and an efficient process. Low butanol titre and product inhibition of microbial growth are the major limitations for commercialization. Use of a consortia of cellulolytic and solventogenic microbes appears to be a feasible approach for ABE fermentation as it enables synergistic utilization of the metabolic pathways of two organisms. Fed batch fermentation with continuous feeding and product recovery or consolidated bio-processing hold promise for near future.

1.10.5. Commercialization of butanol production

1-Butanol is an important chemical ingredient for paints, polymers and plastics. The global market for 1-butanol between 2015-2020 is estimated to touch a CAGR of 5.1% and generate a global market size worth USD 9.9 billion. Asia-Pacific region dominated the global n-butanol market and consumed around 51.3% in 2014.

Rapidly growing end-user industry demand for industrial and architectural products in this region are driving the growth of n-butanol market. In general, solvent titer of about 20 g/L from 55 to 60 g/L of substrate giving solvent yields of around 0.35 g/g sugar is commercially obtained with typical butanol: solvent molar ratio = 0.6, and A:B:E production ratio of 3:6:1 **(Jones & Keis, 1995)**. Butanol is the preferred solvent, since it attracts the highest price in the chemical market. China leads in commercialization of the ABE fermentation process. Over $200 million have recently been invested in China to install 0.21 million TPA of solvent capacity with plans to raise it to one million TPA. There are six major plants that produce about 30000 tonnes butanol per annum from corn

starch. Most plants operate in a semi-continuous fashion, each fermentation lasting up to 21 days. The plant typically houses a chain of up to eight fermentation tanks (300–400 m^3 each) connected together in series. Fresh feedstock, together with periodic additions of seed culture, cascades through the fermenters in a process that provides sufficient retention time for re-assimilation of acids to solvents. Conventional distillation is then used to recover acetone, butanol and ethanol. Most plants are located next to ethanol plants to reduce utility and operating costs. Various challenges associated with ABE fermentation and its solution that will lead to commercialization is shown in Table 1.10. Co-located operations tend to share effluent treatment facilities based on anaerobic digestion (AD). Biogas, produced from the AD process is used to generate heat and power. Although not widely practiced, additional value can be gained from the recovery of hydrogen from the fermentation exhaust gas (typically $1/10^{th}$ of mass of butanol produced). A relatively new plant has been built in Brazil and operated by HC Sucroquimica. This plant produces 8000 TPA solvent from sugarcane juice and is located next to an ethanol distillery and sugar-mill.

1.10.6 Process design in ABE fermentation

In the past 20 years, there have been numerous engineering attempts to improve butanol production in ABE fermentation including: batch culture **(Ishizaki, 1999)**, fed-batch culture **(Yang and Tsao, 1995; Ezeji et al., 2004b**) integrated with a process of butanol removal and continuous culture (**Mutschlechner et al., 2000**) and cell recycle cell immobilization to increase cell density and reactor productivity coupled with extractive fermentation to minimize product inhibition (**Maddox, 1995; Mollah and Stuckey, 1993; Park et al., 1989; Qureshi and Blaschek, 2000; Qureshi and Maddox, 1995; Yang and Tsao, 1995**). The *in-situ* or real time observation, determination and

characterization in biomass pretreatment or reaction system with the help of ultrasound is another avenue of research.

Table 1.10 The challenges and solutions for ABE fermentation (Adopted **Green EM et al., 2011**)

Challenges	**Solutions**
High feedstock cost significantly increases operating cost	Transition towards cheaper (and more sustainable) feedstocks such as wastes and agricultural residues.
Low butanol titres increase recovery costs: Low titres also reduce sugar loadings and increase water usage	Develop improved microbes with improved solvent titers and/or develop methods for insitu product removal to alleviate end product tolerance.
Low butanol yield increases feedstock costs.	Develop improved microbes with higher butanol yields and/or develop microbes with higher butanol: solvent ratios.
Low volumetric solvent productivities increase capital and operating costs.	Develop continuous fermentation processes that reduce down time and increase volumetric productivity.
Solvent recovery using conventional distillation is energy Intensive and relatively expensive.	Develop low energy methods for solvent recovery and purification.
High water usage is not sustainable and increases the cost of effluent treatment.	Recycle process water back through the fermentation.

1.10.7 Sensitivity analysis of butanol production through ABE fermentation

The cost of butanol production increases by 7% when the recovery decreases from 95 to 90%. Sugar utilization is also another input parameter which is inversely proportional to butanol production. Decrease in solid to liquid ratio leads to increase in the number of reactors and heat exchangers, since high volume of water is needed to be handled. The challenges and possible solutions in ABE fermentation are listed in **Table 1.10**. Feedstock cost, severity factor and heat recovery were found to be the most crucial.

1. Feedstock cost directly regulates to butanol cost
2. Heat recovery is inversely proportional to butanol production cost

3. Severity factor is a function of temperature and time which impacts sugar conversion during pretreatment and enzymatic hydrolysis. Heating and cooling processes also impact the butanol production cost.

1.11 Comparison of process economics of ethanol and butanol

In comparison to cellulosic ethanol fermentation, butanol fermentation has still been limited to only glucose utilization. For better comparison, a mixed sugar fermentation slurry with negligible toxic inhibitor is expected in addition to single product formation will foster simpler separation scheme which will ultimately add value to the process economics of butanol production. Purification of n-butanol, ethanol, acetone and H_2 needs more than six major operation units. Approximately, 90% of the water is removed from the first distillation (dehydration) column for butanol purification. Acetone, ethanol and methanol from residual water are further separated and purified from downstream distillation column combined with a decanter and molecular sieve unit to give high grade ethanol. Extractive distillation can be used to break the butanol and water azeotrope. But this makes the process complex and the conversion process less economic. Earlier attempts also explored the advantage of vapor-liquid equilibrium phase behavior between butanol and water **(Tao and Aden., 2009)** by applying a decanter to break the binary azeotrope between butanol and water. To maximize the liquid-liquid separation in the decanter, temperature serves as the primary control mechanism. Number of unit operations of ethanol and butanol purification from fermentation broth are shown in **Table 1.11**.

Table 1.11. Number of unit operations of ethanol and n-butanol purification from fermentation broth**.**

Units Operation	Ethanol	Butanol
Distillation column	2	4
Molecular sieve (adsorption unit)	1	1
Decanter	-	1

1.12 Acceleration of the bioprocess by ultrasound treatment

Ultrasound treatment of the feedstock significantly improves the performance of biomass pretreatment, enzymatic hydrolysis of pretreated biomass and fermentation of the hydrolysate. Improvement of pretreatment and biochemical processes has been reviewed in sections 1.5.1 and 1.5.2. In this section we will discuss the effect of ultrasound on fermentation activity of microbes. **Table 1.12** summarizes few of the significant investigations on the fermentation process.

1.13 Biorefinery approach

Biorefinery unit forms an integral part of the production of materials, chemicals, transportation fuels, energy and heat from biomass (analogous to today's petroleum refineries). Existing biorefinery has two platforms concept namely sugar platform and syn gas platform. The economy of a biofuel industry depends on low cost of substrate but also on more efficient (in terms of total production and selectivity) microbial culture and a simple protocol. In addition, cost of byproducts generated during the process also contribute significantly to lowering of the cost of butanol.

Table 1.12 Summary of ultrasound enhanced fermentation process

Substrate/ Feedstock	Bioprocess	Microorganism	Ultrasound conditions	Observations	Reference
Chili post-harvest residue	SHF	*Saccharomyces cerevisiae*	NA Time (15-20 min)	increase ethanol by 11.15% to that Control. inhibitors were absent there is no need for detoxification of the hydrolysate	**Sindhu et al., 2017**
Parthenium hysterophorus	SSF	*S. cerevisiae MTCC 170*	Frequency = 35 kHz, 10% duty cycle, power = 35 W Intensity = 1.48 W/cm^2, Amplitude = 150 kPa (water medium).	Enhanced cellulose hydrolysis, enhanced trans-membrane transport of substrate and products as well as Toxic substances diluted (due to micro-convection)	**Singh et al., 2015**
Parthenium hysterophorus	SHF	*S. cerevisiae MTCC 170*	Frequency = 35 kHz (10% duty cycle) Power input = 35 W Intensity = 1.48 W/cm^2 Amplitude = 150 kPa (for water medium)	~2x enhanced productivity of ethanol and cell mass Reduced the time to 10 h with an increased ethanol concentration of 12.14 ± 0.6 g/L against 5.26 ± 0.3 g/L was achieved after 18 h	**Singh et al., 2014**
Oil pam fronds	SHF	*S. cerevisiae*	200 W, 37 kHz, 5 h	Ethanol yield was increased by 43%	**Ofori-Boateng and Lee, 2014**
Lignocellulosic fibers of Areca nut husk, moj, and bon bogori.	SSF	*Saccharomyces cerevisae/ cellulase enzyme*	Frequency = 30 kHz, The amplitude 100%., Temperature = 35 ±2°C Intensity = 100 W	Removal of 68% (bon bogori), 65% (Areca nut husk), and 64% (moj) lignin, good recovery of total solid and fermentable sugars yield of ethanol range 0.32 to 0.43 g/g	**Sasmal et al., 2012**
Lactose	SHF	*Kluyveromyces marxianus*	11.8 W/cm^2, 20% duty cycle	Ethanol concentration increased by 3.5 fold	**Sulaiman et al., 2011**
Waste paper	SSF	*Klebsialla oxytoca*	150 W, 15 min exposure/ 240 min cycle	Ethanol production increased by 20%	**Wood et al., 1997**

Abbreviation: SSF= Simultaneous saccharification and fermentation , SHF = Separate hydrolysis and fermentation

1.14 Scope of the present study and specific objectives

The present exercise was aimed at designing a suitable protocol for utilizing multiple invasive weeds as a feedstock for synthesis of bio-alcohol (viz. bioethanol and biobutanol) and increasing its yield with application of ultrasound. Depending upon the type and quantity of the available biomass in different parts of the year, the biofuel industry is required to modify the pretreatment of single or concoction of feedstock. Standardizing optimum pretreatment condition is an uphill task. For achieving maximum efficiency acid/alkali concentration and conditions of autoclaving may have varying effect on different biomasses. In addition, the processing equipment designed for pretreatment of one biomass may not be suitable for another biomass This makes it difficult for a processing unit to frequently change the pretreatment protocols or shit to a new fermenter. It is therefore necessary to first ascertain the alteration in the quality of the hydrolyzates in terms of composition of pentose and hexose sugars with changing feedstock. Earlier reports have been on optimization of pretreatment and fermentation of only few of the invasive weeds. In this study, pretreatment of eight invasive weeds namely *Arundo donax, Chromolena odorata, Eichhornia crassipes, Ipomea carnea, Lantana camara, Mikania micrantha, Parthenium hysterophorus and Saccharum spontaneum* has been carried out under optimized conditions determined for *Parthenium hysterophorus*. The optimum pretreatment conditions for the eight invasive weeds markedly differed from those for *Parthenium hysterophorus*. The major contemplation underlying approach of pretreating the invasive weeds listed above at conditions optimized for *Parthenium hysterophorus* is to assess the output of a bioprocess with feedstock flexibility. In this study, the variations in pretreatment of the eight invasive weeds at conditions optimized for the weed of *Parthenium hysterophorus* were analyzed. The ideal biomass mixture feedstock was determined with the help of statistical mixture design. The hydrolyzates obtained from the composite feedstock were used for ethanol fermentation using

separate hydrolysate fermentation modes and ABE fermentation by separate hydrolysis co-fermentation mode. For acceleration of various processes for alcoholic biofuels production, ultrasound irradiation was introduced in every step comprising acid/alkali pretreatment and enzymatic hydrolysis followed by fermentation. Experimental data obtained by both conventional (mechanical agitation) and ultrasound assisted experiments were coupled to a mathematical model. Cell viability and integrity of the enzyme structure has been studied with the help of flow cytometry, circular dichroism and fluorescence microscope.

The scope and specific objectives of this thesis can be summarized as:

1. Suitability assessment of various invasive weeds as multiple feedstock for biofuel production
2. Comparative study of ultrasound induced enhancement of enzymatic hydrolysis of invasive biomass species with mechanistic model
3. Dilute acid hydrolysis of various invasive weeds and its kinetic modeling, and devising composite feedstock of 8 invasive weeds using statistical mixture design
4. Ultrasound-assisted ethanol production via separate hydrolysis and fermentation routes using hydrolyzates obtained from pretreatment of composite feedstock of invasive weeds.
5. Ultrasound-assisted ABE fermentation using mixed hydrolyzates (pentose + hexose) obtained from pretreatment of composite feedstock of invasive weeds.
6. Mathematical modeling of the enzymatic hydrolysis and ethanol/ABE fermentation to gain physical insight into the process.

References

Abdi, B., 2018. India to announce new biofuel policy soon to realize Rs. 1 lakh crore investment. Economic Times Energy world, (https://energy.economictimes.indiatimes.com/news/oil-and-gas/india-to-announce-new-biofuel-policy-soon-to-realize-rs-1-lakh-crore-investment/63202527) [accessed March7, 2018]

Akhtar, N., Goyal, D., Goyal, A., 2017. Characterization of microwave-alkali-acid pre-treated rice straw for optimization of ethanol production via simultaneous saccharification and fermentation (SSF). Energy Conversion and Management, 141, 133–144.

Alvira, P., Tomas-Pejo, M., Ballesteros, M., Negro, M.J., 2010. Pretreatment technologies for an efficient bioethanol production process based on enzymatic hydrolysis: A review. Bioresource Technology, 101, 4851-4861.

Anderson, W.F., Dein, B.S., Brandon, S.K., Peterson, J.D., 2008. Assessment of Bermuda grass and Bunch grasses as feedstock for conversion to ethanol. Applied Biochemistry and Biotechnology, 145, 13-21.

Avery, J., 2013. Tackling invasive alien species in Europe. Briefing of European Parliamentary Research Service. European Union.

Baral, N.R., Shah, A., 2016. Techno-Economic Analysis of Cellulosic Butanol Production from corn stover through acetone-butanol-ethanol fermentation. Energy Fuels, 30(7), 5779-5790.

Bharadwaja, S.T.P., Singh, S., Moholkar. V.S., 2015. Design and optimization of a sono-hybrid process for bioethanol production from *Parthenium hysterophorus.* Journal of the Taiwan Institute of Chemical Engineers, 51, 71-78.

Boateng, C.O., Lee, K.T., 2014. Ultrasonic-assisted simultaneous saccharification and fermentation of pretreated oil palm fronds for sustainable bioethanol production. Fuel, 119, 285–291.

Bussemaker, M.J., and Zhang, D., 2013. Effect of ultrasound on lignocellulosic biomass as a pretreatment for biorefinery and biofuel applications. Industrial and Engineering Chemistry Resarch, 52, 3563−3580.

Chandel, A.K., Singh, O.V., Rao, L.V., Chandrasekhar, G., Narasu, M.L., 2011. Bioconversion of novel substrate *Saccharum spontaneum*, a weedy material, into ethanol by *Pichia Stipitis* NCIM3498. Bioresource Technology, 102, 1709-1714.

Chapla, D., Parikh, B.S., Liu, L.Z., Cotta, M.A., Kumar, A.K., 2015. Enhanced cellulosic ethanol production from mild-alkali pretreated rice straw in SSF using Clavispora NRRL Y-50464. Journal of Biobased Materials and Bioenergy, 9, 381–8.

Chaudhury, G., Singh, L.K., Ghosh, S., 2012. Alkaline pretreatment methods followed by acid hydrolysis of *Saccharum spontaneum* for bioethanol production. Bioresource technology, 124, 111-118.

Clavero, M., García-Berthou, E., 2005. Invasive species are a leading cause of animal extinctions. Trends in Ecology and Evolution, 20, 110.

CBD, Convention for Biological Diversity (2006), https://www.cbd.int/ibd/2006/default.shtml/.

Davis, S.E., Morton, S.A., 2008. Investigation of ionic liquids for the separation of butanol and water. Separation Science and Technology, 43, 2460-2472.

Deka, J., Barua, I.C., 2015. Problem weeds and their management in the North-East Himalayas. Indian Journal of Weed Science, 47(3), 296–305.

Desai, R.P., 1999. Metabolic flux analysis elucidates the importance of the acid formation pathways in regulating solvent production by *Clostridium acetobutylicum*.

Metabolic Engineering, 1, 206-213.

Durre, P., 2008. Fermentative butanol production – Bulk chemical and biofuel. Annals of the New York Academy of Sciences, 1125, 353-362.

Durre, P., 2007. Biobutanol: an attractive biofuel. Biotechnology Journal, 2, 1525-1534.

Ezeji, T.C., Qureshi, N., Blascheck, H.D., 2004b. Acetone butanol ethanol (ABE) Production from concentrated Substrate: reduction in substrate inhibition by fed-batch technique and product inhibition by gas stripping. Applied Microbiology and Biotechnology, 63, 653-658.

Ezeji, T.C., Qureshi, N., Blascheck, H.D., 2007a. Production of Acetone-butanol-ethanol (ABE) in a continuous flow bioreactor using degermed corn and *Clostridium beijerinckii*. Proceedings, 123, 653-63.

Ezeji, T.C., Qureshi, N., Blascheck, H.D. 2004a. Butanol Fermentation Research: Upstream and Downstream Manipulations. The Chemical Record, 4, 305-314.

Fond, O., 1985. The role of acids on the production of acetone and butanol by *Clostridium acetobutylicum*. Applied Microbiology and Biotechnology, 22, 195-200.

Fernandes, M.C., Ferro, M.D., Paulino, A.F.C., Chaves, H.T., Evtuguin, D.V., Xavier, A.M.R.B., 2018. Comparative study on hydrolysis and bioethanol production from cardoon and rockrose pretreated by dilute acid hydrolysis, Industrial Crops & Products, 111, 633–641.

Gottwald, M., Gottschalk, G., 1985. The internal pH of *Clostridium acetobutylicum* and its effect on the shift from acid to solvent formation. Archives of Microbiology, 143, 42-46.

Green, E.M., 2011. Fermentative production of butanol—the industrial perspective. Current Opinion in Biotechnology, 22, 1–7.

Gupta, R., Khasa, Y.P., Kuhad, R.C., 2011. Evaluation of pretreatment methods in improving the enzymatic saccharification of cellulosic materials. Carbohydrate Polymers, 84, 1103-1109.

Holm, L., Plucknett, D., Pancho, J., Herberger. J., 1977. The World's Worst Weeds. University of Hawaii Press, Honolulu, HI. 609.

Huang, J., Chen, D., Wei, Y., Wang, Q., Li, Z., Chen, Y., Huang, R., 2014. Direct ethanol production from lignocellulosic sugars and sugarcane bagasse by a recombinant *Trichoderma reesei* strain HJ48. The Scientific World Journal, Article ID 798683, 8.

Jang, Y.S., Malaviya, A., Cho, C., Lee, J., Lee, S.Y., 2012. Butanol production from renewable biomass by *Clostridia*. Bioresource Technology, 123, 653-63.

Jones, D.T., Keis, S., 1995. Origins and relationships of industrial solvent producing clostridial strains. FEMS Microbiology Reviews, 17, 223-232.

Jonsson, L.J., Alriksson, B., Nilvebrant, N.O., 2013. Bioconversion of lignocellulose: inhibitors and detoxification. Biotechnology for Biofuels, 6, 16.

Jonsson, L.J., Palmqvist, E., Nilverant, N.O., Hahn-Hageral, B., 1998. Detoxification of wood hydrolysate with laccase and peroxidase from the white rot fungus *Trametes versicolor*. Applied Microbiology and Biotechnology, 49, 691-697.

Jung,Y.H., Park, H.M., Kim, D.H., Park, Y.C., Seo, J.H., Kim, K.H., 2015. Combination of high solids loading pretreatment and ethanol fermentation of whole slurry of pretreated rice straw to obtain high ethanol titers and yields. Bioresource Technology, 198, 861–866.

Kataria, R., Ghosh, S., 2014. NaOH Pretreatment and enzymatic hydrolysis of *Saccharum spontaneum* for reducing sugars production. Energy Sources, 36, 1028-1035.

Kaur, M., Saini, A., Aggarwal, N.K., Sharma, A., Yadav, A., (2014). Utility potential of Parthenium hysterophorus for its strategic management. Advance in agriculture, 1-16.

Keweloh. H., Weyrauch, G., Rehm, H.J., 1990. Phenol-induced membrane changes in free and immobilized *E. coli*. Applied Microbiology and Biotechnology, 33, 66-71.

Khuroo, A.A., Reshi, Z.A., Malik, A.H., Weber, E., Rashid, I., Dar, G.H., 2012. Alien flora of India: taxonomic composition, invasion status and biogeographic affiliations. Biological Invasions, 14, 99–113.

Komolwanich, T., Tatijarern, P., Prasertwasu, S., Khumsupan, D., Thanyalak, C., Luengnaruemitchai, A., Wongkasemjit, S., 2014. Comparative potentiality of Kans grass (*Saccharum spontaneum*) and Giant reed (*Aruno donax*) as lignocellulosic feedstock for the release of monomeric sugars by microwave/ chemical pretreatment. Cellulose, 21, 1327-1340.

Koppram, R., Nielson, F., Albers, E., Lambert, A., Wannstrom, S., Welin, L., Zacchi, G., Olsson, L., 2013. Simultaneous saccharification and co-fermentation for bio-ethanol production using corncob at lab, PDU and demo scales. Biotechnology for biofuels, 6, 2.

Krassig, H.H., 1992. Cellulose, structure, accesibility and reactivity. Switzerland, USA: Gordon and Breach Science publishers.

Kuhad, R.C., Gupta., R., Khasa, Y.P., Singh, A., 2010. Bioethanol production from *Lantana camara* (red sage): pretreatment saccharification and fermentation. Bioresource technology, 1, 8348-8354.

Kuila, A., Banerjee, R., 2014. Simultaneous saccharification and fermentation of enzyme pretreated *Lantana camara* using *S. cerevisiae*. Bioprocess and Biosystems Engineering, 37, 1963-1969.

Kumar, P., Barett, D.M., Delwiche, M.J., Stroeve, P., 2009. Methods for pretreatment of lingocellulosic biomass for efficient hydrolysis and biofuel production. Industrial and Engineering Chemistry Research, 48, 3713-29.

Kumar, A.K., Parikh, B.S., Shah, E., Liu, L.Z., Cotta, M.A., 2016. Cellulosic ethanol production from green solvent-pretreated rice straw. Biocatalysis and Agricultural Biotechnology, 7, 14–23.

Lahkar, B.P., Talukdar, B.K., Sarma. P., 2011. Invasive species in grassland habitat: an ecological threat to one horned rhino (*Rhinoceros unicornis*). Pachydem, 49, 33-39.

Lee, S.Y., 2008a. Fermentative butanol production by Clostridia. [Review]. Biotechnology and Bioengineering, 101(2), 209-228.

Lee, S.Y., 2008b. Continuous butanol production using suspended and immobilized *Clostridium beijerinckii* NCIMB 8052 with supplementary butyrate. Energy and Fuels, 22, 3459-3464.

Liu, Z., Ying, Y., Li, F., Ma, F., Xu, P., 2010. Butanol production by *Clostridium beijerinckii* ATCC 55025 from wheat bran. Journal of Industrial Microbiology and Biotechnology, 37, 495-501.

Lu, J.L., Zhou, P.J., 2015. Ethanol production from microwave-assisted FeCl3 pretreated rice straw. Energy Sources, Part A: Recovery, Utilisation and Environmental Effects, 37, 2367–74.

Lunelli, F.C., Sfalcin, P., Souza, M., Zimmermann, E., Pra, V.D., Foletto, E.L., Jahn, S.L., Kuhn, R.C., Mazutti, M.A., 2014. Ultrasound–assisted enzymatic hydrolysis of sugarcane bagasse for the production of fermentable sugars. Biosystems and Engineering, 124, 24–28.

Lynd, L.R., 1996. Overview and evaluation of fuel ethanol production from cellulosic biomass: technology, economics, the environment, and policy. Annual Review of

Energy and the Environment, 21, 403-465.

Lynd, L.R., Weimer, P.J., Van, Z.W.H., Pretorius, I.S., 2002. Microbial cellulose utilization: fundamentals and biotechnology. Microbiology and Molecular Biology Reviews, 66, 506-577.

Maddox, I.S., 1989. The Acetone-Butanol-Ethanol Fermentation: recent progress in technology. Biotechnology and Genetic Engineering Reviews, 7, 189-220.

Maddox, I.S., 1995. Production of acetone-butanol-ethanol from concentrated Substrates using *Clostridium acetobutylicum*in an integrated fermentation-product removal process. Process Biochemistry, 30, 209-215.

Maiorella, B.L., Blanch, H.W., Wilke, C.R., 1984. Feed component inhibition in ethanolic fermentation by *Sacharomyces cerevisiae*. Biotechnology and Bioengineering, 26, 1155-1166.

Maiti, S., Gallastegui, G., Suresh, G., Kaur, S., Yann, L.B., Patrick, D., Ramirez, A.A., Verma, M., Carlos, R., 2017. Two-phase partitioning detoxification to improve biobutanol production from brewery industry wastes. Chemical Engineering Journal, 330, 1100-1108.

Martin. C., Galbe, M., Nilvebrant, N-O., Jonsson, L.J., 2002. Comparison of the fermentability of enzymatic hydrolysates of sugarcane bagasse pretreated by steam explosion using different impregnating agents. Applied Biochemistry and Biotechnology, 98–100, 699–716.

McFadyen, R.E.C., Chenon, R.D.C., Sipayung, A., 2003. Biology and host specificity of the chromolaena stem gall fly, *Cecidocharesconnexa* (Macquart) (Diptera: Tephritidae), 42, 294-297.

McMillan, J.D. 1997. Bioethanol production: status and prospects. Renewable Energy, 10, 295-302.

Mitchell, W.J., 1998. Physiology of carbohydrate to solvent conversion by Clostridia. Advances in Microbial Physiology, 39, 31–130.

Mollah, A.H., Stuckey, D.C., 1993. Maximizing the production of acetone-butanol in an alginate bead fluidized bed reactor using *Clostridium acetobutylicum*. Journal of Chemical Technology and Biotechnology, 56, 83-89.

Monot, F., 1984. Influence of pH and undissociated butyric acid on the production of acetone and butanol in batch cultures of *Clostridium acetobutylicum*. Applied Microbiology and Biotechnology, 19, 422-426.

Munniappan. R., Bambam, J., 1999. Biological control of *C. Odorata*: successes and failures. in: spencer, N.R.(ed). Proceeding of the X international symposium on biological control of weeds, Bozeman, Montana.81-85.

Mutschlechner, O., Swoboda, H., Gapes, J.R., 2000. Continuous two-stage ABE-fermentation using *Clostridium beijerinckii* NRRL B592 operating with a growth rate in the first stage vessel close to its maximal value. Journal of Molecular Microbiology and Biotechnology, 2, 101-5.

Nanda, S., Dalai, A.K., Kozinski, J.A., 2014. Butanol and ethanol production from lignocellulosic feedstock: biomass pretreatment and bioconversion. Energy Science and Engineering, 2, 138-148.

Nguyen, T.T.T., Le, V.V.M., 2013. Effects of ultrasound on cellulolytic activity of cellulase complex. International Food Research Journal, 20, 557-563.

Nigam, P.S., Singh, A., 2011. Production of liquid biofuels from renewable resources. Progress in Energy and Combustion Science, 37, 52-68.

Nolling, J., 2001. Genome sequence and comparative analysis of the solvent-producing bacterium *Clostridium acetobutylicum*. Journal of Bacteriology, 183, 4823-4838.

Norman, C., Howell, K.A., Millar, A.H., Whelan, J.M., Day, D.A., 2004. Salicylic acid

is an uncoupler and inhibitor of mitochondrial electron transport. Plant Physiology, 134, 492-401.

Olofsson, K., Palmqvist, B., Liden, G., 2010. Improving simultaneous saccharification and co-fermentation of pre-treated wheat straw using both enzyme and substrate feeding. Biotechnology for Biofuels, 3, 17.

Olsson, L., Hahn-Hagerdal, B., 1996. Fermentation of lignocellulosic hydrolysates for ethanol production. Enzyme Microbial Technology, 18, 312-331.

Papoutsakis, E.P., 2008. Engineering Solventogenic Clostridia. Current Opinion in Biotechnology, 19, 420-429.

Park, C.H., Okos, M.R., Wankat, P.C., 1989. Acetone-butanol-ethanol (ABE) fermentation in an immobilized cell trickle bed reactor. Biotechnology and Bioengineering, 34, 18-29.

Patni, N., Pillai, S.G., Dwivedi, A.H., 2011. Analysis of current scenario of Biofuels in India specifically bio-diesel and bio-ethanol. Conference proceedings. Institute of Technology, Nirma University, Ahmedabad – 382 481, 08-10 December.

Phothisantikul, P.P., Tuanpusa, R., Nakashima, M., Charinpanitkul, T., Matsumura, Y., 2013. Effect of CH_3COOH and K_2CO_3 on hydrothermal pretreatment of water Hyacinth (*Eichhornia crassipes*). Industrial and Engineering Chemistry Research, 52, 5009-5015.

Pimentel, D., 2009. Invasive plant: Their role in species extinctions and economic losses to agriculture in the USA. Management of Invasive Weeds, 1-9.

Polman, K., 1994. Review and analysis of renewable feedstocks for the production of commodity chemicals. Applied Biochemistry Biotechnology, 45–46, 709–722.

Qureshi, N., Ezeji, T.C., Ebener, J., 2008a. Butanol production by *Clostridium beijerinckii*part I: use of acid and enzyme hydrolyzed corn fiber. Bioresource Technology, 99, 5915–5922.

Qureshi, N., Saha, B.C., Hector, R.E., Hughes, S.R., Cotta, M.A., 2008b. Butanol production from wheat straw by simultaneous saccharification and fermentation using *Clostridium beijerinckii*: Part I—Batch fermentation. Biomass and Bioenergy, 32, 168-175.

Qureshi, N., Blascheck, H.P., 2000. Butanol production using *Clostridium beijerinckii* BA 101 Hyper-butanol producing mutant strain and recovery by pervaporation. Applied Biochemistry and Biotechnology, 84-86, 225-235.

Qureshi, N., Cotta, M.A., Saha, B.C., 2014. Bioconversion of barley straw and corn stover to butanol (a biofuel) in integrated fermentation and simultaneous product recovery bioreactors. Food and Bio-products Processing, 92, 298–308.

Rajkhowa, D.J., Gogoi, A.K., Yaduraju, N.T., 2005. Weed utilization for vermicomposting – Success story. NRC for weed science, Jabalpur (M.P.), India.

Ranjan, A., Khanna, S., Moholkar, V.S., 2013. Feasibility of rice straw as alternate substrate for biobutanol production. Applied Energy, 103, 32–38.

Sanchez, O.J., Cardona, C.A., 2008. Trends in biotechnological production of fuel ethanol from different feedstock. Bioresource Technology, 99, 5270-5295.

Sasmal, S., Vaibhav, V.G., Mohanty, K., 2012. Ultrasound assisted lime pretreatment of lignocellulosic biomass toward bioethanol production. Energy & Fuels, 26, 3777−3784.

Satyanagalakshmi, K., Sindhu, R., Binod, P., Janu, K.U., Sukumaran, R.K., Pandey, A., 2011. Bioethanol production from acid pretreated water hyacinth by separate

hydrolysis and fermentation. Journal of Scientific and Industrial Research India, 70, 156-161.

Schei, 1996. Invasive Alien plants: An ecological appraisal for the Indian Subcontinent (eds JR Bhat *et al*.)

Scordia, D., Cosentino, S.L., Jeffries, T.W., 2013. Enzymatic hydrolysis, simultaneous saccharification and ethanol fermentation of oxalic acid pretreated giant reed (*Arundo donax* L). Industrial Crops and Products, 49, 392-399.

Scordia, D., Cosentino, S.L., Lee, J.W., Jeffries, T.W., 2011. Dilute Oxalic acid pretreatment for biorefining giant reed (*Arundo donax* L.). Biomass and Bioenergy, 35, 3018-3024.

Scotcher, M.C., Bennett, G.N., 2005. SpoIIE regulates sporulation but does not directly affect solventogenesis in *Clostridium acetobutylicum* ATCC 824. Journal of Bacteriology, 187, 1930-1936.

Secretariat of the convention on biological diversity (2006) Handbook of the convention on biological diversity including its cartagena protocol on biosafety, 4th edition, (Montreal, Canada)

Senatham, S., Chamduang, T., Kaewchingduang, Y., Thammasittirong, A., Srisodsuk, M., Elliston, A., Roberts, I.N., Waldron, K.W., Thammasittirong, S.N.R., 2016. Enhanced xylose fermentation and hydrolysate inhibitor tolerance of *Scheffersomyces shehatae* for efficient ethanol production from non-detoxified lignocellulosic hydrolysate. Springer Plus, 5, 1040.

Shi, Z., Cai, Z., Wang, S., Zhong, Q., Bozell, J.J., 2013. Short-time ultra-sonication treatment in enzymatic hydrolysis of biomass. Holzforschung, 67, 891–897.

Sindhu. R., Binod, P., Mathew, A.K., Abraham, A., Gnansounou, E., Pandey, A., 2017. Development of a novel ultrasound assisted hydrothermal pretreatment strategy for

the production of bioethanol from chili post-harvest residue. Annals of Agricultural and Crop Sciences, 2, 1020.

Singh, S.P., 1998. A review of biological suppression of *C. odorata*.in proceeding of 4th international workshop on biological control and management of *C. odorata*. Bangalore, India, 86-92.

Singh, S., Agarwal, M., Sarma, S., Goyal, A., Moholkar, V.S., 2015. Mechanistic insight into ultrasound induced enhancement of simultaneous saccharification and fermentation of *Parthenium hysterophorus* for ethanol production. Ultrasonic Sonochemistry, http://dx.doi.org/10.1016/j.ultsonch.2015.02.011 1350-4177.

Singh, S., Sarma, S., Agarwal, M., Goyal, A., Moholkar, V.S., 2015a. Ultrasound enhanced ethanol production from *Parthenium hysterophorus*: a mechanistic investigation. Bioresource Technology, 188, 287–294.

Sivanarutselvi, S., Muthukumar, K., Velan, M., 2017. Studies on the effect of hydrothermal pretreatment of sugarcane bagasse for biobutanol production. Energy Sources, Part A: Recovery, Utilization, and Environmental Effects, 39, 1771-1777.

State of conservation report of Manas wildlife sanctuary (N 338), (2015) Manas Tiger Project. Assam Forest Department, Assam.

Subhedar, P.B., Gogate, P.R. 2014. Enhancing the activity of cellulase enzyme using ultrasonic irradiations. Journal of Molecular Catalysis B: Enzymatic, 101, 108–114.

Sulaiman, A.Z., Ajit, A., Yunus, R.M., Christi, Y., 2011. Ultrasound-assisted fermentation enhances bioethanol productivity. Biochemical Engineering Journal, 54, 141-150.

Sun, Y.C., Xu, J.K., Wang, B., Xu, F., Sun, R.C., 2012. Selective separation and recovery of the lignin from lignocellulosic biomass using ionic liquid. Proceedings of the

55th International convention of society of wood science and technology August 27-31, 2012, Beijing, China.

Swana, J., Yang, Y., Behnam, M., Thompson, R., 2011. An analysis of net energy production and feedstock availability for biobutanol and bioethanol. Bioresource Technology, 102, 2112-2117.

Taherzadeh, M.J., Gustafsson, L., Niklasson, C., Liden, G., 2000. Physiological effects of 5-Hydroxymethylfurfural on *Saccharomyces cerevisiae*. Applied Microbiology and Biotechnology, 53, 701-708.

Tao, L., Aden, A., 2009. The economics of current and future biofuels. In Vitro Cellular & Developmental Biology-Plant, 45,199–217.

Ulbricht, R.J., Sharon, J., Thomas, J., 1984. A review of 5-Hydroxymethylfurfural HMF in parental solutions. Fundamental and Applied Toxicology, 4, 843-853.

Vanholme, R., Demedts, B., Morreel, K., Ralph, J., Boerjan, W., 2010. Lignin biosynthesis and structure. Plant Physiology, 153, 110-15511.

Wang, Z., Lin, X., Li, P., Zhang, J., Wang, S., Ma, H., 2012. Effects of low intensity ultrasound on cellulase pretreatment. Bioresource Technology, 117, 222–227.

Wood, B.E., Aldrich, H. C., Ingram, L.O., 1997. Ultrasound stimulates ethanol production during the simultaneous saccharification and fermentation of mixed waste office paper. Biotechnology Progress, 13, 232−237.

Wyman, C.E., 1994. Ethanol from lignocellulosic biomass: technology, economics and opportunities. Bioresource Technology, 50, 3-16.

Xue, C., Wang, Z., Wang, S., Zhang, X., Chen, L., Mu, Y., Bai, F., 2016. The vital role of citrate buffer in acetone-butanol-ethanol (ABE) fermentation using corn stover and high-efficient product recovery by vapor stripping-vapor permeation (VSVP) process. Biotechnology Biofuels, 9, 1461-1469.

Yamada, R., Nakatani, Y., Ogino, C., Kondo, A., 2013. Efficient direct ethanol production from cellulose by cellulase and cellodextrin transporter-co-expressing *Saccharomyces cerevisiae*. Applied and Industrial Microbiology Express, 3, 34.

Yan, J., Zhilei, W., Wang, Q., He, M.H., Li, S., Irbis, C., 2015. Bioethanol production from sodium hydroxide/hydrogen peroxide-pretreated water hyacinth via simultaneous saccharification and fermentation with a newly isolated thermotolerant *Kluyveromyces marxianu* strain. Bioresource Technology, 193, 103-9.

Yang, X., Tsao, G.T., 1995. Enhanced acetone-butanol fermentation using repeated fed batch operation coupled with cell recycle by membrane and simultaneous removal of inhibitory products. Biotechnology and Bioengineering, 47, 444-50.

You, T., Zhang. L., Zhou, S., Xu, F., 2014. Protic acid resin enhanced 1-butyl-3-methylimidazolium chloride pretreatment of *Arundo donax* Linn. Bioresource Technology, 167, 574-577.

Zhang, Y., Fu, E., Liang, J., 2008. Effect of ultrasonic waves on the saccharification processes of lignocellulose. Chemical Engineering and Technology, 31, 1510–1515.

CHAPTER 2 AN ASSESSMENT OF THE POTENTIAL OF INVASIVE WEEDS AS MULTIPLE FEEDSTOCKS FOR BIOFUEL PRODUCTION[§]

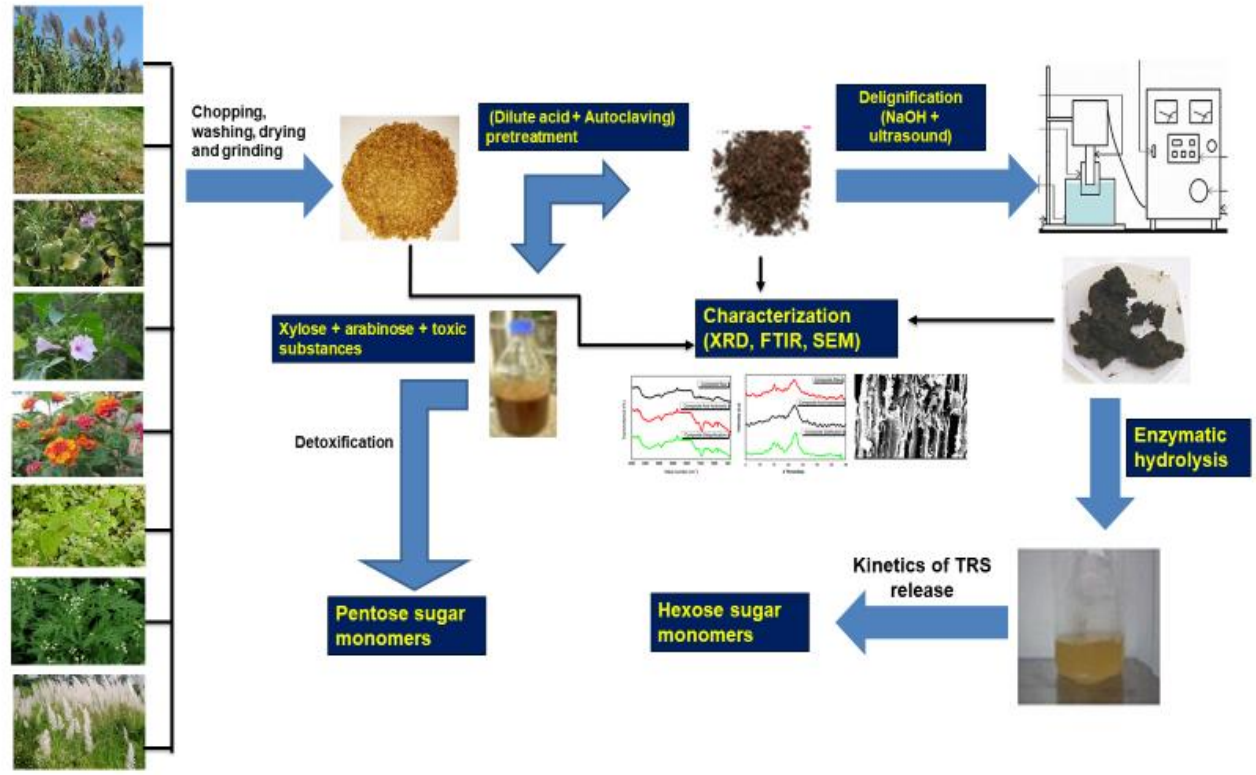

Chapter Highlights

- Assessment of the potential of bioalcohol production from eight highly invasive biomass
- Pretreatment comprising acid hydrolysis, delignification and enzymatic hydrolysis
- Pretreatment is at unoptimized conditions for the invasive weeds
- Average yield of fermentable sugars from weeds is 42.12 per 100 g raw weeds
- Maximum theoretical yield of 21.48 g ethanol and 17.26 g raw weeds

[§] Also see Borah, A.J., Singh, S., Moholkar, V.S., Goyal, A. (2016) An Assessment of Invasive Weeds as Multiple Feedstocks for Biofuels Production. *RSC Advances*, **6**, 47151–47163

CHAPTER 2

AN ASSESSMENT OF THE POTENTIAL OF INVASIVE WEEDS AS MULTIPLE FEEDSTOCKS FOR BIOFUEL PRODUCTION

2.1 Introduction

The quest for alternative and renewable liquid transportation fuel has intensified over the past few years. This is driven by fast and continuing depletion of fossil fuels threatening energy security, and increasing concerns about climatic change as a result of large emission of greenhouse gases through vehicular exhausts. Waste biomasses in the form of noxious invasive weeds (in addition to conventional lignocellulosic substrates of agro– and forestry residues) **(Ranjan et al., 2013; Moholkar and Singh, 2013; Singh et al., 2014)** could form a large potential feedstock source for economic biofuel production **(Raspolli et al., 2013, Ekman et al., 2013, Van et al., 2014).** Large numbers of such invasive species exist in India. These species infest millions of hectares of arable and non–arable (or infertile) land, leading to enormous monetary loss due to a reduction in crops and forage production. The actual biomass produced by these noxious weeds is in the range of 15–20 tons per hectare. Nonetheless, these biomasses can form a feedstock for liquid biofuels due to their significant content of holocellulose (in addition to lignin), which can be hydrolyzed to produce fermentable monomeric sugars. Hexose and pentose sugars produced from the hydrolysis of cellulose and hemicellulose can be used to produce alcoholic biofuels, such as ethanol and butanol. The pretreatment of biomass prior to fermentation encompasses the removal of lignin and the acid/enzymatic

hydrolysis of hemicellulose and cellulose fractions to pentose and hexose sugars. Removal of the lignin matrix in biomass causes a better exposure of the cellulose and hemicellulose fraction to acid/ enzymatic action, which leads to enhancement of the sugar yield. The pretreatment of biomass is also aimed at a reduction in the crystallinity of cellulose and in increasing the biomass porosity and surface area, which all contribute to a faster and higher hydrolysis of the cellulose/hemicellulose, thus maximizing the yield of fermentable sugars.

2.1.1 Aim and approach

The use of a cheap feedstock and optimization of the cost–intensive pretreatment techniques are crucial aspects of the economic feasibility of a sustainable biofuels process. In the present study, we dealt with the pretreatment of multiple invasive species or weeds (which are essentially waste biomasses), and determined the yield of total (hexose + pentose) reducing (or fermentable) sugars, which is a measure of their potential as a feedstock for biofuels. The invasive weeds considered in this work are: (1) *Arundo donax* (AD), (2) *Chromolena odorata* (CO), (3) *Eichhornia crassipes* (EC), (4) *Ipomea carnea* (IC), (5) *Lantana camara* (LC), (6) *Mikania micrantha* (MM), (7) *Parthenium hysterophorus* (PH) and (8) *Saccharum spontaneum* (SS). A number of previous authors have also addressed the matter of the pretreatment of these waste biomasses and a summary of some representative studies in optimization of the pretreatment and fermentation of these invasive weeds is given in **Table 1.5** of Chapter 1. Most of these studies include the following components: acid hydrolysis, delignification, enzymatic hydrolysis and fermentation of the acid/enzyme hydrolyzates to bioethanol. It could be inferred from **Table 1.5** that the optimum pretreatment conditions differ significantly for each biomass. The approach in the present study is

somewhat different from the earlier studies listed in **Table 1.5,** which studied the pretreatment of individual biomasses. In a previous paper, **(Singh et al., 2014)** we presented an extensive study on the assessment and optimization of as many as 17 pretreatment techniques (physical/ chemical/physico–chemical) for the invasive species of *Parthenium hysterophorus* for the maximum production of reducible sugars that could be fermented to produce alcoholic fuels. In the present study, we carried out pretreatment of the eight invasive weeds mentioned above at optimized conditions determined for *Parthenium hysterophorus,* **(Singh et al., 2014)** and assessed the yield of reducible sugars. It could be expected that the optimum pretreatment conditions for the eight invasive weeds could be different than those for *Parthenium hysterophorus*. The major contemplation underlying the approach of pretreating the invasive weeds listed above at conditions optimized for *Parthenium hysterophorus* was to assess the output of a bioprocess with feedstock flexibility. This can be explained in greater details as follows: depending on the availability of biomasses in different parts of the year, the biofuel industry for the large–scale production of alcoholic biofuels may require to change the feedstock or to use a mixed feedstock comprising several biomasses as sufficiently large quantities of a single biomass may not be available throughout the year. In such a situation, it may not be feasible or practical to perform comprehensive optimization of the pretreatment conditions for each biomass used as feedstock. Moreover, the optimum pretreatment conditions (such as acid/alkali concentrations or temperature/pressure of the autoclaving) may show significant variations for different biomasses. Thus, the specifications of processing equipment designed for the pretreatment of one biomass may not be suitable for other biomasses. Obviously, the replacement of process equipment for different biomasses is rather impractical and so under this limitation, it is inevitable to treat different biomasses at conditions optimized

for the representative biomass that was considered for the process design. In such a situation, it is necessary to make a preliminary estimate of the alterations in the quality of the hydrolyzates in terms of the concentrations of pentose and hexose sugars with changing feedstock. The present study essentially attempts to paint a picture of such variations by pretreatment of the eight selected invasive weeds at conditions optimized for the weed of *Parthenium hysterophorus*.

2.2 Materials and methods

2.2.1 Biomass collection and processing

Biomasses of all eight weeds, *viz*. *Arundo donax* (AD), *Chromolena odorata* (CO), *Eichhornia crassipes* (EC), *Ipomea carnea* (IC), *Lantana camara* (LC), *Mikania micrantha* (MM), *Parthenium hysterophorus* (PH) and *Saccharum spontaneum* (SS) were collected from the IIT Guwahati campus. The substrate for pretreatment was the whole plant body except for the roots. After collection, the biomass was dried in ambient air, followed by chopping it into small pieces of a few mm lengths. The chopped biomass was washed with water and again dried in a hot air oven at 60°C for 24 h. Prior to pretreatment; the particle size of the dried biomass was further reduced to < 1 mm using a domestic mixer grinder. The powdered biomass was then stored in air tight containers at room temperature for further experiments.

2.2.2 Proximate and biochemical analysis of invasive biomasses

Proximate analysis of all eight biomasses were determined according to the standard protocols (*viz*. CEN 15104 and ASTM E1755–01). Ultimate analysis was performed by using Euro EA Elemental (C, H, N) analyzer (Eurovector EA 3000). The results of the proximate and ultimate analyses of the invasive weeds are listed in

Appendix A (Table A1). The chemical composition (i.e. determination of cellulose, holocellulose and lignin content) of raw, pretreated and delignified biomass was done by using the standard protocols (*viz*. **Updegraff 1969** and standard TAPPI protocols by **Allan et al., 1992**).

2.2.2.1 ***Determination of holocellulose content*****:** Holocellulose content was measured as the sodium chlorite delignified residue **(Teramoto et al., 2009)**. Two grams of raw biomass was mixed with 100 mL distilled water taken in a 250 conical Erlenmeyer flask. 1.5 g Sodium chlorite and 5 mL of 10% (v/v) acetic acid were added to it. The mixture was kept at 70^{o}C in a water bath for 30 min and stirred at every 10 min. After every time interval of 1 h, 1.5 g sodium chlorite and 5 mL acetic acid added for 4 h. The mixture was cooled to 10°C and then poured into a sintered glass crucible. Residue obtained was then washed five times with ice water followed by acetone to removed dissociated organic compound and then kept for air dried to make acetone free.

2.2.2.2 ***Anthrone method*****:** The method given by **Updegraff (1969)** was followed to estimate the cellulose content in all the biomasses.

Reagents*:* The mixture of acetic/ nitric reagent (150 mL of 80 % acetic acid (13.3 N) and 15 ml of conc. nitric acid (16N) was prepared. Anthrone reagent was freshly prepared by dissolving 0.2 g of anthrone in 100 mL of ice cold conc. H_2SO_4 (37N). The reagent was stored at 4^{o} C for 2 h before use.

Method: 0.1 g of raw biomass was taken in a test tube and 5 ml of acetic/ nitric reagent was added to it and mixed thoroughly. The test tube was placed in a water bath at 100°C for 30 min. The content was allowed to cooled down and then subjected to centrifugation at 5000 g for 20 min. The supernatant was discarded and the residue was collected and

washed with distilled water and it was then dissolved in 10 mL of 67 % H_2SO_4 (approx. 13.7N). The mixture was allowed to stand for 1 h. Then 1 mL of the solution was diluted to 100 mL. 10 mL of anthrone reagent was added to 1 mL of diluted solution. The mixture was boiled for 10 min using a boiling water bath, and was later cooled. Using a spectrophotometer (Varian, Cary 100). The absorbance was recorded at 630 nm using carboxymethyl cellulose (100 µg/ml) a calibration curve was drawn and the amount of cellulose in the sample was estimated.

2.2.2.3 Determination of lignin content

TAPPI, (1992) protocol was followed for lignin estimation. 1 g of raw biomass was kept in a 50 mL beaker and 10 mL of 72% (approx. 14.7 N) sulphuric acid was added to it. The mixture was transferred to a 500 mL round bottom flask and the final volume made to 300 mL with distilled water. The solution was refluxed for 3 h and then transferred to a pre–weighed sintered glass crucible. The biomass was washed with 300 ml of hot distilled water. The residue was dried at 105°C till constant weight was achieved. The residue obtain was the lignin present in biomass sample and was expressed as weight percentage of raw biomass.

2.2.3 Acid hydrolysis of invasive biomasses

The optimum conditions for the acid hydrolysis of *Parthenium hysterophorus* were determined by **(Singh et al., 2014)** as follows: 1% (v/v) H_2SO_4 (equivalent to 0.36 N) mixed with 10% w/v biomass, then autoclaved at 121°C and 15 psi for 30 min, followed by rapid steam release. Dried biomass of all eight weeds species was pretreated under these conditions. After completion of the pretreatment, the biomass from the reaction mixture was separated by filtration through a double–layered muslin cloth. The

residual chemicals left on the biomass surface after acid pretreatment were removed by successive water washes. This procedure was continued until the pH of the wash water became 7 (indicating neutral conditions). This was followed by drying of the biomass residue in a hot air oven for 24 h at 60 °C. The dried biomass containing cellulose and traces of lignin was used for further processing. Acid pretreatment causes hydrolysis of the hemicellulose in biomass, resulting in a release of pentose sugars. The filtrate of the acid pretreatment or the acid hydrolyzate was thus analyzed for the sugar content using NS method. The hydrolysate was detoxified to remove the inhibitory compounds. The pentose sugars predominantly comprise xylose, but other sugars such as arabinose, mannose and galactose are also present; however, their content is negligible as compared to xylose.

2.2.4 Detoxification of acid hydrolysate of invasive biomass

Detoxification of the hydrolyzate from the acid hydrolysis was carried out in two steps. Initially, the pH of the hydrolysate was increased to 10 with the addition of $Ca(OH)_2$, followed by stirring for 30 min. Next, the hydrolyzate was neutralized with the addition of concentrated H_2SO_4, with subsequent centrifugation at 10000 g for 15 min for the removal of suspended solids. 1.5% w/v activated charcoal was added to the hydrolyzate with continuous stirring for 30 min at room temperature (25°C). Inhibitory compounds formed during the acid hydrolysis adsorb on the activated charcoal. The particles of activated charcoal were then removed by vacuum filtration of the hydrolyzate.

2.2.5 Delignification of acid pretreated invasive biomasses

The delignification of the biomass obtained after acid hydrolysis was carried out using the procedure outlined by **(Bharadwaja et al., 2015)**. This procedure makes use of

sonication (or ultrasound irradiation) during delignification. The delignification process is significantly intensified by the physical and chemical effects induced by ultrasound and cavitation. The physical effects of ultrasound and cavitation includes the generation of intense micro–mixing through the phenomena of microstreaming, microturbulence and acoustic waves, while the chemical effects of transient cavitation include the generation of highly reactive radicals through dissociation of gas and vapor molecules entrapped in the bubble **(Chaudhury et al., 2013; Patidar et al., 2012; Chakma et al., 2013).** A probe–type programmable and micro–processor controlled ultrasonic processor (Sonics & Materials, Model VCX 500) with a maximum power of 500 W and frequency of 20 kHz was used for sonication of the reaction mixture. The reaction was carried out in a 100 mL beaker. The total volume of the reaction mixture was 80 mL, with an alkali concentration of 1.5% w/v NaOH and a biomass loading of 2% w/v. The ultrasound probe was set at 30% amplitude, with a theoretical power consumption of 150 W at a duty cycle of 83% (50 s on and 10 s off in 1 min of sonication). The actual power consumption of the ultrasound probe was determined using a calorimetric technique **(Chakma et al., 2013; Sivasankar et al., 2007).** The total sonication time was 10 min, during which the temperature of the reaction medium was maintained at 30°C with the help of a temperature controlled circulating water bath. After the completion of sonication, the reaction mixture was filtered through a double–layered muslin cloth for removal of the solid biomass residue. This cellulose–rich biomass residue (after removal of the lignin and hemicellulose) was washed with hot water several times until the pH of the wash water was neutral, which ensured no chemicals were left on the biomass surface. The biomass residue was dried for 12 h in a hot air oven at 60 ± 3°C, and was then used for the enzymatic hydrolysis.

2.2.6 Saccharification of invasive biomasses by commercial enzymes

The enzymatic hydrolysis (or saccharification) of delignified biomasses of all eight biomass species was carried out using commercial cellulase from *Trichoderma reesei* 6 U/mg and cellobiase from *Aspergillus* sp. enzymes (250 U/g) both procured from Sigma Aldrich, (USA) at the optimum conditions reported by **Bharadwaja et al. (2015)**. The hydrolysis was performed in an incubator shaker (Orbitek, Scigenics Biotech, India) in 50 mM citrate phosphate buffer solution (pH 4.8) at 50°C and at 150 rpm. The reaction mixture was taken in a 150 mL Erlenmeyer flask with a total reaction volume of 20 mL. The concentration of pretreated biomass in the reaction mixture was 4.2% w/v, with cellulase and cellobiase concentrations of 135 and 75 FPU per g biomass, respectively. The hydrolysis was carried out for 120 h. 0.005% w/v sodium azide solution was added to the mixture to avoid external microbial contamination. 0.1 mL samples were withdrawn periodically during hydrolysis and were analyzed to assess the release of sugar.

2.2.7 Determination of reducing sugar in acid and enzyme hydrolysate

Both pentose–rich acid hydrolyzate and hexose–rich enzyme hydrolyzate were subjected to centrifugation for 10 min at 10 000 rpm (26832 g) at 4°C. The total reducing sugar in the hydrolyzate was estimated using NS (Nelson and Somogyi) method of **Nelson (1944)** and **Somogyi (1945)**. The presence of individual sugars in the hydrolyzate was confirmed through HPLC analysis (Perkin Elmer series 200). The chromatogram HPLC profile of the standard sugars and sugar in each biomass are reproduce in the **Appendix A Fig. A2** and **Fig**. **A3.** The HPLC instrument comprised a pump, a refractive index detector, a vacuum degasser and a Hi–plex–H column (Varian, 300 mm × 5 mm × 4.6 mm). Deionized Milli Q water at a flow rate of 0.4 mL min^{-1} was used as the mobile phase. Prior to injection in to the HPLC column, samples withdrawn from the reaction

mixture were diluted and filtered through a 0.2 mm membrane filter to remove any suspended particulate matter.

2.2.7.1 ***Reagents used for sugar analysis*****:** Composition of the reagents used in total reducing sugar analysis is as follows (Nelson, 1944; Somogyi, 1945): **Reagent A**: A mixture of 2.5 g sodium carbonate, 2.5 g potassium sodium tartrate tetra hydrate, 2.0 g sodium bicarbonate and 20.0 g sodium sulphate is dissolved in 100 mL of distilled water. **Reagent B**: 4.5 g copper sulphate pentahydrate and 2 drops concentrated sulphuric acid are added to 30 mL of distilled water. **Reagent C**: 2.5 g ammonium molybdate tetrahydrate and 2.1 mL concentrated sulphuric acid were added to 45 mL of distilled water. Solution of 0.3 g sodium arsenate heptahydrate in 2.5 mL of distilled water was mixed to it and stored in an amber bottle at 37 °C for 24 hours prior to use. **Reagent D** Reagents A and B are mixed in a ratio 25:1 to obtain **Reagent D**. 100 µl of samples was prepared by dilution with distilled water in Eppendorf tube volume of 2mL. To this sample solution prepared 100 µl of reagent D is added and boiled in water bath for 20 min. After 20 min, the solution is allowed to stand, at 25°C until it get cooled to room temperature. 100 µl of reagent C added to the reaction mixture followed by 700 µl of distilled water to make the final volume to 1 mL. The final sample mixture was analyzed for quantification of total reducing by reading the absorbance at 500 nm on UV–VIS spectrophotometer (Varian–Cary 100 UV–Vis spectrophotometer).

2.2.8 Characterization of the raw, acid pretreated and delignified biomasses

2.2.8.1 ***SEM analysis*****.** The morphologies of the eight biomass species at various stages of pretreatment, namely raw biomass, post acid pretreatment and post alkaline delignification, were analyzed with a Scanning Electron Microscope (JEOL, Model:

JSM–6360, USA). For SEM analysis, the samples were prepared by drying the biomass at 60°C for 24 h and then spreading the dried samples onto carbon tape placed over the surface of the SEM stub. The samples were sputtered with 10 nm gold in a sputter–coater. The SEM micrographs of raw, acid–pretreated and delignified biomass were taken at a similar magnification for comparison of the different micrographs to discern the effects of pretreatment on the biomass structure and morphology.

2.2.8.2 ***FTIR spectroscopy*****.** The raw, acid–pretreated and delignified biomasses of all eight species were characterized for the change in structural composition following pretreatment. An FTIR spectrophotometer (Perkin Elmer, Spectrum Two, USA) was used to characterize the samples. The samples for analysis were prepared by mixing a small quantity of biomass (10 mg) and KBr in a ratio (w/w) of 1:100. The mixtures were ground well and the spectra were recorded in the range of 400–4000 cm1 using 200 mg of biomass + a KBr mixture in the form of pellets.

2.2.8.3 ***X–ray diffraction***. The effect of acid pretreatment and delignification on the crystallinity of residual cellulose in pretreated biomass was assessed using X–ray diffractometer (D8 Advance, Bruker, Germany). The diffractometer was operated at 40 KV and 40 mA using Cu–Kα (λ = 1.54 Å) radiation. Samples of the pretreated and delignified biomasses of all eight species were scanned in the range of 2θ = 5–35^o with step size of 0.05^o. The crystallinity index (*CrI*) of the residual cellulose in biomass was determined with formula of **Segal et al., (1962):**

$$CrI\,(\%) = \frac{I_{crystalline} - I_{amorphous}}{I_{crystalline}} \times 100$$

where, $I_{\text{crystalline}}$ = intensity of the crystalline peak at 2θ = 22^o and $I_{\text{amorphous}}$ = intensity of the amorphous peak at 2θ = 18^o.

2.3 Results and discussion

2.3.1 Results of dilute acid and enzymatic hydrolysis

The experimental results on the pretreatment and enzymatic hydrolysis of the eight biomass species considered in this work are given in **Tables 2.1** and **2.2A**. It should be noted that in **Table 2.1**, the cellulose content of biomass after dilute acid hydrolysis is expressed as a percentage of raw biomass, while that after delignification is expressed as a percentage of biomass after acid pretreatment. For the biomass of *Saccharum spontaneum* and *Eichhornia crassipes,* the percentage cellulose content of biomass after pretreatment was above 95%, indicating almost the complete removal of lignin and hemicellulose followed by *Ipomea carnea* with 94.6%. This was also confirmed by the large positive values for the percentage relative changes to various bands in the IR spectrum of *Saccharum spontaneum* and *Eichhornia crassipes* (as depicted in **Table 2.3**) corresponding to different functional groups in the biomasses. However, for the biomasses of *Arundo donax* and *Lantana camara,* the percentage cellulose content after delignification and acid hydrolysis was less than 85%, which indicates the presence of residual lignin in biomass after pretreatment. The results given in **Table 2.1** demonstrate the potentials of the weed species for biofuel production. The holocellulose content of *Eichhornia crassipes* was the highest, while *Lantana camara* had the highest lignin content. The lignin hinders the hydrolysis of hemicellulose during dilute acid pretreatment. The subsequent alkali pretreatment at 1.5% w/v NaOH assisted with sonication could also not remove the lignin completely. As a consequence, the pretreated biomass undergoing enzymatic hydrolysis comprised only 80% cellulose. An interesting result was seen for the biomasses *Arundo donax* and *Saccharum spontaneum*, where the initial lignin content of these biomasses was almost similar, yet the biomass of *Saccharum spontaneum* after pretreatment had a far higher content of cellulose than

Arundo donax. An explanation for this discrepancy can be given in terms of the structural composition of lignin in *Arundo donax*. **You et al. (2014)** recently published an analysis of the lignin structure from the stems and foliage of *Arundo donax*, and described how lignin is an amorphous polymer, and is made up of three aromatic alcohols or monolignols, namely *p*–coumaryl, coniferyl and syringyl. These monolignols form distinct lignin units during the lignification process, known as p–hydroxy phenyl (H), guaiacyl (G) and syringyl (S) units. The analysis of **You et al. (2014)** clearly indicated that the milled wood lignin (both stem and foliage) of *Arundo donax* were HGS–type lignin with an S/G ratio in the range of 0.15–0.62, with a strong predominance of G units. The main lignin inter unit linkages were β–0–4 alkyl–aryl ethers followed by β–β', β–1', α, β–diaryl ethers together with cinnamyl alcohol and cinnamaldehyde end groups. The foliage lignin with higher condensed G units contained a greater amount of tricin. The linkages between lignin and tricin could be alkaline stable. As a result of its structural characteristics, the lignin in *Arundo donax* is not removed completely during alkaline pretreatment at 1.5% w/v NaOH.

2.3.1.1 *Enzymatic hydrolysis*

The results of enzymatic hydrolysis of the pretreated biomasses of the eight invasive weeds are depicted in **Fig. 2.1** below. The kinetics of sugar release during enzymatic hydrolysis with respect to both pretreated biomass (post acid hydrolysis and delignification) and only cellulose is given in **Table 2.2B**. The trend in sugar release in 36 h of treatment for the eight biomasses are as follows: *Saccharum spontaneum* > *Ipomea carnea* > *Eichhornia crassipes* > *Arundo donax* > *Lantana camara* > *Parthenium hysterophorus* > *Chromolena odorata* > *Mikania micrantha*. Comparing this trend

against the cellulose content of the pretreated biomasses, we find an anomaly that the biomasses of Arundo donax and *Lantana camara* (which have 18% and 20% residual lignin, respectively) have a higher release of sugars than the biomass of *Mikania micrantha*, which has 96.7% cellulose. A possible explanation for this inconsistency can be given in terms of hydrolysis of some portion of the cellulose (in addition to hemicellulose) during the dilute acid treatment. The reason underlying this could be the lesser crystallinity of the biomass of *Mikania micrantha*, as indicated by the crystallinity index in **Table 2.4**. As a consequence, the absolute quantity of cellulose in the pretreated biomass available for enzymatic hydrolysis is reduced. This is manifested in terms of a lower and slower sugar release during the enzymatic hydrolysis. For greater details on the enzymatic hydrolysis of invasive weeds, we refer readers to our recent paper **(Borah et al., 2016).** Some other observations on the results of the enzymatic hydrolysis and their plausible explanations on the basis of characterization of the biomasses are as follows:

Table 2.1 Results of lignocellulosic composition of different biomasses

Sample	Holocellulose* (wt% raw biomass)	Lignin (wt% raw biomass)	Cellulose Content of Biomass (wt % of biomass after preceding treatment)		
			Raw	After dil. acid hydrolysis	After Delignification
AD	69.0 ± 2.8	22.5 ±0.6	55.0 ± 4.2	74.2 ± 1.2	82.3 ± 3.5
CO	65.3 ± 0.8	20.2 ± 2.1	52.0 ± 2.3	55.7 ± 2.7	91.7 ± 3.9
EC	82.2 ± 2.1	04.1 ± 0.4	47.3 ± 1.7	72.7 ± 2.1	96.7 ± 3.9
IC	67.2 ± 2.1	19.4 + 1.8	54.3 ± 0.8	51.7 ± 2.1	94.6 ± 1.9
LC	61.8 ± 1.9	27.2 ± 4.5	38.3 ± 3.7	69.0 ± 3.4	80.7 ± 2.6
MM	61.5 ± 1.4	19.1 ± 0.7	50.2 ± 2.5	58.2 ± 3.1	93.6 ± 4.3
PH	65.2 ± 1.2	20.2 ± 2.1	32.6 ± 4.2	52.6 ± 2.1	93.0 ± 0.9
SS	61.0 ± 3.5	23.0 ± 3.2	49.3 ± 3.0	76.6 ± 3.2	96.1 ± 3.2

The values are mean ± SE (n = 3) Abbreviation: *A. donax* (AD), *C. odorata* (CO), *E. crassipes* (EC), *I. carnea* (IC), *L. camara* (LC), *M. micrantha* (MM), *P. hysterophorus* (PH), and *S. spontaneum* (SS).

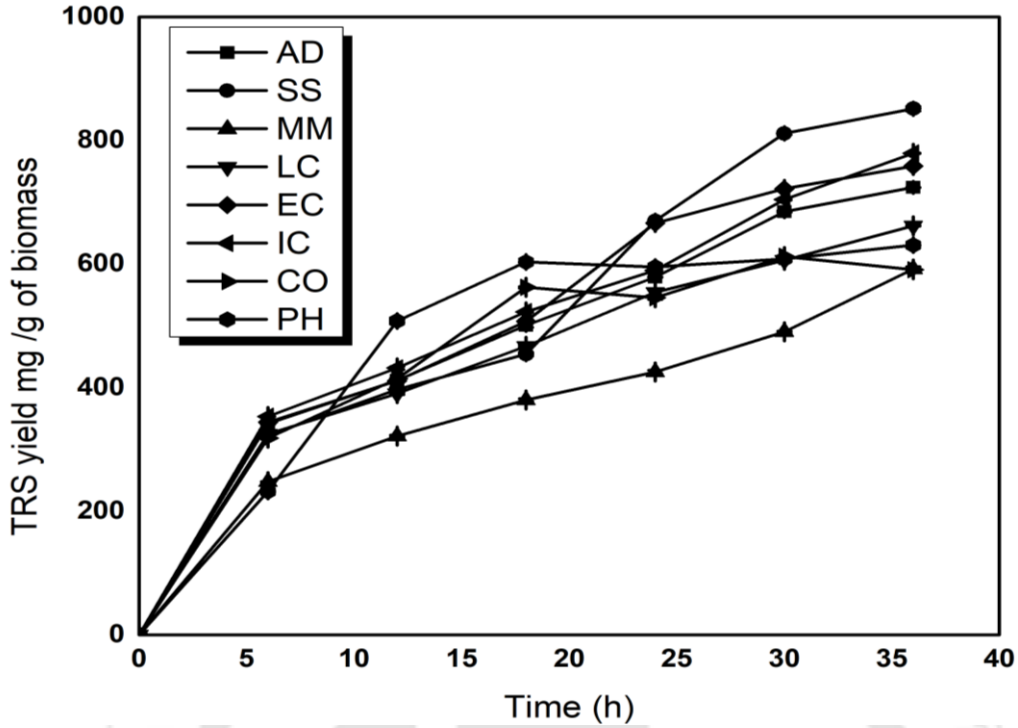

Figure 2.1 Time Profile of TRS release during enzymatic hydrolysis of delignified biomasses of different invasive weeds for 36 h of treatment.
Abbreviation: *A. donax* (AD), *C. odorata* (CO), *E. crassipes* (EC), *I. carnea* (IC), *L. camara* (LC), *M. micrantha* (MM), *P. hysterophorus* (PH), and *S. spontaneum* (SS).

(1) Delignification causes depolymerization of lignin through homolytic cleavages of the phenyl ether β–O–4 and α–O–4 bonds, resulting in exposure of the cellulose moieties in the biomass. The residual biomass after delignification is rich in cellulose and has an increased crystallinity due to removal of the amorphous lignin and hemicellulose. However, we find that the order of crystallinity of delignified biomass (i.e. AD > SS > IC > LC > MM > CO > EC > PH) does not follow the order of the cellulose content of biomass (i.e. EC > SS > IC > MM > PH > CO > AD > LC). This disparity is attributed to two factors: (1) loss of crystallinity during acid hydrolysis due to partial hydrolysis of the cellulose (in addition to hemicellulose), as noted earlier, and (2) the presence of residual lignin in biomass after pretreatment.

(2) The lesser the crystallinity of the cellulose, the faster its reactivity during enzymatic hydrolysis, thus resulting in high hexose sugar yields. However, the order of sugar yields in enzymatic hydrolysis (i.e. SS > IC.> EC > AD > LC > PH > CO.> MM) does not follow the order of the post–delignification crystallinity of the biomass (i.e. AD > SS > IC > LC > MM > CO > EC.>PH). This disaccord is also ascribed to other factors affecting the reaction between the enzymes and the cellulose substrate, such as the presence of residual lignin in the biomass, which may compete with cellulose for adsorption of the enzyme, and hindrance offered by the ash content of the cellulose.

2.3.1.2 *Total fermentable sugar (TFS) yield*

Some peculiar features of the total reducible sugar (TRS) release from different biomasses under dilute acid pretreatment and enzymatic hydrolysis are evident from the results presented in **Table 2.2A**. The highest sugar release is seen (in terms of concentration in g L^{-1}, and yield in mg g^{-1} of raw biomass and mg g^{-1} of delignified biomass) for the biomass of *Saccharum spontaneum*. Although the biomasses of *Saccharum spontaneum*, *Mikania micrantha* and *Lantana camara* have similar holocellulose contents (as a percentage of raw biomass), the extent of sugar release during their acid pretreatment and enzymatic hydrolysis differs drastically. This difference is attributed to the presence of lignin in the biomass after pretreatment, which hinders the access to hemicellulose and cellulose during acid/enzymatic hydrolysis. **Table 2.2A** also lists the total fermentable sugar (TFS) produced by each biomass during pretreatment. A peculiar result is seen for the biomass of *Eichhornia crassipes*. The biomass has more than 96% cellulose after acid pretreatment, yet the yield of total fermentable sugar is 36.36 g per 100 g of raw biomass. This discrepancy could be a consequence of the high

Table 2.2 (A) Results of TRS release from biomasses during different pretreatments and subsequent enzymatic hydrolysis (A) TRS yield in acid and enzyme hydrolysis

Biomass	TRS released in AH (g/L)	TRS yield in AH (mg/g of raw biomass)	TRS released in EH till 36 hour (g/L)	TRS yield in EH till 36 hour (mg/g of delignified biomass)	TFS (mg/g of raw Biomass)	TFS yield (g/100 g of raw biomass)
AD	31.60	315.9	30.41	724.0	492.9	49.29
CO	17.63	176.3	25.77	613.6	360.2	36.02
EC	23.86	238.6	31.86	758.6	363.6	36.36
IC	11.95	119.5	32.73	779.5	350.2	35.02
LC	11.80	118.0	27.81	662.2	306.7	30.66
MM	27.21	272.1	24.90	592.0	449.7	44.37
PH	27.27	277.27	27.22	630.2	466.3	46.63
SS	39.45	394.5	35.81	851.7	394.7	39.47

Abbreviations: *TRS, Total reducing sugar; TFS – total fermentable sugar, AH, Acid hydrolysis; EH, Enzymatic hydrolysis, A. donax* (AD), *C. odorata* (CO), *E. crassipes* (EC), *I. carnea* (IC), *L. camara* (LC), *M. micrantha* (MM), *P. hysterophorus* (PH), and *S. spontaneum* (SS).

(B) Kinetics of TRS release during enzyme hydrolysis and theoretical alcohol (ethanol/ butanol) yield.

Biomass	TRS released in EH (mg/ g–delignified biomass/ h)	TRS released in EH (mg/ g–cellulose/ h)	Theoretical ethanol yield (g/ 100g raw biomass)	Theoretical butanol yield (g/ 100g raw biomass)
AD	23.36	28.52	25.14	20.20
CO	20.69	22.03	18.37	14.77
EC	24.75	25.60	18.54	14.90
IC	27.51	29.11	17.86	14.36
LC	21.47	26.61	15.63	12.51
MM	17.83	19.05	22.62	18.19
PH	22.21	23.90	23.78	19.12
SS	26.24	27.34	29.88	24.02

Abbreviations: *TRS – Total reducing sugar; AH – Acid hydrolysis; EH – Enzymatic hydrolysis A. donax* (AD), *C. odorata* (CO), *E. crassipes* (EC), *I. carnea* (IC), *L. camara* (LC), *M. micrantha* (MM), *P. hysterophorus* (PH), and *S. spontaneum* (SS). [a] Maximum theoretical yield for ethanol from hexose as well as pentose sugars is 0.51 g/g sugar and Butanol is 0.41 g/g sugar

ash content of *Eichhornia crassipes*, which may hinder both (acid and enzyme) hydrolyses, especially the enzymatic hydrolysis, which has relatively slower kinetics and stronger limitations in the mass transfer. For all the biomasses except *Lantana camara*,

more than 60% of the TFS per unit raw biomass is released during the acid hydrolysis itself. For *Lantana camara*, about 38% of the TFS per unit raw biomass is released during acid hydrolysis and the rest during the enzymatic hydrolysis. Therefore, the trend in TFS yields per unit raw biomass (i.e. SS > AD > PH > MM > EC > CO> IC > LC) follows the trend in the reducible sugar yield after acid hydrolysis (i.e. SS > AD > PH >MM > EC > IC > LC). The highest TFS yield was obtained for *Saccharum spontaneum*, while the least yield was obtained for *Lantana camara*. We assign this result to the high lignin content of LC (approx. 27%), which may hinder both the acid and enzymatic hydrolysis. The highest TFS yield after acid and enzymatic hydrolysis was observed for *Saccharum spontaneum*, although the initial holocellulose content was approx. 61–64%. This is possibly an outcome of the effective delignification during alkaline pretreatment due to which the resultant biomass comprises almost pure cellulose (approx. 96%), with a moderate–to–low crystallinity index of 62.5%. These features contribute to the efficacy of the enzymatic hydrolysis, leading to high yields of hexose sugars.

2.3.2 Assessment of biofuels production potential

The potential of the eight invasive weeds as feedstock for biofuels can be assessed on the basis of the maximum theoretical production of alcoholic biofuels, such as ethanol and butanol from fermentation of the hydrolyzates resulting from acid pretreatment and enzymatic hydrolysis. The theoretical yields of ethanol and butanol resulting from the total fermentable sugars (inclusive of both the pentose and hexose hydrolyzates obtained from the acid and enzymatic treatments) from each of the eight invasive weeds are listed in **Table 2.2(B)**. It can be seen that the biomass of *Saccharum spontaneum* had a maximum yield of 29.88 g ethanol and 24.02 g butanol per 100 g of raw biomass. The

least yields of 15.63 g ethanol and 12.51 g butanol per 100 g of raw biomass were observed for the biomass of *Lantana camara*. For the biomass of *Mikania micrantha*, which is a relatively novel feedstock for bioalcohol production, the theoretical yields were 22.62 g ethanol and 18.19 g butanol per 100 g of raw biomass. The average yield of ethanol from all eight invasive weeds was 21.48 g per 100 g of raw biomass, while the average yield of butanol was 17.26 g per 100 g of raw biomass. These yields are at par with the yields reported by **Singh et al. (2014)** for *Parthenium hysterophorus*, i.e. 20 g ethanol per 100 g raw biomass and 16 g butanol per 100 g raw biomass. The similar yields of ethanol and butanol for the eight invasive weeds, as compared to *Parthenium hysterophorus*, are indicative of the promising potential of these weeds for biofuels production – even under un–optimized pretreatment conditions for each of the biomass. This result also highlights that these invasive weeds could be used as multiple feedstocks in a biorefinery, and could be expected to support an overall consistent and sustainable production of alcoholic biofuels. For the efficient production of alcoholic biofuels with a maximum yield per unit raw biomass, it is essential that the hydrolyzates from both the acid and enzymatic treatments can be utilized for fermentation. These hydrolyzates could be fermented separately (as demonstrated by **Bharadwaja et al. 2015**) or simultaneously using mixed cultures. The theoretical bioalcohol yields from the eight tested invasive weeds (with a proper utilization of pentose and hexose sugars) are on par with the yields from conventional fermentation substrates, such as corn and molasses, and also second–generation lignocellulosic substrates, such as agro residues of rice/wheat crops. However, the invasive weeds being waste biomasses (with no other outlet such as cattle feed or domestic fuel) are likely to be available at far cheaper prices than agro–residues. Thus, the processes for biofuels production with invasive weeds as a feedstock are expected to

offer significantly lower production costs and contribute to an attractive economy that should interest the stakeholders in the biofuels industry.

2.3.3 Results of biomass characterization

The characterization of the raw biomass and the biomass after two stages of pretreatment, namely acid pretreatment and alkaline delignification, was carried out using three techniques, namely scanning electron microscopy (SEM), FTIR and X–ray diffraction. The results of these analyses are presented below.

2.3.3.1 ***SEM analysis*****:** The surface morphology of the biomass after acid pretreatment and alkaline delignification was assessed using SEM micrographs. The representative micrographs of the raw biomass, the acid–pretreated biomass and the delignified biomass of all eight biomasses are shown in **Fig. 2.2A.1** to **H.3**. Some distinct features of the surface morphology that are evident from the SEM micrographs are given below. Irrespective of the type of biomass, the observed effects of pretreatment on the fibre structure of all the biomasses were almost similar. The total amount of residue on the sample surface reduced after pretreatment. Dilute acid pretreatment mainly removes the hemicellulosic fraction. Removal of this fraction creates microspores or holes on the surface of the biomass, as evident from the micrographs shown in **Fig. 2.2C.2** and **D.2** corresponding to the biomasses of *Mikania micrantha* and *Lantana camara*. Another common feature of the micrographs of all the biomasses was the presence of globular structures on the surface of biomass after dilute acid pretreatment. These structures are associated with lignin condensation and agglomeration. As noted by **Lima et al., (2013)**, formation of the globular structures is related to the severity of the pretreatment conditions for that particular biomass. During acid pretreatment at elevated pressure and

temperature, the lignin molecules become fluid and coalesce, giving rise to the formation of droplets within the cell matrix. Due to hydrostatic pressure within the cell wall layers, some lignin droplets get redeposited on the biomass surface during cooling of the bulk liquid medium. The SEM micrographs after alkali treatment or delignification reveal the disappearance of the lignin globules from the biomass surface, with a concurrent rise in the surface roughness of the biomass. This result indicates that alkaline treatment causes degradation of the fibrillar structure or tissue of cellulose and lignin. Destruction of the tissues with removal of the lignin helps in gaining a better access of the cellulose to enzyme action, which results in a faster and higher yield of fermentable sugar from the hydrolysis.

2.3.3.2 ***FTIR analysis***: The changes in composition of the lignocellulosic biomass after different pretreatments can be monitored with FTIR spectroscopy. The effect of dilute acid hydrolysis and alkaline delignification on the composition of the eight biomass species was monitored in terms of the relative change in absorbance at specific band positions representing certain biomass components. The vibrational frequencies of different functional groups in the IR spectrum of biomass, along with percentage change in the intensities of these bands after pretreatment, in comparison to raw biomass, are listed in **Table 2.3B, (Singh et al., 2014, Sun et al., 2005; Kuhad et al., 2010)**. The definition of the percentage relative change is given as:

$$\%\ \text{Relative change} = 100 \times \left[\frac{\text{band intensity in untreated solid} - \text{band intensity of pretreated solid}}{\text{band intensity of untreated solid}} \right]$$

As per the above definition, a positive relative percentage change of intensity at all specific bands indicates a reduction in the particular component assigned to that band.

The IR spectra of biomasses at three stages, namely raw biomass, post dilute acid pretreatment and post delignification, are given in the Fig. 2.3.

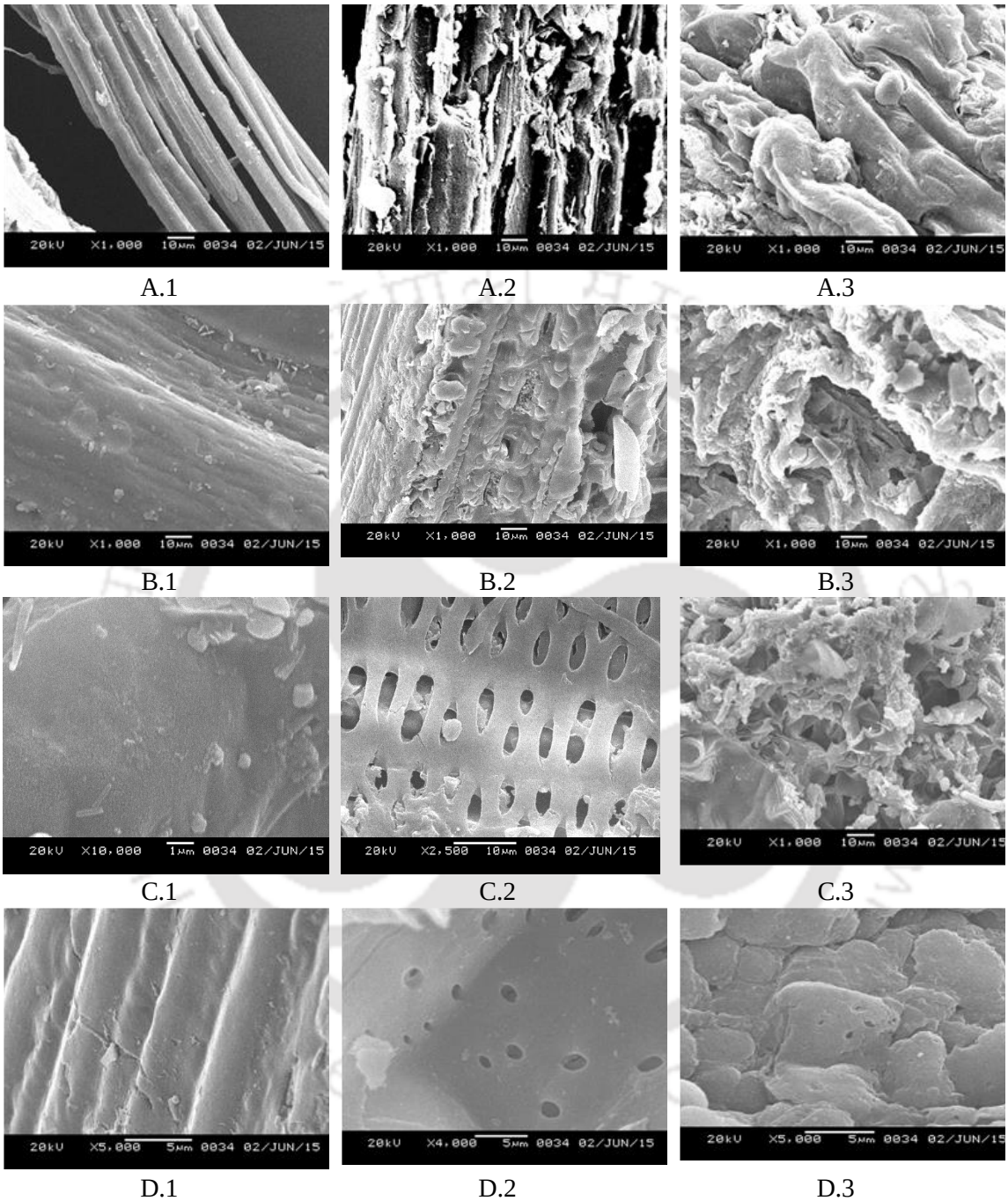

Figure 2.2 SEM micrographs of eight biomass species in native or raw state and after various stages of pretreatment. (1) raw biomass, (2) biomass after acid hydrolysis with autoclaving (1% v/v H_2SO_4, 121^oC, 15 lb pressure), (3) delignified biomass (alkaline treatment with 1.5% w/v NaOH with sonication). (A) *Arundo donax*; (B*) Saccharum spontaneum*; (C) *Mikania Micrantha;* (D) *Lantana camara*;.

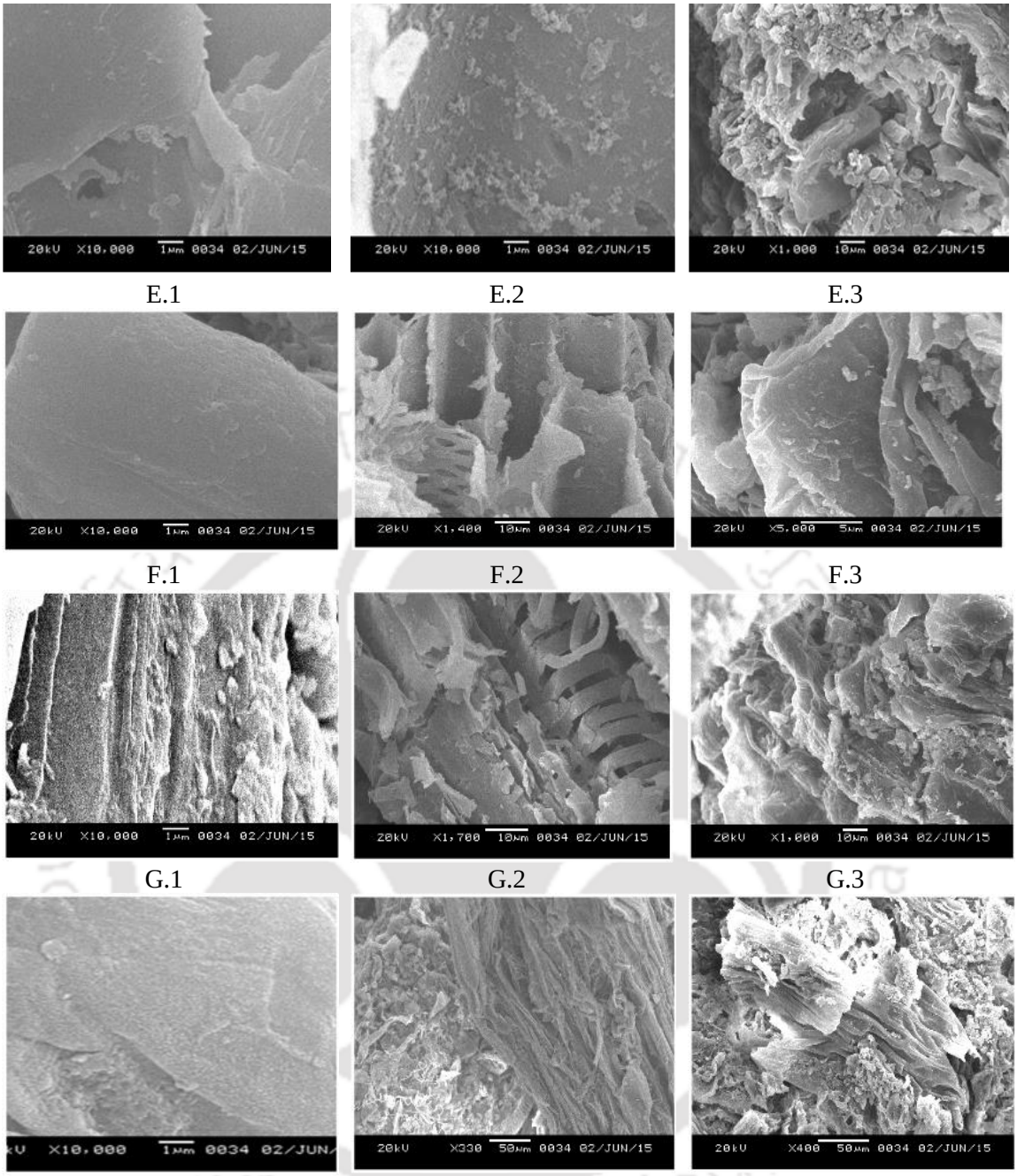

Conti..Figure 2.2 SEM micrographs of eight biomass species in native or raw state and after various stages of pretreatment. (1) raw biomass, (2) biomass after acid hydrolysis with autoclaving (1% v/v H_2SO_4, 121^oC, 15 lb pressure), (3) delignified biomass (alkaline treatment with 1.5% w/v NaOH with sonication). (E) *Eichhornia crassipes* (F) *Ipomea carnea* (G) *Chormolena odorata* (H) *Parthenium hysterophorus*.

Table 2.3 (A) Assignment of band position of different lignocellulosic biomasses using FTIR Spectroscopy

Band position	**Assignments (cm^{-1})**
900	Band of cellulose
1098	Amorphous to crystalline cellulose ratio
1059	C=O stretching due to carbohydrate–lignin Linkage
1238	Hemicellulose–lignin linkage
1245	C=O adsorption resulting from acetyl group cleavage
1260	Ester absorbance related to removal of uronic acid
1378	Band of hemicellulose
1428	Band of cellulose
1458	Aromatic ring variation related to lignin removal
1508	Aromatic ring vibration related to ligini removal
1595	Aromatic ring stretch relating to lignin removal
1720	Carboxylic acids/ ester groups
1738	C=O stretching related to rupture of methyl/methylene
1745	Carbonyl bonds related to Lignin side chain removal
2900	C–H stretching related to rupture to rupture of methyl/ methylene group of cellulose
3348	O–H stretching related to rupture of cellulose–hydrogen bonds

For most absorption bands, the values of the relative change in the intensity were positive after completion of both pretreatments. The changes indicate the efficient removal of hemicellulose and lignin after the biomass treatments. Positive changes for the band positioned at 1378 cm^{-1} indicates the removal of hemicellulose during acid hydrolysis. Positive changes for the band positioned at 900 and 1098 cm^{-1} indicate a reduction in cellulose crystallinity, which assists in enzymatic hydrolysis. The overall conclusion of the FTIR analysis is that treatment of acid hydrolysis at 1% v/v H_2SO_4, 121°C and 15 psi pressure, and alkaline delignification at 1.5%w/v NaOH assisted by ultrasound are able to induce desired changes in the biomass structure; although these conditions have not been individually optimized for each of the eight biomasses considered in the present work.

Table 2.3(B) Summary of characterization of pre–treated biomass using FTIR Spectroscopy (relative changes in intensities for various bands)

Band position (cm^{-1})	Relative change in intensities (%)															
	AD AH	AD DELG	MM AH	MM DELG	LC AH	LC DELG	WH AH	WH DELIG	SS AH	SS DELG	IC AH	IC DELG	PH AH	PH DELG	CO AH	CO DELIG
900	3.6	34.7	–6.8	16.7	0.5	29.9	33.5	76.6	–0.4	19.7	1.1	38.11	–0.2	38.11	–1.73	27.17
1098	2.4	27.1	–10.8	2.7	6.9	15.8	32.7	74.5	11.5	16.5	0.2	34.98	0.21	34.98	0.91	15.79
1059	1.8	26.4	11.7	2.3	–5.3	14.1	33.4	73.7	11.9	15.7	4.2	34.18	1.32	34.18	–2.31	15.11
1238	1.1	34.8	5.6	14.9	4.3	31.3	31.6	76.5	4.2	20.3	1.8	35.47	3.4	35.47	0.64	27.51
1245	0.2	35.0	–5.3	16.1	–4.6	32.0	31.3	76.5	–4.3	21.2	–0.3	35.87	–4.5	35.87	–0.74	28.27
1260	–0.3	36.9	–5.2	18.5	–5.5	33.8	31.2	77.2	–0.5	26.6	1.1	37.18	4.2	37.18	–1.29	30.32
1378	2.5	37.7	8.6	19.2	13.4	32.0	29.3	77.4	7.7	25.4	0.3	38.89	6.1	38.89	3.97	30.28
1428	–1.4	40.9	–11.2	21.4	–12.5	38.4	27.6	78.3	–11.1	28.1	–13.4	39.26	4.5	39.26	–6.57	33.52
1458	–4.0	19.6	–8.0	–1.3	–11.0	13.0	25.7	68.9	5.4	9.0	–12.5	26.86	2.5	26.86	2.05	10.66
1508	–6.1	15.2	–8.3	–7.8	–14.7	8.1	25.1	65.7	–2.5	1.2	1.2	18.94	–2.1	18.94	–2.31	5.94
1595	–4.3	30.3	–11.5	7.6	–20.1	26.2	25.5	75.3	–3.4	19.8	–11.0	25.90	–.12	25.90	–1.42	21.33
1720	–5.9	27.7	–0.8	14.3	–6.2	30.1	26.7	72.8	–23.6	11.7	0.24	26.74	–4.2	26.74	–2.61	25.54
1738	–9.0	28.6	–4.1	16.1	–9.6	32.1	24.0	72.7	–31.5	12.5	3.4	25.23	–2.1	25.23	–6.16	27.15
1745	–11.9	29.2	–6.0	15.0	–12.7	33.3	22.9	72.8	–40.5	11.1	1.21	24.53	–1.1	24.53	–8.58	27.08
2900	11.5	37.2	–5.2	20.9	–15.5	40.7	18.8	76.5	–21.5	25.5	–2.31	36.32	–.23	36.32	–5.28	31.76
3348	1.4	17.6	–9.1	–9.4	–21.2	20.0	18.2	74.9	–14.8	9.6	0.23	18.99	–3.22	18.99	–9.13	8.45

Relative change (%) = (Intensity of untreated biomass – intensity of pretreated biomass) / intensity of untreated biomass x 100.

Abbreviations AH – post acid hydrolysis; DELIG – Post delignification. Assignment (cm^{-1}) of band position are adopted from Kumar et al., 2009; Sun et al., 2005.

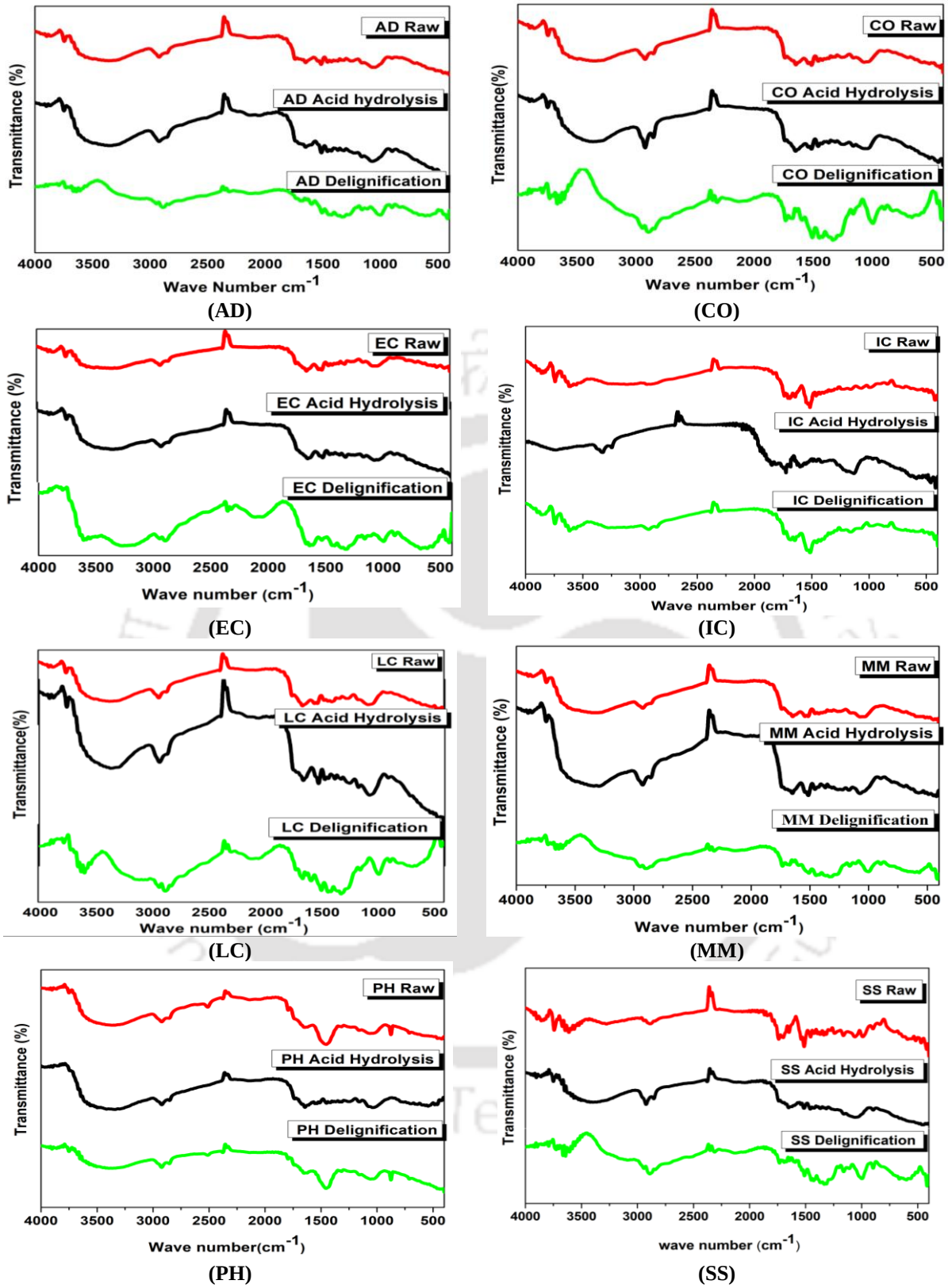

Figure 2.3 FTIR spectra of native or raw biomass, biomass after dilute (1%) acid hydrolysis with autoclaving (121ºC, 15 psi) and biomass after alkaline delignification (1.5% w/v NaOH with sonication). (AD) *Arundo donax*; (CO) *Chromolena odorata*, (EC) *Eichhornia crassipes*, (IC) *Ipomea carnea*, (LC) *Lantana camara*. , (MM) *Mikania micrantha*, (PH) *Parthenium hysterophorus* (SS) *Saccharum spontaneum*.

2.3.3.3 ***XRD analysis:*** Changes in the biomass composition and structure induced by the two pretreatments, i.e. dilute acid hydrolysis and alkaline delignification, can also be mapped by X–ray diffraction. The crystallinity index (CrI) determined by XRD analysis is an excellent tool to assess the extent of removal of the two components of biomass, i.e. hemicellulose and lignin, which have a relatively more amorphous structure as compared to cellulose. A rise in crystallinity index essentially indicates an increase in the percentage of the cellulose content of biomass after pretreatment. The crystallinity indices of the eight biomass species at various stages, namely raw biomass, dilute acid treatment and alkaline delignification, are given in **Table 2.4**. The actual X–ray diffractograms of the eight biomasses are given in **Fig. 2.4.** It could be seen from **Table 2.4** that the crystallinity of the biomass increases after treatment with 1% v/v H_2SO_4 at 121^oC and 15 psi pressure, which indicates removal of the hemicellulose. The extent of the rise in crystallinity is, however, different for the eight biomass species. The biomasses of *Eichhornia crassipes* and *Mikania micrantha* showed close to a 100% increase in crystallinity, while the biomass of *Saccharum spontaneum* showed a very marginal rise. For the biomass of *Lantana camara,* the crystallinity showed a slight reduction with dilute acid treatment. The crystallinity index shows a further rise with alkaline delignification. Alkali pretreatment in the presence of ultrasound leads to delignification, with saponification of the intermolecular ester bonds cross–linking the xylan hemicelluloses and lignin, in addition to breakage of the linkages between cellulose and lignin. **Singh et al., (2014)** observed that the alkaline treatment of lignocellulosic biomass results in a swelling of the biomass, also with an increase in surface area a decrease in the degree of polymerization, separation of the structural linkages between lignin and carbohydrates and disruption of the lignin structure. All these effects contribute to a reduction in the amorphous fraction of biomass and exposure of the crystalline cellulose

fraction, which is reflected in an increase in crystallinity of all the eight biomasses after delignification. These results are in concurrence with the results of **Singh et al., (2014)** who observed an increase in the crystallinity of *Parthenium hysterophorus* after 1% v/v H_2SO_4 treatment at 121°C and 15 psi pressure and delignification with 1.5% w/v NaOH treatment in presence of ultrasound. The results of the X–ray diffraction analysis are additional corroborations that, although conditions for the dilute acid hydrolysis and delignification are not optimized for the eight invasive weeds used in the present study, the pretreatment of the weed biomasses at these conditions was still able to induce desired changes in their composition.

Table 2.4 Characterization of pre–treated biomass by XRD in terms of crystallinity index

Biomass	Crystallinity Index, *CrI* (%)		
	Raw	Post dil. acid hydrolysis	Post delignification
AD	37.50	60	64.70
SS	52.00	56.52	62.50
MM	20.00	38.70	48.57
LC	50.00	47.50	57.14
EC	16.67	33.33	42.85
IC	29.41	45.00	57.89
CO	28.57	43.75	44.40
PH	24.13	27.77	30.76

Abbreviation: *A. donax* (AD), *C. odorata* (CO), *E. crassipes* (EC), *I. carnea* (IC), *L. camara* (LC), *M. micrantha* (MM), *P. hysterophorus* (PH), and *S. spontaneum* (SS).

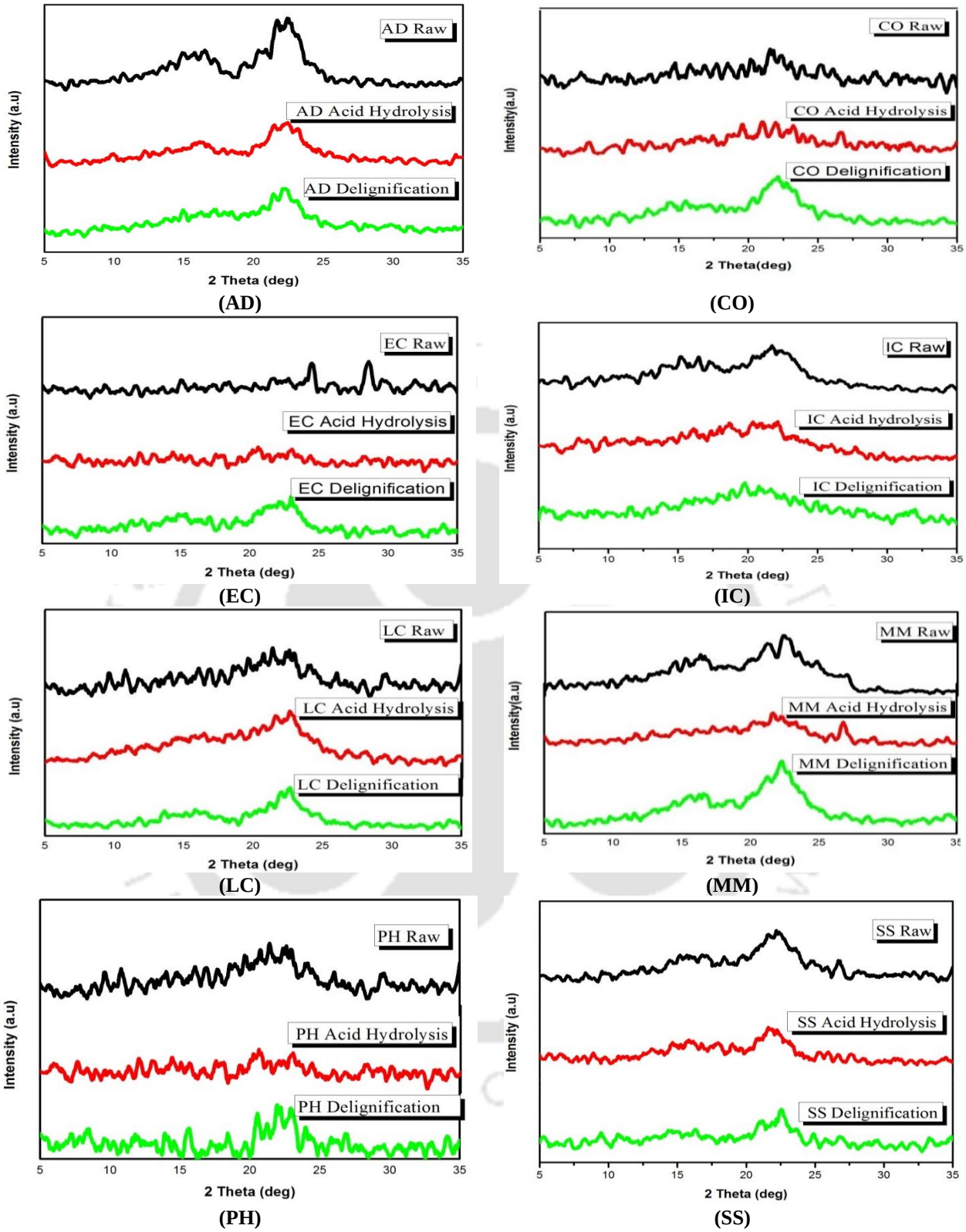

Figure 2.4 X–ray diffractograms of eight biomass species, viz. native biomass and the biomass after different pretreatments. (AD) *Arundo donax*; (CO) *Chromolena odorata*, (EC) *Eichhornia crassipes*, (IC) *Ipomea carnea*, (LC) *Lantana camara*. , (MM) *Mikania micrantha*, (PH) *Parthenium hysterophorus* (SS) *Saccharum spontaneum*

2.4 Conclusion

The present study investigated the bioalcohol production potential of eight invasive weeds, *viz*. *Arundo donax* (AD), *Chromolena odorata* (CO), *Eichhornia crassipes* (EC), *Ipomea carnea* (IC), *Lantana camara* (LC), *Mikania micrantha* (MM), *Parthenium hysterophorus* (PH) and *Saccharum spontaneum* (SS) in terms of the yield of total fermentable sugars from pretreatment and enzymatic hydrolysis. The pretreatment comprised two steps: dilute acid hydrolysis and alkaline delignification with sonication, followed by enzymatic hydrolysis of the pretreated biomass.

These pretreatments were carried out at conditions optimized for the waste biomass of *Parthenium hysterophorus*. Thus, the pretreatment conditions were not optimized specifically, for any of the eight biomasses considered in this study. Despite this limitation, the average TFS yield from the eight invasive weeds was 42.12 g per 100 g of raw biomass, which is on par with the yield from *Parthenium hysterophorus* for optimized pretreatment conditions. This TFS yield corresponded to a (theoretical) bioethanol yield of 22.36 g and a biobutanol yield of 17.26 g per 100 g of raw biomass. These results vividly demonstrate that a consistent production of alcoholic biofuels could be achieved from the use of invasive weeds as multiple feedstocks, even if the pretreatment conditions are not optimized for each of the weeds. The results of the present study have also demonstrated the feasibility of the large–scale production of alcoholic biofuels employing multiple biomass feedstocks of different invasive weeds.

References

Allan, G.G., Carroll, J.P., Negri, A.R., (1992). TAPPI JOURNAL., 75(1), 175.

Bharadwaja, S.T.P., Singh, S., Moholkar, V.S., 2015. Design and optimization of a sono–

hybrid process for bioethanol production from *Parthenium hysterophorus*. Journal of Taiwan Institute Chemical Engineering, 51, 71–78.

Borah, A.J., Agarwal, M., Poudyal, M., Goyal, A., Moholkar, V.S., 2016(b). Mechanistic investigation in ultrasound induced enhancement of enzymatic hydrolysis of invasive biomass species, Bioresource Technology, 213, 342-349.

Chakma, S., Moholkar, V.S., 2013. Physical mechanism of sono–fenton process. AIChE Journal, 59(11), 4303–4313.

Chaudhury, G., Singh, L.K., Ghosh, S., 2012. Alkaline pretreatment methods followed by acid hydrolysis of *Saccharum spontaneum* for bioethanol production. Bioresource Technology, 124, 111–118.

Ekman, A., Wallberg, O., Joelsson, E., Borjesson, P., 2013. Possibilities for sustainable biorefineries based on agricultural residues – A case study of potential straw–based ethanol production in Sweden. Applied Energy, 102, 299–308.

Kuhad, R.C., Gupta, R., Khasa, Y.P., Singh, A., 2010. Bioethanol production from *Lantana camara* (red sage): pretreatment saccharification and fermentation. Bioresource Technology, 101, 8348–8354.

Kumar, R., Mago, G., Balan, V., Wyman, C.E., 2009. Physical and chemical characterizations of corn stover and poplar solids resulting from leading pretreatment technologies. Bioresource Technology, 100, 3948–3962.

Lima, M.A., Lavorente, G.B., Da Silva, H.K.P., Bragatto. J., Rezende, C.A., Bernardinelli, O.D., DeAzevedo, E.R., Gomez, L.D., McQueen–Mason, S.J., Labate, C.A., Polikarpov, I., 2013. Effects of pretreatment on morphology, chemical composition and enzymatic digestibility of eucalyptus bark: a potentially valuable source of fermentable sugars for biofuel production – Part 1.

Biotechnology Biofuels, 6, 75.

Moholkar, V.S., Singh, S., 2013. A corrigendum to 'Feasibility of rice straw as alternative substrate for biobutanol production' by Ranjan *et al.* Applied Energy, 116, 436–8.

Nelson, N.A., 1944. Photometric adaptation of the Somogyi method for the determination of glucose. Journal of Biological Chemistry, 153(2), 375–80.

Patidar, R., Khanna, S., Moholkar, V.S., 2012. Physical features of ultrasound assisted enzymatic degradation of recalcitrant organic pollutants. Ultrasound Sonochemistry, 19(1), 104–118.

Ranjan, A., Khanna, S., Moholkar, V.S., 2013. Feasibility of rice straw as alternate substrate for biobutanol production. Applied Energy, 103, 32–38.

Raspolli Gallettia, A.M., Antonettia, C., Ribechinia, E., Colombinia, M.P., Nassi o Di Nassob, N., Bonarib, E., 2013. From giant reed to levulinic acid and gamma–valerolactone: A high yield catalytic route to valeric biofuels. Applied Energy, 102, 157–162.

Segal, L., Creely, J.J., Martin, A.E., Jr., Conrad, C.M., 1962 An empirical method for estimating the degree of crystallinity of native cellulose using the X–ray diffractometer. Textile Research Journal, 29, 786–94.

Singh. S., Khanna, S., Moholkar, V.S., Goyal, A., 2014. Screening and optimization of pretreatments for *Parthenium hysterophorus* as feedstock for alcoholic biofuels. Applied Energy, 129, 195–206.

Sivasankar, T., Paunikar, A.W., Moholkar, V.S., 2007. Mechanistic approach to enhancement of the yield of a sonochemical reaction. AIChE Journal, 53(5), 1132–1143.

Somogyi, M., 1945. A new reagent for the determination of sugars. Journal of Biological Chemistry, 160, 61–68.

Sun, X.F., Xu, F., Sun, R.C., Fowler, P., Baird, M.S., 2005. Characteristics of degraded cellulose obtained from steam exploded wheat straw. Carbohydrate Research Journal, 340(1), 97–106.

Teramoto, Y., Lee, S.H., and Endo, T. 2009. Cost reduction and feedstock diversity for sulphuric acid– free ethanol cooking of lignocellulosic biomass as a pretreatment to enzymatic saccharification. Bioresource Technology, 100, 4783–4789.

Updegraff, D.M., 1969. Semi micro determination of cellulose in biological materials. Analytical Biochemistry 3,2, 420–424.

You, T., Zhang. L., Zhou, S., Xu, F., 2014. Protic acid resin enhanced 1-butyl-3-methylimidazolium chloride pretreatment of *Arundo donax* Linn. Bioresource Technology, 167, 574-577.

CHAPTER 3: MECHANISTIC INVESTIGATION IN ULTRASOUND INDUCED ENHANCEMENT OF ENZYMATIC HYDROLYSIS OF INVASIVE BIOMASS SPECIES[§]

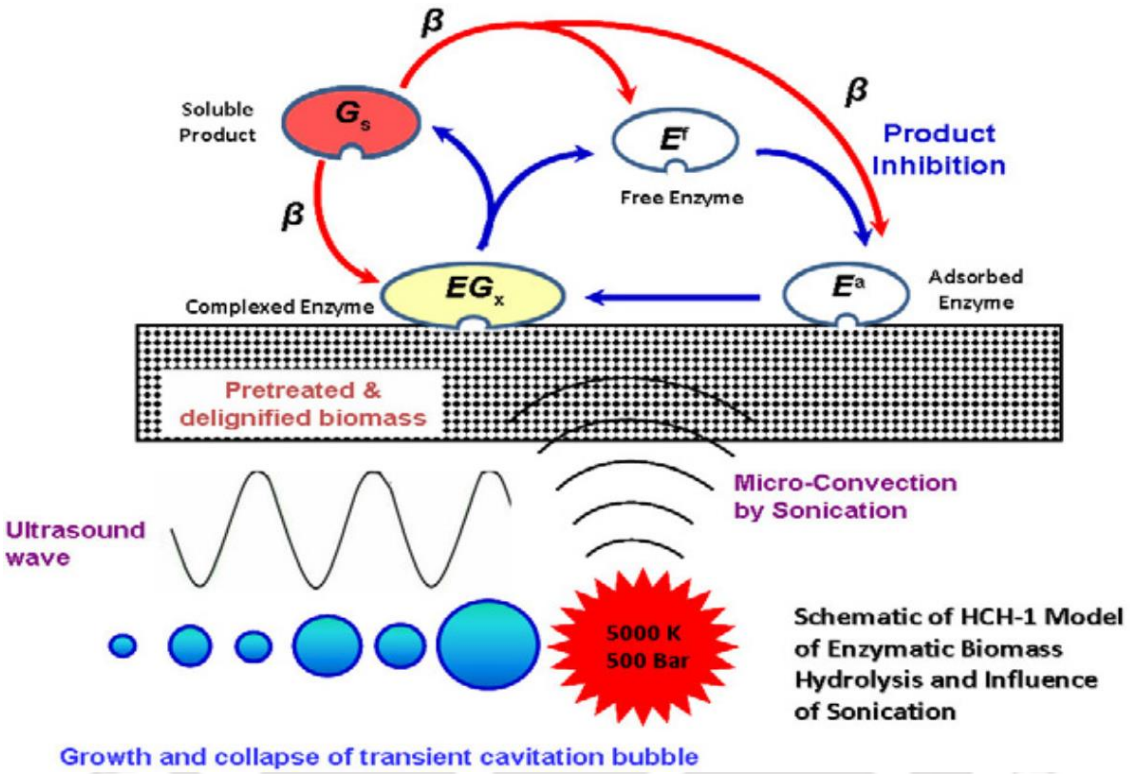

Chapter Highlights

- Enzymatic hydrolysis of eight invasive weeds with mechanical agitation and sonication
- Experimental results fitted to HCH-1 model of hydrolysis using Genetic Algorithm
- Sonication enhances kinetics of enzymatic hydrolysis by more than 10-fold.
- Sonication augments enzyme activity by conformational changes in secondary structure.
- Reduction in product inhibition and increase in substrate affinity of enzyme by sonication.

[§] Also see Borah A.J., Agarwal, M., Poudyal, M., Goyal, A., Moholkar, V.S. (2016) Mechanistic investigation in ultrasound induced enhancement of enzymatic hydrolysis of invasive biomass species. *Bioresource Technology*, 213, 342-349.

CHAPTER 3

MECHANISTIC INVESTIGATION IN ULTRASOUND INDUCED ENHANCEMENT OF ENZYMATIC HYDROLYSIS OF INVASIVE BIOMASS SPECIES

3.1 Introduction

Bioalcohol production from lignocellulosic biomass (also known as second generation biofuel) involves three steps: (1) biomass pretreatment (acid hydrolysis and delignification), (2) enzymatic hydrolysis and (3) fermentation of pentose and hexose rich hydrolyzate obtained from biomass pretreatment and enzymatic hydrolysis. Bioalcohol production from common invasive weeds such as *Arundo donax* **(Silva et al., 2015; Loaces et al., 2017)**, *Parthenium hysterophorus* **(Singh et al., 2015a, b; Bharadwaja et al., 2015)** *Lantana camara* **(Kuhad et al., 2010; Kuila and Banerjee, 2014)** *Saccharum spontaneum* **(Chandel et al., 2011; Kataria and Ghosh, 2014)**, *Eichhornia crassipes* (**Photisantikul et al., 2013; Yan et al., 2015)** and *Ipomea carnea* **(Kumari and Pramanik, 2013)** have been reported. The productivity of bioalcohol can be enhanced by intensification of kinetics and yield of above three steps. Especially, the second step of enzymatic hydrolysis is of crucial due to high cost of enzymes and slow kinetics. Intensification of the process essentially involves exploring efficient ways of introducing energy into the system for bringing out desired physical/chemical change. Ultrasound irradiation (or sonication) is an efficient method for intensification of physical, chemical and biological processes. Sonication of the liquid medium essentially induces phenomenon of cavitation, which is nucleation, growth and implosive collapse of

gas/vapor bubbles driven by pressure radiation due to ultrasound. Both sonication and cavitation create intense energy concentration on temporal and spatial scale, which markedly improves the kinetics of the process. The technique of ultrasound treatment has been previously employed for enhancement of rice straw pretreatment **(Suresh et al., 2014)**, delignification **(Singh et al., 2014; Bharadwaja et al., 2015)**, enzymatic hydrolysis **(Singh et al., 2015a)** and fermentation **(Singh et al., 2015a, b)**. In these reports, we have explored enzymatic hydrolysis of multiple invasive weeds with ultrasound. The weeds used were: *Arundo donax* (AD), *Chromolena odorata* (CO), *Eichhornia crassipes* (EC), *Ipomea carnea* (IC), *Lantana camara* (LC), *Mikania micrantha* (MM), *Parthenium hysterophorus* (PH) and *Saccharum spontaneum* (SS) which are abundantly found in the northeastern region of India. A peculiarity of the present study is that enzymatic treatments of all biomasses have been carried out under constant conditions. These conditions have been adopted from our earlier study **(Bharadwaja et al., 2015)** on sono-hybrid process for bioethanol production from waste biomass of *Parthenium hysterophorus*. The pretreatment of the invasive weeds prior to enzymatic hydrolysis has also been carried out under constant conditions, which have been optimized for *P. hysterophorus* **(Singh et al., 2014)**. The rationale underlying this strategy is explained subsequently. Commercial cellulase and cellobiase enzymes have been used for hydrolysis.

Another objective of this study is to gain mechanistic insight into ultrasonic enhancement of enzymatic hydrolysis. Previous authors have reported studies in ultrasonic enhancement of the enzymatic hydrolysis of pretreated biomass. A review of literature in this area is given in **Table 1.6** of Chapter 1. However, most of these studies have a black-box approach and are focused on the results rather than rationale. Little

attempt is dedicated in these studies to establish the physical mechanism of ultrasound induced enhancement of the enzymatic hydrolysis by identifying links between physics of ultrasound/cavitation and biophysical mechanism of hydrolysis. We have adopted a dual strategy in our investigation, *viz*. (1) comparative analysis of secondary structure of cellulase and cellobiase enzymes in native form and after sonication, and (2) fitting of the time profiles of reducing sugar release to the HCH-1 model for enzymatic cellulose hydrolysis. This model describes the heterogeneous hydrolysis of cellulose (in solid form) taking into account adsorption, complexation and inhibition of enzyme in free, adsorbed and complex form. Circular dichroism analysis has revealed the conformational changes in the secondary structure of enzyme induced by ultrasound and cavitation, which led to unfolding of the enzyme proteins and augmentation of the enzyme activity. On the other hand, comparative analysis of values of kinetic and physiological parameters obtained after fitting of HCH-1 model **(Holtzapple et al., 1984)** to the experimental data helped in getting a mechanistic insight into the synergistic effects between mechanism of enzyme action and physics of ultrasound and cavitation.

3.2 Materials and methods

3.2.1 Materials

Following chemicals have been procured from Fisher Scientific, India: citric acid, sodium mono-phosphate, sodium azide, sulphuric acid and Sodium hydroxide. Commercial enzyme cellulase (6 U/mg) produced by *Trichoderma reesei* (ATCC 26921) and cellobiase (or β–1,4-glucosidase, 250 U/g) produced by *Aspergillus niger* was procured from Sigma Aldrich, USA.

3.2.2 Biomass collection and processing

The lignocellulosic biomass of all eight weeds: *Arundo donax* (AD), *Chromolena odorata* (CO), *Eichhornia crassipes* (EC), *Ipomea carnea* (IC), *Lantana camara* (LC), *Mikania micrantha* (MM), *Parthenium hysterophorus* (PH) and *Saccharum spontaneum* (SS) were collected from IIT Guwahati campus and nearby areas. The entire process followed was same as described in Chapter 2 (Subsection 2.2.1).

3.2.3 Pretreatment of raw biomass and hydrolysis of pretreated biomass

As noted earlier, all eight biomasses have been pretreated under constant conditions, viz. 1% (v/v) H_2SO_4 (equivalent to 0.36 N), 10% w/v biomass, autoclaving at 121°C and 15 psi for 30 min followed by rapid steam release. These conditions have been optimized for acid hydrolysis of the invasive weed of *P. hysterophorus* in our earlier study **(Singh et al., 2014).** The solid residue obtained after pretreatment was subjected to delignification by ultrasound assisted alkaline treatment. The conditions for delignification were as follows: 1.5% w/v NaOH, 2% w/v biomass, 30°C with treatment time of 10 min. These conditions have also been optimized for the invasive weed of *P. hysterophorus* in our previous study **(Bharadwaja et al., 2015)**. The residue obtained after both acid hydrolyzed and delignification was washed several times till neutral pH was obtained. The residual biomass was dried in a hot air oven at 60 ± 3 °C for 12 h. This residue was subjected to enzymatic hydrolysis using commercial cellulase and cellobiase (*β*– 1,4-glucosidase) enzymes under two protocols, *viz.* mechanical shaking and sonication. The lignocellulosic composition of the eight invasive weeds in native and post-treatment form is given in Table 2.1 (B) of chapter 2.

3.2.4 Protocol of enzymatic hydrolysis of biomass with mechanical shaking

Enzymatic hydrolysis with mechanical shaking (henceforth called as control experiments) was carried out in 150 mL Erlenmeyer flask with total reaction volume of 20 mL using an incubator–shaker (Scigenics, India). Mechanical shaking was applied at 150 rpm and temperature of 50 °C. pH of the reaction mixture was maintained 5 using citrate–phosphate buffer in all experiments. Other parameters of enzymatic hydrolysis (or saccharification) of delignified biomasses of all eight weed species were maintained at the optimum values reported by **Bharadwaja et al. (2015)** as follows: (1) concentration of pretreated biomass in reaction mixture = 4.2% w/v, and (2) concentrations of cellulase and cellobiase as 135 and 75 FPU/g biomass, respectively. Total time of enzymatic hydrolysis was 120 h. 0.005% w/v Sodium azide solution was added to the mixture to avoid external microbial contamination **(Singh et al., 2015)**. The progress of the enzymatic hydrolysis was monitored by withdrawing 0.1 mL samples of reaction mixture periodically and analyzing for release of sugar.

3.2.5 Protocol for enzymatic hydrolysis of biomass with sonication

The protocol for enzymatic hydrolysis with sonication (henceforth called test experiments) was very similar to that with mechanical shaking. Parameters such as reaction volume, biomass concentration, enzyme concentration were exactly same as for the mechanical shaking. Experiments were carried out in an ultrasound bath (Elma, Germany; model: Transonic T-460, volume: 2 L, dimensions: 25 cm x 15 cm x 10 cm) operating at a frequency of 35 kHz and theoretical power input of 35 W. This bath was filled with water, which acted as medium for propagation of ultrasound. This bath had facility of automatic amplitude compensation due to which the net acoustic power delivered to the bath remained constant irrespective of the changes occurring in the bath

during course of reaction. Prior to the experiments, the pressure amplitude of the ultrasound wave generated in the bath was determined using calorimetric technique as 1.5 bar **(Sivasankar et al., 2007; Bhasarkar et al., 2013).** The temperature of water in the bath increased during sonication. By periodic replacement of some quantity of water in the bath, the temperature of water was maintained at 30°C during the sonication period. A 100 mL conical flask made of borosilicate glass was used for the experiments with total reaction volume of 20 mL. The temperature of the reaction mixture inside the flask was same as that of water outside. The flask was dipped to about 1/4th of its height in water inside the bath. Due to significant spatial variation of the acoustic intensity in the bath, the position of reaction flask was carefully maintained constant in all experiments. Total time of sonication of the enzymatic hydrolysis reaction mixture was 10 h with 10% duty cycle (i.e. 1 min of sonication and 9 min of mechanical shaking for every 10 min of treatment). Similar to the control experiments, progress of the sugar release in enzymatic hydrolysis was monitored by periodic withdrawal of 0.1 mL aliquots of reaction mixture and analyzing them for concentration of reducing sugar.

3.2.6 Total reducing sugar estimation

Hexose-rich enzyme hydrolysates collected intermittently from both set of experiments were subjected to centrifugation for 10 min at 10,000 rpm (26,832g) at 4°C to remove particulate matter. Total reducing sugar in the hydrolyzate was estimated using method of **Nelson (1944) and Somogyi (1945).**

3.2.7 Analysis of enzyme structure

The morphological changes in the structure (i.e. secondary and tertiary structures) of cellulase and cellobiase enzyme induced by physical and chemical effects of

ultrasound/cavitation have been determined using intrinsic fluorescence and circular dichroism analysis. The procedures for the same have been described below.

3.2.7.1 Intrinsic fluorescence analysis of enzymes before and after exposure to sonication

Three samples of cellulase and cellobiase enzymes were used for measurement of intrinsic fluorescence, viz. (1) native enzyme (i.e. without any treatment), (2) enzyme after treatment with mechanical agitation, and (3) enzyme after ultrasound treatment at ambient pressure of 101.3 kPa. The total treatment time was 1 h with both mechanical agitation and sonication. A duty cycle of 10% was employed for enzyme treatment with ultrasound (as stated previously in the experimental section). Intrinsic fluorescence spectra of all three enzyme samples were measured at temperature of 25° ± 1°C with fluorescence spectrophotometer (Horiba Scientific, model: FluoroMax-4) at 280 nm excitation wavelength (slit = 10 nm), 300–500 nm emission wavelength (slit = 10 nm) and 10 nm/s of scanning speed. Citrate phosphate buffer (0.05 M, pH 5) used for dissolution of cellulase enzyme was used as a blank solution for these measurements.

3.2.7.2 Circular dichroism (CD) analysis of enzymes before and after exposure to sonication

Far UV circular dichroism (CD) spectra of the cellulase and cellobiase enzymes were recorded from the difference in absorption of left and right-circularly polarized light in a Jasco J-815 spectro-polarimeter using a suprasil quartz cuvette of 1 mm optical path length at temperature (25 ± 1°C). The spectra were recorded between 240 and 190 nm with 3 replicates at a scan rate of 100 nm/min with 1 nm bandwidth and a path length of the sample cell of 1 mm. The CD data were expressed in terms of mean residue ellipticity

[h] based on the average molecular weight range of (42–68 kDa) and concentration 50 mM of cellulase or cellobiase solution **(Coral et al., 2002)**. The spectrum of phosphate buffer solution was used as blank and subtracted from the average of three spectra to obtain a corrected spectrum for each samples. The secondary structures of native enzyme and enzyme after treatment with mechanical agitation or sonication were analyzed using an online server DICHROWEB **(Sreerama and Woody, 2000; Whitmore and Wallace, 2004 & 2008).**

3.3 Mathematical model of enzyme hydrolysis of delignified biomass

The mathematical model for enzymatic hydrolysis of pretreated biomass used in this study is the HCH-1 model proposed by **Holtzapple (1981) and Holtzapple et al. (1984).** This first order model is essentially applicable for small particle size biomass substrates (or finely ground substrates as in present study), which are rich in cellulose content. In our previous paper on enzymatic hydrolysis of *P. hysterophorus* **(Singh et al., 2015),** a description of this model along with relevant equations has been given. However, for the convenience of the reader, we have reproduced this description of HCH-1 model. In general, pure cellulose substrates exhibit 1st order kinetic for enzymatic hydrolysis, while impure substrates exhibit 2nd order kinetics **Holtzapple et al. (1984)**. This feature was independent of the size of the particles of biomass. This essentially signifies secondary role of mass transfer in the enzymatic hydrolysis process and also that chemical reaction kinetics limits the hydrolysis reactions (**Holtzapple et al., 1984)**. The basic mechanism of the enzymatic hydrolysis of cellulose according to HCH-1 model is depicted in **Fig. 3.1.** The first step in this mechanism is the reversible adsorption of free cellulase, E^f, onto free site cellulose, G_x^f , characterized by equilibrium constant, $1/\delta$. The next step is formation of enzyme/substrate complex with combination of the active site of

adsorbed enzyme, E^a, with a glucose site. The equilibrium constant of this step is $1/\eta$. The equilibrium constants are expressed as follows:

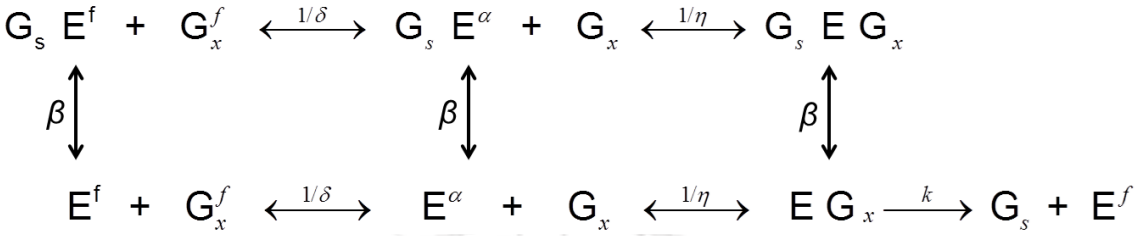

Fig. 3.1. Basic mechanism of the enzymatic hydrolysis of cellulose according to HCH-1 model.

$$\frac{1}{\delta} = \frac{[E^a]}{[E^f][G_x^f]} \quad (1)$$

$$\frac{1}{\eta} = \frac{[EG_x]}{[E^a]} \quad (2)$$

An underlying assumption in expression for equilibrium constant η is that for pure cellulosic material, the concentration of active sites does not change with hydrolysis. The enzyme–substrate complex is then irreversibly converted into the soluble product G_s with rate constant of k. This step is assumed to be the slowest and hence rate controlling step of enzymatic hydrolysis in HCH-1 model. Hence, overall reaction velocity is written as:

$$v = k[EG_x] \quad (3)$$

Inhibition of enzyme: As depicted in **Fig. 3.1**, enzyme exists in the system in three forms, viz. free form, E^f, adsorbed form, E^a, and complexed form, EG_x. The products of the hydrolysis, *viz.* cellobiose and glucose, can inhibit the enzyme in all of these forms. However, cellobiose is a transient and intermediate product of hydrolysis process, and gets rapidly transformed into glucose. Hence, HCH-1 model accounts only for glucose inhibition, which is characterized by the product binding constant, β. This equilibrium

constant for product binding is assumed to be same for all enzyme species. A material balance on enzyme species yields:

$$\beta = \frac{\left[G_s E^f\right]}{\left[G_s\right]\left[E^f\right]} \equiv \frac{\left[G_s E^a\right]}{\left[G_s\right]\left[E^a\right]} \equiv \frac{\left[G_s E G_x\right]}{\left[G_s\right]\left[E G_x\right]} \tag{4}$$

The inhibition factor is given as: $i = \frac{1}{1+\beta\left[G_s\right]}$ (5)

Taking material balances of the substrate and enzyme species yield following expressions:

$$\left[G_x^f\right] = \frac{\left[G_x\right]}{1+\varepsilon\ \left(1+\beta\left[G_s\right]\right)\left[\frac{1}{\delta}+\frac{1}{\delta}\frac{1}{\eta}\right]\left[E^f\right]} \tag{6}$$

$$\left[E^f\right] = \frac{\left[E\right]}{\left(1+\beta\left[G_s\right]\right)\left(1+\left[\frac{1}{\delta}+\frac{1}{\delta}\frac{1}{\eta}\right]\left[G_x^f\right]\right)} \tag{7}$$

Elimination of the term [EG_x] in the expression for reaction velocity finally gives:

$$v = \frac{d\left[G_s\right]}{dt} = \frac{\kappa\left[G_x\right]\left[E\right]\left(\frac{1}{1+\beta\left[G_s\right]}\right)}{\alpha+\phi\left[G_x\right]+\varepsilon\left[E\right]} \tag{8}$$

where, $\kappa = \frac{k}{\eta+1}$ and $\alpha = \frac{\eta\delta}{\eta+1}$ (9)

Factor φ, represents extent of enzyme adsorption onto cellulose, and is determined as follows:

$$\phi = \frac{\left[G_x^f\right]}{\left[G_x\right]} = \frac{\text{free cellulose sites}}{\text{total cellulose sites}} \tag{10}$$

(1) Elimination of the term $\left[E^f\right]$ in expression for $\left[G_x^f\right]$ yields a quadratic equation in terms of $\left[G_x^f\right]$, whose positive root is:

$$\phi = \frac{[G_x] - \alpha - \varepsilon[E] + \sqrt{\left([G_x] - \alpha - \varepsilon[E]\right)^2 + 4\alpha[G_x]}}{2[G_x]} \tag{11}$$

(2) φ can also be obtained by substitution for $\left[G_x^f\right]$ in equation for φ:

$$\phi = \frac{\alpha}{\alpha + \varepsilon\ (1 + \beta\ [G_s]\ \left[E^f\right]} \tag{12}$$

Values of different parameters required for simulation of enzyme hydrolysis using HCH-1 model are as follows:

(1) Pretreated and delignified biomass concentration of 4.21% w/v or 42.1 g/L. It should be noted that, as depicted in **Table 2.1B** of Chapter 2, there is varying residual concentration of lignin in the biomass of all eight weeds even after delignification. Therefore, the actual cellulose concentration in the reaction mixture for the eight weeds is as follows: AD = 38.32 g/L, CO = 39.59 g/L, EC = 40.73 g/L, IC = 39.84 g/L, LC = 39.04 g/L., MM = 39.44 g/L, PH = 39.17 g/L and SS = 40.43 g/L.

(2) Cellulase concentration = 0.94 g/L (calculated on the basis of specific activity = 6 U/mg, and optimized concentration = 135.85 FPU/g pretreated and delignified biomass), β-glucosidase concentration = 12.6 g/L (calculated on the basis of specific activity = 250 U/g, and optimized concentration = 75 FPU/g pretreated and delignified biomass).

Profiles of total reducible sugar release for 10 h treatment have been considered for simulation of ultrasound-assisted enzymatic hydrolysis, while profile for 36 h treatment has been considered for enzymatic hydrolysis with mechanical agitation. These

time periods have been selected on the basis of incremental sugar release during hydrolysis. The incremental sugar release was less than 5% for every hour of treatment beyond 36 h for mechanical shaking and beyond 10 h for sonication. HCH-1 model has been derived for a single enzyme having dual activity of endoglucanase and cellobiase. Correspondingly, the enzyme concentration used in the simulations of HCH-1 model is 6.77 g/L, which is the average of cellulase and β-glucosidase concentration mentioned above. The expression for reaction velocity contains four parameters, *viz*. α, β, ε and κ, which characterize kinetics and physiology of the enzymatic hydrolysis. The numerical values of these parameters are obtained by comparison of the numerical solution of the ordinary differential equation (ODE) for reaction velocity with experimental profile of total reducing sugar (i.e. the soluble product, G_s). For calculating the simulated profile for soluble product of hydrolysis, and matching it with experimental profile, optimum values of the model parameters in Eq. (8) need to be determined. This ODE was solved using Runge–Kutta 4th order method. The optimum values of the model parameters were determined by calculating root mean square (RMS) error between experimental values and model results using Genetic Algorithm (GA) (Flowchart given in **Appendix B Fig. B1**). The objective function for optimization was defined on the basis of squared error as:

$$obj = \min\left[\sum_{i=1}^{n} er_i\right] \tag{13}$$

where, n is the number of data points for reducing sugar concentration. The error term, er, is defined as:

$$er = \left(G_s^{\exp} - G_s^{\text{model}}\right)^2 \tag{14}$$

The Genetic Algorithm minimizes the objective function and gives the optimized values of model parameters, for which the experimental and simulated profiles of total reducible sugar release match as closely as possible. A quantitative comparison of the model

parameters, *viz.* α, β, ε and κ, for control and test experiments gives the mechanistic account of the influence of ultrasound on enzymatic hydrolysis of pretreated biomass.

3.4 Results and Discussion

As noted earlier, a peculiar feature of the present study is that enzymatic hydrolysis of pretreated biomass of all eight invasive weeds has been carried out under constant conditions instead of the conventional approach of statistical optimization of the conditions for every biomass. Before proceeding to the results and discussion section, we would like to explain the rationale underlying enzymatic hydrolysis at constant conditions. Commercial scale production of bioalcohol requires very large quantities of biomass feedstocks. Considering production/availability of different biomasses in different parts of the year, the biofuel industry may require to change the feedstock. Sufficiently large quantities of a single biomass may not be available throughout the year. It may not be practical to optimize hydrolysis conditions for every biomass used as feedstock. Even if such studies are conducted, the optimum conditions of hydrolysis, *viz.* pH, enzyme concentration, biomass concentration and temperature, may show significant variations for different biomasses. Hence, equipment designed for hydrolysis of one biomass may not be suitable for another biomass. Frequent replacement of process equipment with biomass feedstock is rather impractical for the industry. Under this limitation, it is inevitable to keep hydrolysis conditions same for all biomasses employed as feedstock. The quality of the hydrolyzates resulting from hydrolysis of different biomasses, in terms of reducible sugar content, can show significant variations, which would ultimately affect the net production of alcoholic biofuel. The present study essentially attempts to address this issue with mechanistic approach of concurrent analysis of experimental and simulations results of each biomass.

3.4.1 Experimental results of enzymatic hydrolysis

The time profiles of total reducible sugar release during enzymatic hydrolysis of pretreated and delignified biomass of eight invasive weeds have been depicted in **Figs. 3.2** and **3.3**. **Fig. 3.2** depicts the results for mechanical agitation (or shaking) of the hydrolysis mixture, while **Fig. 3.3** depicts the results for hydrolysis with ultrasound irradiation. **Figs**. **3.2** and **3.3** also show the simulated profile of sugar release using HCH-1 model for enzymatic hydrolysis. It could be inferred that experimental and simulated profiles match well, which essentially shows that enzymatic hydrolysis of all eight invasive weeds under both mechanical agitation and sonication is well described by the HCH-1 model. **Table 3.1** summarizes the total reducible sugar release from the eight biomasses under conditions of mechanical agitation and sonication. The data shown in **Table 3.1** is a clear representation of the beneficial effect of ultrasound and cavitation in accelerating the kinetics of sugar release in enzymatic hydrolysis of all 8 biomasses more than 10×. Nearly same TRS yield has been obtained using sonication in 10 h of treatment against 120 h treatment with mechanical agitation. *Arundo donax* (AD) showed the least amount of sugar release in the stipulated time of ultrasound treatment. The possible explanation could be the partial removal of residual lignin after delignification (in our earlier study) and complex structure of lignin with predominance of G unit interlinked with greater amount of tricin **(You et al., 2014**), which may enhance the stability during NaOH treatment.

3.4.2 Simulation results of enzymatic hydrolysis using HCH-1 model

The results of simulations of enzymatic hydrolysis using HCH-1 model are depicted in **Table 3.2**, which lists the values of the model parameters under conditions of

mechanical agitation and sonication for the eight invasive weeds obtained through Genetic Algorithm optimization.

Table 3.1 Total reducing sugar yield (TRS) after enzymatic hydrolysis for various biomasses

Biomass	Mechanical agitation*		Sonication
	Treatment period: 36 h (considered for simulations)	Total treatment period: 120 h (g/L)*	Treatment period: 10 h (g/L)
AD	30.48 ± 0.56	39.94 ± 0.28	22.41 ± 0.26
CO	25.77 ± 0.46	36.12 ± 0.18	39.04 ± 0.32
EC	31.86 ± 0.24	41.03 ± 0.12	38.09 + 0.45
IC	32.73 ± 0.25	37.22 ± 0.24	32.54 ± 0.46
LC	27.81 ± 0.42	35.90 ± 0.62	36.09 ± 0.72
MM	24.86 ± 0.65	33.42 ± 0.70	35.90 ± 1.02
PH	27.22 ± 0.32	38.10 ± 0.12	34.71 ± 0.46
SS	35.77 ± 1.20	40.21 ± 0.46	40.02 ± 0.42

** The total treatment period for enzymatic hydrolysis with mechanical agitation was 120 h. However, incremental sugar release after 36 h was negligible, and hence, the total reducing sugar released after 36 h has been considered for analysis.*

Table 3.2. Simulation results of enzymatic hydrolysis: Values of the kinetic and physiological parameters in HCH–1 model

Biomass species	Control experiment (mechanical agitation)					Test experiment (under sonication)				
	κ	A	β	ε	F–best	K	α	B	ε	F–best
AD	0.72	0.74	0.38	0.06	5.81	1.21	0.51	0.27	0.06	2.21
CO	1.41	0.79	0.93	0.20	3.30	2.39	0.20	0.22	0.20	4.70
EC	1.01	0.34	0.56	0.14	4.60	1.85	0.25	0.25	0.15	4.76
IC	1.59	0.52	0.43	0.41	2.98	1.93	0.30	0.29	0.42	3.76
LC	1.05	0.49	0.79	0.03	5.00	1.69	0.35	0.32	0.04	5.60
MM	0.38	0.55	0.33	0.11	3.40	1.66	0.42	0.28	0.10	4.20
PH	1.22	0.50	0.60	0.22	4.76	1.99	0.15	0.42	0.22	2.59
SS	0.51	0.31	0.21	0.10	4.60	1.98	0.26	0.12	0.11	6.10

Notation: *κ – Lumped kinetic constant of enzymatic hydrolysis (h^{-1}); α - Lumped constant for enzyme-substrate complexation (g/L); β - Product binding constant (L/g); ε - Number of cellulose sites covered by adsorbed or complexed enzyme; F-best – Best fitness value for the model parameters.*

The four parameters, *viz*. κ, α, β and ε, which represent kinetics and physiology of the hydrolysis process show following trends in test and control experiments, which reveal the mechanics of the effect of sonication on enzymatic hydrolysis system: (1) enhancement in lumped kinetic constant (κ) of the hydrolysis; (2) reduction in lumped constant for enzyme/substrate complexation (α) indication enzyme/substrate affinity; (3) reduction in product binding constant (β) indicative of extent of product inhibition, and (4) no change in value of ε in test and control experiments, which indicates practically constant adsorption of cellulase/cellobiase on cellulose substrate. Enhancement in κ with concurrent reduction in α is attributed to microturbulence and intense micro-mixing generated by ultrasound and cavitation in the hydrolysis reaction mixture, which promotes faster transport and enhanced interaction of enzyme with substrate. Intense micro-convection also helps in faster diffusion of the soluble product away from cellulose surface and its dilution in the medium. This reduces the extent of product inhibition of the enzyme, as indicated by reduction in product binding constant, β. Intense micro-convection also assists faster splitting of the enzyme–substrate complex, which results in enhanced reaction velocity – as indicated by trend in lumped kinetic constant, κ. Practically same values of ε with mechanical agitation and sonication indicate that adsorption of the enzyme on cellulose is not limited by mass transfer.

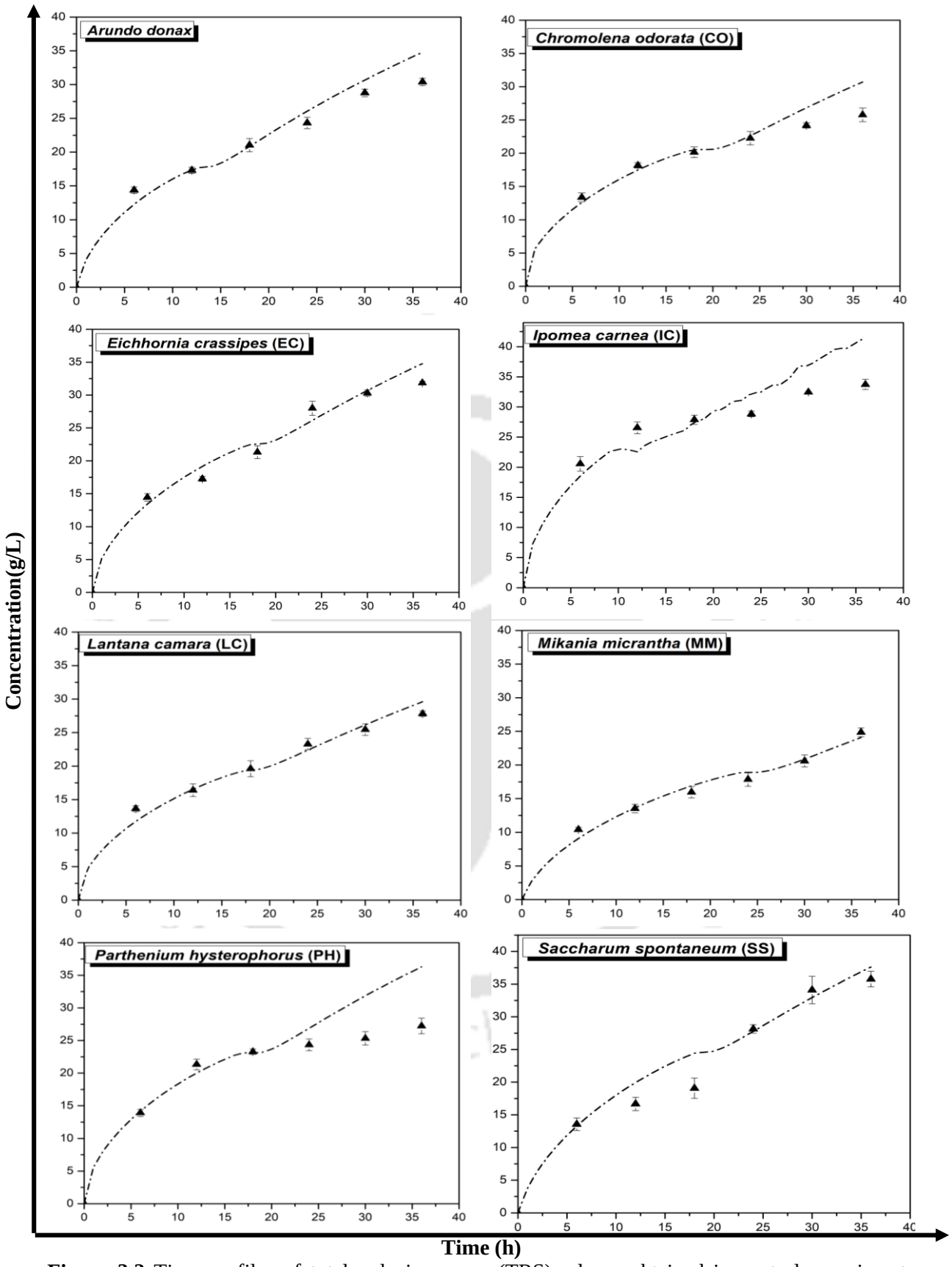

Figure 3.2 Time profiles of total reducing sugar (TRS) release obtained in control experiments (employing mechanical agitation for enzymatic hydrolysis mixture) for various invasive weeds. ▲: denotes the experimental time profiles of TRS, ----- : denotes Simulation time profile of TRS

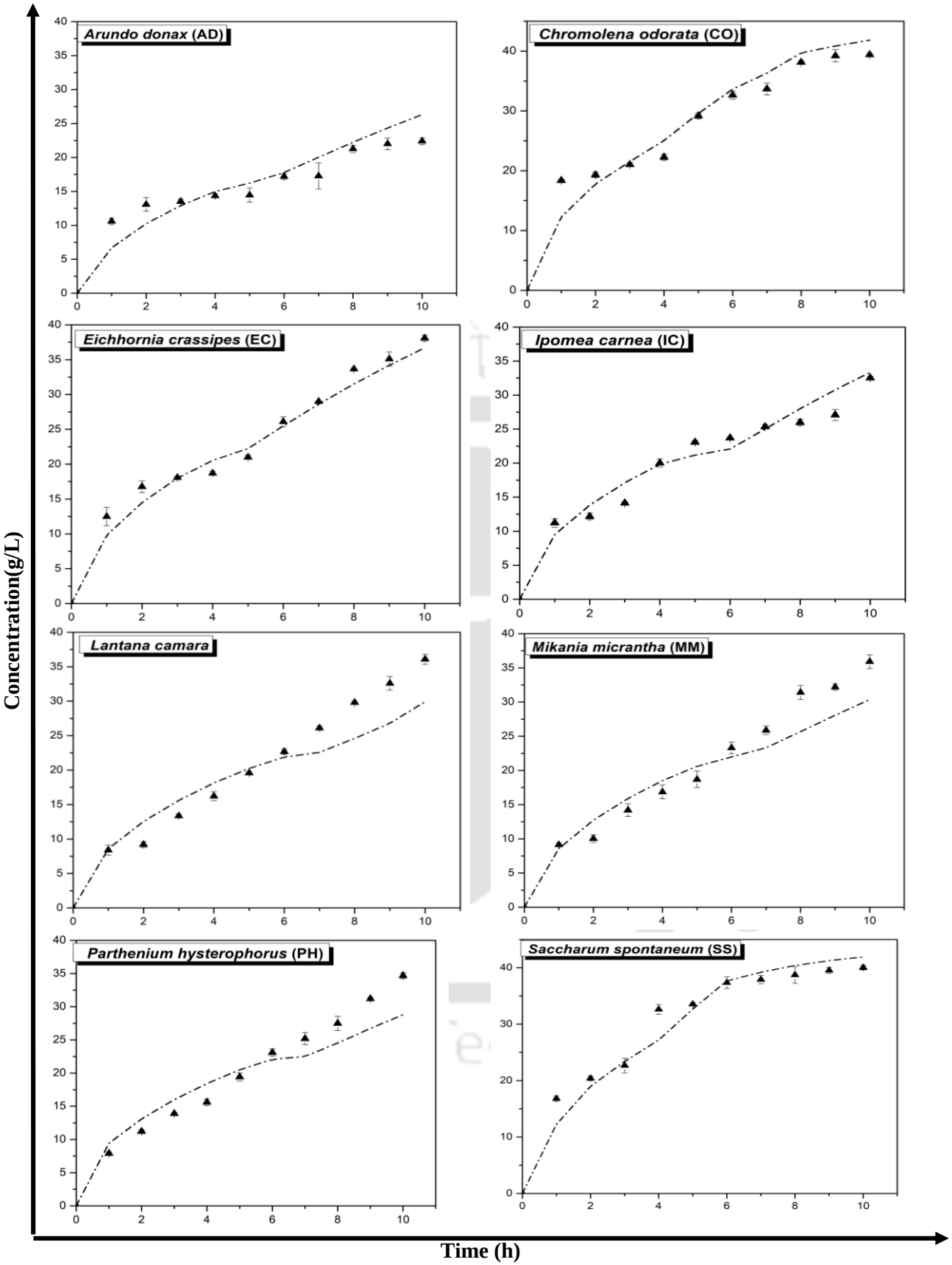

Figure 3.3 Time profiles of total reducing sugar (TRS) release obtained in Test experiments (employing mechanical agitation for enzymatic hydrolysis mixture) for various invasive weeds.
▲: denotes the experimental time profiles of TRS, ----- : denotes Simulation time profile of TRS

3.4.3 Results of intrinsic fluorescence and circular dichroism analysis.

It is known that exposure of enzyme protein to ultrasound induce conformational changes in the secondary structure of the protein, which augments it activity (**Subhedar and Gogate, 2014; Wang et al., 2012)**. The structures and hydrolysis mechanism of the cellulase and cellobiase enzymes has been explained by many authors. **Rouvinen et al., (1990)** have reported that the 3-D structure of a cellulose reveals an α-β protein with a fold similar to the widely occurring barrel topology. The active site of cellobiohydrolase is located at the carboxyl terminal and at a parallel β-barrel in an enclosed tunnel, through which the cellulase threads. The probable catalytic sites are two aspartic acid residues located in the center of the tunnel. **Davies and Henrissat (1995)** have also explained the mechanism of processivity of cellobiohydrolases. The enzyme remains bound to the cellulose polysaccharide chain by several substitutes, the lid closing active site, and the glyocosyl enzyme. The two empty sites created due to release of a disaccharide product and other factors such as loop movement provide driving force for enzyme motion along the chain or chain threading along enzyme's active site. Hydrolysis proceeds iteratively until the enzyme movement is stopped by steric factors. **Bras et al. (2011)** have reported biochemical properties and crystal structure of a protein CtCel 124 in the cellulase system. They showed that crystal structure of CtCel 124 displays a superhelical fold, in which a constellation of α-helices encircles a central helix, in which the catalytic site is located. The substrate binding cleft has two topographical domains in which the bound substrate (cellobiose) displays twisted and linear conformations. This suggested that the enzyme targeted the interphase between crystalline and disordered regions of cellulase.

Influence of sonication on secondary and tertiary structure of cellulase and cellobiase was assessed using intrinsic fluorescence spectra and circular dichroism spectra. The intrinsic fluorescence spectra are depicted in **Fig. 3.4**, while circular

dichroism spectra are shown in **Fig. 3.5**. The analysis of the circular dichroism spectra using Dichroweb online server is given in **Table 3.3**. Change in pH or microenvironment can induce change in the state and structure of amino acid residues. Mainly three amino acid residues (*viz*. Trp, Tyr and Phe) contribute to the intrinsic fluorescence. **Fig. 3.4** shows the Trp fluorescence spectrum for cellulase and cellobiase enzymes individually, with maximum fluorescence emission wavelength at 348 nm. The enzyme treatment with both mechanical agitation and sonication reduced the fluorescence intensity, but the reduction was more marked in the case of sonication treatment. This is attributed to the denaturation of protein caused due to strong shear and micro-convection arising from collapsing bubbles as well as by destruction of hydrophobic interactions between protein molecules, causing different movements of hydrophobic groups **(Yu et al., 2014)**. It has been also reported that ultrasound can lead to the thermo-sonolysis of water molecules to form intermediates such as hydroxyl and hydrogen radicals, which can react with tryptophan and oxidize into kynurenine **(Chowdhury et al., 1995).** The spectra in **Fig. 5.4** also do not show any red or blue shift in maximum fluorescence emission wavelength.

The causes leading to this effect is rupture of hydrophobic interaction between protein molecules leading to molecular unfolding of protein. These effects are eventually induced by intense microconvection generated by ultrasound and cavitation. Decrease of population of exposed tryptophan residues on the surface of cellulase and cellobiase, probably due to aggregation of protein after treatment with mechanical agitation or sonication, leads to reduction in fluorescence intensity. These conformational changes cause exposure of hydrophobic amino acid groups and structures inside enzyme molecules leading to augmentation of activity.

The CD spectra of cellulase and cellobiase enzymes depicted in **Fig. 3.5**, along with the structural analysis presented in **Table 3.3** which also further corroborate the

results of intrinsic fluorescence spectroscopy shown in **Fig. 3.4**.The data on content of secondary structure components of the enzymes presented in **Table 3.3** clearly shows reduction in α-helix conformation content of the enzyme, with rise in β-sheet and random coil structure after sonication. Reduction in α-helix structure is more marked for ultrasound (or sonication) treatment than mechanical agitation. Moreover, greater reduction in α-helix structure is seen for cellulase enzyme than cellobiase enzyme. These conformational changes help in augmenting the activities of both cellulase and cellobiase enzyme. As per the analysis of **Davies and Henrissat (1995)** and **Rouvinen et al. (1990**), increase in β-sheet/ β-turn components in enzyme structure can increase the active sites (β-barrel tunnels) for cellulose polysaccharide chains. Moreover, as per analysis of **Bras et al., (2011),** reduction in α-helix components can also expose catalytic sites located inside them, due to which the enzyme cellobiase can bind to substrate more easily - without requiring undergoing twisted and linear conformations. These effects also contribute to augmentation of catalytic efficiency of the enzymes.

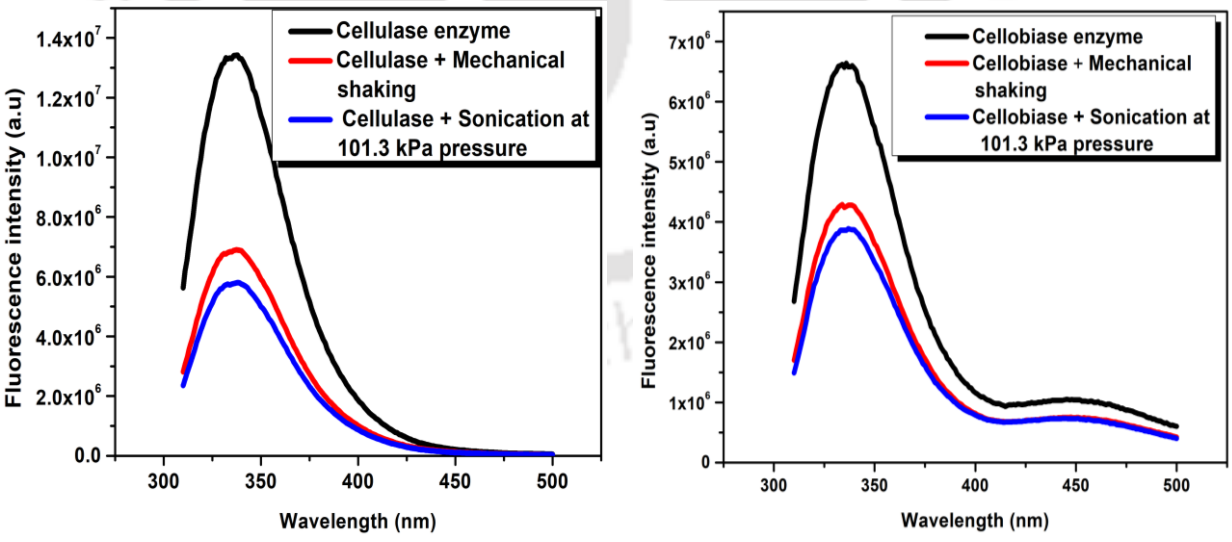

A. Intrinsic spectra of Cellulase B. Intrinsic spectra of Cellobiase

Figure 3.4 Intrinsic fluorescence spectra of enzymes in various forms (native enzyme and post–treatment with mechanical shaking and sonication at atmospheric or 101.3 kPa pressure). (A) Spectra of cellulase; (B) Spectra of cellobiase

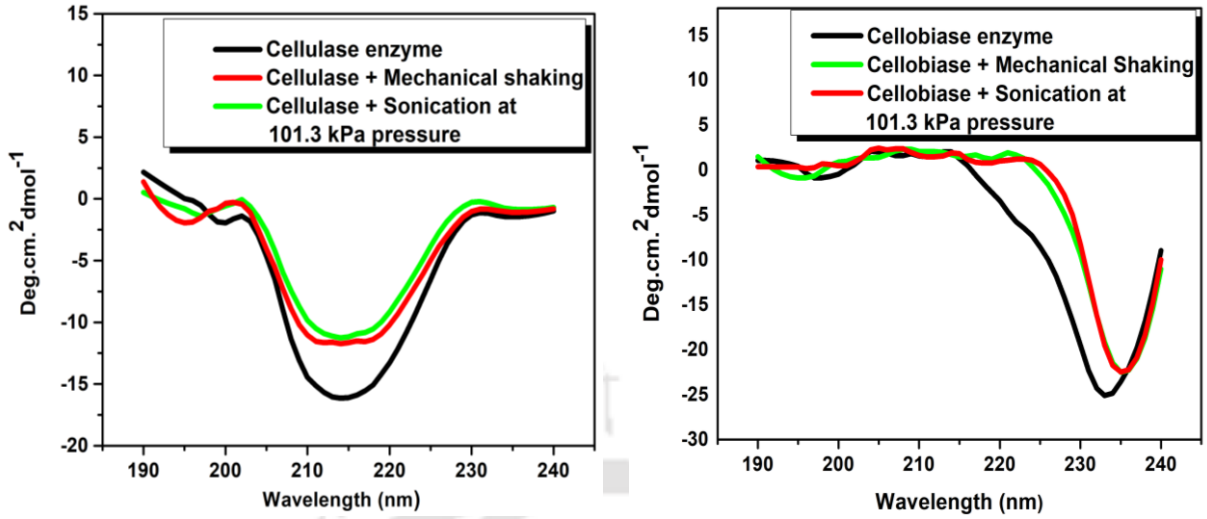

A. CD Spectra of Cellulase B. CD Spectra of Cellobiase

Figure 3.5 Circular dichroism of spectra of enzymes in various forms (native enzyme and post–treatment with mechanical shaking and sonication at atmospheric or 101.3 k Pa pressure). (A) Spectra of cellulase; (B) Spectra of cellobiase.

Table 3.3. Secondary structure element of the enzymes by CD using Dichroweb server.

	α–helix (%)	β–sheet (%)	β–turn (%)	Random coil (%)
Cellulase				
1. Native Cellulase	32.7	13.20	23.14	30.82
2. Cellulase + mechanical shaking	30.67	25.24	18.54	25.53
3. Cellulase + sonication (at atmospheric conditions)	19.10	29.75	18.40	32.73
Cellobiase				
1. Native cellobiase	11.68	44.46	10.23	33.71
2. Cellobiase + mechanical shaking	9.84	45.50	10.76	33.50
3. Cellobiase sonication (at atmospheric conditions)	9.80	45.68	10.77	33.74

3.5. Conclusion

Enzymatic hydrolysis of pretreated biomass of eight invasive weeds was carried out with mechanical agitation and sonication under identical (un-optimized) conditions. Structural integrity of the secondary structures of the enzymes involved in the enzymatic hydrolysis were also analyzed by intrinsic fluorescence and circular dichroism. Concurrent analyses of both the experiments gives a mechanistic insight into the ultrasound-induced enhancement of hydrolysis of biomasses of invasive weeds. The main enhancement effect of ultrasound/cavitation is in terms of acceleration of the kinetics of hydrolysis. A 10-fold higher kinetics of hydrolysis was seen with application of sonication as compared with mechanical agitation. Essentially, same TRS yield was obtained after 120 h of treatment with mechanical agitation as obtained after 10 h treatment of sonication applied with just 10% duty cycle. On the other hand, the net TRS yield from hydrolysis showed only marginal improvement with sonication. The enhancement in kinetics of hydrolysis with sonication can be attributed to two factors:

(1) Conformational changes in secondary structure of the enzyme, viz. reduction in α-helix content with concurrent rise in β-sheet and random coil content. These conformational changes cause unfolding of enzyme proteins with creation/exposure of active sites, as noted in previous section.

(2) Generation of intense micro-convection in the medium, which enhances enzyme/substrate affinity and reduces product inhibition of enzyme The micro-convection also augments reaction velocity with faster splitting of enzyme/ substrate complex.

Moreover, it is noteworthy that enhancement effect of ultrasound and cavitation is observed even under non-optimum conditions of enzymatic hydrolysis. These results essentially point that process intensification due to ultrasound/cavitation helps in

overcoming the limitations of enzymatic hydrolysis by increasing the reaction velocity, increase in enzyme-substrate affinity by unfolding of enzyme exposing active site, reduction in product inhibition and enhancement of enzyme activity due to conformational changes in its secondary structure. The enhancement effect of sonication was revealed to be independent of the conditions of enzymatic hydrolysis – whether optimized or un- optimized.

References

Bharadwaja, S.T.P., Singh, S., Moholkar, V.S., 2015. Design and optimization of a sono-hybrid process for bioethanol production from *Parthenium hysterophorus*. Journal of. Taiwan Institute of Chemical Engineers, 1, 1–8.

Bhasarkar, J.B., Chakma, S., Moholkar, V.S. 2013. Mechanistic features of oxidative desulfurization using sono-Fenton–peracetic acid (ultrasound/Fe2+–CH3COOH–H2O2) system. Industrial & Engineering Chemistry Research, 52, 9038-9047.

Bras, J.L., Cartmell, A., Carvalho, A.L., Verze, G., Bayer, E.A., Vazana, Y., Correia, M.A., Prates, J.A., Ratnaparkhe, S., Boraston, A.B., Romao, M.J., Fontes, C.M, Gilbert HJ., 2011. Structural insights into a unique cellulase fold and mechanism of cellulose hydrolysis. Proceedings of National Academy of Science (USA), 108, 5237-42.

Chandel, A.K., Singh, O.V., Rao, L.V., Chandrasekhar, G., Narasu, M.L., 2011. Bioconversion of novel substrate *Saccharum spontaneum*, a weedy material, into ethanol by *Pichia Stipitis* NCIM 3498. Bioresource Technology, 102, 1709-1714.

Chowdhury, S.K., Eshraghi, J., Wolfe, H., Diane, F., Allan, G., David, J. 1995. Mass spectrometric identification of amino acid transformations during oxidation of

peptides and proteins: modifications of methionine and tyrosine. Analytical Chemistry, 67:390–398

Coral, G., Arikan, B., Ünaldi, M.N., Guvenmez, H., 2002. Some properties of crude carboxymethyl cellulase of *Aspergillus niger* Z10 wild-type strain. Turkish Journal of Biology, 26, 209-213.

Davies, G. and Henrissat, B., 1995. Structures and mechanisms of glycosyl hydrolases. Structure, 3, pp.853-859.

Holtzapple, M.T., 1981. The pretreatment and enzymatic saccharification of Poplar wood (Ph.D. thesis). Department of Chemical Engineering, University of Pennsylvania, USA.

Holtzapple, M.T., Caram, H.S., Humphrey, A.E. 1984. The HCH–1 model of enzymatic cellulose hydrolysis. Biotechnology and Bioengineering, 26, 775–780.

Kataria, R., Ghosh, S., 2014. NaOH Pretreatment and enzymatic hydrolysis of *Saccharum spontaneum* for reducing sugars production. Energy Source, 36,1028-1035.

Kuhad, R.C., Gupta, R., Khasa, Y.P., Singh, A., 2010. Bioethanol production from *Lantana camara* (red sage): pretreatment saccharification and fermentation. Bioresource technology, 101, 8348–8354.

Kuila, A., Banerjee, R., 2014. Simultaneous saccharification and fermentation of enzyme pretreated *Lantana camara* using *S. cerevisiae*. Bioprocess and Biosystem Engineering, 37, 1963-1969.

Kumari, R., Pramanik, K., 2013. Bioethanol production from *Ipomoea carnea* biomass using a potential hybrid yeast strain. Applied Biochemistry Biotechnology, 171,771–785.

Loaces, I., Schein, S., Noya, F., 2017. Ethanol production by *Escherichia coli* from *Arundo donax* biomass under SSF, SHF or CBP process configurations and in situ production of a multifunctional glucanase and xylanase. Bioresource Technology, 224, 307–313.

Nelson, N., 1944. A photometric adaptation of the Somogyi method for the determination of glucose. Journal of Biological. Chemistry, 153, 375–380.

Phothisantikul, P.P., Tuanpusa, R., Nakashima, M., Charinpanitkul, T., Matsumura, Y., 2013. Effect of CH_3COOH and K_2CO_3 on hydrothermal pretreatment of water hyacinth (*Eichhornia crassipes*). Industrial Engineering Chemistry Research, 52, 5009-5015.

Rouvinen, J., Bergfors, T., Teeri, T., Knowles, J. K.C., Jones, T.A., 2013. Three-dimensional structure of cellobiohydrolase II from *Trichoderma reesei*. Science, 249, 380-6.

Silva, C.F.L., Schirmer, M.A., Maeda, R.N., Barcelos, C.A., Pereira Jr. N., 2015. Potential of giant reed (*Arundo donax* L.) for second generation ethanol production. Electronic Journal of Biotechnology, 18, 10–15.

Singh, S., Agarwal, M., Sarma, S., Goyal, A., Moholkar, V.S. 2015b. Mechanistic insight into ultrasound induced enhancement of simultaneous saccharification and fermentation of *Parthenium hysterophorus* for ethanol production. Ultrasound Sonochemistry, 26, 249–256.

Singh, S., Bharadwaja, S.T.P.,Yadav, P.K., Moholkar, V.S., Goyal, A., 2014. Mechanistic investigation in ultrasound–assisted (alkaline) delignification of *Parthenium hysterophorus* biomass. Industrial and Engineering. Chemistry Research, 53, 14241–14252.

Singh, S., Sarma, S., Agarwal, M., Goyal, A., Moholkar, V.S. 2015a. Ultrasound enhanced ethanol production from *Parthenium hysterophorus*: a mechanistic investigation. Bioresource Technology, 188, 287–294.

Sivasankar, T., Paunikar, A.W., Moholkar, V.S., 2007. Mechanistic approach to enhancement of the yield of a sonochemical reaction. AIChE Journal, 53, 1132–1143.

Somogyi, M., 1945. A new reagent for the determination of sugars. Journal of Biological Chemistry, 160, 61–68.

Sreerama, N. and Woody, R.W., 2000. Estimation of protein secondary structure from circular dichroism spectra: comparison of CONTIN, SELCON, and CDSSTR methods with an expanded reference set. Analytical biochemistry, 287, 252-260.

Subhedar, P.B., Gogate, P.R., 2014. Enhancing the activity of cellulase enzyme using ultrasonic irradiations. Journal of Molecular Catalysis B: Enzymatic, 101, 108–114.

Suresh, K., Ranjan, A., Singh, S., Moholkar, V.S. 2014. Mechanistic investigations in sono–hybrid techniques for rice straw pretreatment. Ultrasounics Sonochemistry, 21, 200–207.

Wang, Z., Lin, X., Li, P., Zhang, J., Wang, S., Ma, H.. 2012. Effects of low intensity ultrasound on cellulase pretreatment. Bioresource Technology, 117, 222–227.

Whitmore, L. and Wallace, B.A., 2008. Protein secondary structure analyses from circular dichroism spectroscopy: methods and reference databases. Biopolymers: Original Research on Biomolecules, 89(5), pp.392-400.

Yan, J., Zhilei, W., Wang, Q., He, M.H., Li, S., Irbis, C., 2015. Bioethanol production from sodium hydroxide/ hydrogen peroxide-pretreated water hyacinth via

simultaneous saccharification and fermentation with a newly isolated thermotolerant *Kluyveromyces marxianu* strain. Bioresource Technology, 193, 103-109.

You, T., Zhang, L., Zhou, S., Xu, F. 2014. Protic acid resin enhanced 1-butyl-3-methylimidazolium chloride pretreatment of *Arundo donax* Linn. Bioresource Technology, 167, 574-577.

Yu, Z.L, Zeng WC, Zhang WH. 2014. Effect of ultrasound on the activity and conformation of α-amylase, papain and pepsin. Ultrasonics Sonochemistry, 21, 930–936.

CHAPTER 4: KINETIC MODELING OF DILUTE ACID HYDROLYSIS OF VARIOUS INVASIVE WEEDS TO DEVELOP A COMPOSITE FEEDSTOCK FOR BIOFUEL PRODUCTION

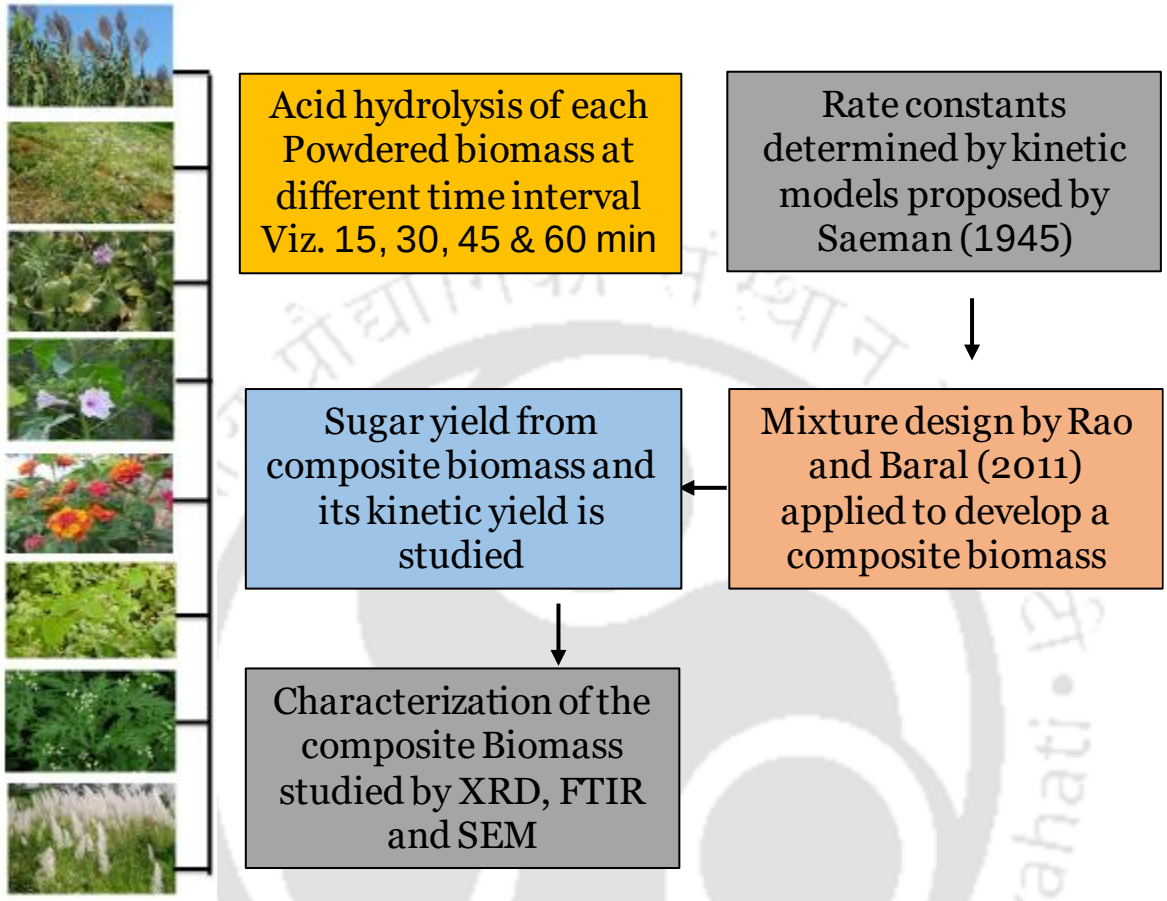

Chapter Highlights

- Used single optimized condition of for all biomass.
- Study of hydrolysis kinetics of 8 individual biomasses.
- Develop a composite biomass with the best ratio from mixture design TRS yield 496.3 mg/g of raw biomass
- Sugar estimation of composite biomass and its characterization after pretreatment

CHAPTER 4

KINETIC MODELING OF DILUTE ACID HYDROLYSIS OF VARIOUS INVASIVE WEEDS TO DEVELOP A COMPOSITE FEEDSTOCK FOR BIOFUEL PRODUCTION

4.1 Introduction

Among various challenges, year round availability of biomass feedstock is the most critical part in biofuel industry. Transition towards cheaper and most sustainable feedstock such as waste and agriculture residues will answer to lot of query to the existing biofuel economy. **Qureshi and Blaschek (2000)** reported 30~32% of total cost of the biofuel cost is due to the feedstock processing/collection followed by pretreatment (~19-20%). This leads to higher upstream cost contributing approximately one half of the total production cost of biofuel. To achieve such target of large scale production, year round availability of feedstock is the utmost necessity. Single commodity feedstock cannot supply sufficient feedstocks to meet national biofuel targets owing to various constraint such as competing demands from other markets (e.g., food, feed etc.). Blending of different lignocellulosic biomass as a composite feedstock can be an alternative solution to overcome current challenges on biomass supply. It will encompass a board portfolio feedstock, initiate more geographical diversity and ultimately exert less resource pressure on any location or feedstock.

The invasive weeds are a population exhibiting a net negative impact to the target ecosystem across the globe. European commission of parliamentary services (2013), provided the data around 1000 billion losses due to invasive weeds followed by loss of

US$90 billion per year in India. Managing and manipulating such invasion with various regimes has been associated with labor intensive, feasibility and cost effective issue. One of the best ways to minimize the impact of such invasive weeds on the ecosystem is to exploit its biomass as a feedstock for biofuel production. It may significantly control the damage inflicted by these weeds on ecosystem; also enhancing economy of biofuel production.

The present work was intended to establish the potential of various invasive biomass prevalent in this region by assessing the kinetics of TRS yield during acid hydrolysis followed by making a composite biomass comprising the best ratio of all the invasive biomass with the help of mixture design. This would bring down the cost to a marginal rate and also open a new window for sustainable utilization.

The invasive weeds considered in this work are: (1) *Arundo donax* (AD), (2) *Saccharum spontaneum* (SS), (3) *Mikania micrantha* (MM), (4) *Lantana camara* (LC), (5) *Eichhornia crassipes* (EC), (6) *Ipomea carnea* (IC), (7) *Chromolena odorata*, (8) *Parthenium hysterophorus* (PH). According to data reported by **Rajkhowa (2005)** all the biomass produced at the range of 15-20 tons per hectare. In most of earlier studies, the research has been mostly focused on single biofuel crop with several liabilities regarding its sustainability and demands. To overcome such problem, an attempt was made to mix all the biomasses and use as composite biomass. In most earlier studies, the proportions of the mixture components are selected randomly, by which we have a very little information on optimizing the biomass proportions to maximize the sugar yield.

In this work, irreversible pseudo first order kinetics of each biomass was studied by hydrolyzing the hemicellulose fraction. Time profiles of TRS yield and rate constant of each biomass under study were taken into account. The mixture design method by **Rao**

and Baral (2011) was then applied to investigate the synergetic effects of mixed substrates in batch experiments, and to establish the optimum mixture composition of eight biomass on the basis of sugar yield after acid and enzymatic hydrolysis. Characterization of the composite biomass after various treatment was done by XRD, FTIR and SEM micrograph to validate the effectiveness of the pretreatment process.

4.1.1 Assessment of biofuels production potential

The use of this model has been demonstrated to seek the potential of these invasive weeds (namely *Arundo donax, Chromolena odorata, Eichhornia crassipes, Ipomea carnea, Lantana camara, Mikania micrantha, Parthenium hysterophorus and Saccharum spontaneum*) as feedstock for biofuels by hydrolysis of hemicellulose to fermentable sugars. The dilute acid hydrolysis of different biomass using 1% v/v H_2SO_4 was carried out at different time intervals (*viz.*15, 30, 45 and 60 min). The reaction constants representing the rate of conversion (k_1), rate of degradation (k_2) and maximum conversion at a specific time were determined. The eight biomasses were divided into two category based on the results obtained from kinetic analysis. The best four of the eight biomass were considered as set 1 for mixed design and the rest four biomasses were placed in set 2. The distribution of these biomasses was also favored on the basis of their flowering season and classifications. The best run from each set (category) will be mixed to obtain the best combination ratio of the eight biomasses in terms of TRS yield. The motive behind this segregation was the flexibility of use when there is a surplus amount of the required biomasses which gives maximum conversion in minimum time from industrial prospect. Moreover, use of eight biomasses altogether in a single design will give innumerable run which is impractical and cannot backed by valid justification.

4.2 Materials and Methods

4.2.1 Materials

All the chemicals used for the experiments (*viz*. sulphuric acid, sodium hydroxide, sodium borate dihydrate, disodium ethylene diamine tetra acetate dihydrate (EDTA), sodium lauryl sulphate, disodium hydrogen phosphate, ethoxy ethanol, cetyl trimethyl ammonium bromide (CTAB), decahydro-naphthalene and sodium sulphite) were purchased from Fisher Scientific, India and glucose (HPLC grade) was procured from Sigma Aldrich, USA. All chemicals were used as received without any further pretreatment.

4.2.2 Biomass collection and processing

The lignocellulosic feedstock of all eight weeds, *viz*. *Arundo donax* (AD), *Chromolena odorata* (CO), *Eichhornia crassipes* (EC), *Ipomea carnea* (IC), *Lantana camara* (LC), *Mikania micrantha* (MM), *Parthenium hysterophorus* (PH) and *Saccharum spontaneum* (SS) were collected from within campus. Biomass was chopped into pieces and washed with water, dried at 60^{o}C for 24 h and ground to powder with mixer grinder (pass through mesh giving particle size <1 mm). The powdered biomass was stored in air-tight containers at 25°C for further experiments.

4.2.3 Protocol for hemicellulose estimation

Hemicellulose content in all the biomass samples were determined by following the protocol established by **Goering** and **Van Soest (1970)**. Neutral detergent fiber (NDF) and acid detergent fiber (ADF) were estimated separately to determine the hemicellulose content. The deduction of ADF from NDF determine the hemicellulose content of the biomass. Reagent used in neutral detergent solution was prepared by

dissolving 6.81 g of sodium borate dihydrate, 18.61 g of disodium ethylene diamine tetraacetate dihydrate (EDTA) in 800 mL distilled water by heating. Following this, 30 g sodium lauryl sulphate, 4.5 g disodium hydrogen phosphate and 10 mL of 2 ethoxy ethanol were added to the solution. The solution was made up to 1 L by adjusting the pH to 7.0. Acid detergent solution was prepared by dissolving 20 g of cetyl trimethyl ammonium bromide (CTAB) In 1 L of 1 N H_2SO_4.

4.2.3.1 ***Neutral detergent fiber (NDF) estimation***1 g of dry powdered biomass sample was taken in a refluxing flask and 100 mL of cold neutral detergent solution was added to it. 2 mL of decahydro-naphthalene and 0.5 g of sodium sulphite was added to the solution. The solution was refluxed for 1 h. The solution was transferred to a pre-weighed sintered glass crucible and filtered by applying suction. The residue was washed with hot water followed by acetone and dried at 100°C till constant weight was achieved.

4.2.3.2 ***Acid detergent fiber (ADF) estimation*****:** 1 g of raw biomass was transferred to a refluxing flask and 100 mL of cold acid detergent solution was added to it. The solution was refluxed and processed similarly as described in NDF.

4.2.4 Dilute acid pretreatment of raw biomasses, delignification and enzymatic hydrolysis of composite biomass.

The conditions optimized for acid hydrolysis of *Parthenium hysterophorus* in our prior study (Singh et al. 2014), which have been adapted in present study, are as follows: 1% (v/v) H_2SO_4 (equivalent to 0.36 N), 10% (w/v) biomass, autoclaving at 121^{o}C and 15 psi for different interval (*viz*. 15, 30, 45 and 60 min) followed by rapid steam release. The composite biomass later obtained by mixing the best run from the two category will further undergo delignification and enzyme hydrolysis. The conditions used for

delignification and enzyme hydrolysis have been previously discussed in greater detail in chapter 3 (subsections 3.3.4 -3.3.7) (Bharadwaja et al. 2015; Borah et al., 2016).

4.2.5 Characterization of raw and pretreated composite biomass

The structural variation in various stages of pretreatment *viz*. acid pretreatment and delignification of composite biomass from raw biomass were characterized by SEM, FTIR and XRD.

***Surface analysis using SEM*:** The change in structure morphology during various stages of pretreatment *viz*. acid pretreatment and delignified composite biomass from raw biomass was analyzed by Field Emission Scanning Electron Microscope (FESEM) at a magnification of 500X (JSM-6360, JEOL., USA Inc.). The specimens were prepared by mounting on aluminum stubs using double sided carbon adhesive tapes and sputter coated with 10 nm thin layer of gold powder at 200 Å before analysis. These specimens were observed at operating voltage of 5.0 kV. The SEM micrograph of raw, acid pretreated and delignified biomass were taken at similar magnification to discern the effect of pretreatment on the biomass structure and morphology.

Spectroscopy measurement by FTIR: The changes in the structural composition of raw composite biomass after pretreatment with respect to the functional groups were determined by FTIR spectroscopy. The spectra were recorded in the range of 4000-400 cm^{-1} (Perkin Elmer, Spectrum Two, USA). Samples for analysis were prepared by mixing dried biomass (10 mg approx.) sample with KBr spectroscopic grade salt with ratio (w/w) of 1: 100 in a granite mortar. The pellet was then grinded and pressed well before reading the spectra.

***Crystallinity index measurement by XRD*:** X-ray diffractometer (D8 Advance, Bruker, Germany) was used to test and measure the crystalline index of acid treated and delignified samples with respect to the raw samples. X-ray beams operated at 40 kV and 40 mA were then charged to the sample, using Cu-Kα radiation (λ = 1.54184 Å), a grade range between 5°-35° and a step size of 0.05°. The crystallinity of the residual cellulose in the composite biomass was calculated according to the empirical method proposed by **Segal et al. (1962)** or peak height method. CrI is simply calculated by dividing the height of (2 0 0) peak (the maximum interference; I200) and the height of the minimum among the (2 0 0) and (1 1 0) peaks (the intensity at 28 = 18°).

$$\mathrm{CrI}(\%)= \frac{I_{\mathrm{crystalline}} - I_{amorphorus}}{I_{crystalline}} \times 100$$

4.2.6 Kinetic Modeling to determine the rate constant of acid hydrolysis

The dilute acid hydrolysis reactions are very complex in nature, mainly because the substrate is in a solid phase and the catalyst is in a liquid phase. The kinetics of hydrolysis depends on a number of variables, such as: temperature, acid concentration, time, substrate concentration and substrate composition **(Lenihan et al., 2010).** Although optimization of all these variables have been conducted in our early studies for one of the biomass based on one-to-one hypothesis. Conducting the same experiments for all the individual biomass is quite impractical, if the intention of the stakeholders is to utilize the multiple biomasses as a mixed feedstock for bio alcohol production in a single reactor. This will cut down the year round dependency on single feedstock availability. The practical objective of studying the kinetic model is, on a first level, is to optimize the process and, on a second level, to obtain Equations useful for economical estimations.

The models usually associated with dilute acid hydrolysis which were first proposed by **Saeman (1945).**

The model proposed by **Saeman (1945)** involves hydrolysis of the polymer (such as glucan, xylan) being degraded to monomer (glucose, xylose etc.), which subsequently converted to decomposition products. This is represented below:

$$Polymer \overset{k_1}{\rightarrow} Monomer \overset{k_2}{\rightarrow} Decomposed\ products \quad (1)$$

where k_1 is the rate of conversion of polymer to Monomer and k_2 is the rate of decomposition of glucose. Both have units of the reciprocal of time (min^{-1}).

$$Glucan\ (A) \overset{k_1}{\rightarrow} Glucose(B) \overset{k_2}{\rightarrow} HMF(C) \quad (2)$$

The formation rate of the product glucose (B) with respect to time is represented by Eqn. (3):

$$\frac{dC_B}{dt} = k_1 C_A - k_2 C_B \quad (3)$$

Integrating and solving above equation with respect to time gives concentration of sugar as a function of time:

$$C_B = k_1 C_{A0} \left(\frac{e^{-k_1 t} - e^{-k_2 t}}{k_2 - k_1} \right) \quad (4)$$

Using this equation, it will be possible to accurately model the reactions kinetics at each of the operating conditions of temperature and acid concentration and therefore determine the reaction constants. The reaction constants k_1 and k_2 are determined through using the Matlab tools. By minimizing the sum of the square of the error between the experimental data and the model data obtained accurate reaction parameters can be found. The solver function operates by attempting to acquire a value of zero error through changing of the k_1 and k_2 values. On this basis quantitative saccharification is used to determine the

concentration of the reactants. By taking into account the solid liquid ratio, the initial concentrations C_{A0} can be established by determining the concentration of their products in an assumed 100% conversion reaction. Through quantitative saccharification, the hexosans (glucan) and pentosan (xylan) are hydrolysed completely to form hexose (glucose) and pentose (xylose, arabinose), respectively. The concentration of the sugars produced, which are obtained from analyzing the chromatograms are fixed as the initial concentrations of the cellulose and hemicellulose. Therefore, the initial concentration of glucose, xylose and arabinose is assumed to be that of the C_{A0} of glucan, xylan and hemicellulose These values will satisfy the respective parameters within the mathematical model. The reaction was modeled to determine the kinetics for 1% (v/v) sulphuric acid concentration with an operating temperature of 121^{o}C for different time intervals.

4.3 Results and Discussion

4.3.1 Kinetic modeling of acid hydrolysis

A comparative study of quantitative saccharification obtained experimentally and the results of the kinetic model constructed to represent sugar yield at different time interval at an acid concentration of 1.0% (v/v) and temperature of 121^{o}C is shown in Fig. 4.1. The model was constructed through calculating best fit reaction coefficients for k_1 and k_2. From observing these graphs, it can be seen that the models generated for sugars production at 1.0% (v/v) acid concentration are highly accurate. Along with the model for the reaction, the experimental values against the model values are constructed to determine if the data fits. The correlations represented by all R^2 are seen to be well above 0.9 which indicated the high level of accuracy achieved from the model. The kinetic model is of first order principles further demonstrated that the glucose generation reaction

is a first order reaction as has been noted in numerous studies **(Saeman, 1945**; **Tizazu and Moholkar, 2018).**

When taking into account the reaction kinetics involved in the formation of sugars through hydrolysis, it is seen that the larger the value of k_1, the higher the rate of sugar formation and therefore the lower the cycle time required to maximize yield. In contrast to this, the larger the value of k_2 the higher the rate of sugar degradation. Hence, the most desirable operating conditions will result in a high value of k_1 and a low value of k_2. This assumption is clearly reflecting from the k_1 value of *E. crassipes* and *L. camara* (LC) which is 0.266 and 0.038. Faster kinetics of *E. crassipes* (EC) results in higher conversion rate of 87.9% in contrast to 57.4% of *L. camara*. Time required for this bioconversion of TRS nearly reduced to 3.5 times for *E. crassipes* in comparison to *L. camara.* The outcome of the results can be attributed to the biochemical constituent of the lignocellulose. In previous paper, **Borah et al. (2016a)** have reported that lignin constituent of LC to be around 27% which is nearly seven times more than *E. crassipes* which might hinder the access of carbohydrate moiety for hydrolysis **(Bahuguna and Shukla, 2010)**

In this regard, optimum time for both *S. spontaneum* (SS) and *Ipomea carnea* (IC) is 30 min. The maximum conversion for the same treatment time differs drastically which is 91.4% in case of SS and 52.4% for IC. This consequence is due to increasing k_2 value of IC with respect to SS which signifies there is more degradation of product during the process which limit the overall bioconversion process. *A. donax* (AD) and *M. micrantha* (MM) has the same k_1 value, yet the overall sugar bioconversion of AD is 76.6%, which is comparatively less then to that of MM which is 90.2%. This is imputed due to higher k_2 value of AD, which signifies the degradation of product. In practice this scenario is difficult to achieve so the optimum conditions available at the current operating

conditions must be investigated. The value of k_1 and k_2 both increase exponentially with temperature as per the Arrhenius Equation. Increase in temperature would increase sugar production rate but a rapid sugar degradation would render the process highly inefficient as was seen earlier. Therefore, to preserve sugars, it is best to limit the temperature of the reaction and to try and manipulate the *k* values by varying the acid concentration. *S. spontaneum* gave 91.4 % conversion at 30 min whereas *M. micrantha* gives 90.15 % conversion at 51 min. Similarly, *I carnea* gives only 52.45% conversion, which is maximum for 30 min. Another important observation the initial hemicellulose concentration of biomass is different for all the biomass as well as optimum conversion & time for optimum conversion is also different.

If biomass availability is not a limiting issue, then those biomasses which gives maximum conversion at minimum time can be used as a composite biomass which would cut down the economy cost. And if it is a limiting issue, we can use the composite biomass optimized based on available sugar concentration, conversion rate and time. Based on the criteria of sugar yield and maximum conversion, we have divided the eight biomasses into two categories. **Category A** consisted of those biomass where initial hemicellulose and sugar yield was more than 25 g/L and percentage conversion was more than 75%. Four out of the eight biomasses met the required condition for category A. These four biomass were mixed in various ratio to form a composite biomass based on the run generated from statistical mixture design. 19 sets of run were generated in this category. Each run consisted of various proportions of the four biomasses which was mixed accordingly to form the composite of that particular run. Acid hydrolysis of each such composite obtained from each run was done. The sugar obtained from such hydrolysis was conducted for sugar estimation by NS methods. The best 2 runs from 19 sets of experiments of category A were short-listed for enzyme hydrolysis, and the best of

these runs were considered for further experiments. The rest of four biomasses which could not meet the criteria for category A were considered in **category B.** In this case as well, 19 sets of experiments were obtained and same protocols were followed like the category A to get the best combination with high sugar yield.

The best result from this category was carried forward as per composition. From **Table 4.3(A)** experiment no. 6, and experiment no. 32 from **Table 4.3 (B)** emerged as the best combinations of mixed biomass that gave maximum sugar yields of 26.9 g/L (269.04 mg/g of raw biomass) and 107.09 g/L (10.71 mg/g of raw biomass) respectively from acid hydrolysis. Enzyme hydrolysis of the delignified biomass of these two runs gave total reducing sugar yield of 30.45 g/L (544.54 mg/g of raw biomass) and 24.43 g/L (275.87 mg/g of raw biomass). Under limitation of biomass availability, the best biomass compositions from both categories can be blended and used as feedstock.

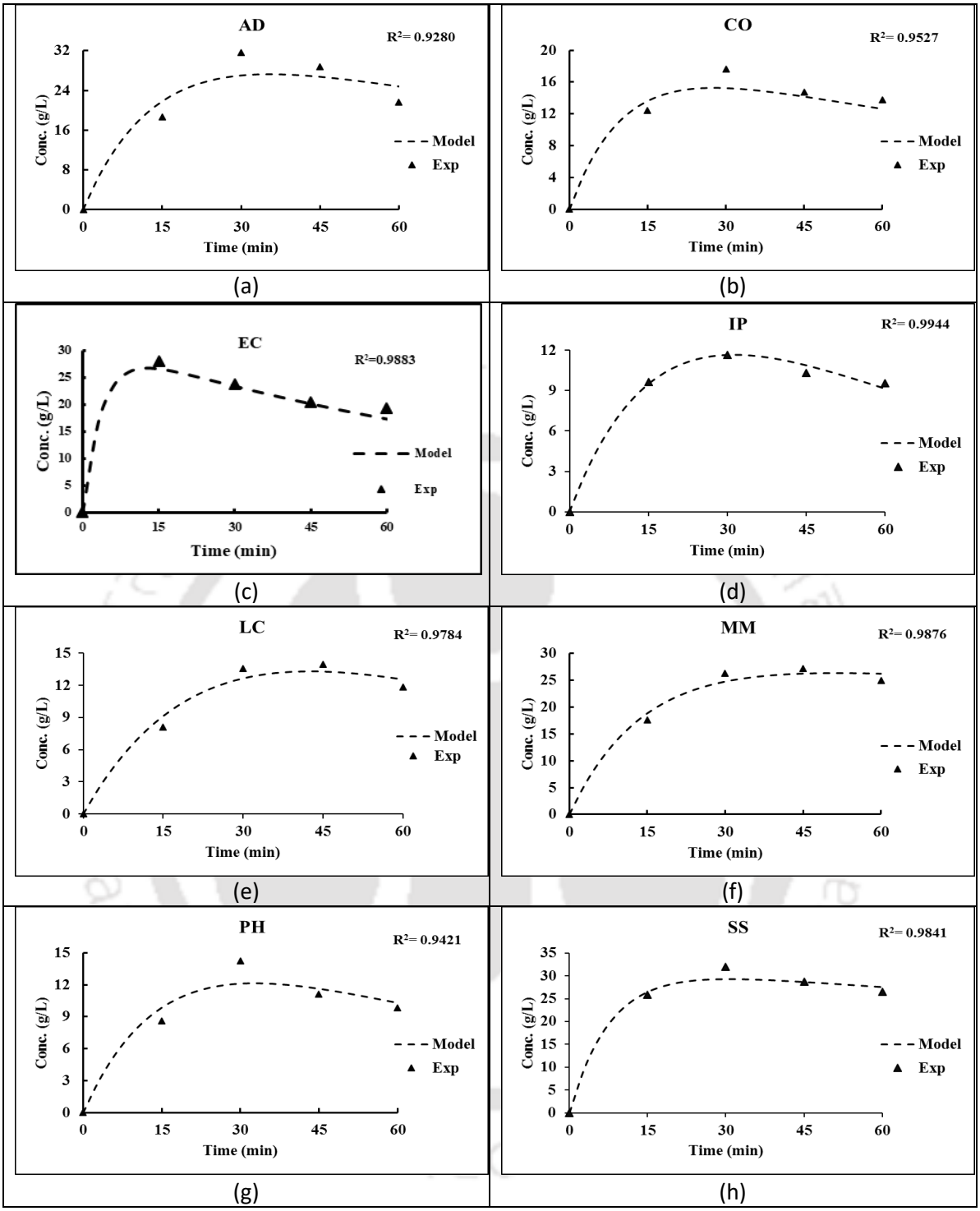

Figure 4.1. Experimental and model fitting of kinetics for acid hydrolysis (a) AD, (b) CO, (c) EC, (d) IP, (e) LC, (f) MM, (g) PH, (h) SS.

Table 4.1 Results of hemicellulose composition of different biomasses

Samples	Filter paper wt.	Final wt.	NDF	ADF	Hemicellulose (NDF - ADF) × 100
AD	0.947	1.915	0.968		35.6
	0.942	1.554		0.612	
CO	0.910	1.856	0.946		19.4
	0.940	1.692		0.752	
EC	0.952	1.902	0.948		30.5
	0.948	1.590		0.643	
IP	0.917	1.850	0.940		22.0
	0.947	1.667		0.72	
LC	0.924	1.870	0.951		23.2
	0.935	1.650		0.719	
MM	0.938	1.890	0.952		29.2
	0.952	1.610		0.658	
PH	0.953	1.901	0.948		18.0
	0.938	1.706		0.768	
SS	0.951	1.907	0.956		32.1
	0.910	1.546		0.635	

Table 4.2 (A) Results of kinetic modelling of biomasses with hemicellulose and sugar concentration ≥ 25 g/L

Parameters	AD	EC	MM	SS
C_{A0} (g/litre)	35.61	30.52	29.21	32.10
k_1(min^{-1})	0.071	0.266	0.071	0.153
k_2(min^{-1})	0.007	0.010	0.002	0.003
R^2	0.928	0.988	0.987	0.984
Time $_{opt}$ (min)	36	12	51	30
Concentration $_{opt}$ (g/litre)	27.26	26.80	26.31	29.34
Max. Conversion (%)	76.6	87.9	90.2	91.4

(B) Results of kinetic modelling of biomasses with hemicellulose and sugar concentration ≤ 25 g/L

Parameters	CO	IP	LC	PH
C_{A0} (gm/litre)	19.42	22.21	23.20	18.02
k_1(min^{-1})	0.095	0.047	0.038	0.062
k_2(min^{-1})	0.009	0.020	0.013	0.012
R^2	0.953	0.994	0.978	0.942
Time $_{opt}$ (min)	27	30	42	33
Concentration $_{opt}$ (g/litre)	15.25	11.64	13.32	12.12
Max. Conversion (%)	78.5	52.4	57.4	67.3

Table 4.3 (A). Results of mixture design with biomasses obtained from Table 4.2 (A)

Expt. No.	AD	EC	MM	SS	TRS yield in AH (mg/g of raw Biomass)	TRS yield in EH mg/g of delignified BM	TFS yield mg/ g of Raw BM
1	0	0.5	0	0.5	171.41		
2	0	0.333	0.333	0.333	142.17		
3	0.125	0.625	0.125	0.125	156.24		
4	0.333	0.333	0.333	0	156.32		
5	0.5	0	0	0.5	224.54	778.4	516.29
6	0.625	0.125	0.125	0.125	269.04	725	544.54
7	0.333	0.333	0	0.333	192.14		
8	0.25	0.25	0.25	0.25	160.72		
9	0.5	0	0.5	0	166.32		
10	0	0	0.5	0.5	151.59		
11	0	0.5	0.5	0	217.54		
12	0.125	0.125	0.125	0.625	212.09		
13	0.125	0.125	0.625	0.125	190.36		
14	0	1	0	0	210.72		
15	0.5	0.5	0	0	172.72		
16	0	0	1	0	198.68		
17	0	0	0	1	219.63		
18	0.333	0	0.333	0.333	186.86		
19	1	0	0	0	221.23		

Abbreviation: AH- Acid hydrolysis, EH- Enzyme hydrolysis, TRS – Total reducing sugar, TFS- Total fermentable sugar TFS= (TRS of AH +EH)

(B) Results of mixture design with biomasses obtained from Table 4.2

Expt. No.	CO	IC	LC	PH	TRS yield in AH (mg/g of raw Biomass)	TRS yield in EH mg/g of delignified BM	TFS yield mg/ g of Raw BM
20	0.333	0.333	0	0.333	85.40		
21	0	0	1	0	87.92		
22	0.5	0.5	0	0	104.42	536.36	270.58
23	0.25	0.25	0.25	0.25	99.54		
24	0.5	0	0.5	0	103.95		
25	1	0	0	0	112.18		
26	0.125	0.125	0.125	0.625	81.90		
27	0	0.5	0	0.5	72.34		
28	0	0.5	0.5	0	81.86		
29	0.125	0.625	0.125	0.125	52.45		
30	0.5	0	0	0.5	32.54		
31	0	1	0	0	96.36		

Expt. No.	CO	IC	LC	PH	TRS yield in AH (mg/g of raw Biomass)	TRS yield in EH mg/g of delignified BM	TFS yield mg/ g of Raw BM
32	0.625	0.125	0.125	0.125	107.09	581.81	275.87
33	0	0.333	0.333	0.333	48.31		
34	0.125	0.125	0.625	0.125	78.31		
35	0.333	0.333	0.333	0	78.82		
36	0.333	0	0.333	0.333	80.59		
37	0	0	0.5	0.5	77.27		
38	0	0	0	1	93.36		

4.3.2 Biochemical analysis of composite biomass

The data obtained from acid and enzymatic hydrolysis of the composite biomass (both category A and B) are given in **Table 4.4(A)**. The cellulose content of the composite biomass was 52.80 ± 0.32% w/w biomass. The concentration of cellulose slightly increases after acid hydrolysis to 62.40 ± 1.2 owing to removal of hemicellulose during the acid pretreatment. The total reducing sugar yield after acid hydrolysis was 22.7 g/L (227 mg/g of raw biomass), as shown in **Table 4.4(A).** Lignin content of composite biomass was 20 ± 0.24. After delignification, cellulose concentration increased to 90.03 ± 0.23%. This is indicative of almost complete removal of lignin owing to effective alkaline delignification process with intermittent sonication **(Borah et al., 2016a,b)**. These results also draw a parallel outcome with the results of crystallinity index of cellulose, which shows a marginal increase in the crystallinity obtained after delignification. The case was nearly double when the cellulose crystallinity was analyzed for acid-pretreated biomass in comparison to raw biomass. This is mainly accredited to the fact that although sonication-assisted alkaline delignification extensively removes lignin content of biomass, it may also reduce crystallinity of cellulose. Removal of both lignin and hemicellulose results in exposure of cellulose fraction of biomass. However, acid hydrolysis for hemicellulose removal maintains crystallinity of cellulose, while delignification results in reduction of

crystallinity of cellulose making it increasingly amorphous. This enables the enzymes to adequately bind with the carbohydrate moieties of cellulose and give better yield of reducing sugar which will be later used as carbon source for bioalcohol production.

4.3.3 Kinetic assessment of enzymatic hydrolysis

The results of TRS yield of the delignified composite biomass after enzyme hydrolysis for both mechanical agitation (control) and ultrasound agitation (Test) are shown in **Fig. 4.2.** Enzyme hydrolysis with mechanical agitation gave TRS yield of 27.7 g/L (659 g/g of delignified biomass after 42 h). The yield of total fermentable sugar was 49.6 g /100 g of raw biomass depicted in **Table 4.4(A).** The kinetics of TRS release during enzymatic hydrolysis of the delignified biomass is represented in **Table 4.4(B).**

Preliminary, though enzyme hydrolysis was conducted for 120 h, but the time profile of 42 h is considered, since the incremental sugar release was less than 5% for every hour of treatment after 42 h. On the contrary, similar amount of sugar was obtained through ultrasound-assisted enzyme hydrolysis at 14 h with 10% duty cycle mentioned in **Table 4.4(A).** This is a clear elucidation of beneficial effect of sonication that has augmented the yield of sugar and also reduced the time required for hydrolysis. Sonication also significantly accelerated the kinetics of hydrolysis. The TRS yield per gram of delignified composite biomass and the corresponding cellulose conversion per hour is 56 mg and 62.5 mg respectively, which is nearly 2× the control experiments, as evident from **Table 4.4(A).** A theoretical bioalcohol yield from TRS obtained from composite biomass is: ethanol = 25.29 ± 0.14; butanol = 20.17 ± 0.12 g/L.

Table 4.4 Results of TRS release from composite biomass during different pretreatments and subsequent enzymatic hydrolysis

(A) TRS yield in acid and enzyme hydrolysis

Composite Biomass	TRS released in AH (g/L)	TRS yield in AH (mg/g of raw biomass)	TRS released in EH till 36 hour (g/L)	TRS yield in EH till 36 hour (mg/g of delignified biomass)	TFS yield (mg/g of raw Biomass)	TFS yield (g/100 g of raw biomass)
Control	22.70	227.0	27.7	659.0	492.1	49.2
Test	22.70			662.0	496.3	49.6

TRS – total reducing sugar; TFS – total fermentable sugar, AH – acid hydrolysis; EH – enzymatic hydrolysis. Control experiments = mechanical shaking, Test experiments = mechanical with intermittent sonication.

(B) Kinetics of TRS release during enzyme hydrolysis and theoretical alcohol (ethanol/butanol) yield.

Composite Biomass	TRS released in EH (mg/ g-delignified biomass/ h)	TRS released in EH (mg/ g-cellulose/ h)	Theoretical ethanol yield (g/ 100g raw biomass)	Theoretical butanol yield (g/ 100g raw biomass)
Control	20.79	23.1	25.09	20.17
Test	56.33	62.5	25.29	20.34

[a] *Maximum theoretical yield for ethanol from hexose as well as pentose sugars is 0.51 g/g sugar and Butanol is 0.41 g/g sugar*

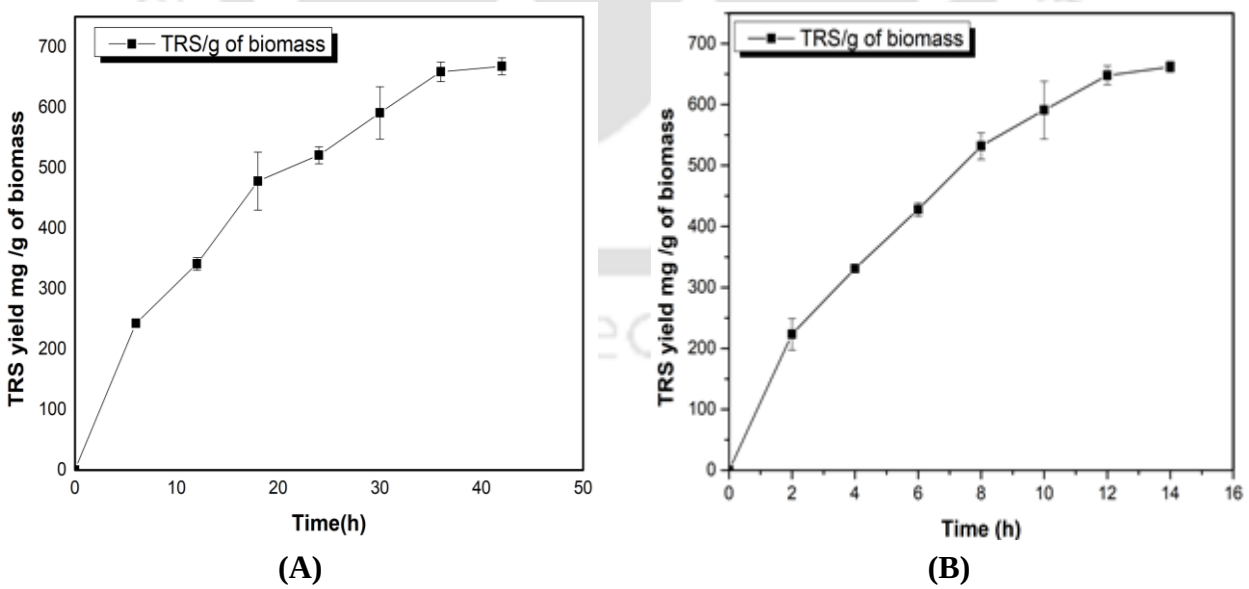

(A) **(B)**

Fig. 4.2 Time profile of TRS release during enzymatic hydrolysis of delignified biomasses (A) Control (Mechanical shaking @150 rpm) (B) Test (Shaking with intermittant sonication)

4.3.4 Results of composite biomass characterization

Compositional analysis alone is not sufficient to investigate the dynamic change of multifunctional component in lignocellulose. For instance, lignin localization and its interaction with cellulose and hemicellulose will give a valuable insight into the effects of various pretreatments into the structure that cannot be inferred from other analysis. The analysis of three widely used techniques, viz. FTIR, XRD and SEM are presented below.

FTIR analysis of composite biomass: The effect of dilute acid pretreatment and alkaline delignification on the composition of composite biomass was monitored in terms of relative change in the vibrational frequencies of different functional groups in the IR spectrum of the biomass. A relative positive change in all the characteristic band position is visible from the **Table 4.5** below after both pretreatments. Positive change for the band position indicates removal of the corresponding functional group from lignin.

XRD analysis of composite biomass: Crystallinity index (CrI) is a traditional parameter used for the quantitative representation of the crystallinity, indicating the relative amount of the crystalline (ordered) and amorphous (less ordered) regions of a cellulosic structure or glucan from hemicellulose. Its crystallinity is believed to play a major role in its biological conversion. Changes in cellulose structure induced by dilute acid pretreatment and alkaline delignification is plotted in Figure 4.3 below. Amorphous part also incorporates all other constituent such as lignin, pectin and protein etc. apart from crystalline cellulose **(Ciolacu et al., 2011)**. The amorphous regions are able to adsorb the water; moreover, their chemical, enzymatic, and microbial hydrolysis are easier and faster than the crystalline regions **(Karimi et al., 2013)**. Rise in crystalline value after acid hydrolysis is indicative of removal of hemicellulose which leads to more exposure of

cellulose content. Further increase in crystallinity after alkaline delignification is attributed to the rupture of the linkage between cellulose and lignin **(Borah et al., 2016)**. Alkali treatment with intermittent sonication results in disruption of lignin structure and swelling of biomass with increase surface area and decrease in degree of polymerization **(Singh et al, 2014).**

SEM analysis of composite biomass: Surface characterization, morphology, and analysis of microstructure can be performed by SEM. The representative micrographs of raw and various pretreated composite biomass are shown in **Fig. 4.4.** Existence of micro pores after dilute acid pretreatment marked the effectiveness of the process. Delignification process results in surface destruction and re-localization of the cell wall components implies the idea of better accessibility and the enzymatic hydrolysis **(Donohoe et al., 2011).**

Table 4.5 Summary of pretreated composite biomass using FTIR spectroscopy (relative change in intensity for various band)

Band position and assignment[#] (cm^{-1})	**Relative change in intensities**	
	Composite AH	Composite DLG
900 (Band of cellulose)	13.05	26.27
1098 (Amorphous to crystalline cellulose ratio)	7.90	20.73
1059 (C=O stretching due to carbohydrate–lignin linkage)	7.53	19.46
1238 (Hemicellulose–lignin linkage)	10.59	27.89
1245 (C=O absorption resulting from acetyl group cleavage)	10.86	28.22
1260 (Ester absorbance related to removal of uronic acid)	11.27	28.47
1378 (Band of hemicellulose)	13.89	13.37
1428 (Band of cellulose)	14.20	-3.18
1458 (Aromatic ring vibration related to lignin removal)	14.55	23.57
1508 (Aromatic ring vibration related to lignin removal)	14.91	3.35
1595 (Aromatic ring stretch related to lignin removal)	18.36	29.08
1720 (Carboxylic acids / ester groups)	14.42	34.31
1738 (C=O stretching due to carbohydrate linked with lignin)	15.20	35.80
1745 (Carbonyl bonds related to lignin side chain removal)	15.72	36.71
2900 (C–H stretching related to rupture of methyl/group of cellulose)	19.75	37.38
3348 (O–H stretching related to rupture of cellulose-hydrogen bonds)	19.51	35.93

Relative change (%) = (Intensity of untreated biomass – Intensity of pretreated biomass)/ Intensity of untreated biomass × 100Abbreviations: AH - Acid hydrolysis; DLG - Delignified biomass
Data taken from Kumar *et al*. (2009), Singh *et al*. (2014), Sun *et al*. (2005)

Table 4.6 Characterization of pretreated composite biomass by XRD in term of crystallinity index.

Biomass	Crystallinity Index, *CrI* (%)		
	Raw	Post dil. acid hydrolysis	Post delignification
Composite	37.5	60	64.70

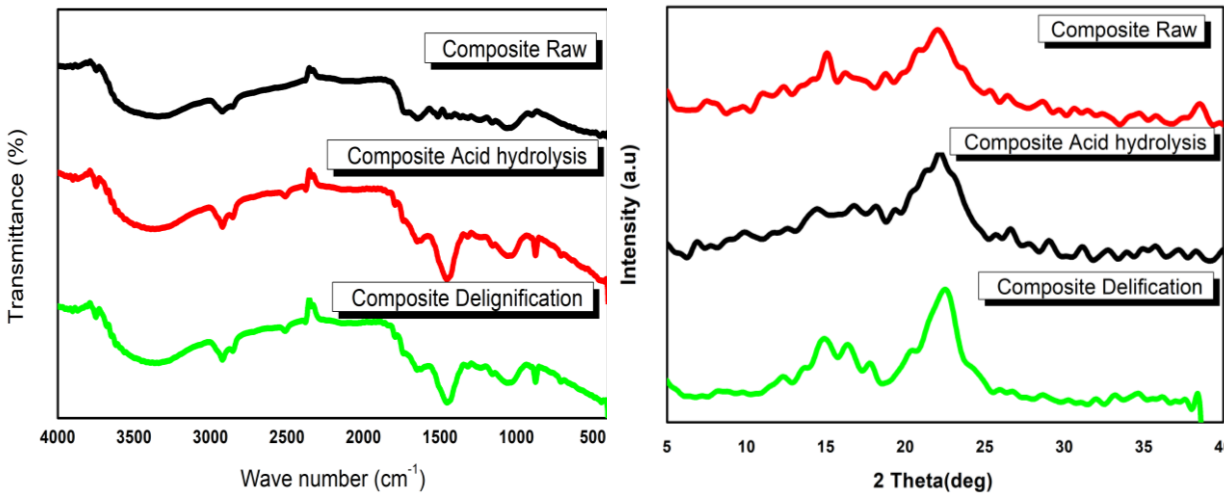

Figure 4.3 (1) FTIR spectra and **(2)** X-ray diffractograms of native or raw composite biomass, biomass after dilute (1%) acid hydrolysis with autoclaving (121ºC, 15 psi) and biomass after alkaline delignification (1.5% w/v NaOH with sonication).

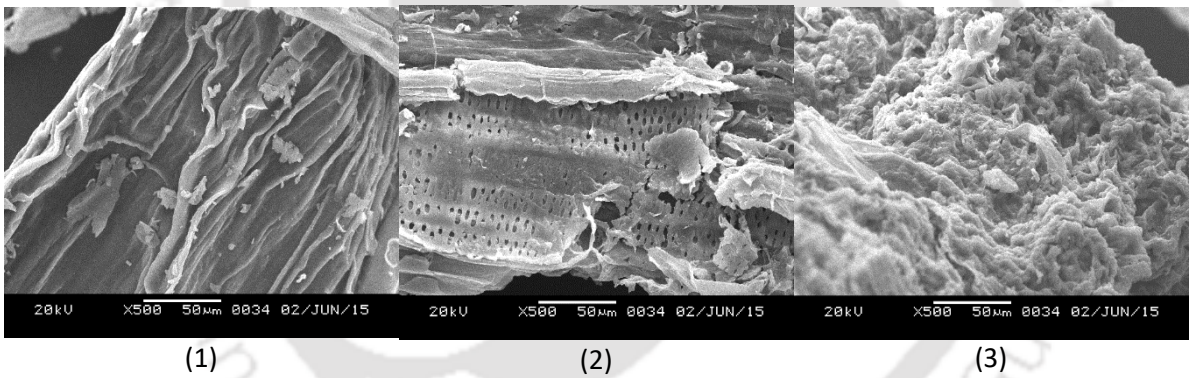

Figure 4.4 SEM micrographs of composite biomass species in native or raw state and after various stages of pretreatment. (1) raw biomass, (2) biomass after acid hydrolysis with autoclaving (1% v/v H_2SO_4, 121ºC, 15 lb pressure), (3) delignified biomass (alkaline treatment with 1.5% w/v NaOH with sonication).

4.4 Conclusion

During feedstock limited condition, all eight biomasses can be mixed at two best ratios obtained from mixture design experiments to form a composite biomass. Total fermentable sugar (both pentose and hexose) obtained by acid hydrolysis and enzyme hydrolysis from the whole composite was 49.6 ± 0.28 g/100 g of raw biomass which could be directly used for bioalcohol production via fermentation route. Characterization of the composite biomass revealed that the pretreatments of the biomass induced a positive change in the structure and biochemical composition. A theoretical yield of around 25.29 ± 0.14 ethanol and 20.17 ± 0.12 butanol was estimated from the available TRS from the composite biomass.

References

Bahuguna, U., Shukla, R.N., 2010. A study on investigation of the chemical constituents & milled wood lignin analysis of *Lantana camara* & *Prosopis chinnsis*. International Journal of Applied Biology and Pharmaceutical Technology, 830-839.

Bharadwaja, S.T.P., Singh, S., Moholkar, V.S., 2015. Design and optimization of a sono-hybrid process for bioethanol production from Parthenium hysterophorus. Journal of Taiwan Institute of Chemical Engineering, 51, 71–78.

Borah, A.J., Agarwal, M., Poudyal, M., Goyal, A., Moholkar, V.S., 2016b. Mechanistic investigation in ultrasound induced enhancement of enzymatic hydrolysis of invasive biomass species. Bioresource Technology, 213, 342-349.

Borah, A.J., Singh, S., Sarma, S., Goyal, A., Moholkar, V.S., 2016a. An assessment of the potential of invasive weeds as multiple feedstocks for biofuel production, Royal Society of Chemistry Advance, 6, 47151.

Ciolacu, D., Ciolacu, F., Popa, V.I., 2011. Amorphous cellulose structure and characterization. Cellulose Chemical Technology, 45, 13–21.

Donohoe, B.S., Vinzant, T.B., Elander, R.T., Pallapolu, V.R., Lee, Y.Y., Garlock, R.J., Balan, V., Dale, B.E., Kim, Y., Mosier, N.S., Ladisch, M.R., Falls, M., Holtzapple, M. T., Sierra-Ramirez, R., Shi, J., Ebrik, M.A., Redmond, T., Yang, B., Wyman, C.E., Hames, B., Thomas, S., Warner, R.E., 2011. Surface and ultrastructural characterization of raw and pretreated switch grass. Bioresource. Technology, 102, 11097–11104.

Goering, H.K. and Van Soest, P.J., 1970. Forage fiber analysis: apparatus, reagents, procedures and some applications. USDA-ARS Agricultural Handbook 379, Washington DC.

Karimi, K., Shafiei, M., Kumar, R., 2013. Progress in physical and chemical pretreatment of lignocellulosic biomass. In: Gupta, V.K., Tuohy, M.G. (Eds.), Biofuel Technologies. Springer, Berlin, Heidelberg, 53–96.

Kumar, R., Mago, G., Balan, V., Wyman, C.E., 2009. Physical and chemical characterizations of corn stover and poplar solids resulting from leading pretreatment technologies. Bioresource Technology, 100, 3948–3962.

Lenihan, P., Orozco, A., O'Neill, E., Ahmad, M., Rooney, D., & Walker, G. 2010. Dilute acid hydrolysis of Lignocellulosic biomass. Chemical Engineering Journal,156, (2), 395-403.

Qureshi, N., Blascheck, H.P., (2000). Butanol production using *Clostridium beijerinckii* BA 101 Hyper–Butanol producing mutant strain and recovery by Pervaporation. Applied Biochemistry Biotechnology, 84–86, 225–235.

Rajkhowa, D.J., Gogoi, A.K., Yaduraju, N.T., 2005. Weed utilization for vermicomposting – Success story. NRC for weed science, Jabalpur (M.P.), India.

Rao, P.V., Baral, S.S., 2011. Experimental design of mixture for the anaerobic co-digestion of sewage sludge. Chemical Engineering Journal, 172, 977–986

Saeman, J.F., 1945. Kinetics of wood saccharification. Hydrolysis of cellulose and decomposition of sugars in dilute acid at high temperature. Industrial and Engineering Chemistry, 37, 43-52.

Segal, L., Creely, J.J., Martin, A.E. Jr, Conrad, C.M., 1962. An empirical method for estimating the degree of crystallinity of native cellulose using the x-ray diffractometer. Textile Research Journal, 29, 786–794.

Singh, S., Khanna, S., Moholkar, V.S., Goyal, A., 2014. Comparative assessment of pretreatment strategies for enzymatic saccharification of *Parthenium hysterophorus*. Applied Energy, 129, 195–206.

Sun, X.F., Xu, F., Sun, R.C., Fowler, P., Baird, M.S., 2005. Characteristics of degraded cellulose obtained from steam exploded wheat straw. Carbohydrate Research, 340, 97–106.

Tizazu, B. Z., Moholkar, V.S., 2018. Kinetic and thermodynamic analysis of dilute acid hydrolysis of sugarcane bagasse. Bioresource Technology, 250, 197–203.

CHAPTER 5: PHYSICAL INSIGHTS OF ULTRASOUND-ASSISTED ETHANOL PRODUCTION FROM COMPOSITE FEEDSTOCK OF INVASIVE WEEDS[§]

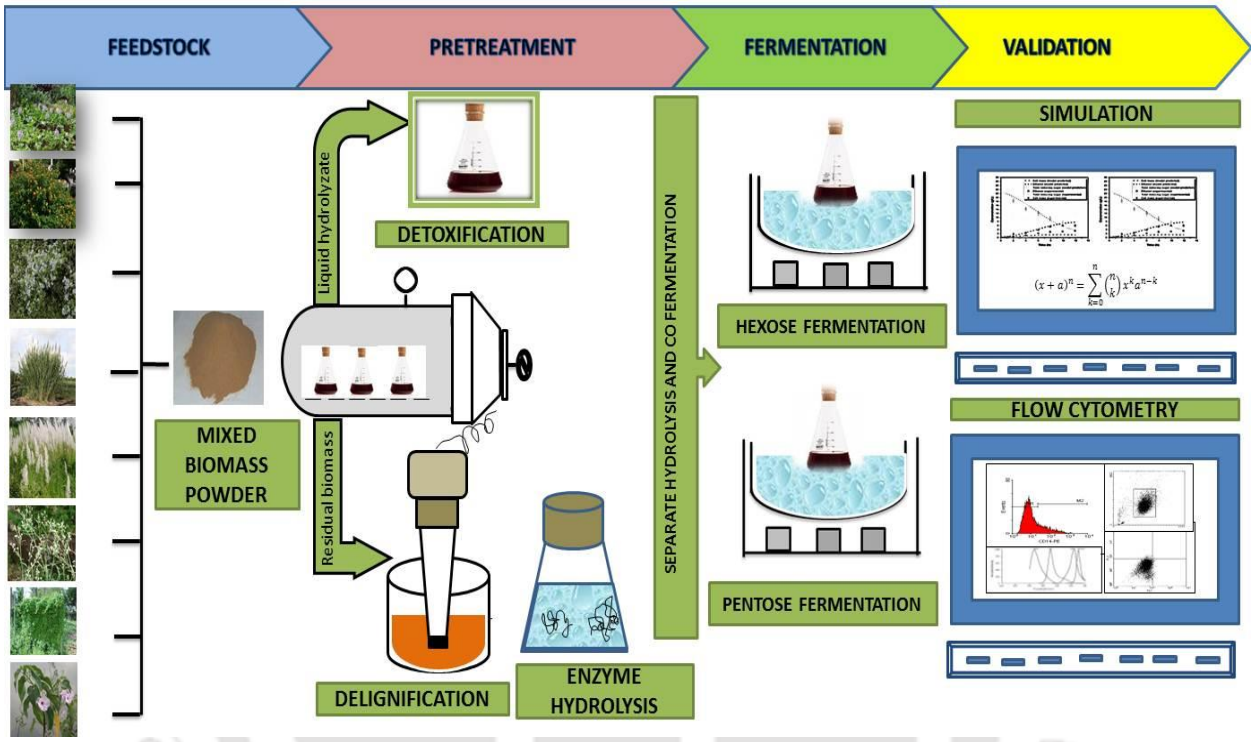

Chapter Highlights

- Bioethanol fermentation (SHF protocol) using mixed feedstock of 8 invasive weeds
- Fitting of fermentation profiles to biokinetic model using Genetic Algorithm
- Total ethanol yield from pentose and hexose fermentation = 220 g/kg raw biomass
- Faster transport of nutrients, substrate and products across cell membrane with sonication
- Rise in Monod saturation constant for substrate with reduction in substrate inhibition

[§] *See also* **Borah A.J.**, Agarwal, M., Goyal, A., Moholkar, V.S. (2018) Physical insights of ultrasound-assisted ethanol production from composite feedstock of invasive weeds, *Ultrasonics Sonochemistry*. doi: 10.1016/j.ultsonch.2018.07.046.

CHAPTER 5

PHYSICAL INSIGHTS OF ULTRASOUND-ASSISTED ETHANOL PRODUCTION FROM COMPOSITE FEEDSTOCK OF INVASIVE WEEDS

5.1 Introduction

High production cost of lignocellulosic ethanol has been attributed primarily due to the price of the feedstock. **Qureshi and Blaschek (2000)** reported that 30~32% of the bioalcohol production cost is contributed by the feedstock, followed by ~19-20% contribution by cost of pretreatment. For a viable lignocellulosic ethanol production (2nd generation bioethanol), continuous supply of biomass feedstocks at a rational cost must be warranted. Most of the studies on bioethanol production have been based on single feedstock, which limits their practical viability owing to unassured year-long supply of the biomass because of logistics, intrinsic and extraneous factors. In this context, use of mixed feedstocks as substrate for bioethanol production has been poorly explored. Invasive weeds present in every ecosystem worldwide form potential feedstocks for biofuel generation. Quantitatively, these weeds constitute an abundant biomass ranging from 5 t/ha to as high as 20 t/ha depending upon the species, prevailing season and the growth conditions **(Rajkhowa et al., 2005)**. These invasive weeds have adverse impact on both terrestrial and aquatic ecosystem **(Bhatt et al., 2011).** However, use of mixed substrate for bioethanol production has its own limitations and challenges, since each individual feedstock could have widely varying properties such as moisture and ash content, structural composition of cellulose, hemicellulose and lignin, particle size and distribution, bulk density, etc. **(Anukam et al., 2016)**. Accordingly, different feedstocks have different optimal conditions for pretreatment, hydrolysis and fermentation.

Ultrasound is an established technique for intensification of diverse physical and chemical processes and has also been employed for enhanced bioethanol production **(Nikolic et al., 2010; Subhedar et al., 2015; Battista et al., 2016; Berlowska et al., 2016)**. Ultrasound exhibits its effect on the reaction system through cavitation bubbles of implosive collapse that create intense energy concentration on an immensely small spatial and temporal scale **(Nalajala et al., 2010; Choudhury et al., 2014)**. The main physical influence of ultrasound and cavitation is generation of intense micro-turbulence that gives micromixing in the medium, which terminates mass transfer limitations. The chemical effect of transient cavitation is generation of highly reactive radicals and other smaller species through thermal dissociation of vapor entrapped in the bubble at the moment of transient collapse.

The objective of this study was to investigate the influence of ultrasound in enhancing bioethanol production from mixed biomass of invasive weeds in comparison to the conventional process employing mechanical agitation. A mixture of 8 invasive weeds found in Northeastern India, viz. *Arundo donax* (AD), *Chromolena odorata* (CO), *Mikania micrantha* (SS), *Lantana camara* (LC), *Eichhornia crassipes* (EC), *Ipomea carnea* (IC), *Parthenium hysterophorus* (PH) and *Saccharum spontaneum* (SS) was used as the substrate. Fermentation was carried out using the procedure of SHF (separate hydrolysis and fermentation). Both hydrolyzates obtained from dilute acid hydrolysis and enzymatic hydrolysis were used for fermentation. Time profiles of substrate, biomass and product in fermentation were fitted to a mathematical model using Genetic Algorithm. The flow chart of genetic Algorithm is given in **Appendix Fig. 3A**. Relative variations in the parameters of the kinetic model provide mechanistic insight into the effect of sonication on enhancement of bioethanol fermentation process. Moreover, the physiological status and heterogeneity within bacterial population subjected to stress

during fermentation with mechanical agitation and sonication was assessed using multicolor flow cytometry (FCM) analysis **(Amor et al., 2002)**.

5.2 Materials and Methods

5.2.1 Chemicals and reagents

Each of the medium components (*viz*. yeast extract, Potassium dihydrogen phosphate, ammonium disulphate and magnesium sulphate) and sodium hydroxide pellets were obtained from Himedia Pvt. Ltd., India. Sulphuric acid used for reagent preparation was acquired from Fisher Scientific, India. Glucose (99.5% purity) used as standard for reducing sugar estimation, and commercial enzymes (cellulase 8 U/mg and β-glucosidase 250 U/mg, Novozyme 188) were procured from Sigma Aldrich, USA. Ethanol (99.5%), used as standard in gas chromatography, was procured from Loba Chemicals, USA.

5.2.2 Biomass collection and its processing

All the eight weeds, *viz.* AD, CO, EC, IC, LC, MM, PH, and SS were collected from the campus of our institute. The chopped biomass was washed with water followed by drying in hot air oven at 60^{o}C for 18-24 h followed by grinding (using a mixer grinder) into powdered biomass. The powdered biomass (particle size < 1 mm) was stored in air–tight containers at room temperature.

5.2.3 Pretreatment of raw composite biomass (acid pretreatment and delignification)

Composite biomass comprising mixture of 8 invasive weeds (in ratio pre-optimized using statistical mixture design as described in Chapter 4) was subjected to dilute acid hydrolysis under following conditions: 1% (v/v) H_2SO_4 (equivalent to 0.36 N), 10% w/v biomass, autoclaving at 121°C and 15 psi for 30 min followed by rapid steam

release. These conditions were optimized for acid hydrolysis of different invasive weeds and are mentioned in Chapter 3, section 3.3.3 for acid hydrolysis, and section 3.3.4 for detoxification. The hydrolysate was filtered using muslin cloth and the filtrate (i.e. pentose-rich hydrolyzate) was cooled to room temperature. After pretreatment, the solid residue was subjected to delignification by ultrasound-assisted alkaline treatment. The conditions for ultrasound-assisted delignification of acid-pretreated composite biomasses was as follows: 2% (w/v) biomass, 1.5% (w/v) NaOH, 30°C and10 min of sonication with having duty cycle of 83% (50 s ON and 10 s OFF) **(Singh et al., 2014)**. These conditions were optimized earlier and reported in a previous study in chapter 3 in subsection 3.3.5, adopted from **Bharadwaja et al. (2015)**. The composite biomass residue obtained after both acid hydrolysis and delignification was washed several times till neutral pH was obtained. The residual biomass was dried in a hot air oven at 60°± 3°C for 12 h. The cellulose content of the delignified solid residue was determined as 90.3 ± 3.2 g/g of delignified biomass according to standard TAPPI protocols **(Allan et al., 1992)**. This cellulose-rich residue was subjected to enzymatic hydrolysis, as explained in the section 5.2.4.

5.2.4 Enzymatic hydrolysis

The enzymatic hydrolysis of composite biomass was performed in 150 mL Erlenmeyer flask with 50 mL of total working volume. Reaction mixture for enzymatic hydrolysis comprised of 4.2% (w/v) of delignified residue in 100 mL of 50 mM citrate phosphate buffer solution (pH 5.0 ± 0.2, actual cellulose concentration = 38.03 g/L) with cellulase and cellobiase concentrations of 135 and 75 FPU/g biomass, with bath temperature maintained at 30° ± 3°C, respectively **(Bharadwaja et al., 2015)**. In order to enhance the kinetics of enzymatic hydrolysis with concurrent rise in sugar yield,

sonication was applied to the reaction mixture at duty cycle of 10% as per the protocol reported earlier by **(Singh et al., 2015a).** The ultrasound system used for sonication is described in subsection 5.2.6.1. The presence of total reducing sugars (glucose, pentose) sugar in the enzymatic hydrolysate was confirmed by HPLC analysis (Perkin–Elmer, Series 200, with a refractive index detector) using HiPlex-H column (300 mm × 5 μm × 4.6 mm, Varian) with MilliQ water as eluent at flow rate 0.6 mL/min.

5.2.5 Microorganism, culture revival and maintenance

Saccharomyces cerevisiae MTCC 170 was obtained from Microbial Type Culture Collection (MTCC), Chandigarh, India. The powdered microbial culture was grown in YEPD medium (at pH 5) consisting of 10 g/L yeast extract, 10 g/L peptone and 20 g/L glucose. *S. cerevisiae* MTCC 170 culture was incubated at 30°C and 150 rpm in an incubator shaker (Orbitek, Scigenics Biotech, India) for 18 h **(Singh et al., 2015)**. *Candida shehatae* NCIM 3500 was procured from National Chemical Laboratory (NCL), Pune, India. This yeast was grown in MGYP media comprising 3 g/L malt extract, 3 g/L yeast extract, 5 g/L peptone and 10 g/L glucose at pH 6.0 ± 0.4. *C. shehatae* NCIM 3500 culture was incubated at 30°C, 120 rpm in an incubator shaker (Orbitek, Scigenics Biotech) for 48 h. before inoculating into the fermentation medium **(Bharadwaja et al., 2015)**. Both cultures were preserved at 4°C as agar slants and sub-cultured after a regular interval of approx. 2 weeks.

5.2.6 Fermentation of composite biomass for ethanol production

The hydrolysate obtained from both dilute acid pretreatment and enzymatic hydrolysis of composite biomass was used for ultrasound-assisted fermentation. The hydrolysate from acid pretreatment consisted of pentose sugars resulting from hydrolysis

of hemicellulose; while the hydrolyzate obtained from enzymatic hydrolysis of cellulose comprised hexose sugars. The pentose hydrolysate also contained inhibitory compounds like hydroxyl methyl furfural and furfural generated due to oxidation of reducing sugars. Therefore, the hydrolysate was detoxified by neutralization with 2% (w/v) $Ca(OH)_2$ followed by adsorptive removal of inhibitory compounds **(Nguyen et al., 2017)**. Which had been discussed in **chapter 2** under **subsection 2.2.4**.

***5.2.6.1 Ultrasound system for fermentation*:** Sonication of reaction mixture was performed in an ultrasound bath (Make: Elma, Germany; Model: Trans-sonic T-460, 2 L, Power = 35 W, frequency = 35 kHz). Calorimetric technique was used to estimate actual acoustic power input to the medium in the bath as 18.58 W, and on this basis acoustic pressure amplitude in the bath was calculated as 1.5 bar **(Chakma et al., 2011)**. The Erlenmeyer flask was positioned at the center of the ultrasound bath and the flask was immersed in about 50% of its height in the water. The bath was mapped for spatial variation of acoustic intensity **(Gogate et al., 2002)**. The position of the flask was carefully retained similar in all experiments conducted to avoid artifacts generated due to fluctuating ultrasound intensity **(Moholkar et al., 2000)**. The temperature of the water bath was kept at 30°±2°C by substituting water in the bath at regular intervals. Sonication was applied with 10% duty cycle (i.e. 1 min ON and 9 min OFF in every 10 min of treatment), which was optimized earlier on the basis of the viability of cells.

5.2.6.2 Pentose fermentation: Fermentation of dilute acid (or pentose-rich) hydrolysate was carried out in a 150 mL Erlenmeyer flask at 30°C and 150 rpm in an incubator shaker for 30 h. The final fermentation medium consisted of 1 g/L yeast extract, 22.7 ± 1.8 g/L reducing sugars, 1 g/L potassium dihydrogen phosphate, 5 g/L ammonium sulphate and

0.5 g/L magnesium sulphate heptahydrate. 10% (v/v) inoculum of *Candida shehatae* was added to the fermentation medium. The total volume of fermentation medium was 50 mL. In the control experiments, fermentation was carried out in a shaker incubator at 30°C for 30 h at 150 rpm, while in test experiments; intermittent sonication was applied to fermentation mixture at duty cycle of 10%. Experiment was conducted till the residual sugar concentration in fermentation mixture reduced to ≤ 5 g/L. 100 µL samples of fermentation broth were withdrawn at 2 h of regular intervals followed by centrifugation at 10,000 rpm at 4°C for 20 min. These samples were used for determination of progress of fermentation, i.e. the time profiles of substrate, product and the biomass. All experiments were conducted in triplicate to assess the reproducibility of the results.

***5.2.6.3 Hexose fermentation*:** Fermentation of the enzymatic (or hexose-rich) hydrolyzate was carried out in a 150 mL Erlenmeyer flask with working volume of 50 mL. The final fermentation medium contained with 3 g/L yeast extract, 27.7 g/L reducing sugars (mainly glucose), 3 g/L peptone, 1 g/L potassium dihydrogen phosphate, 0.5 g/L ammonium sulphate and 0.5 g/L magnesium sulphate heptahydrate and 10% (v/v) inoculum (10^6 cells/ml) of *Saccharomyces cerevisiae* was added to the medium **(Karuppaiya et al., 2010)** and medium pH adjusted to 5.0. Rest of the protocol for the control and test experiments was same as described earlier for hexose fermentation **(Singh et. al., 2015)**.

5.2.7 Analysis

The residual concentration of total reducing sugars (TRS) in the samples of both pentose and hexose fermentation mixtures was quantified with the standard protocol of **Nelson (1944)** and **Somogyi (1945)** with glucose (99.5% purity) used as standard. The

samples of fermentation mixture were centrifuged at 10,000 rpm for 15 min to form pellets of cell biomass. The cell pellets were dried at 60° ± 3°C in hot air oven and the dry cell weight (DCW) weight was measured for estimation of cell biomass. Ethanol in the samples withdrawn from fermentation mixture was quantified by Gas Chromatograph (Thermo Fischer CP 202N) using a CP Wax 52 CB capillary column (250 mm × 0.25 mm × 0.39 mm, Varian) and ethanol (99.5% purity) as standard. The oven temperature was set from 45°C to 100°C with 3°C/min increment and after 100°C, 5°C/min increment up to 200°C. The temperatures of the detector and injector were maintained at 250°C and 230°C, respectively. Nitrogen gas was used as a carrier with a flow rate of 2 mL/min.

5.2.8 Viability analysis of sonication-exposed yeast cells by FACS

Acquisition of fermentation samples was carried out with a multi-parametric BD FACS calibur (Becton Dickson, 488 nm argon ion laser, 15 mW). Carboxyfluorescein diacetate (CFDA) and propidium iodide (PI) were used for assessment of the viability of ultrasound induced micro-organism during fermentation. Cells of *Clostridium acetobutylicum* (10^6 cfu/mL) were centrifuged at 10,000 rpm for 10 min and resuspended in 50 mM phosphate buffer saline (PBS, pH 7). Unstained, single and double stained along with heat killed stained cells were used as positive and negative controls to program the instrument detectors. The cell samples were stained and acquired as per the protocol described by **Mahato et al. (2016)**. The signals were collected in log mode by BD Cell Quest Pro software, and were further analyzed and refined by FloJo software (Tree Star, Stanford, USA). All experiments were conducted in duplicate to assess reproducibility.

5.3 Mathematical model

A mathematical model proposed by **Philippidis et al., (1992)** for ethanol fermentation, was used in this study. The model assumes that the pH of the fermentation mixture has no significant effect on enzyme activity and cell growth and remained constant during the fermentation. The growth medium supplies an excess of all nutrients except for the carbon source (total reducing sugars), which was derived by dilute acid/enzymatic hydrolysis of delignified composite biomass. The fermentation process comprised of following steps: (a) diffusion of sugar towards cell wall, (b) uptake of sugars by cells, (c) sugar metabolism and ethanol synthesis and (d) ethanol secretion into the aqueous phase. Ethanol and carbon dioxide are the major products of fermentation. The process of aerobic fermentation has been well represented by following three equations that give time variations of cell mass (X), total reducing sugars or TRS (G) and ethanol (E). The main equations of the model and the underlying assumptions are as follows.

Cell mass: Fermentative organism assumed glucose to be the primary carbon source, which is metabolized into cell mass, X, with concomitant synthesis of ethanol and CO_2. Other metabolic products obtained is of insignificant amount. The Monod kinetic expression, which involves both non-competitive substrate and product inhibition, relates the microbial growth as a function of ethanol and TRS concentration:

$$\frac{d(X)}{dt} = \mu_m \left[\frac{(G)}{K_3 + (G) + \frac{(G)^2}{K_1}} \right] \left[\frac{K_{3E}}{K_{3E} + (E)} \right] (X) - k_d (X)$$

Notations: K_3 – Monod constant for total reducing sugars, K_i – substrate inhibition constant, K_{3E} – inhibition constant of cell growth by ethanol, μ_m – maximal specific growth rate of the microorganism, the second term on the RHS is potential cell lysis,

which is assumed to be proportional to cell mass X and characterized by constant k_d, which is specific rate of cell death.

Total Reducing Sugars (TRS): TRS consumption in the fermentation broth occurs via two mechanisms, viz. cell mass synthesis and as a source of cell maintenance requirement. Thus, the total TRS consumption rate by two mechanisms is:

$$\frac{d(G)}{dt} = -\left[\frac{1}{Y_{X/G}}\frac{d(X)}{dt} + m(X)\right]$$

where, $Y_{X/G}$ – average yield coefficient of cell mass on the substrate (total reducing sugar), and m – specific rate of substrate consumption for maintenance requirements. The above balance for glucose does not include additional term corresponding to ethanol fermentation, as ethanol is a product directly associated with energy generated by the fermentative microorganism.

Ethanol: Ethanol formation occurs through two contributions, *viz*. growth-associated ethanol formation and non-growth associated ethanol formation and it also relies on the concentration of TRS in the medium:

$$\frac{d(E)}{dt} = \left[\alpha\frac{d(X)}{dt} + b(X)\right]\left[\frac{G}{K_4 + (G)}\right]$$

where, a – constant for growth associated ethanol formation, b – constant for non-growth associated specific ethanol production, and K_4 – Monod constant for ethanol synthesis.

The above set of ordinary differential equations (ODEs) for three independent variables, viz. X, G and E, and the parameters therein characterize the fermentation process. These equations have total of 10 parameters, *viz*. K_3, K_1, K_{3E}, k_d, μ_m, a, b, $Y_{X/G}$, m and K_4. The numerical solution of above equations was compared with the experimental time profiles of X, G and E. The unknowns in this model are the kinetic and physiological parameters, whose optimum values need to be determined by iteration so as to match the time profiles of the cell mass, substrate, and ethanol concentrations calculated using the model with the

experimental data. As per the findings of **Philippidis et al. (1992)**, K_4 is assumed to be zero. The Runge–Kutta 4th order method was used to solve the three ordinary differential equations of the main model, and parameters optimization was done by calculating root mean square (RMS) error between experimental and model results using Genetic Algorithm (GA). The objective function (Obj) for the optimization was defined as follows: $Obj = \min\left(\sum_{i=1}^{n} er_i\right)$ where n is the number of experimental data points for TRS concentration, ethanol concentration and cell mass concentration. The error (er) is defined as:

$er_i = \left[(G_i^{exp} - G_i^{pred})^2 + (X_i^{exp} - X_i^{pred})^2 + (E_i^{exp} - E_i^{pred})^2\right]^{1/2}$. GA minimizes the objective function (which is summation of root mean square of errors) and gives the corresponding optimized values of model parameters.

5.4 Results and Discussion

5.4.1 Acid hydrolysis and enzymatic hydrolysis of composite biomass

The total reducing sugar (TRS) content of pentose-rich dilute acid hydrolyzate after detoxification was determined as 22.7 ± 1.8 g/L. Enzymatic hydrolysis of composite biomass resulted in hexose-rich hydrolysate with TRS concentration of 27.7 ± 1.6 g/L, which corresponded to a yield of 659.5 mg/g of delignified biomass.

5.4.2 Experimental results of ethanol fermentation

Time profiles of ethanol, cell mass and TRS concentrations in control and test experiments for both pentose and hexose fermentations are shown in **Figs. 5.1** and **5.2**, respectively. The results of pentose and hexose fermentations under control and test conditions are summarized in **Table 5.1**.

Pentose fermentation: An ethanol titre of 9.78 ± 0.6 g/L (0.43 g/g reducing sugar, 0.073 g/g raw biomass) and biomass concentration of 3.26 ± 0.6 g/L was achieved after 24 h of fermentation in control experiment. Nevertheless, application of intermittent sonication during fermentation in test experiments reduced the fermentation period to 12 h with an increased ethanol titre to 11.58 ± 0.24 g/L (0.51 g/g reducing sugar, 0.087 g/g raw biomass) with biomass concentration 3.30 ± 0.2 g/L. Thus, a 2-fold rise in both ethanol and biomass productivity was observed in the test experiments shown in **Table 5.1** below.

Hexose fermentation: In the control experiments conducted for 24 h, an ethanol titer of 7.37 ± 0.8 g/L (0.26 g/g reducing sugar, 0.074 g/g raw biomass) and biomass concentration of 3.43 ± 0.4 g/L was achieved. In test experiments, ethanol titre increased to 13.3 ± 0.4 g/L (0.48 g/g reducing sugar, 0.13 g/g raw biomass) with biomass concentration of 3.80 ± 0.2 g/L in 12 h fermentation. Thus, application of sonication during hexose fermentation not only reduced the fermentation period by 50%, but also enhanced ethanol yield 1.8-fold. The net ethanol productivity, therefore, increased almost 4-fold.

5.4.3 Simulation results of ethanol fermentation

Simulated profiles of TRS, ethanol and biomass concentrations in pentose and hexose fermentation are shown in **Figs. 5.1** and **5.2**. It could be observed that the experimental and simulated profiles matched quite well. The kinetic and physiological parameters values of the fermentation model obtained after fitting of simulated profiles to experimental data by applying GA optimization are given in **Table 5.2**. Comparative evaluation of the model parameters for both pentose and hexose fermentation under control and test conditions provide an insight into the effect of sonication on physiology of fermentation as follows:

a) K_3 represents Monod constant for TRS for cell growth. The value of K_3 reduced marginally in test experiments for both pentose and hexose fermentation, as compared to respective control experiments. Reduction in K_3 with sonication is indicative of faster transport of substrate (or total reducing sugars) all across the cell membrane, which implies that sonication assists in better utilization of total reducing sugars for cell growth by rapid mass transfer and achieve maximum specific growth rate with limited TRS concentration.

b) K_i is the substrate inhibition constant for cell growth. Increase in K_i signifies high tolerance of cells towards non-competitive inhibition by the substrate. K_i increased in test experiment as compared to control experiment in both pentose and hexose fermentation. This effect is also attributed to enhanced of substrate transfer across cell membrane and faster utilization of substrate in the cells under influence of sonication, which reduces cell growth inhibition by substrate. Monod constant reduction for TRS and rise in the inhibition are synergistic phenomena, which are essentially manifested in terms of rise in values of $Y_{X/G}$ and $\mu_{max.}$

c) K_{3E} is designated as cell growth inhibition constant by products. No considerable difference in the values of K_{3E} value were observed in control and test experiments. This implies that the inhibition mechanism of cell growth by ethanol remains unaltered by the physical and chemical effects of ultrasound and cavitation.

d) In both pentose and hexose fermentations, specific cell death rate (k_d) and specific rate of substrate consumption for cell maintenance diminished in the test experiments. This essentially means that energy expenditures of the cells for mass transfer (nutrients,

substrate and product) across cell membrane reduce after exposure to sonication. These results are attributed to intense microconvection generated by sonication. Due to reduced energy requirements for cell maintenance, larger fraction of the substrate is utilized for cell metabolism that results in enhanced productivity of ethanol. Additional favorable effect of microconvection is deagglomeration of the cells and regulation of the osmolarity of cell's interior volume. Accumulation of toxic substances produced during fermentation in the mixture may result in death of cells. Strong micro-convection could also result in effective dilution of these substances in the bulk volume that may reduce the death rate of the cells, as evident from flow cytometry analysis presented in next section.

e) *a* and *b* are the constants for growth associated and non-growth associated ethanol production. In both control and test fermentations with pentose and hexose hydrolyzates, value of constant a is one order of magnitude higher than b. This indicates that sonication does not influence the intrinsic functioning of the microbial cells, and ethanol still remains a predominantly growth associated product even with application of sonication – only the productivity of ethanol increases for the reasons discussed in preceding paragraphs.

Table 5.1 Summary of experimental results of fermentation under control and test conditions

Parameter	Fermentation of pentose-rich hydrolyzate		Fermentation of hexose-rich hydrolyzate	
	Control experiment*	Test experiment#	Control experiment*	Test experiment#
Maximum ethanol concentration (g/L)	9.78 ± 0.6	11.58 ± 0.2	7.37 ± 0.8	13.3 ±0.4
Maximum cell mass concentration (g/L)	3.26 ± 0.6	3.30 ± 0.4	3.43 ±0.4	3.80 ±0.2
Ethanol yield on reducing sugar (g/g)§	0.43	0.51	0.26	0.48
Ethanol yield on raw biomass (g/g)§	0.073	0.087	0.074	0.13
Ethanol productivity (g/L/h)§	0.41	0.96	0.31	1.10
Cell mass productivity (g/L/h)§	0.14	0.27	0.14	0.32
Cell mass yield on reducing sugar (g/g)§	0.39	0.28	0.46	0.28

* Values after 24 h of fermentation, # Values after 12 h of fermentation, § Yields and productivities have been determined using average values of ethanol and cell mass concentrations.

Table 5.2. Physiological and kinetic parameters in fermentation model for control and test fermentations of pentose-rich and hexose-rich hydrolyzates

Parameter	Fermentation of pentose-rich hydrolysate		Fermentation of hexose-rich hydrolysate	
	Control experiment	Test experiment	Control experiment	Test experiment
Monod constant for cell growth, K_3 (g/L)	22.1	20.0	25.9	19.6
Inhibition constant of cell growth by substrate, K_i (g/L)	94.2	96.2	90.3	99.7
Inhibition constant of cell growth by ethanol, K_{3E} (g/L)	30.13	30.0	31.8	32.1
Specific cell death rate, K_d (1/h)	0.20	0.13	0.19	0.15
Maximal specific growth rate, μ_m (1/h)	0.79	0.96	0.94	0.98
Constant for growth associated ethanol formation, a (g/g)	2.95	2.98	2.84	2.99
Non-growth associated specific ethanol production rate, b (g/g/h)	0.35	0.59	0.37	0.48
Average yield coefficient of cell mass on TRS, $Y_{X/G}$ (g/g)	0.25	0.32	0.15	0.27
Specific rate of substrate consumption for cell maintenance requirement, m (1/h)	0.78	0.74	0.95	0.70
F-best	11.4	11.4	10.4	10.4

.

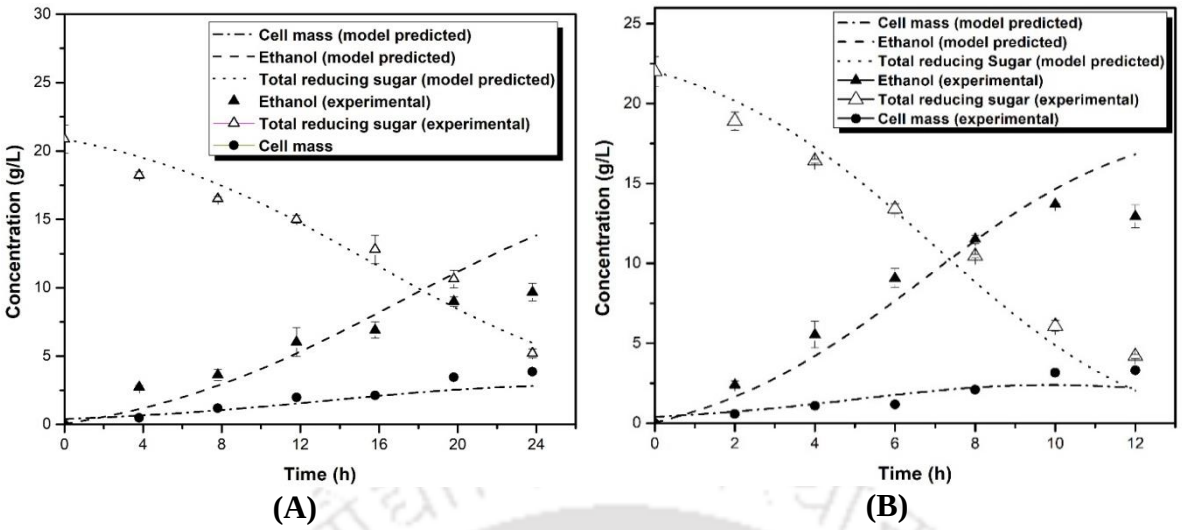

Figure 5.1. Experimental and simulated profiles of ethanol production, TRS consumption and biomass production in pentose fermentation. (A) control experiment, (B) test experiment.

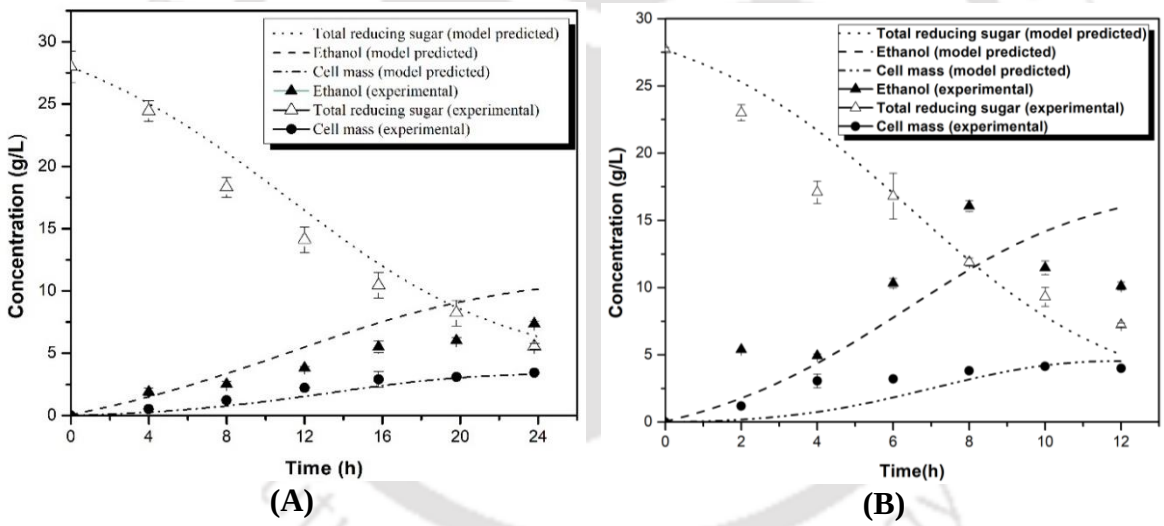

Figure 5.2. Experimental and simulated profiles of ethanol production, TRS consumption and biomass production in hexose fermentation. (A) control experiment, (B) test experiment.

5.5 Flow cytometry analysis of cells used in fermentations.

Multiparametric flow cytometry was conducted for assessing the viability of *S. cerevisiae* MTCC 170 and *Candida shehatae* NCIM 3500 cells after exposure to sonication during fermentation. Live, membrane compromised and dead bacteria were

observed in contour plots based on their differential staining characteristics with PI and cFDA stain. From the contour plots shown in **(Fig. 5.3)** the upper left quadrant (Q1) signifies the live population, upper right quadrant (Q2) consists of membrane compromised cells. Dead cells appeared in the lower right quadrant (Q3) and unstained cells in the lower left quadrant (Q4).

From the **Fig. 5.3**, negative control ($cFDA^-$ PI^-) showed least fluorescence signals while positive control ($cFDA^-$ PI^+) showed highest fluorescence intensity of PI (99% of population), Live population stain with cFDA ($cFDA^+$, PI^-) and heat killed population stained with PI ($cFDA^-$, PI^+) was adequately seen in their respective upper left (Q1) and lower right quadrant (Q3) with relative high intensity (87.8 % and 97.8% for native *S. cerevisiae* and *C. shehatae* cells, respectively) of their corresponding strain. The following controls have been performed to set the flow cytometry detector, from collecting any irrelevant light signal against any debris present in the samples. The graphs obtained from the experimental results clearly show that majority of cell intensity (*viz.* > 65.9% and 88.7% for native cells of *S. cerevisiae* and *C. shehatae* and 75.5% and 87.1% for ultrasound-treated *S. cerevisiae* and *C. shehatae*) falls in the live quadrant (Q1). Although there is negligible intensity in the dead zone (Q3) for both the cells, there is a considerable amount of cell population in the second quadrant (Q2) with 24% in case of *S. cerevisiae* and relatively lower in case of C. *shehatae* with 5-6%. This confirmed that the major cell populations existed as viable, if not exposed to any harsh treatment. It is thus revealed that use of sonication does not have any inhibiting effect on the cells. The mean fluorescence intensities (MFI) of fluorescent dyes for the two bacterial strains are also shown in **Table 5.3**. in addition to better the understand the cell physiological state. These contour plots are machine generated based on the relative intensity collected in the two filter chambers, viz. FL1 and FL3, for live and dead cells respectively.

Treatment	*Candida Shehate*	*Sacharomyces cerevisiae*
Cells with no stain (CDN)	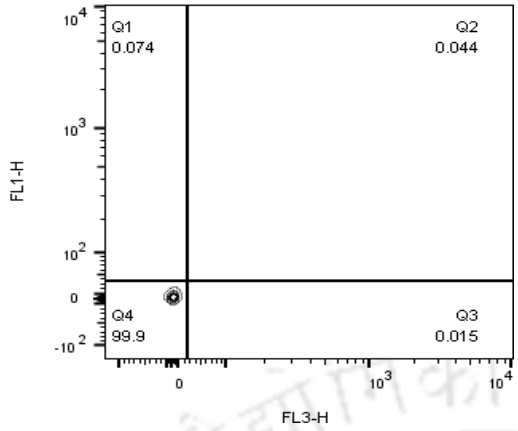	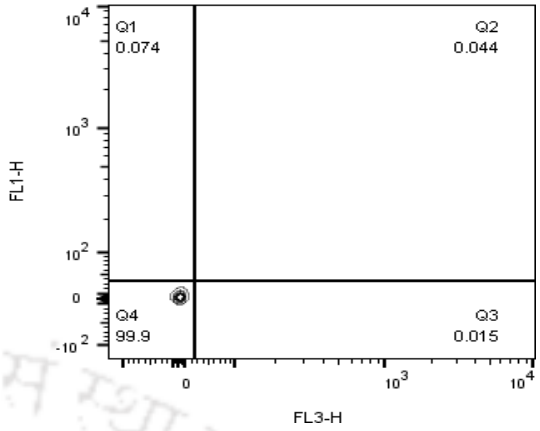
Cell stain with live cell stain CFDA. (CCFDA)	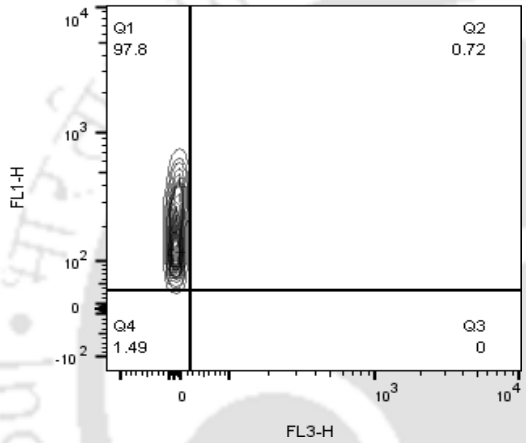	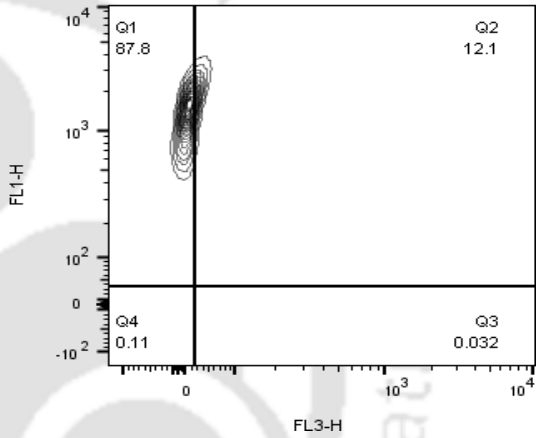
PI stain with heat killed cells (HPI)	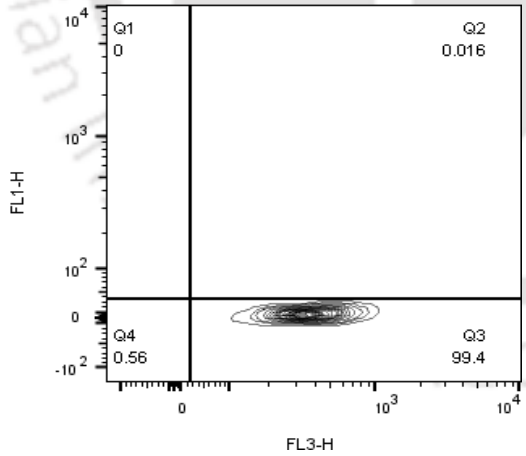	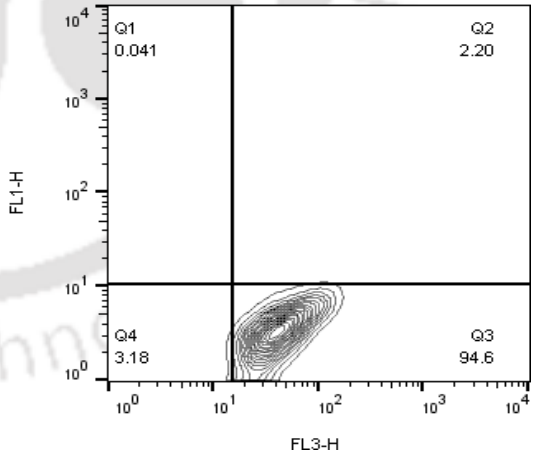

Figure 5.3. Results of viability analysis of *Candida shehatae* and *Saccharomyces cerevisiae* against ultrasound by flow cytometry.

Native cells

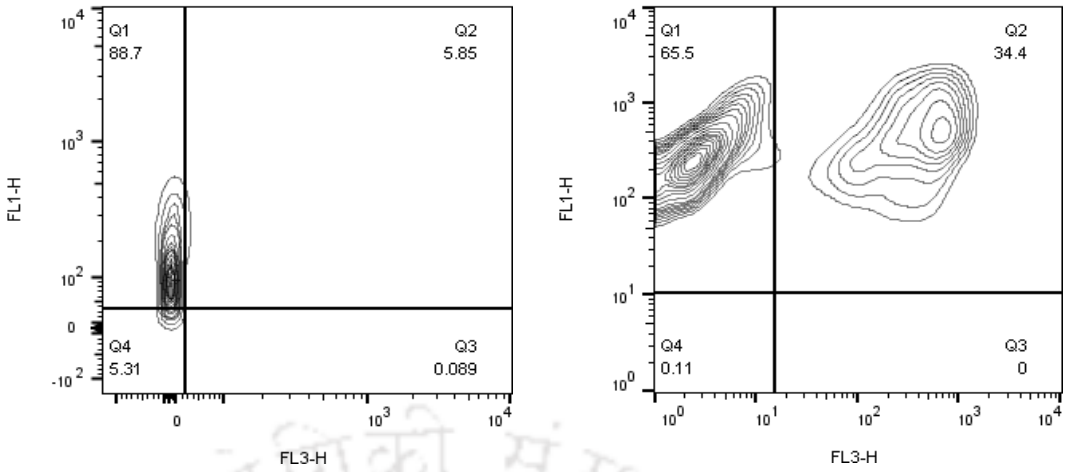

Ultrasound treated cells

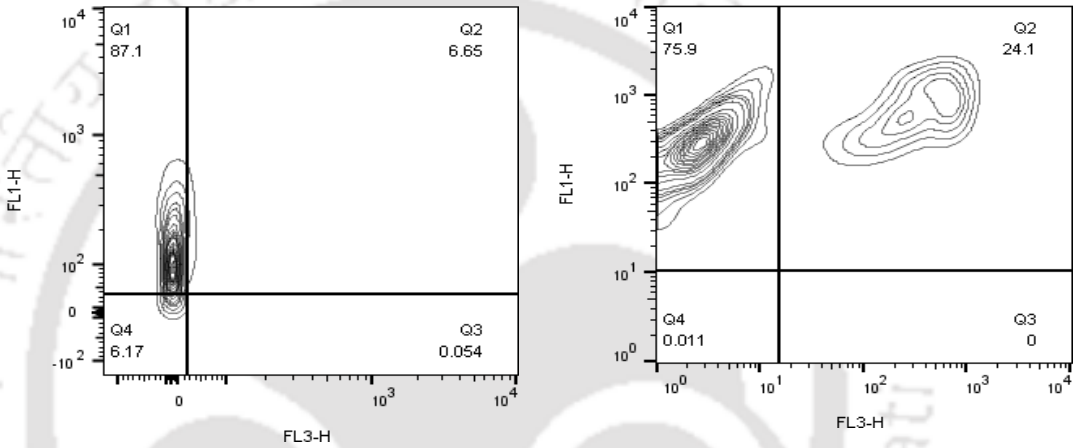

Figure 5.3 (*continued*….). Results of viability analysis of *Candida schehatae* and *Saccharomyces cerevisiae* against ultrasound by flow cytometry.

.

Table 5.3. Flow cytometry results of viability assessment of (a) *Saccharomyces cerevisiae*, and (b) *Candida schehatae* during exposure to sonication

(a) *Saccharomyces cerevisiae*						
Treatment	Mean (FL1)	Mean (FL3)	Quadrant 1 (Live) %	Quadrant 2 (Compromised) %	Quadrant 3 (Dead) %	Quadrant 4 (No stain) %
Cells with no stain (CDN)	3.64	1.13	1.60	0.04	0.03	98.3
Cell stain with live cell stain CFDA (CCFDA)	1613	18.9	87.8	12.1	0.11	0.03
PI stain with heat killed cells (HPI)	6.08	46.3	0.04	2.20	94.6	3.18
Native cells (T-1)	438	92.9	65.9	34.1	0	0.01
Ultrasound treated cells (T-2)	408	140	75.5	24.4	0	0.11
(b) *Candida shehatae*						
Treatment	Mean (FL1)	Mean (FL3)	Quadrant 1 (Live) %	Quadrant 2 (Compromised) %	Quadrant 3 (Dead) %	Quadrant 4 (No stain) %
Cells with no stain (CDN)	5.64	1.20	0.07	0.04	0.01	99.9
Cell stain with live cell stain CFDA (CCFDA)	283	3.61	97.8	0.72	0	1.49
PI stain with heat killed cells (HPI)	8.09	395	0	0.02	99.4	0.56
Native cells (T-1)	202	10.8	88.7	5.85	0.09	5.31
Ultrasound treated cells (T-2)	218	12.5	87.1	6.65	0.05	6.17

Abbreviations: *CDN = Cell with double negative cell, CCFDA =cell stained with carboxy fluorescein diacetate (cFDA), HPI = Heat killed propidium iodide*

5.6 Conclusion

The present study has reported a bioprocess for synthesis of ethanol using mixed invasive weeds as the feedstock. The optimized composite biomass comprising 8 invasive weeds was subjected to dilute acid hydrolysis, alkaline delignification and enzymatic hydrolysis. The pentose-rich and hexose-rich hydrolyzates were separately fermented with application of sonication, with bioethanol yields of 87 and 133 g/kg, respectively. Thus the total bioethanol yield from mixed feedstock of invasive weeds is ~ 220 g/kg. Application of sonication during fermentation had marked effect on kinetics of fermentation and ethanol productivity. The kinetics of both pentose and hexose fermentation were enhanced 2-fold with sonication at 10% duty cycle. No significant change in structural morphology of the microbial cells was observed after exposure to

sonication in flow cytometry analysis. Analysis of fermentation profiles with bio-kinetic model has given insight into the physical mechanism of ultrasound-assisted enhancement in fermentation kinetics. Sonication assists faster transport of nutrients, substrate and products across cell membrane, increase in enzyme-substrate affinity and reduction in substrate inhibition. We believe that results of this study will form useful inputs for further studies in synthesis of second generation bioethanol.

References

Allan, G.G., Carroll, J.P., Negri, A.R., (1992). TAPPI Journal., 75(1), 175.

Amor, K.B., Breeuwer, P., Verbaarschot, P., Rombouts, F.M., Akkermans, A.D., De Vos, W.M. and Abee, T., 2002. Multiparametric flow cytometry and cell sorting for the assessment of viable, injured, and dead Bifidobacterium cells during bile salt stress. Applied Environmental Microbiology., 68, 5209-5216.

Anukam, A., Mamphweli, S., Reddy, P., Meyer, E., Okoh, O., 2016. Pre-processing of sugarcane bagasse for gasification in a downdraft biomass gasifier system: A comprehensive review, Renewable and Sustainable Energy Reviews, 66, 775-801.

Bharadwaja, S.T.P., Singh, S., Moholkar, V.S., 2015. Design and optimization of a sono-hybrid process for bioethanol production from *Parthenium hysterophorus*. Journal of Taiwan Institute of Chemical Engineering. http://dx.doi.org/10.1016/j.jtice.2015.01.022.

Bhatt, J.R., Singh, J.S., Singh, S.P., Tripathi, R.S. and Kohli, R.K., 2011. Invasive Alien Plants an ecological appraisal for the Indian subcontinent (Vol. 1). Cabi.

Battista, F., Mancini, G., Ruggeri, B. and Fino, D., 2016. Selection of the best pretreatment for hydrogen and bioethanol production from olive oil waste products. Renewable energy, 88, pp.401-407.

Berłowska, J., Pielech-Przybylska, K., Balcerek, M., Dziekonska-Kubczak, U., Patelski, P., Dziugan, P. and Kręgiel, D., 2016. Simultaneous saccharification andfermentation of sugar beet pulp for efficient bioethanol production. BioMed research international, 1-10.

Chakma, S., Moholkar, V.S., 2011. Mechanistic features of ultrasonic desorption of aromatic pollutants. Chemical Engineering Journal, 175, 356–367.

Choudhury, H.A., Chakma, S. and Moholkar, V.S., 2014. Mechanistic insight into sonochemical biodiesel synthesis using heterogeneous base catalyst. Ultrasonics sonochemistry, 21, 169-181.

Gogate, P.R., Tatake, P.A., Kanthale, P.M., Pandit, A.B., 2002. Mapping of sonochemical reactors: review, analysis, and experimental verification. AIChE Journal, 48, 1542–1560.

Karuppaiya, M., Sasikumar, E., Viruthagiri, T., Vijayagopal, V., 2010. Optimization of process variables using response surface methodology (RSM) for ethanol production from cashew apple juice by *Saccharomyces cerevisiae*. Asian Journal of Food and Agro-Industry, 3, 462–73.

Mahato, S., Singh, A., Rangan, L., Jana, C.K., 2016. Synthesis, In silico studies and in vitro evaluation for antioxidant and antibacterial properties of diaryl methylamines: A novel class of structurally simple and highly potent pharmacophore. European Journal of Pharmaceutical Sciences, 88, 202–209.

Moholkar, V.S, Sable, S.P., Pandit, A.B., 2000. Mapping the cavitation intensity in an ultrasonic bath using the acoustic emission. AIChE Journal, 46, 684–694.

Moulin, G., Helen, B., Galzy, P., 1984. Inhibition of alcoholic fermentation. Biotechnology & Genetic Engineering Reviews, 2, 365–382.

Nalajala, V.S. and Moholkar, V.S., 2011. Investigations in the physical mechanism of sonocrystallization. Ultrasonics Sonochemistry, 18,.345-355.

Nelson, N., 1944. A photometric adaptation of the Somogyi method for the determination of glucose. Journal of Biological Chemistry, 153, 375–380.

Nguyen, T.Y., Cai, C.M., Kumar, R., Wyman, C.E., 2017(a). Overcoming factors limiting high-solids fermentation of lignocellulosic biomass to ethanol, Proceedings of the National Academy of Sciences of the United States of America, 114(44), 11673-11678.

Nikolic, S., Mojović, L., Rakin, M., Pejin, D. and Pejin, J., 2010. Ultrasound-assisted production of bioethanol by simultaneous saccharification and fermentation of corn meal. Food Chemistry, 122(1), 216-222.

Philippidis, G.P., Spindler, D.D., Wyman, C.E., 1992. Mathematical modeling of cellulose conversion to ethanol by simultaneous saccharification and fermentation process, Applied Biochemistry and Biotechnology, 34, 35, 543–556.

Qureshi, N., Blascheck, H.P., 2000. Butanol production using *Clostridium beijerinckii* BA 101 Hyper-butanol producing mutant strain and recovery by pervaporation. Applied Biochemistry and Biotechnology, 84-86, 225-235.

Rajkhowa, D.J., Gogoi, A.K., Yaduraju, N.T., 2005. Weed Utilization for Vermicomposting – Success Story. NRC for Weed Science, Jabalpur (M.P.), India.

Singh, S., Khanna, S., Moholkar, V.S., Goyal, A., 2014. Comparative assessment of

pretreatment strategies for enzymatic saccharification of Parthenium hysterophorus. Applied. Energy 129, 195–206.

Singh, S., Sarma, S., Agarwal, M., Goyal, A., Moholkar, V.S., 2015(a). Ultrasound enhanced ethanol production from *Parthenium hysterophorus*: a mechanistic investigation. Bioresource Technology, 188, 287–294.

Singh, S., Agarwal, M., Sarma, S., Goyal, A., Moholkar, V.S., 2015(b). Mechanistic insight into ultrasound induced enhancement of simultaneous saccharification and fermentation of *Parthenium hysterophorus* for ethanol production. Ultrasonic Sonochemistry, 26, 249–256.

Somogyi, M., 1945. A new reagent for the determination of sugars. Journal of Biological Chemistry, 160, 61–68.

Subhedar, P.B. and Gogate, P.R., 2015. Ultrasound-assisted bioethanol production from waste newspaper. Ultrasonics sonochemistry, 27, 37-45.

CHAPTER 6: MECHANISTIC INVESTIGATIONS IN BIOBUTANOL SYNTHESIS VIA ULTRASOUND ASSISTED ABE FERMENTATION USING MIXED FEEDSTOCK OF INVASIVE WEEDS§

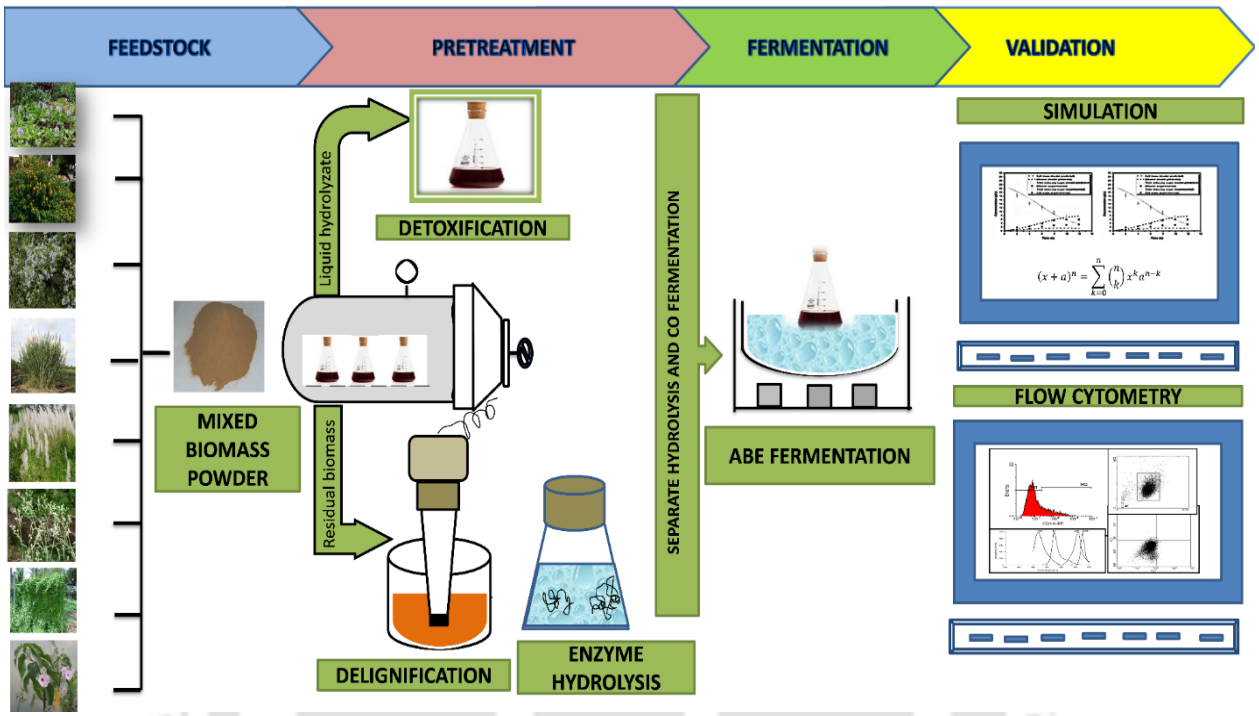

Chapter Highlights

- Ultrasound-assisted ABE fermentation using *C. acetobutylicum* and mixed invasive weeds
- Net ABE solvent yield with sonication was 0.288 g/g raw biomass in 92 h fermentation
- Analysis of substrate and metabolites profiles in fermentation using biokinetic model
- Sonication enhanced kinetics of metabolic reactions with reduced saturation constants
- Flow cytometry analysis revealed high cell viability during exposure to sonication

§ *See also* Borah, A.J., Roy, K., Goyal, A., Moholkar, V.S. (2018) Mechanistic Investigations in Biobutanol Synthesis via Ultrasound–Assisted ABE Fermentation Using Mixed Feedstock of Invasive Weeds. *Bioresource technology.* doi.org/10.1016/j.biortech.2018.10.063.

CHAPTER 6

MECHANISTIC INVESTIGATIONS IN BIOBUTANOL SYNTHESIS VIA ULTRASOUND–ASSISTED ABE FERMENTATION USING MIXED FEEDSTOCK OF INVASIVE WEEDS

6.1 Introduction

Alcoholic biofuels are potential carbon–neutral liquid transportation fuels that can be blended with gasoline. The most popular biofuel in this category is bioethanol. However, bioethanol has demerit of having relatively low heat of combustion as compared to gasoline and only 5 to 10% blend is recommended for present IC engines. An alternate alcoholic biofuel is biobutanol, which has attracted attention of scientific community in recent years owing to its distinct properties (Energy density = 29.2 MJ/kg, Heat of vaporization = 0.43 MJ/kg, Research Octane Number = 96, Motor Octane Number = 78) **(Ranjan and Moholkar, 2009; 2012)**. These properties are similar to that of gasoline, due to which biobutanol can blended with gasoline to much larger extent than ethanol without requiring modifications in the engine. Other merits of biobutanol are its non–corrosive nature, lower volatility, small absorption of moisture, high boiling point (118°C) and low Reid vapor pressure making it less evaporative/explosive. Despite high potential of biobutanol as renewable and carbon–neutral liquid transportation fuel, the commercial production encounters two major issues: (1) high cost of substrate and (2) low productivity and yield of fermentation. In addition, the microbial species of genera *Clostridia* for biobutanol fermentation (popularly known as ABE or acetone–butanol–

ethanol fermentation) are strict anaerobes. Thus, maintenance of strict anaerobic conditions during fermentation increases the operating cost **(Qureshi and Blaschek, 2000)**. Clostridium spp. are well-known bacteria for efficient fermentation of lignocellulosic hydrolysates (*viz*. both hexose and pentose rich) predominantly to ABE (acetone-butanol-ethanol) solvents **(Xin et al. 2014, Zhao et al., 2016; Kandia et al., 2018). Ranjan et al. (2013)** in their study reported that carbon substrate concentration of 4-6% w/v is optimum for butanol production. **Maddox et al. (1994)** stated that substrate concentration of ≤ 8% w/v resulted in reduced solvent production due to substrate inhibition. **Girbal and Soucaille, (1994)** reported that substrate concentration > 6% w/v reduced solvent yield due to product inhibition.

In the present study, an attempt was made to simultaneously address the above two issues associated with ABE fermentation. As a solution to high cost of substrate **(Demirbas, 2009, Cherubini et al. 2010, Farmanbordara et al. 2018)**, the present study has employed mixed (or composite) biomass of multiple invasive weeds as the feedstock for fermentation. These weeds cause enormous loss to both terrestrial and aquatic ecosystems. However, these weeds have high holocellulose content (in the form of hemicellulose and cellulose), which can be hydrolyzed to produce fermentable pentose and hexose sugars **(Singh et al. 2015a, Borah et al. 2016a, Borah et al., 2016b)**. The yield and kinetics of ABE fermentation also plays a significant role in overall economy and efficiency of the process. The biochemistry of ABE fermentation leads to formation of three solvents *viz.* acetone, butanol and ethanol with CO_2 and H_2 as gaseous byproducts *via* two intermediate metabolites (acetic and butyric acids). The intriguing microbial physiology involved with the obligatory anaerobic *Clostridial* species enable it a perplex system for study and further optimization. Usual practice of augmenting performance of fermentation systems is use of recombinant or genetically engineered micro-organism that

have faster kinetics with high yield and selectivity and tolerance to inhibition.

In this study, an attempt to introduce sonication (or ultrasound irradiation) as a mdeium to intensify the ABE fermentation process. This technique has been widely applied for ethanol fermentation **(Sulaiman et al., 2011; Sasmal et al., 2012; Singh et al., 2015b; Borah et al., 2018).** Sonication resulted in marked enhancement of both kinetics and yields of ethanol fermentation with both pentose and hexose-rich hydrolysates obtained from the pretreatment of lignocellulosic biomass.

Another aim of this study was to gain mechanistic understanding of the enhancement of fermentation induced by ultrasound irradiation. For this purpose, the experimental profiles of substrate and various metabolites were analyzed using a kinetic model reported in literature. **Votruba et al. (1986)** have stated a mathematical model for batch ABE fermentation. This model represents biochemical and physiological aspects of microbial growth and synthesis of metabolites during fermentation with batch culture of *Clostridium acetobutylicum*. This model comprises set of 8 ordinary differential equations that essentially symbolize the mass balances of the bioreactor for substrate, biomass, the intermediates of metabolic pathway and main final end products. This model tries to capture the batch culture stages using physiological culture as a state marker. **Votruba et al., (1986)** synthesized the model equations on the rate kinetic analysis of batch fermentation data under optimum conditions of media composition and physical parameters. The experimental data obtained from fermentation was fitted to the model (using Runge–Kutta ODE solver coupled with Genetic Algorithm), the variation in the trends of physiological and kinetic parameters of the mathematical model, gave a fascinating mechanistic influence of ultrasound assisted fermentation process, as stated in the consequent sections. Sonication generates intense microconvection in the medium that creates high shear. Microbial cells are subjected to this shear and can undergo

morphological changes that could hamper their activity. In this context, the influence of sonication on the physiological status and heterogeneity within bacterial population has been explored using multi–parametric flow cytometry.

6.2. Materials, methods and mathematical model

6.2.1 Chemicals and reagents

Following chemicals of fermentation media were procured from HiMedia Pvt. Ltd., India: RCA (Reinforced Clostridia Agar), RCM (Broth), anaerobic culture bag etc. Following GC standards were procured from Sigma Aldrich, USA: butanol (99.8%), ethanol, acetone (99.5% purity). Commercial enzymes *viz.* Cellulase (8 U/mg) and *β*–glucosidase (250 U/mg, Novozyme 188 were procured from Sigma Aldrich, USA.

6.2.2 Composite biomass

All the eight biomasses, viz. *Arundo donax, Chromolena odorata, Eichhornia crassipes Ipomea carnea, Lantana camara, Mikania micrantha, Parthenium hysterophorus and Saccharum spontaneum* were collected from local sources. Biomass was chopped into pieces and washed down with deionized water, dried at 60 ± 3°C for 24 hours and ground to powder with mixer grinder (pass through particle mesh size >1 mm). All the powdered biomasses were mixed with the ratio optimized in our previous study to form the composite biomass with the help of statistical mixture design. 31.25 wt% of composite biomass was contributed by *A. donax* and *C. odorata* each, while the fraction of other six biomasses (viz. *Eichhornia crassipes Ipomea carnea, Lantana camara, Mikania micrantha, Saccharum spontaneum and Parthenium hysterophorus*) was 6.25 wt%. The composite biomass was exposed to dilute acid hydrolysis followed by alkaline delignification and enzymatic hydrolysis to obtain pentose and hexose–rich hydrolysates,

which could form substrates for fermentation. Greater details on physical conditions and exact protocol of dilute acid hydrolyses and delignification have been mentioned in Chapter 3, section 3.3.3 for acid hydrolysis, 3.3.4 for detoxification and 3.35 for delignification **(Borah et al. 2016a, Borah et al. 2016b**).

6.2.3 Microorganism, culture revival and maintenance

Clostridium acetobutylicum 11274 used for ABE fermentation was procured from Microbial Type Culture Collection (MTCC), Institute of Microbial Technology (IMTECH), Chandigarh, India. The cells were revived anaerobically inside an anaerobic culture bag system (Himedia; India) and was maintained in both RCA (Reinforced Clostridial Agar) and RCM (Reinforced Clostridial Medium: Broth) culture media at 37°C **(Ranjan et al., 2013)**. Anaerobic environments in broth was maintained by adding 0.05% of cysteine hydrochloride and nitrogen sparging at regular intervals.

6.2.4. Experimental setup for ultrasound assisted enzymatic hydrolysis and fermentation

ABE fermentation subjected to sonication was set up in an ultrasound bath (Make: Elma, Germany; Model: Trans–sonic T–460, 2 L) operating at a rated power input of 35 W and 35 kHz frequency. Actual acoustic power input to the medium in the bath, and acoustic pressure amplitude in the bath was calculated as 18.58 W and 1.5 bar based on calorimetric techniques **(Moholkar et al. 2000, Chakma and Moholkar, 2011)**. Both experiments were implemented in 250 mL custom fabricated flask placed at the center of the ultrasound bath. The location of the flask was projected and carefully retained similar throughout the experiments to avoid the change in acoustic intensity due to spatial variation **(Moholkar et al., 2000, Gogate et al., 2002, Sutkar and Gogate, 2002)**. The

water bath temperature was retained at 37 ± 2°C by partial replacement of water at routine interim. Sonication with 10% duty cycle (i.e. 1 min ON and 9 min OFF in every 10 min of time interval), was applied for both enzymatic biomass hydrolysis and ABE fermentation **(Borah et al., 2018)**. The protocol for enzyme hydrolysis has been described in and protocol followed for enzymatic hydrolysis has been detailed described in Chapter 5, section 5.2.4 respectively **(Borah et al. 2016a)**.

6.2.5 ABE Fermentation of Composite hydrolysate

Fermentation of the reducing monomeric sugars hydrolysate was carried out using *Clostridium acetobutylicum* in 250 mL custom–fabricated flask with a bottom sprout and screw cap for anaerobic clostridial culture with working volume of 50 mL. Fermentation media containing hydrolysate was supplemented with yeast extract (3 g/L), PABA (4 g/L), sodium acetate (3 g/L), magnesium sulphate (0.5 g/L), and 0.05% of cysteine hydrochloride and medium pH was adjusted to 6.8 ± 0.2 (**Ranjan et al., 2013**). Nitrogen gas sparging was done to maintain the anaerobic environment inside the flask. The fermentation medium was inoculated with 18 h old, 5% (v/v) *Clostridium acetobutylicum* culture and incubated at 37°C and 150 rpm in an incubator shaker (Scigenics Biotech, Model: Orbitek). In the test experiment, 1 min of sonication followed by 9 min of mechanical shaking for each 10 min of reaction time interval were adopted for ABE fermentation. Fermentation in control (mechanical shaking) and test experiments (intermittent sonication + mechanical shaking) was carried out for 120 and 96 h, respectively. The duration of fermentation was decided on the basis of percentage change in concentrations of substrate (TRS) and all final metabolites in consecutive samples withdrawn from fermentation broth in both test and control experiments. Fermentation was discontinued at the moment when the percentage changes in contents of substrate and

all solvents (acetone, ethanol, butanol) in two consecutive fermentation samples was ≤ 5%. pH of the samples of fermentation was also monitored as it is the characteristic feature of phase of metabolism and more importantly the physiological shift from acidogenesis to solventogenesis that triggers formation of final solvents from intermediate metabolites of acids. In addition to the profiles of final solvents, the profiles of intermediate metabolites of acids (*viz*. acetic and butyric acid) and cell biomass concentration in the fermentation broth were also monitored.

6.2.6 Analytical methods

The residual concentration of total fermentable sugars (pentose + hexose) in the fermentation broth was detected by **Nelson (1944)** and **Somogyi (1945)** method, and re–confirmed with HPLC analysis (Perkin–Elmer, Series 200, RI Detector) using HiPlex–H column (300 mm × 5.l mm × 4.6 mm, Varian) with water as eluent at flow rate of 1 mL/min. The fermentation samples (*viz*. acetone, butanol and ethanol concentration) was quantified using GC analysis (Varian, CP 3800) using a CPWax 52 CB capillary column (250 mm × 0.25 mm × 0.39 mm, Varian) with acetone, ethanol and butanol (HPLC grade) as standards (listed in **Appendix C Fig. C1** and **Fig**. **C2**) respectively. The oven temperature was conditioned from 45^{o}C to 100^{o}C with an increment of 3^{o}C /min and 100^{o}C to 200^{o}C with an increment of 5^{o}C/min. The injector and detector temperatures were kept at 230^{o}C and 250^{o}C, respectively with a flow rate of 2 mL/min using nitrogen as a carrier gas.

6.2.7 Mathematical model of ABE fermentation

Powell (1969) has proposed the probability of modeling relationship between specific growth rate (representative of history of microbial culture) and a variable

environment using metabolic activity functional (represented as Q). They defined the relationship as: $\mu = Y_{X/S} Q g(S)$, where $Y_{X/S}$ is macroscopic yield coefficient, and $g(S)$ is a simple environmental depending function. For a stable culture with access to substrate in the medium, the value of $g(S)$ can be assumed to be unity **(Harder et al. 1982)**. The metabolic activity functional $Q(t)$ depends on history of the culture and consumed variable substrate rate during development of microbial culture. In the general form, Q(t) is defined as: $Q(t) = \int_0^\infty f(\xi) q\left[S(t-\xi)\right] d\xi$.

$f(\xi)$ is distribution function representing age–dependent structure of microbial population, and q is the specific substrate consumption rate (which in turn is a function of age of the microbial population). **Powell (1969)** has proposed that $Q(t)$ can be considered similar with concentration variation of some cell constituent concentration which is interrelated to growth rate. **Powell (1969)** has further proposed to use intracellular RNA concentration as a representative of $Q(t)$, as RNA shows linear relationship with cell growth rate, and moreover, the ratio of individual RNA sub–components (mRNA, tRNA and rRNA) remain constant with wider culture conditions. With these hypotheses, the relationship between growth rate and intracellular RNA (indicator of culture's physiological state) is given as: $\mu = K(RNA - RNA_{\min}) g(S)$, where RNA_{min} is the RNA concentration in the cell at μ = 0. The dynamic mass balance for intracellular RNA was given on the basis that culture growth rate is directly related to the substrate (reducing sugar) concentration and a term describing inhibition of culture growth (in the present context product inhibition by butanol), as:

$$\frac{d(\mathrm{RNA}\cdot X)}{dt} = k_1 S \frac{K_I}{K_I + B}(\mathrm{RNA}\cdot X)$$

Indicator of culture's physiological state (y) was dimensionless concentration of RNA:

$y = RNA/RNA_{\min}$. A linear relation was defined between specific growth rate of culture and the cellular RNA content as: $\mu = ay - b$. On the basis of results of **Harder** and **Roels (1982)**, who demonstrated that numerical values of coefficients *a* and *b* are same for most bacterial cultures, a parameter λ can be defined as: $\lambda = Kg(S)/RNA_{\min} = 0.56$. In simplest form, the dynamics of culture associated with indicator of physiological state is written as:

$$\frac{d(yX)}{dt} = \mu(S,B)yX$$

$$\frac{dy}{dt} = \mu(S,B)y - 0.56(y-1)y$$

The initial value of y depends on the physiological state of the microbial culture or the inoculum. For inoculum in stationary phase, y (0) = 1. For inoculum in exponential growth phase, y (0) ≥ 1, while for inoculum in declining phase where only a fraction of biomass is capable of growth, $y(0) \leq 1$. A generalized metabolic pathway of acetone-butanol-ethanol fermentation is shown in **Fig. 6.1**, below with main intermediate metabolites and the final products.

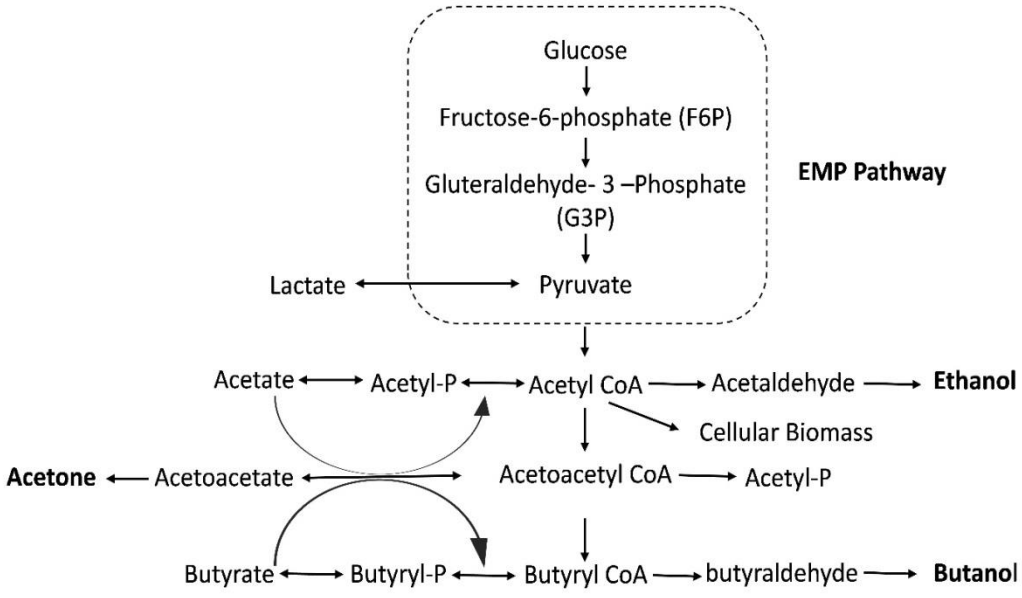

Figure 6.1 Generalized metabolic pathway of acetone-butanol-ethanol (ABE) fermentation

On the basis of this pathway, the overall mass balance equations of metabolism of ABE fermentation have been formulated as follows: Assuming a linear relationship with substrate and simultaneous product inhibition expressed by Yerusalimski–Monod type expression, the differential mass balances for biomass and its physiological state are written as:

$$\frac{dX}{dt} = \lambda\left(y-1\right)X - k_2 XB \tag{1}$$

$$\frac{dy}{dt} = \left[k_1 S\frac{K_I}{K_I + B} - \lambda\left(y-1\right)\right]y \tag{2}$$

Rate of consumption of sugar(s) or substrate (S) for various cellular functions including growth and production of acids and solvents, is written as:

$$\frac{dS}{dt} = -k_3 SX - k_4\frac{S}{K_s + S}X \tag{3}$$

Mass balance for butyrate is written in following form:

$$\frac{dBA}{dt} = \underbrace{k_5\frac{K_I}{K_I + B}S\cdot X}_{\substack{\text{Biosynthesis of butyrate from}\\ \text{sugar substrate inhibited by butanol}}} - \underbrace{k_6\frac{BA}{K_{BA} + BA}X}_{\substack{\text{Consumption of butyrate for}\\ \text{bioconversion into butanol}}} \tag{4}$$

k_5 and k_6 are kinetic constants, while K_I and K_{BA} are inhibition (by butanol) and saturation constants, respectively. The differential mass balance for butanol, which represents initial delay in butanol production and accumulation of intermediate butyrate in the fermentation mixture (including inhibitory effect of butanol on reactions related to growth and synthesis of cellular materials), is represented as:

$$\frac{dB}{dt} = \left(k_7 S\cdot X + 0.841k_6\frac{BA}{K_{BA} + BA}X\right) - 0.841k_5\frac{K_I}{K_I + B}S\cdot X \tag{5}$$

k_7 is the kinetic constant for direct production of butanol from biomass, while 0.841 is stoichiometric coefficient (determined as the ratio of molecular weights of butanol and butyric acid) for specific rate of butyric acid production from butanol. Since we have not

measured profiles of gaseous metabolites generated in fermentation, these have not been included in the model. The differential mass balances for other liquid phase metabolites such as acetic acid (*AA*), ethanol (*E*), acetone (*A*) are written as:

$$\frac{dAA}{dt} = k_8 \frac{S}{K_s + S} \frac{K_I}{K_I + B} X - k_9 \frac{AA}{K_{AA} + AA} \frac{S}{K_s + S} X \tag{6}$$

$$\frac{dA}{dt} = k_{10} \frac{S}{K_s + S} X - 0.484 \frac{dAA}{dt} \tag{7}$$

First term on RHS of eq. 6 represents rate of acetate synthesis, while the second term represents rate of acetate conversion into acetone. In eq. 7, the coefficient 0.484 corresponds to stoichiometric conversion of acetate to acetone. Finally, the ethanol production rate in ABE fermentation can be described using a Monod type function:

$$\frac{dE}{dt} = k_{11} \frac{S}{K_s + S} X \tag{8}$$

The ordinary differential equations (ODEs) cited above for 8 independent variables, viz. *y*, *X*, *G*, *AA*, *BA*, *A*, *B* and *E*, and the parameters therein describe the physiology of ABE fermentation process. These equations have total of 11 kinetic parameters, *viz.* k_1, k_2, k_3, k_4, k_5, k_6, k_7, k_8, k_9, k_{10}, k_{11}, one inhibition constant K_I, and three saturation constants, K_S, K_{BA}, and K_{AA}. The numerical elucidation of all above stated equations was matched with the experimental time profiles of *X*, *G*, *AA*, *BA*, *A*, *B* and *E*. The unidentified physiological and kinetic parameters in this model need to be determined by iteration to determine an optimum value so as to compare the time profiles of the cell mass, substrate, acids and solvent concentrations estimated using this model with the experimental profiles. The set of eight ODEs of the fermentation model was solved as initial value problem using Runge–Kutta adaptive step size method. Optimum values of the model parameters (within pre–specified bounds – provided in supplementary material) were determined by calculating root mean square (RMS) error between experimental and

model results and minimizing the same using Genetic Algorithm (GA). The objective function (*Obj*) for the GA optimization was defined as: $Obj = \min\left(\sum_{i=1}^{n} er_i\right)$ where *n* is the number of experimental data points for the variables *X*, *G*, *AA*, *BA*, *A*, *B* and *E*.

6.2.8 Accessing the viability of bacteria subjected to sonication

The two dyes, viz. carboxyfluorescein diacetate (CFDA) and propidium iodide (PI) from Sigma Aldrich were used for analysis of the live and dead cells in the samples. Physiological state of *Clostridium acetobutylicum* cells under the impact of ultrasound were explored using Flow Cytometry (BD Calibur™ Flow Cytometer, BD Biosciences, USA). FACS Flow solution (BD) as the sheath fluid was used for the analysis of cell suspension. Cell suspension approx.10^6 fpu/mL were centrifuged at 10,000 rpm and was resuspended in phosphate buffer saline (PBS) maintained at pH 7. Various parameters, viz. CDN = cell double negative (no stain), HDN = heat–killed double negative, cCFD = cell stain with live stain CFDA, CPI = cell stain with dead stain PI, HPI = heat killed stain with PI, HDP = heat–killed double positive (i.e. both stains, 95°C for 15 min), CDP = cell with double positive (i.e. both stains), were considered for understanding the membrane integrity and functionality of the cytoplasmic enzymes.

Bacterial samples were stained individually by adding 10 µL CFDA (0.25 mM) or 10 µL PI (10 µg/mL) and nurtured at 37°C in the dark for 30 min. All stained bacterial samples were later washed with PBS to decant the residual dye. Bacterial samples were also double stained by following the protocol as described in **Amor et al. (2002)** and **Mahato et al. (2016).** All the cell samples were retained at medium flow rate (24 µL/min ± 5 µL/min) up to a total event of 10,000 events per sample. Bacterial cells were analyzed by forward scattered (FSC) and side scattered (SSC) light. The detection of CFDA was done through FL1 channel with 530 nm bandpass filter. Red fluorescence signal of PI was

collected in the FL3 channel with N600 nm long pass filter for membrane permeability. The fluorescence signals of individual cells were gathered in biexponential mode. Gating was done in dot–plot of FSC–SSC to discriminate bacteria from noise and artifacts. Data was obtained by BD Cell Quest Pro software and was analyzed and refined by FloJo software (Tree Star, Stanford, USA).

6.3 Results and Discussion

6.3.1 Fermentation experiments under control and test conditions

Fermentation substrates: A mixture of pentose and hexose hydrolysates acquired from dilute acid and enzymatic hydrolysis of composite biomass was used as substrate for fermentation under both control and test conditions. Total fermentable sugar (TFS) concentration of the composite hydrolyzates was 50 $g{\cdot}L^{-1}$ (comprising pentose sugars = 22.7 $g{\cdot}L^{-1}$ and hexose sugars = 27.7 $g{\cdot}L^{-1}$).

pH profile: The time profiles of pH of fermentation broth under control and test experiments are shown in **Fig. 6.2.** The butterfly shifts of pH that trigger solventogenesis from initial acidogenesis phase are clearly visible. The minimum pH of fermentation broth reached was 4.1 and 3.9 in control and test experiments respectively. However, marked difference in the time required to reach minimum pH in control and test experiments was seen. In the control experiment, minimum pH reached after 46 h from commencement of fermentation, while in test experiment the minimum pH was achieved at 24 h. This clearly was the consequence of faster metabolism of microbial culture that augments rate of acid formation which can been seen in the **Fig. 6.3 (c and d)** below.

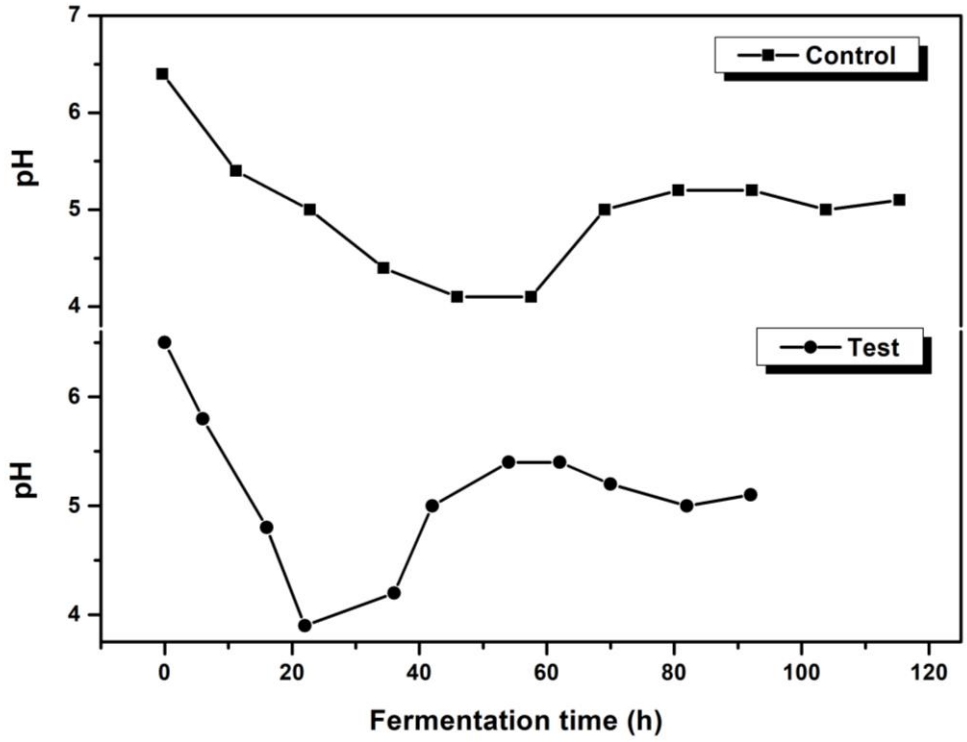

Figure 6.2 Time profiles of pH of fermentation broth in control (mechanical shaking) and test (mechanical shaking + sonication @ 10% duty cycle) experiments.

Fermentation experiments: The time profiles of acidogenesis phase of fermentation (formation of acetic and butyric acids) in control and test experiments are depicted in **Figs. 6.3c** and **d**, respectively. The time profiles of solventogenesis phase (formation of acetone, ethanol and butanol) in control and test experiments are displayed in **Figs. 6.3a** and **b**, respectively. Finally, the time profiles of substrate (total fermentable sugars) and the cell biomass are depicted in **Figs. 6.3e** and f. The briefing of the results in the control and test experiments is presented in **Table 6.1**.

Control experiments (fermentation with mechanical shaking): Control experiments yielded maximum acetone and ethanol concentrations of 0.76 and 3.04 g/L after 120 h of fermentation. The butanol concentration peaked at 5.81 g/L at 120 h of fermentation. Butanol formation commenced at 41 h of fermentation with drop in pH to 4.1 (which corresponds to the butterfly shift mentioned earlier). The total solvent (acetone, butanol

and ethanol) yield was 0.376 g/g TFS or 0.168 g/g raw biomass. The final cell mass concentration was 3.70 g/L. ABE solvent productivity in control experiments was 0.08 g L^{-1} h^{-1}.

Test experiments (fermentation with mechanical shaking with intermittent sonication): The most notable effect of intermittent sonication on fermentation process was in terms of reduction in time of fermentation. 3–Fold reduction in fermentation time was seen with sonication (92 h) in test experiments against 120 h fermentation in control experiments. In addition, final ABE titer increased to 4.56, 9.12 and 2.82 g/L, respectively with a total ABE yield of 0.646 g /g TFS. Net butanol yield was 0.159 g/g raw biomass with overall solvent productivity of 0.18 g L^{-1} h^{-1}. Net solvent yield with respect to raw biomass was 0.288 g/g, while final cell mass concentration in the broth was 4.10 g/L. Notably, butanol formation commenced much earlier in test experiments, i.e. within 30 h of fermentation, with drop in pH to 3.9 corresponding to the butterfly shift seen in **Fig. 6.2**. Final cell mass concentration in the broth also increased to 4.10 g/L. These results are suggestive of enhanced metabolism of the microbial culture under influence of sonication.

Table 6.1 Summary of acetone–butanol–ethanol (ABE) fermentation under control and test conditions

Parameter	Control experiments (mechanical shaking @ 150 rpm)	Test experiments (mechanical shaking sonication @ 10% duty cycle)
Final concentrations of acids, solvents and biomass		
Acetic acid (g L^{-1})	4.05 ± 0.2	4.58 ± 0.63
Butyric acid (g L^{-1})	4.35 ± 0.4	5.06 ± 0.30
Total acids (g L^{-1})	8.4 ± 0.6	9.64 ± 0.93
Acetone (g L^{-1})	0.76 ± 0.02	4.56 ± 1.01
Butanol (g L^{-1})	5.81 ± 0.36	9.10 ± 1.3
Ethanol (g L^{-1})	3.04 ± 0.04	2.82 ± 0.29
Total ABE (g L^{-1})	9.61 ± 0.38	16.5 ± 2.6
Maximum biomass concentration (g L^{-1})	3.70 ± 0.17	4.10 ± 0.08
Substrate utilization		
Initial TFS (g L^{-1})	50	50
Final TFS (g L^{-1})	10.18 ± 0.72	8.84 ± 1.24
TFS utilized (g L^{-1})	39.82	41.16
TFS utilization (%)	79.64	82.32
TFS utilization rate (g L^{-1} h^{-1})	0.33	0.45
Yields and productivities		
Fermentation time (h)	120	92
ABE productivity (g L^{-1} h^{-1})	0.08	0.18
Butanol yield (g·g^{-1} TFS)	0.149	0.233
ABE yield (g·g^{-1} TFS)	0.376	0.645
ABE yield (g·g^{-1} raw biomass)	0.168	0.288

*Abbreviation TFS= TRS obtain from both Glucose and xylose.

6.3.2 Simulation results of ABE fermentation

Comparative analysis of the values of the physiological parameters derived from fitting of the fermentation model to the experimental profiles of substrates and different metabolites in control and test fermentation gave a mechanistic insight of the ultrasound effect on the fermentation process. The trends in the values of model parameters for the control and test experiments (as given in **Table 6.2**), and the explanations for these trends are as follows:

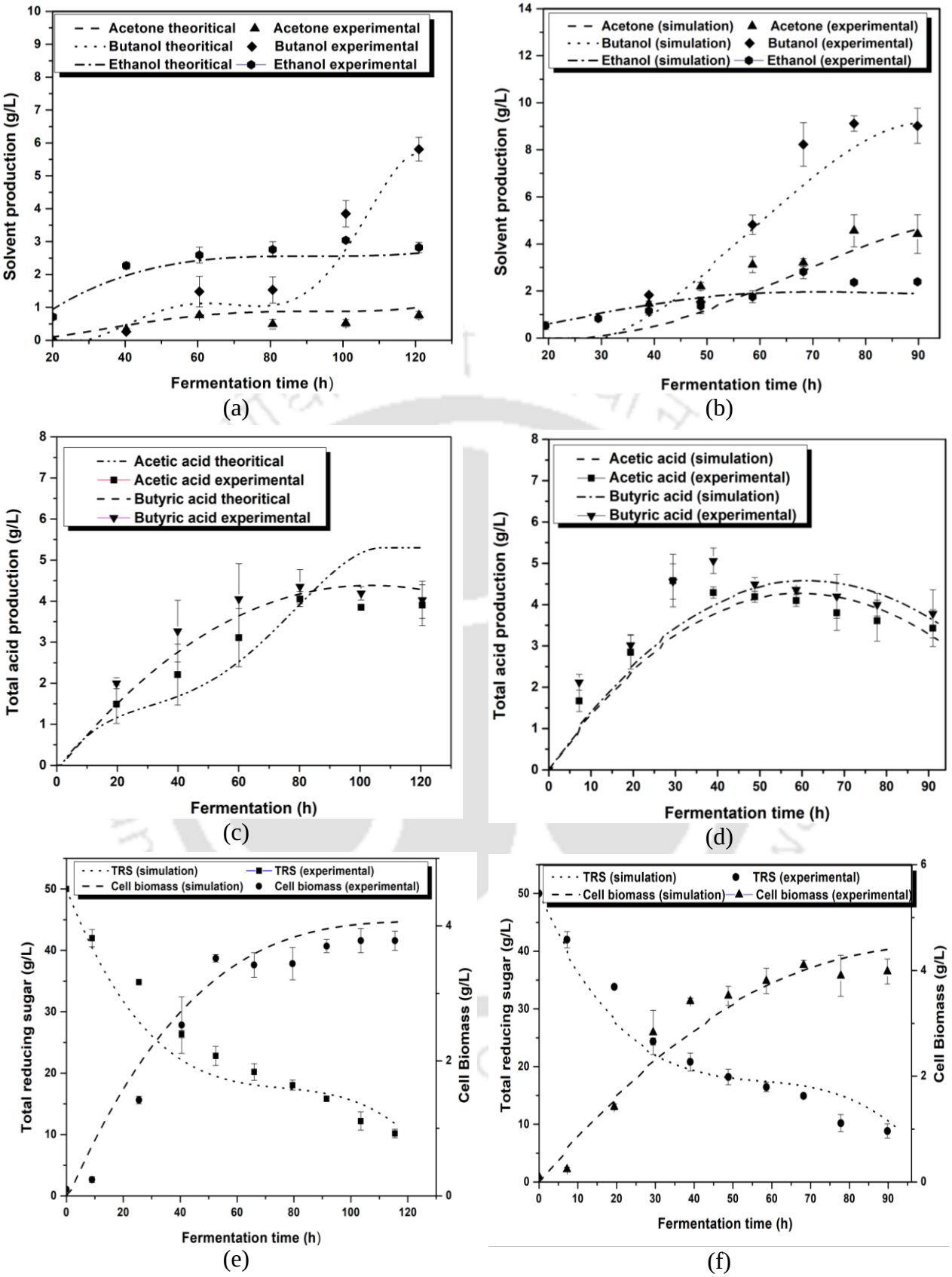

Figure 6.3 Experimental and simulated time profiles of acids and solvents during ABE fermentation under control and test conditions. **(a)** acetone, butanol and ethanol profiles (control experiments). **(b)** acetone, butanol and ethanol profiles (test experiments) **(c)** acetic and butyric acid profiles (control experiments). **(d)** acetic and butyric acid profiles (test experiments). **(e)** TRS utilization and cell biomass profiles (control experiments). **(f)** TRS utilization and cell biomass profiles (test experiments).

(1) The constant k_1 characterizes the kinetics of biomass growth with respect to substrate utilization. Increase in rate constant (k_1) in ultrasound-assisted fermentation indicates higher consumption of substrate for cell growth. This is a possible consequence of enhanced mass transfer of sugars through cell membrane due to strong micro–convection caused by ultrasound. The kinetic constant (k_2), which represents cell lysis and decay due to butanol (and which is directly proportional to the concentration of butanol in the broth) also increases in test experiments. This is attributed to higher and faster production of butanol in the test experiments. (2) Rise in K_I (inhibition constant of butyrate synthesis from sugar substrate by butanol) in test experiments indicated rise in inhibition tolerance of the enzymes involved in metabolic pathway leading to butyrate formation. By definition, K_I is the concentration of inhibitory product (i.e. butanol) required to cause half of maximum inhibition of butyrate synthesis. An increase in K_I signifies that higher concentration of inhibitory products required for a certain degree of inhibition. Higher tolerance of enzymes towards inhibition is a possible consequence of faster mass transfer across cell membrane due to microconvection induced by ultrasound. Due to faster transport of substrate/product across cell, the inhibitory products do not accumulate within the cells for a longer period of time, thus reducing inhibition. K_S is the Monod's saturation constant for substrate. It is defined as the substrate concentration when the specific growth rate of biomass is half of the maximum specific growth rate. Decrease of K_S in test experiments is also a possible consequence of faster transport of substrate across cell, due to which lesser bulk substrate concentration is required for achieving maximum specific growth rate. Moreover, reduction in K_S also signifies better utilization of the substrate for cell growth and metabolism, which is corroborated by rise in the values of other kinetic constants of the model. The saturation constants are also representative of the substrate-enzyme affinity. It has been demonstrated that intracellular

enzymes undergo conformational changes in their secondary structure, as the cells are subjected to sonication **(Bhasarkar et al., 2015; Borah et al., 2016b; Dikshit et al., 2017)**. These conformational changes are in terms of breaking down of the rigid α-helix structure and rise in β-sheet and random coil content. This helps in unfolding of the enzyme with exposure of the inner hydrophobic and other amino acid residues. This essentially eases out access of the substrate to the binding site, which is manifested as enhanced enzyme-substrate affinity. (3) On the other hand, the saturation constants of butyric acid K_{BA} increased in test experiments, while the saturation constant of acetic acid, K_{AA}, showed marginal reduction. Increase in K_{BA} signifies the requirement of higher concentration of butyric acid for the cell metabolism. A possible cause leading to this effect is, the secretion of these metabolites into the medium after their formation inside the cell, as a result of faster cellular transport. This phenomenon results in restricted access of the substrate butyric acid for the enzymes in butanol pathway, *viz*. butyrate kinase, butyraldehyde dehydrogenase and butanol dehydrogenase.

Kinetic constants related to substrate consumption, *viz*. k_3 – characterizing the substrate consumption for biomass growth and k_4 – characterizing the substrate consumption for acids and solvents production, increase with sonication. However, the rise in k_3 (~ 65%) is much higher than the that in k_4 (~ 20%).

The kinetic constants, k_6 and k_7 reduced with application of sonication. These constants are associated with production of butanol. k_6 is the kinetic constant for consumption of butyrate for formation of butanol, while k_7 is the kinetic constant for production of butanol directly from biomass. As noted by **Votruba et al., (1984)** k_6 and k_7 also represent initial delay in butanol production and accumulation caused by intermediate accumulation of butyrate in the broth. From this study it was hypothesized that the reduction in k_6 and k_7 is essentially a manifestation of secretion of the butyric acid

from the cells due to sonication – as a result of which its intracellular concentration reduces. It is interesting to note that despite reduction in specific kinetic constants related to butanol production, the net production of butanol shows significant rise in test experiments. This result is clearly attributed to higher formation of butyric acid in the test experiments, as characterized by higher value of kinetic constant k_5.

The kinetic constants k_8 and k_{10} representing acetic acid formation from substrate with inhibition from butanol and direct acetone formation from substrate, respectively, show enhancement with sonication. The kinetic constant k_9, representing conversion of acetic acid into acetone, reduces with sonication. In concurrence with a similar trend in k_6, the reduction in k_9 is a probable consequence of secretion of acetic acid from cell into the medium due to which its intracellular concentration reduces.

Finally, the specific kinetic constant related to ethanol formation, k_{11} stays practically unaltered with sonication. However, augmentation in net ethanol formation in test experiments is a consequence of higher biomass production. **Srivastava** and **Volesky (1990)** showed that ethanol is essentially a growth associated product, and negligible production of ethanol occurs in the stationary phase of microbial culture. The results of present study concur with the conclusions of **Srivastava and Volesky (1990)** as significant ethanol concentration is observed in the fermentation broth during initial stages of fermentation (≤ 24 h) in both test and control experiments.

Table 6.2 The kinetic and physiological parameters in ABE fermentation

Kinetic / Saturation / Inhibition Constants	Control experiments (With mechanical shaking)	Test experiments(With intermittent sonication)
k_1 Eq. (1) $(g/L)^{-1}\cdot h^{-1}$	0.002	0.005
k_2 Eq. (2) $(g/L)^{-1}\cdot h^{-1}$	0.0014	0.0055
k_3 Eq. (3) $(g/L)^{-1}\cdot h^{-1}$	0.017	0.028
k_4 Eq. (3) h^{-1}	0.588	0.705
k_5 Eq. (4) $(g/L)^{-1}\cdot h^{-1}$	0.045	0.098
k_6 Eq. (4) h^{-1}	0.188	0.136
k_7 Eq. (5) $(g/L)^{-1}\cdot h^{-1}$	0.004	0.0015
k_8 Eq. (6) h^{-1}	0.471	0.753
k_9 Eq. (7) h^{-1}	0.118	0.098
k_{10} Eq. (7) h^{-1}	0.090	0.176
k_{11} Eq. (8) h^{-1}	0.025	0.024
Inhibition constant K_I (g/L)	0.287	0.356
Substrate saturation constant K_S (g/L)	1.654	1.484
Butyric acid saturation constant K_{BA} (g/L)	0.187	0.527
Acetic acid saturation constant K_{AA} (g/L)	0.688	0.647

Table 6.3 Viability assessment results of *Clostridium acetobutylicum*

Treatment	Mean (FL1)	Mean (FL3)	Quadrant 1 (Live) in %	Quadrant 2(Compro-mise) in %	Quadrant 3 (Dead) in %	Quadrant 4 (No stain) in %
Cells with no stain (CDN)	2.80	3.04	0.29	0	0.015	99.7
Heat killed with not stain (HDN)	3.16	6.02	0.53	0.29	3.43	95.8
Cell stain with live cell stain CFDA (CCFDA)	454	4.37	84.5	0.09	0	15.4
CFDA stain with Heat killed cell (HCFDA)	12	2.15	39.1	0	0	60.3
PI stain with dead cells (CPI)	2.81	9.50	0.03	0.04	19.6	80.3
PI stain with heat killed cells (HPI)	3.94	30.6	0.24	0.54	77.9	21.3
Heat killed cells stained with both the stain (HDP)	7.76	34.9	2.29	18.4	69.9	9.47
Normal cells stained with both the stain	379	12.4	63.3	17.0	10.1	9.64
Ultrasound treated cells 1	588	13.8	59.2	19.5	7.83	13.5
Ultrasound treated cells 2	519	13.2	57.6	17.5	9.11	15.8

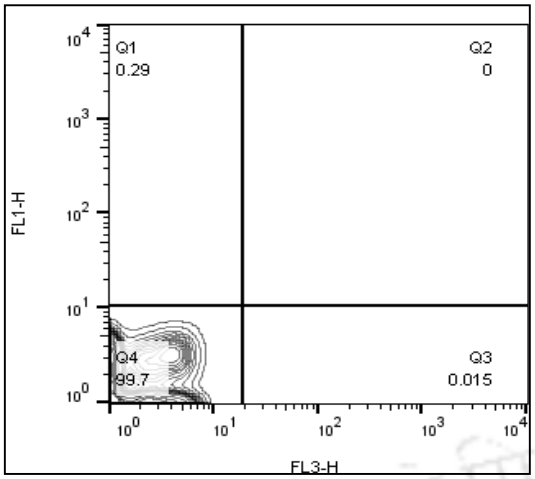

Cells with no stain (CDN)

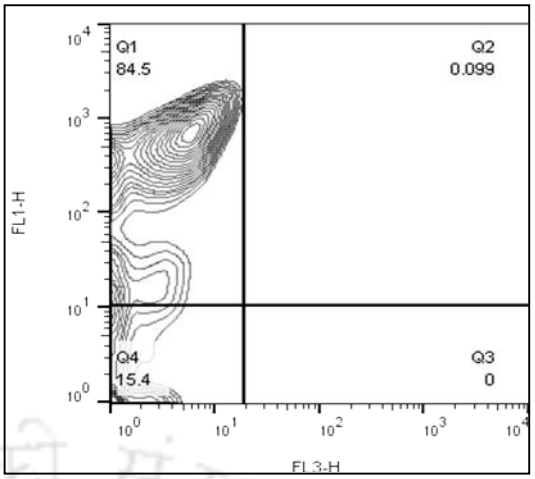

Cell stain with live stain CFDA. (CCFDA)

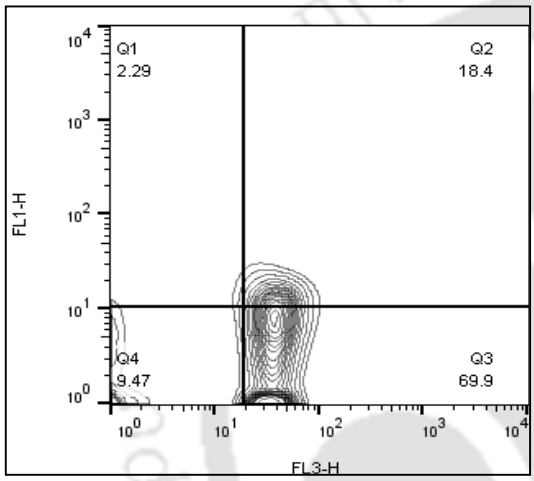

PI stain with heat killed cells (HPI)

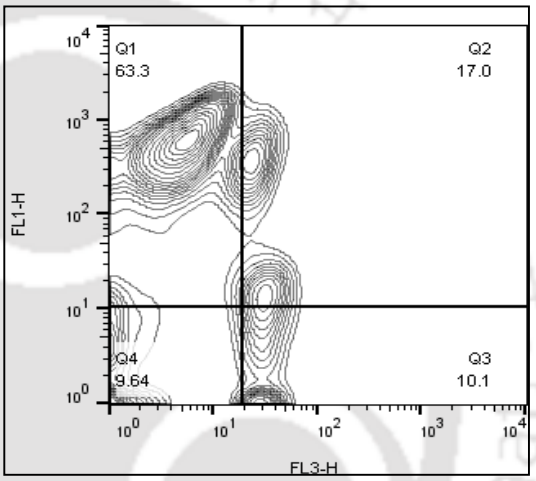

Cell stain with both live & dead stain (CFDA, PI)

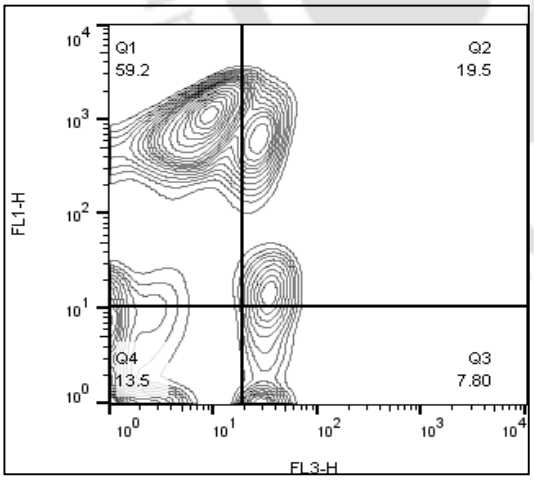

Ultrasound treated cells 1

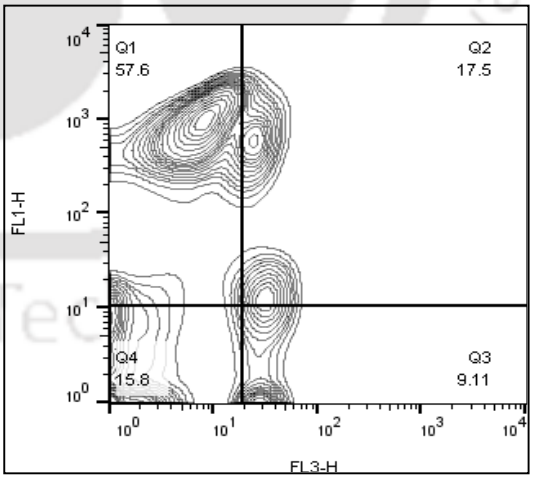

Ultrasound treated cells 2

Figure 6.4. Results of viability assessment of *C. acetobutylicum* against ultrasound by flow Cytometry **(**CDN=cell double negative (no stain), HDN= heat killed double negative, cCFD. cell stain with live stain CFDA, CPI=Cell stain with dead stain PI & HPI =heat killed, HDP= Heat killed double positive (i.e both stain), CDP= Cell with double positive (ie both stain.) Ultrasonicaton 1 and 2 are the replicates of two test sample. Mean FL1 = mean fluorescence intensity of cFDA, Mean FL3 = mean fluorescence intensity of cPI

6.3.3 Flow cytometry analysis of *C. acetobutylicum*

Multiparametric Flow Cytometry (MFC) was carried out to assess viability of *Clostridium acetobutylicum* cells during exposure to sonication in test experiments, in comparison to viability in control experiments with mechanical shaking. Live, dead and cell membrane-compromised bacteria were determined based on the mean intensity value recorded by both the filters based on the cell physiology, and also graphical representation in contour plots based on their differential staining characteristics with PI and CFDA stain. The upper left quadrant (Q1) of the contour plot **(Fig. 6.4)** signifies live population, while upper right comprised of membrane compromised cells (Q2). The dead cells (Q3) and unstained cells can be seen in the lower right and left quadrant (Q4) of the contour plot.

From **Table 6.3**, negative control ($CFDA^{-}$, PI^{-}) showed least fluorescence signals with 99.7 cell retaining in quadrant Q4, while positive control ($CFDA^{+}$, PI^{+}) showed highest mean fluorescence density value of 454 nm in FL1 (fluorescence intensity of CFDA) with 63% of live cell population. Live population stain with CFDA ($CFDA^{+}$, PI^{-}) and heat killed population stained with PI ($CFDA^{-}$, PI^{+}) is sufficiently appeared in their respective upper left (Q1) and lower left quadrant (Q3) with relative high intensity (84.5% and 77.9 % for *C. acetobutylicum*) of their corresponding strain.

In the test sample (cells exposed to sonication), the highest mean florescence intensity value was seen for both replicates in FL1 (588 and 519 nm) filter which take the live stain CFDA stain shown in **Table 6.3**. The contour plots also show majority of cell intensity (> 59% cells) in the live quadrant (Q1). However, considerable amount of cells can be seen in other quadrants, *viz*. average of both the test samples 18.5% in Q2, 8.47% in Q3 and 14.65% in Q4. These changes in the cell population can be attributed to the predominant physiology of Clostridial cells. It is already known from the literature

(Amor et al., 2002; Mahato et al., 2016) that Clostridial cells exhibit different morphologies according to their environments. The cells in Q4 are those which are likely to form spores, and thus, are not able to take any of the stains used in the experiments. The cells in Q2 correspond to membrane-compromised cells, whose membrane integrity is probably affected due to the mechanical shear generated during exposure to sonication.

6.4 Conclusions

This study demonstrated the ultrasound-assisted ABE fermentation process using mixture of pentose and hexose hydrolysates, obtained from pretreatment of composite feedstock of 8 invasive weeds, as substrate. Sonication reduced fermentation period from 120 h to 92 h, and caused ~70% rise in ABE solvent yield. Analysis of fermentation profiles vis-à-vis biokinetic model has given mechanistic insight into the process. Sonication enhanced kinetic constants of metabolic reactions with reduction in saturation constants of substrates, and also increased substrate inhibition resistance. These phenomena resulted in faster metabolism. Flow cytometry results revealed no adverse effect of sonication on cell morphology.

References

Amor, K.B., Breeuwer, P., Verbaarschot, P., Rombouts, F.M., Akkermans, D.L., Devos, W.M., 2002. Multiparametric flow cytometry and cell sorting for the assessment of viable, injured, and dead Bifidobacterium cells during bile salt stress. Applied Environmental Microbiology, 68, 5209–5216.

Bhasarkar, J., Borah, A.J., Goswami, P., Moholkar, V.S., 2015. Mechanistic analysis of ultrasound assisted enzymatic desulfurization of liquid fuels using horseradish peroxidase. Bioresource Technology, 196, 88-98.

Borah, A.J., Agarwal, M., Goyal, A., Moholkar, V.S., 2018. Physical insights of ultrasound-assisted ethanol production from composite feedstock of invasive weeds. Ultrasounics Sonochemistry. doi: 10.1016/j.ultsonch.2018.07.046.

Borah, A.J., Agarwal, M., Poudyal, M., Goyal, A., Moholkar, V.S., 2016(b). Mechanistic investigation in ultrasound induced enhancement of enzymatic hydrolysis of invasive biomass species, Bioresource Technology, 213, 342-349.

Borah, A.J., Singh, S., Goyal, A., Moholkar, V.S., 2016(a). An assessment of invasive weeds as multiple feedstocks for biofuels production. RSC Advances, 6, 47151-47163.

Chakma, S., Moholkar, V.S., 2011. Mechanistic features of ultrasonic desorption of aromatic pollutants. Chemical Engineering Journal, 175, 356–367.

Cherubini, F., 2010. The biorefinery concept: using biomass instead of oil for producing energy and chemicals. Energy Conversion and Management, 51, 1412-1421.

Demirbas, A. 2009. Biofuels securing the planet's future energy needs. Energy Conversion and Management, 50, 2239-2249.

Dikshit, P.K., Padhi, S.K., Moholkar, V.S., 2017. Process optimization and analysis of product inhibition kinetics of crude glycerol fermentation for 1,3-dihydroxyacetone production. Bioresource. Technology, 244, 362-370.

Farmanbordara, S., Karimia, K.B., Amiric, H., 2018. Municipal solid waste as a suitable substrate for butanol production as an advanced biofuel. Energy Conversion and Management, 157, 396-408.

Girbal, L., Soucaille, P., 1994. Regulation of *Clostridium acetobutylicum* metabolism as related by mixed-substrate steady state continuous cultures: role of NADH/NAD ration and ATP pool. Journal of Bacteriology. 176, 6433-6438.

Gogate, P.R., Tatake, P.A., Kanthale, P.M., Pandit, A.B. 2002. Mapping of sonochemical

reactors: review, analysis and experimental verification., AIChE Journal, 48, 1542–1560.

Harder, A., Roels, J.A., 1982. Application of simple structured models in bioengineering. Advances in Biochemical Engineering and Biotechnology, 21, 56-107.

Kandia, F.B., Rondags, E., Framboisier, X., Mauviel, G., Dufour, A., Guedon1, E., 2018. Diauxic growth of *Clostridium acetobutylicum* ATCC 824 when grown on mixtures of glucose and cellobiose. AMB Express, 8, 85-92.

Maddox, I.S., Qureshi, N., Roberts, T.K., 1994. Production of acetone-butanol-ethanol from concentrated substrates utilizing *C. acetobutylicum* in an integrated fermentation product removal process. Process Biochemistry, 30, 209-215.

Mahato, S., Singh, S., Rangan, L., Jana, C.K., 2016. Synthesis, In silico studies and in vitro evaluation for antioxidant and antibacterial properties of diarylmethylamines: A novel class of structurally simple and highly potent pharmacophore. European Journal of Pharmaceutical Science, 88, 202–209.

Nelson, N., 1944. A photometric adaptation of the Somogyi method for the determination of glucose. Journal of Biological Chemistry, 153, 375–380.

Qureshi, N., Blascheck, H.P., 2000. Butanol production using *Clostridium beijerinckii* BA 101 hyper-butanol producing mutant strain and recovery by Pervaporation. Applied Biochemistry and Biotechnology. 84, 225-235.

Powell, E. Proceedings of the 4th symposium on continuous cultivation of microorganisms, I. Malek, Ed. (Publishing House Academia, Prague,1969; 275.

Ranjan, A., Mayank, R., Moholkar, V.S., 2013b. Development of semi-defined rice straw-based medium for butanol production and its kinetic study. 3 Biotech, 3, 353–364.

Ranjan, A, Moholkar, V.S. 2012. Biobutanol: Science, engineering and economics. Int. J Energy Res. 36, 277-323.

Ranjan, A., Moholkar, V.S. 2009. Biobutanol: A viable gasoline substitute through ABE fermentation. Proc. World Acad. Sci: Eng. Technol. 51, 497-503.

Ranjan, A., Moholkar, V.S., 2013a. Comparative study of various pretreatment techniques for rice straw saccharification for the production of alcoholic biofuels. Fuel. 112, 567-571.

Sasmal, S., Goud, V.V., Mohanty, K., 2012. Ultrasound assisted lime pretreatment of lignocellulosic biomass toward bioethanol production. Energy and fuels, 26, 3777–3784.

Singh, S., Agarwal, M., Sarma, S., Goyal, A., Moholkar, V.S., 2015(b). Mechanistic insight into ultrasound induced enhancement of simultaneous saccharification and fermentation of *Parthenium hysterophorus* for ethanol production. Ultrasonics Sonochemistry. 26, 249–256.

Singh, S., Sarma, S., Agarwal, M., Goyal, A., Moholkar, V.S., 2015(a). Ultrasound enhanced ethanol production from *Parthenium hysterophorus*: a mechanistic investigation. Bioresource. Technology, 188, 287–294.

Somogyi, M., 1945. A new reagent for the determination of sugar. Journal. Biological Chemistry, 160, 61–68.

Srivastava, A.K., Volesky. B., 1990. Updated model of the batch acetone-butanol fermentation Biotechnoogy Letters, 9, 693-698.

Sulaiman, A.Z., Azilah, A., Yunus, R.M., Chisti, Y., 2011. Ultrasound-assisted fermentation enhances bioethanol productivity. Biochemical Engineering Journal, 54, 141–150.

Sutkar, V.S., Gogate, P.R., 2009. Design aspects of sonochemical reactors: techniques for

understanding cavitational activity distribution and effect of operating parameters. Chemical Engineering Journal, 155, 26–36.

Moholkar, V.S., Sable, S.P., Pandit. A.B., 2000. Mapping the cavitation intensity in an ultrasonic bath using the acoustic emission, AIChE Journal, 46, 684–694.

Votruba, J., Volesky, B., Yerushalmi, L., 1986. Mathematical model of a batch acetone-butanol fermentation. Biotechnology and Bioengineering. 28, 247–255.

Xin, F., Rui, Y., Wu, He, J., 2014. Simultaneous fermentation of glucose and xylose to butanol by clostridium *sp.* strain BOH3. Applied and Environmental Microbiology, 80, 15, 4771–4778.

Zhao, X., Condruz, S., Chen, J., Jolicoeur, M., 2016. A quantitative metabolomics study of high sodium response in *Clostridium acetobutylicum* ATCC 824 acetone–butanol–ethanol (ABE) fermentation. Scientific Reports, 6, 28307-12.

CHAPTER 7: OVERVIEW AND SUGGESTION FOR FUTURE WORK

CHAPTER 7

OVERVIEW AND SUGGESTION FOR FUTURE WORK

7.1 Overview

The present thesis was aimed at designing a suitable process of utilizing multiple invasive weeds as a feedstock for synthesis of bio alcohol and intensifying its yield in every step by applying ultrasound. Earlier research on biofuel has dealt with optimization of pretreatment and fermentation of these few individual invasive weeds. Here, we have carried out pretreatment of the eight invasive weeds namely (viz. *A. donax, C. Odorata, E. crassipes, I. carnea, L. Camara, M. micrantha, P. hysterophorus, S. spontaneum*) under optimized conditions determined for *Parthenium hysterophorus* and have assessed the yield of reducible sugars. Perceptibly, the optimum pretreatment conditions for the eight invasive weeds could be different than those for *Parthenium hysterophorus*. The major contemplation underlying approach of pretreating the invasive weeds listed above at conditions optimized for *Parthenium hysterophorus* is to assess the output of a bioprocess with feedstock flexibility. This can be explained in greater details as follows: Depending on the availability of biomasses in different parts of the year, the biofuel industry for large–scale production of alcoholic biofuels may require to change the feedstock or use mixed feedstock comprising several biomasses. Sufficiently large quantities of a single biomass may not be available throughout the year. In such situation, it may not be feasible and practical to conduct a comprehensive assessment and optimization of pretreatment conditions for each of the biomass used as feedstock. Even if such studies are conducted, the optimum conditions of pretreatment, such as acid/alkali

concentration or temperature/pressure of autoclaving, may show significant variations for different biomasses. Thus, processing equipment designed for pretreatment of one biomass may not be suitable for another biomass (in terms of design parameters such as material of construction or the thickness of the reactor wall). Obviously, replacement of process equipment with biomass is rather impractical. Under this limitation, it is rather inevitable to treat different biomasses at conditions optimized for the representative biomass that has been considered for the process design. In such situation, it is necessary to have a preliminary estimate of the alterations in the quality of the hydrolyzates in terms of concentrations of pentose and hexose sugars with changing feedstock. The study essentially attempts to give a picture of such variations by pretreatment of the eight invasive weeds at conditions optimized for the weed of *Parthenium hysterophorus*. We then studied the kinetic constant of the reaction necessary for designing the reactor and to also calculate theoretical yield. It also optimizes sugar release time and content. Based on the results obtained from the above criteria we have used mixture design experiments to get the best ratio of biomass component to form a composite biomass. The hydrolyzates obtained from the composite biomass were used for ethanol fermentation by separate hydrolysate fermentation mode and ABE fermentation by separate hydrolysis co-fermentation mode. For intensification of the processes for alcoholic biofuels synthesis, ultrasound irradiation is introduced in every step comprising acid/alkali pretreatment and enzymatic hydrolysis followed by fermentation. Experimental data obtained by both conventional (mechanical agitation) and ultrasound assisted experiments were coupled to a mathematical model. The viability of the cell and integrity of the enzyme structure has been studied with the help of Flow Cytometry, Circular dichroism and Fluorescence microscope.

The compendium consists of 7 chapters dwelling on different aspects of bioalcohol

fermentation. A brief summary of each chapter is outlined below:

- Chapter 1 presents the general introduction to the subject of biofuel synthesis from lignocelluloses, various policies involve and a brief discussion of invasive species and their potential to become next generation energy feedstock for biofuel production, abridged review of literature on various aspects of bioalcohol production using invasive weeds including its pretreatment studies and description of aim, approach and scope of the thesis.
- Chapter 2 embodies information on a sustainable bioprocess with feedstock flexibility by pretreatment of the eight selected waste invasive weeds at conditions optimized for a single weed. Assessment of the yield of reducible sugars of each biomass and study the kinetics of TRS releases has been presented. Effect of pretreatment on the surface and structural morphology of all biomasses is also characterized by XRD, SEM and FTIR.
- Chapter 3 deals with dilute acid hydrolysis of all biomasses and determining kinetics of the process using model proposed by Saeman in 1945. An irreversible pseudo-homogeneous 1st-order reaction is discussed for hydrolysis of the polymers like glucan, xylan to monomers like glucose, xylose and formation of decomposition products. The reaction constants k_1 and k_2 (representing polysaccharide to monosaccharide conversion, and further degradation of monosaccharide to other products, respectively) are determined by using solver function of the Matlab. Composite biomass is further developed based on the reaction constants and mixer design. Total fermentable sugar obtained from the composite biomass was estimated followed by characterization of its surface and structural morphology.
- Chapter 4 reveals the mechanistic insight into ultrasonic enhancement of enzymatic

hydrolysis of eight biomasses. Most of the earlier studies had a black-box approach and were focused on the results rather than rationale. This chapter has tried to find the physical mechanism of ultrasound induced enhancement of the enzymatic hydrolysis by identifying links between physics of ultrasound/ cavitation and biophysical mechanism of hydrolysis. We have adopted a dual strategy in our investigation, viz. (1) comparative analysis of secondary structure of cellulase and cellobiase enzymes in native form and after sonication, with the help of circular dichroism and florescence microscopy, and (2) fitting of the time profiles of reducing sugar release to the HCH-1 model for enzymatic cellulose hydrolysis.

- Chapter 5 centers around the mechanistic investigations on ultrasound-assisted bioethanol production by SHF mode of fermentation using optimized composite biomass as feedstock. Ultrasound at 35 kHz, 10% duty cycle was used for sonication. Experimental results were fitted to mathematical model and the kinetic and physiological parameters in the model were obtained using Genetic Algorithm (GA) based optimization. The viability of ultrasound-treated cell was analyzed through flow cytometry.
- Chapter 6 details our studies on solving two daunting problems associated with ABE fermentation namely adequate availability of biomass and low product yield by using the invasive biomass as feedstock and ultrasound irradiation as an intensification process. The biochemistry leading to accumulation of three solvent end products and two intermediate metabolites (acetic and butyric acids) were expressed through a mathematical modeling. The cell viability affected by ultrasound was studied through flow cytometry.

7.2 Suggestions for future work

Some of the suggestions for future work can be given as follows:

- All the experiments carried out in this thesis were conducted in batch mode (lab scale). The yield can more increased using continuous and fed batch operation mode. These studies are more suitable for large scale process.
- Real time product estimation with inbuilt sonication features need to be designed to monitor the physiology of the biochemical process.
- Sustainable mode of solvent recovery with specific enzyme immobilization can also help reduce the solvent inhibition and get the desired results of improve yield.
- Organism tolerances to product and substrate inhibition need to be studied in the form of co-culture etc.
- Reactor with inbuilt ultrasound system need to be design and the process enhancement need to be further optimized in terms of ultrasound power input as well as frequency.
- Assessment of complete cost analysis of bioethanol and biobutanol production (both upstream and downstream of the process) will help to take the research to commercial scale.
- Biorefinery prospect need to be seek to extract various intermediate product with commercial value, this will in turn bring down the economy involve in biofuel commercialization.

Research publications

RESEARCH OUTPUT

PUBLISHED IN PEER REVIEWED INTERNATIONAL JOURNALS

Research papers published from thesis

1. **Arup Jyoti Borah**, M Agarwal, M Poudyal, A Goyal, VS Moholkar. (2016) Mechanistic investigation in ultrasound induced enhancement of enzymatic hydrolysis of invasive biomass species. *Bioresource Technology*, 213, 342-349.

2. **Arup Jyoti Borah**, S Singh, A Goyal, VS Moholkar. (2016) An Assessment of Invasive Weeds as Multiple Feedstocks for Biofuels Production. *RSC Advances*, **6**, 47151-47163.

3. **Arup Jyoti Borah**, M. Agarwal, A. Goyal, V.S. Moholkar. (2018) Physical insights of ultrasound-assisted ethanol production from composite feedstock of invasive weeds, *Ultrasonics Sonochemistry* doi: 10.1016/j.ultsonch.2018.07.046.

4. **Arup Jyoti Borah**, K. Roy, A. Goyal, V.S. Moholkar. (2018). Mechanistic investigations in biobutanol synthesis via ultrasound–assisted abe fermentation using mixed feedstock of invasive weeds. *Bioresource Technology*, 272, 389-397.

5. **Arup Jyoti Borah,** R. Malani, A. Goyal, V.S. Moholkar. Kinetic modeling of dilute acid hydrolysis of various weedy invasive species as feedstock for biofuel production. (Manuscript under preparation)

6. **Arup Jyoti Borah,** A. Goyal, V.S. Moholkar. Development of a composite biomass and its assessment as a feedstock for biofuel production. (Manuscript under preparation)

Other research papers published

7. J Bhasarkar, **Arup Jyoti Borah**, P Goswami, VS Moholkar. (2015). Mechanistic analysis of ultrasound assisted enzymatic desulfurization of liquid fuels using horseradish peroxidase. Bioresource technology, 196, 88-98.

8. M Agarwal, PK Dikshit, JB Bhasarkar, **Arup Jyoti Borah**, VS Moholkar. (2016) *Physical insight into ultrasound-assisted biodesulfurization using free and immobilized cells of Rhodococcus rhodochrous MTCC 3552*. Chemical Engineering Journal, 295, 254-267.

9. S Pradhan**, Arup Jyoti Borah**, M Agarwal, M Poudyal, A Goyal, VS Moholkar. (2017) *Mechanistic investigation in ultrasound induced enhancement of enzymatic hydrolysis of invasive biomass species*. Bioresource technology, 213, 342-349.

Book chapter

V. S. Moholkar, P. K. Dikshit, S. Chakma, S. Khanna, R. Malani, Arup Jyoti Borah, J. Bhasarkar. Mechanistic issues of Sono-Biodegradation. Vol. 8: Biodegradation and Bioremediation, Environ. Sci. & Engg. Vol. 8. Stadium Press LLC. (2017), pp. 74-118.

CONFERENCE PRESENTATIONS

Poster Presentation:

AJ Borah, VA Selvi **.** *Synthesis of Silica nanoparticles from biomass its characterization and application in agricultural pest control***.** On 18th International conference Perspectiveand challenges in Chemcial and Biological Sciences innovation. (post ISCBC-2012, IASST, Boragaon, India) january 30th.

AJ Borah, A Goyal, VS Moholkar. *Comparative assessment of various biomass as potential feedstock for biofuel production.* International conference on Harnessing Natural resources for Sustainable development: Global trend. Jan29- 31th, 2014.

AJ Borah, A Goyal, VS Moholkar. *Establishing invasive weeds as a new feedstock for biorefinery: From Pain to Gain*. On Indo-US Conference on Advanced Lignocellulosic Biofuels (Indo-US CALB-2014).

AJ Borah, M Agarwal, M Poudyal, A Goyal, VS Moholkar. *Mechanistic investigation in ultrasound induced enhancement of enzymatic hydrolysis of invasive biomass species*. International conference on New Horizon in Biotechnology. (NHBT-2015, Trivandrum, India) Nov22-25.

Appendix A

Table A1: Results of proximate and ultimate analyses of eight biomass

Biomass feedstock	Ultimate analysis[#]					Proximate analysis	
	C (%)	H (%)	N (%)	S (%)	O (%)	Ash[*] (%)	Calorific Value[*] (MJ/kg)
AD	46.4	5.8	3.0	0.2	44.7	6.5 ± 0.2	18.7 ± 0.4
CO	42.4	5.4	3.9	0.0	48.2	6.2 ± 0.5	17.2 ± 0.7
EC	41.0	5.3	4.2	0.0	49.4	20.6 ± 0.1	9.2 ± 0.3
IC	42.2	4.3	1.7	0.2	51.2	3.2 ± 0.6	21.2 ± 0.2
LC	50.2	6.4	5.1	0.0	38.2	7.2 ± 0.4	18.2 ± 0.3
MM	43.1	5.6	4.6	0.0	46.7	8.5 ± 0.7	19.1 ± 0.7
PH	41.0	5.2	3.2	0.11	37.1	3.4 ± 0.7	13.1 ± 0.1
SS	49.1	6.2	2.7	0.0	41.9	9.0 ± 0.9	15.7 ± 0.3

* *The values are mean ± SE (n = 3).* # – An approximate variation of ±5% is expected in these values for various samples drawn from same source.

Fig A2: HPLC Standard graph of Glucose, Cellobiose, Xylose and Arabinose

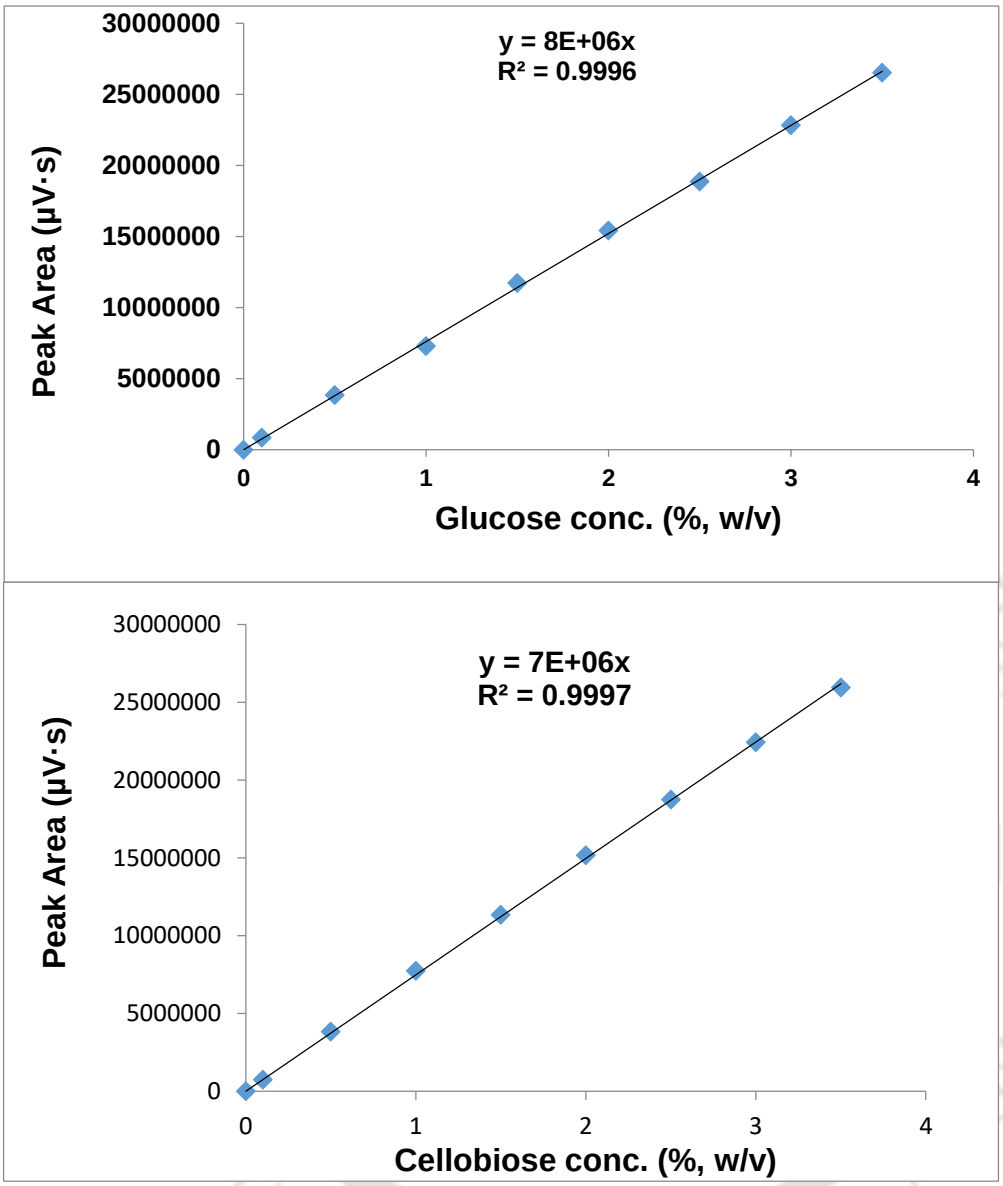

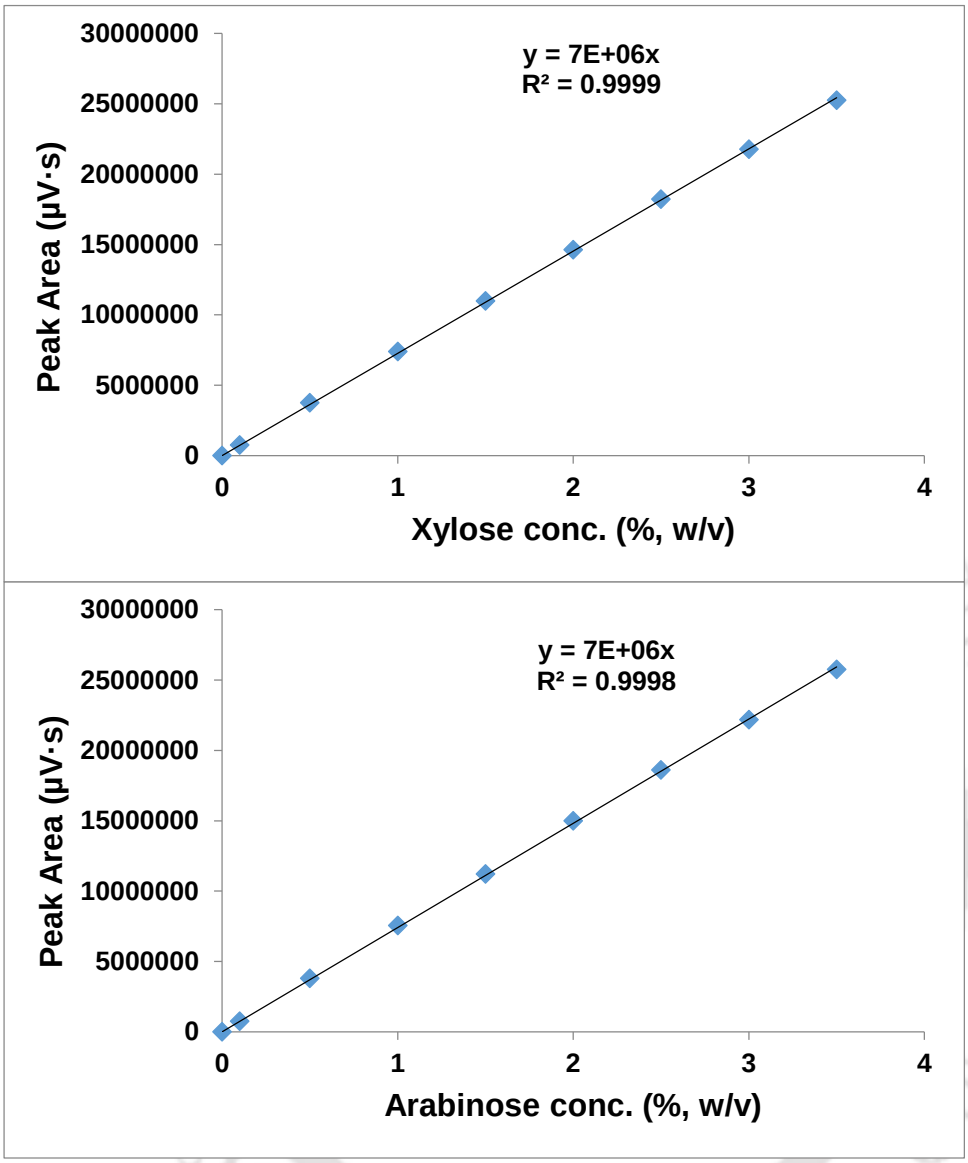

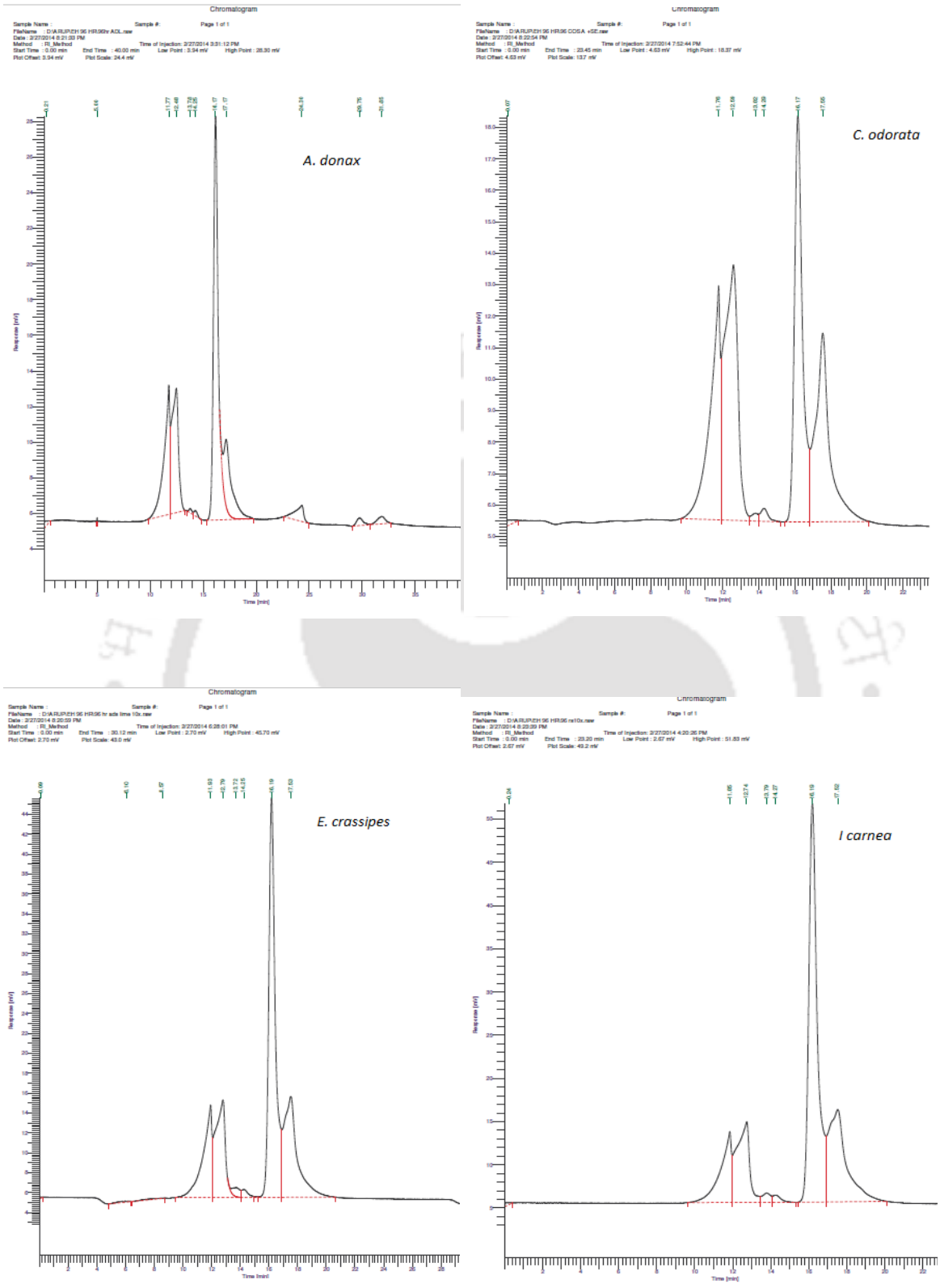

Fig A3: HPLC profile of sugars in eight different biomass

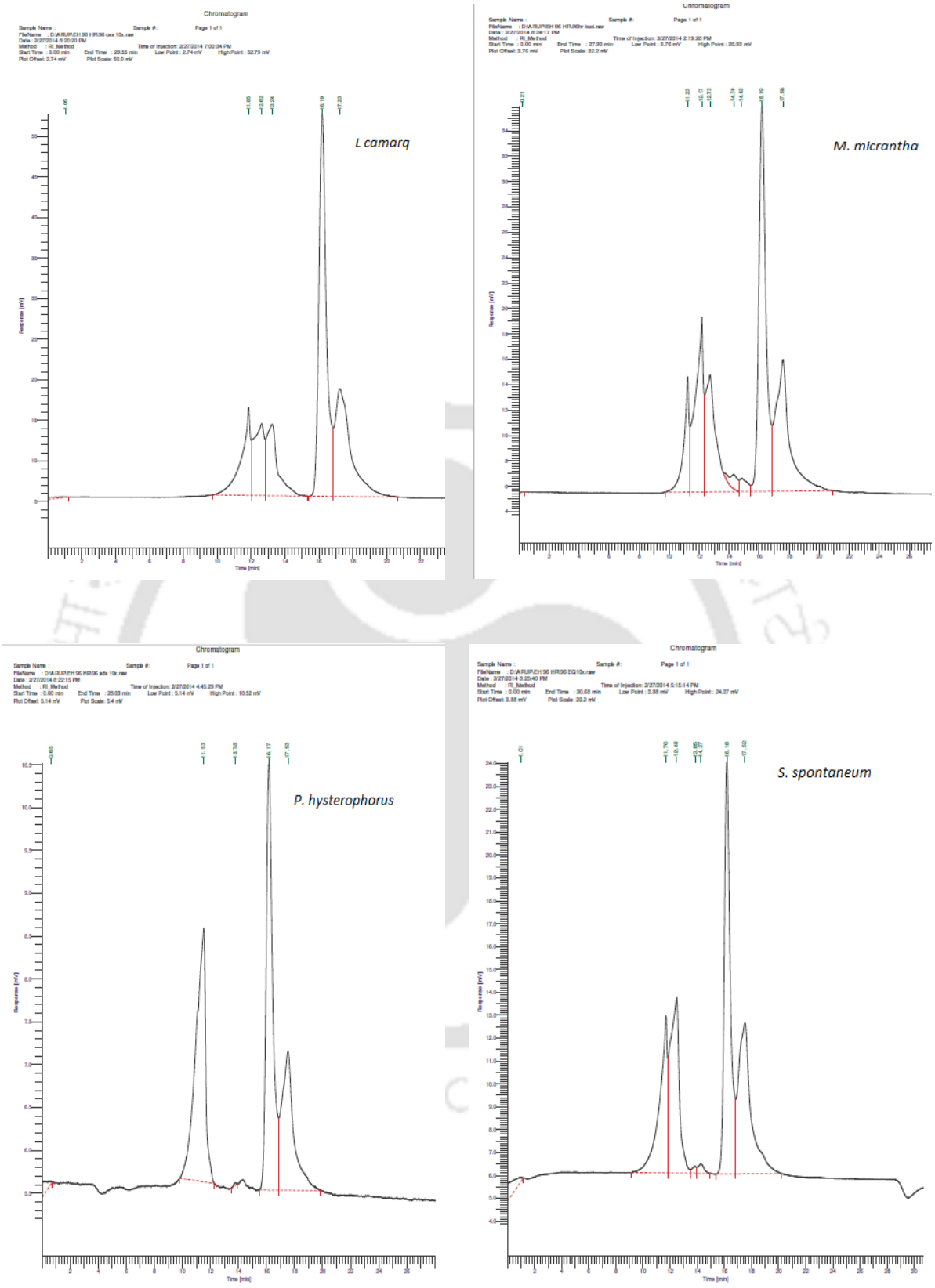

Figure A3: HPLC profile of sugars in eight different biomass

Appendix B

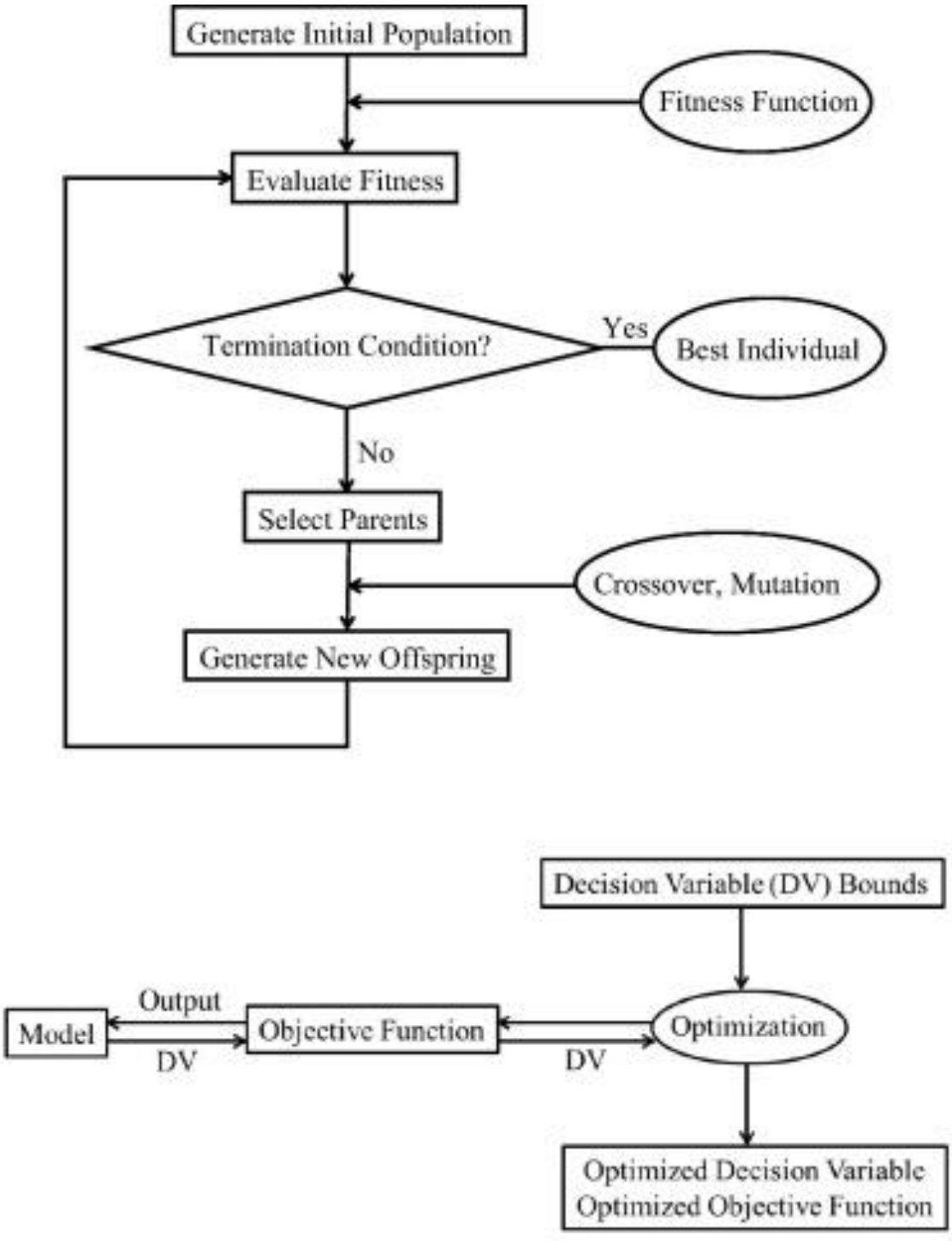

Figure B1: Flow chart of genetic algorithm

Reproduced from Singh et al., 2015 with permission from Elsevier®

Appendix C

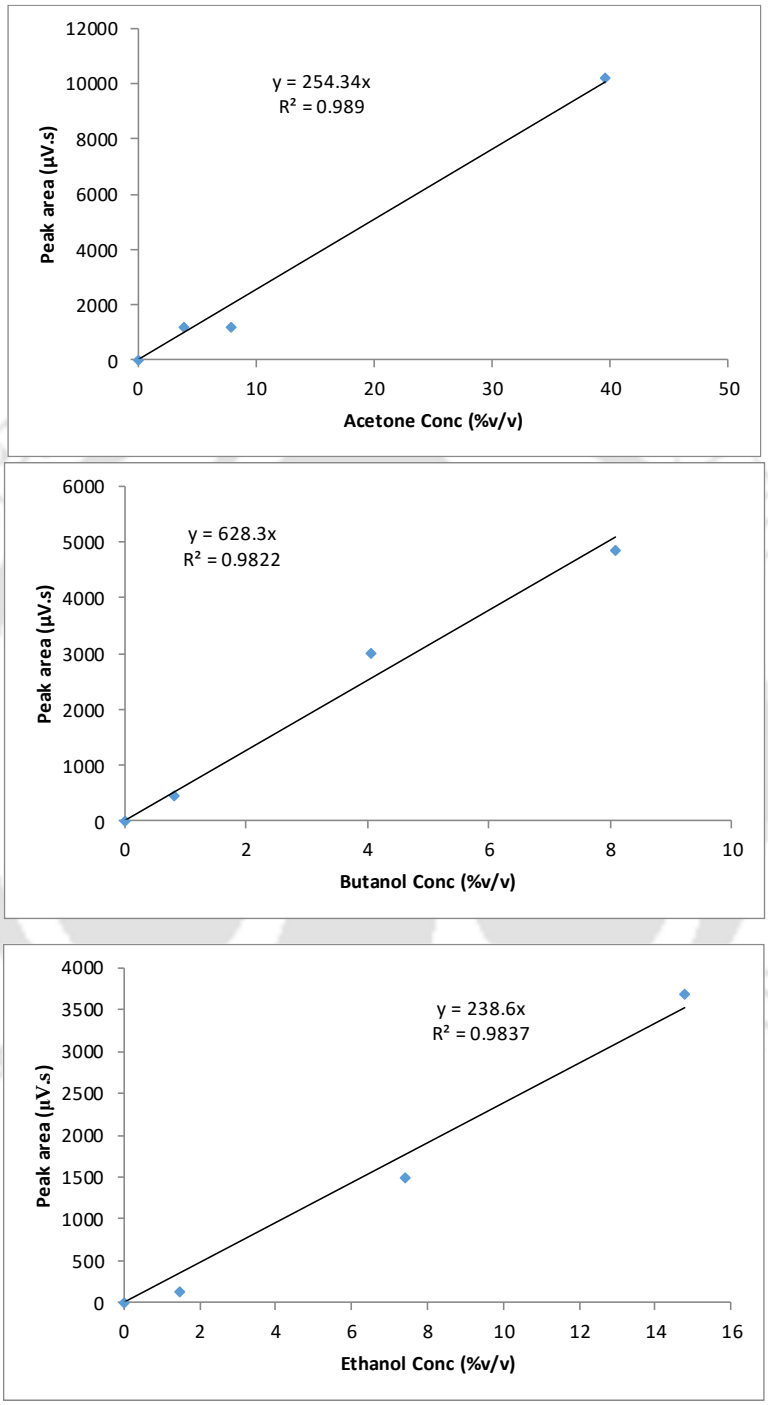

Figure C1: GC Standard of Acetone, butanol and Ethanol

CENTRE FOR ENERGY
IIT, GUWAHATI

Chromatogram Info:

File Name	: c:\Iris32\Work.2\CALIB\00_3812-May-20152878 4th day imm.PRM	File Created	: 5/12/2015 12:38:34 AM
Origin	: Acquired	Acquired Date	: 5/12/2015 12:38:34 AM
Project	: c:\Iris32\Projects\Work.2.PRJ	By	: Centre for Energy

Printed Version Info:

Printed Version	: 5/12/2015 12:38:34 AM	Printed Date	: 5/12/2015 12:39:02 AM
Report Style	: c:\Iris32\Common\Chromatogram.sty	By	: Centre for Energy
Calibration File	: None		

Sample Info:

Sample ID	: 2878 4th day imm	Amount	: 0
Sample	:	ISTD Amount	: 0
Inj. Volume [ml]	: 0	Dilution	: 1

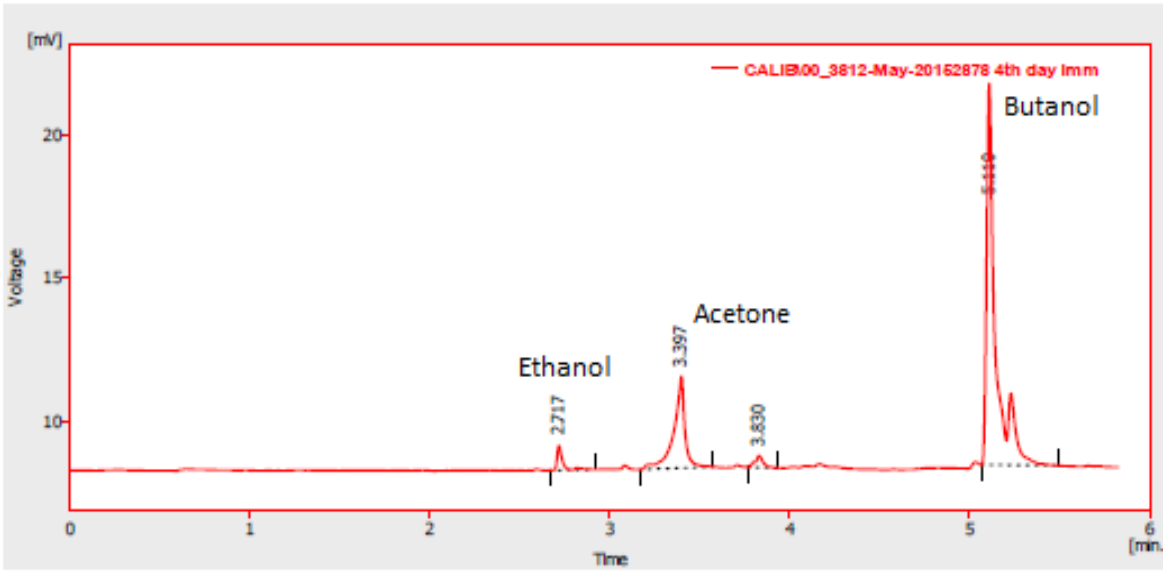

Figure C2: GC chromatogram profile of ABE fermentation